SOILS and ROCKS

An International Journal of Geotechnical and Geoenvironmental Engineering

Editor Waldemar Coelho Hachich - University of São Paulo, Brazil

Co-editor Manuel Matos Fernandes - University of Porto, Portugal

Special Issue: In Situ Testing for Ground Characterization

Guest-editors: Roberto Quental Coutinho - Universidade Federal de Pernambuco, Brazil

António Viana da Fonseca - University of Porto, Portugal

Executive Board

Alberto Sayão
Pontifical Catholic University of Rio de Janeiro, Brazil
Jorge Almeida e Sousa
University of Coimbra, Portugal
Ian Schumann Martins
Federal University of Rio de Janeiro, Brazil
João Maranha
LNEC, Portugal

Associate Editors

H. Einstein
MIT, USA
John A. Hudson
Imperial College, UK
Kenji Ishihara
University of Tokyo, Japan
Michele Jamiolkowski
Studio Geotecnico Italiano, Italy
Willy A. Lacerda
COPPE/UFRJ, Brazil
E. Maranha das Neves
Lisbon Technical University, Portugal
Nielen van der Merve
University of Pretoria, South Africa
Paul Marinos
NTUA, Greece
James K. Mitchell
Virginia Tech., USA
Lars Persson
SGU, Sweden
Harry G. Poulos
University of Sidney, Australia
Niek Rengers
ITC, The Netherlands
Fumio Tatsuoka
Tokyo University of Science, Japan
Luiz González de Vallejo
UCM, Spain
Roger Frank
ENPC-Cermes, France

Editorial Board Members

Roberto F. Azevedo
Federal University of Viçosa, Brazil
Milton Kanji
University of São Paulo, Brazil
Antonio M.S. Oliveira
University of Guarulhos, Brazil
Omar Y. Bitar
IPT, Brazil
Lázaro V. Zuquette
University of São Paulo, Brazil
Fabio Taioli
University of São Paulo, Brazil
Tarcisio Celestino
University of São Paulo-SC, Brazil
Roberto Q. Coutinho
Federal Univ. of Pernambuco, Brazil
Nilo C. Consoli
Federal Univ. Rio Grande do Sul, Brazil
Sandro S. Sandroni
Consultant, Brazil
Sérgio A.B. Fontoura
Pontifical Catholic University, Brazil
Ennio M. Palmeira
University of Brasilia, Brazil
Luciano Décourt
Consultant, Brazil
Faiçal Massad
University of São Paulo, Brazil
Marcus Pacheco
University of the State of Rio de Janeiro, Brazil
Paulo Maia
University of Northern Rio de Janeiro, Brazil
Renato Cunha
University of Brasília, Brazil
Orencio Monje Vilar
University of São Paulo at São Carlos, Brazil
Maria Eugenia Boscov
University of São Paulo, Brazil
Vinod Garga
University of Ottawa, Canada
Richard J. Bathurst
Royal Military College of Canada
Robert Mair
University of Cambridge, UK
Serge Leroueil
University of Laval, Canada
Mario Manassero
Politécnico di Torino, Italy
Luis Valenzuela
Consultant, Chile
Jorge G. Zornberg
University of Texas/Austin, USA
Andrew Whittle
MIT, USA
Pierre Bérest
LCPC, France
Peter Kaiser
Laurentian University, Canada
He Manchao
CUMT, China
Teruo Nakai
Nagoya Inst. Technology, Japan
Claudio Olalla
CEDEX, Spain
Frederick Baynes
Baynes Geologic Ltd., Australia
R. Kerry Rowe
Queen's University, Canada
R. Jonathan Fannin
University of British Columbia, Canada
Laura Caldeira
LNEC, Portugal
António S. Cardoso
University of Porto, Portugal
José D. Rodrigues
Consultant, Portugal
António G. Coelho
Consultant, Portugal
Luís R. Sousa
University of Porto, Portugal
Rui M. Correia
LNEC, Portugal
João Marcelino
LNEC, Portugal
António C. Mineiro
University of Lisbon, Portugal
António P. Cunha
LNEC, Portugal New
António G. Correia
University of Minho, Portugal
Carlos D. Gama
Lisbon Technical University, Portugal
José V. Lemos
LNEC, Portugal
Nuno Grossmann
LNEC, Portugal
Luís L. Lemos
University of Coimbra, Portugal
Ricardo Oliveira
COBA, Portugal

Soils and Rocks publishes papers in English in the broad fields of Geotechnical Engineering, Engineering Geology and Geo-environmental Engineering. The Journal is published in April, August and December. Subscription price is US$ 90.00 per year. The journal, with the name "Solos e Rochas", was first published in 1978 by the Graduate School of Engineering, Federal University of Rio de Janeiro (COPPE-UFRJ). In 1980 it became the official magazine of the Brazilian Association for Soil Mechanics and Geotechnical Engineering (ABMS), acquiring the national character that had been the intention of its founders. In 1986 it also became the official Journal of the Brazilian Association for Engineering Geology and the Environment (ABGE) and in 1999 became the Latin American Geotechnical Journal, following the support of Latin-American representatives gathered for the Pan-American Conference of Guadalajara (1996). In 2007 the journal acquired the status of an international journal under the name of Soils and Rocks, published by the Brazilian Association for Soil Mechanics and Geotechnical Engineering (ABMS), Brazilian Association for Engineering Geology and the Environment (ABGE) and Portuguese Geotechnical Society (SPG). In 2010, ABGE decided to publish its own journal and left the partnership.

Soils and Rocks

1978,	1 (1, 2)
1979,	1 (3), 2 (1,2)
1980-1983,	3-6 (1, 2, 3)
1984,	7 (single number)
1985-1987,	8-10 (1, 2, 3)
1988-1990,	11-13 (single number)
1991-1992,	14-15 (1, 2)
1993,	16 (1, 2, 3, 4)
1994-2010,	17-33 (1, 2, 3)
2011,	34 (1, 2, 3, 4)
2012-2013,	35-36 (1, 2, 3)
2014,	**37 (1, 2, 3)**

ISSN 1980-9743 CDU 624.131.1

ISSN 1980-9743

SOILS and ROCKS

An International Journal of Geotechnical and Geoenvironmental Engineering

Publication of

ABMS - Brazilian Association for Soil Mechanics and Geotechnical Engineering

SPG - Portuguese Geotechnical Society

Volume 37, N. 3, September-December 2014

Table of Contents

Articles

Examination of the Potential of the Seismic Dilatometer (SDMT) to Estimate *In Situ* Stiffness Decay Curves in Various Soil Types

S. Amoroso, P. Monaco, B.M. Lehane, D. Marchetti

Abstract. This paper illustrates the use of the seismic dilatometer (SDMT) to assess the decay of in-situ stiffness with strain level in different soil types. The approach adopted in this study relies on the ability of the SDMT to provide routinely at each test depth both a *small strain* stiffness (G_0 from V_S) and a *working strain* stiffness (constrained modulus M_{DMT} derived from the usual DMT interpretation). At various test sites, *working strain* DMT moduli are compared with reference stiffness decay curves back-figured from (i) the behavior observed under a full-scale test embankment (at Treporti) or footings (in Texas), (ii) from laboratory tests (at L'Aquila, Fucino plain and Po plain) and (iii) various combinations of in-situ and laboratory testing techniques (Western Australia). Typical ranges of the shear strains γ_{DMT} associated with *working strain* DMT moduli are inferred to assist construction of stiffness - strain decay curves for different soil types.
Keywords: seismic dilatometer, *in situ* stiffness decay curves, working strain stiffness, small strain stiffness.

1. Introduction

Methods for deriving stiffness decay curves (G-γ curves or similar, G = shear modulus, γ = shear strain) from *in situ* tests have been proposed by various Authors e.g. Robertson & Ferrera (1993) and Fahey (1998) used the unload-reload (u-r) cycles from self-boring pressuremeter tests; Mayne *et al.* (1999) and Marchetti *et al.* (2008) employed the SDMT; Elhakim & Mayne (2003) and Mayne (2003) adopted the seismic cone tests (SCPTs) while Lehane & Fahey (2004) combined the SCPT and DMT.

The seismic dilatometer (SDMT) is the combination of the flat dilatometer (DMT) with an add-on seismic module for the measurement of the shear wave velocity V_S. The approach adopted in this study relies on the ability of the SDMT to provide routinely, at each test depth, both the stiffness at *small strains* (the small strain shear modulus G_0 obtained from the shear wave velocity V_S as $G_0 = \rho\ V_S^2$) and the stiffness at *operative strains* (as represented by the constrained modulus M_{DMT} obtained by the usual DMT interpretation). The potential for these two stiffness values to provide guidance when selecting the G-γ curve of a soil element is examined.

2. Flat Dilatometer Test (DMT)

The flat dilatometer, introduced by Marchetti (1980), consists of a steel blade having a thin, expandable, circular steel membrane mounted on one face. When at rest, the membrane is flush with the surrounding flat surface of the blade. The blade is connected, by an electro-pneumatic tube running through the insertion rods, to a control unit on the surface (Figs. 1a and 1b). The control unit is equipped with pressure gauges, an audio-visual signal, a valve for regulating gas pressure (provided by a tank) and vent valves. The blade is advanced into the ground using common field equipment, i.e. penetrometers normally used for the cone penetration test (CPT) or drill rigs.

The test starts by inserting the dilatometer into the ground. When the blade has advanced to the desired test depth, the penetration is stopped. The operator inflates the membrane and takes, in about 30 sec, two readings: the *A* pressure, required to just begin to move the membrane ("lift-off" pressure), and the *B* pressure, required to expand the membrane center of 1.1 mm against the soil. A third reading *C* ("closing pressure") can also optionally be taken by slowly deflating the membrane soon after *B* is reached. The blade is then advanced to the next test depth, with a depth increment of typically 20 cm.

The interpretation proceeds as follows. First the field readings are used to derive the DMT intermediate parameters material index I_D, horizontal stress index K_D, dilatometer modulus E_D. Then I_D, K_D, E_D are used, by means of commonly used correlations, to estimate the constrained modulus M, the undrained shear strength s_u, the *in situ* earth pressure coefficient K_0 (clays), the overconsolidation ratio *OCR* (clays), the friction angle φ' (sands), the bulk unit weight γ. Consolidation and permeability coefficients may be estimated by performing dissipation tests. The

Sara Amoroso, Researcher, Department of Seismology and Tectonophysics, Istituto Nazionale di Geofisica e Vulcanologia, Italy. e-mail: sara.amoroso@ingv.it.
Paola Monaco, Assistant Professor, Department of Civil, Architectural and Environmental Engineering, University of L'Aquila, Italy. e-mail: paola.monaco@univaq.it.
Barry M. Lehane, Winthrop Professor, School of Civil, Environmental and Mining Engineering, University of Western Australia, Western Australia. e-mail: barry.lehane@uwa.edu.au.
Diego Marchetti, Engineer, Studio Prof. Marchetti, Italy. e-mail: diego@marchetti-dmt.it.
Submitted on March 2, 2014; Final Acceptance on December 15, 2014; Discussion open until April 30, 2015.

(a) (b) (c)

Figure 1 - (a) Schematic layout of the flat dilatometer test. (b) Seismic dilatometer equipment. (c) Schematic layout of the seismic dilatometer test (Marchetti *et al.*, 2001; Marchetti *et al.*, 2008).

C-reading, in sand, approximately equals the equilibrium pore pressure.

More detailed information on the DMT equipment, test procedure and all the interpretation formulae may be found in the comprehensive report by ISSMGE Technical Committee TC16 (Marchetti *et al.*, 2001).

3. Seismic Dilatometer Test (SDMT)

The seismic dilatometer (SDMT) is a combination of the mechanical flat dilatometer (DMT) with an add-on seismic module for measuring the shear wave velocity V_S. First introduced by Hepton (1988), the SDMT was subsequently improved at Georgia Tech, Atlanta, USA (Martin & Mayne, 1997, 1998; Mayne *et al.*, 1999). A new SDMT system (Figs. 1b and 1c) has been more recently developed in Italy (Marchetti *et al.*, 2008).

The seismic module (Fig. 1b) is a cylindrical element placed above the DMT blade, equipped with two receivers spaced at 0.50 m. The shear wave source, located at ground surface, is an automatic hammer or a pendulum hammer (≈ 10 kg) which hits horizontally a steel rectangular plate pressed vertically against the soil (by the weight of the truck) and oriented with its long axis parallel to the axis of the receivers, so that they can offer the highest sensitivity to the generated shear wave. When a shear wave is generated at the surface (Fig. 1c), it reaches first the upper receiver, then, after a delay, the lower receiver. The seismograms acquired by the two receivers, amplified and digitized at depth, are transmitted to a PC at the surface, which determines the delay. V_S is obtained as the ratio between the difference in distance between the source and the two receivers (S_2 - S_1) and the delay of the arrival of the impulse from the first to the second receiver (Δt).

The determination of the delay from SDMT seismograms, normally obtained using a cross-correlation algorithm rather than relying on the first arrival time or specific single points in the seismogram, is generally well conditioned. The *true-interval* test configuration with two receivers avoids possible inaccuracy in the determination of the “zero time” at the hammer impact, sometimes observed in the *pseudo-interval* one-receiver configuration. Moreover, the couple of seismograms recorded by the two receivers at a given test depth corresponds to the same hammer blow and not to different blows in sequence, which are not necessarily identical. Hence the repeatability of V_S measurements is considerably improved (observed V_S repeatability ≈ 1%, i.e. a few m/s). V_S measurements are taken every 0.50 m of depth (while the mechanical DMT readings are taken every 0.20 m). Validations of V_S measurements by SDMT by comparison with V_S measured by other *in situ* seismic tests at various research sites are reported by Marchetti *et al.* (2008).

4.Tentative Method for Deriving *in situ G*-γ Decay Curves from SDMT

Marchetti *et al.* (2008) first proposed the possible use of the SDMT for deriving *in situ* elemental soil stiffness variations with strain level (*G*-γ curves or similar). Such curves could be tentatively constructed by fitting “reference typical-shape” laboratory *G*-γ curves through two points, both obtained by SDMT: (1) the initial *small strain* modulus G_0 (obtained as $G_0 = \rho\ V_S^2$), and (2) a *working strain* modulus G_{DMT}.

To locate the second point on the *G*-γ curve it is necessary to know, at least approximately, the elemental shear strain corresponding to G_{DMT}. Indications by Mayne (2001) locate the DMT moduli at an intermediate level of strain (γ ≈ 0.05-0.1%) along the *G*-γ curve. Similarly Ishihara (2001) classified the DMT within the group of methods of measurement of soil deformation characteristics involving an intermediate level of strain (0.01-1%). The above qualitative indications are investigated in this paper.

As suggested by Marchetti *et al.* (2008), a *working strain shear modulus* G_{DMT} can be derived from the constrained modulus M_{DMT} provided by the usual DMT interpretation (Marchetti, 1980, Marchetti *et al.*, 2001). As a first approximation, by referring to linear elasticity:

$$G_{DMT} = \frac{1-2\nu}{2(1-\nu)} M_{DMT} \tag{1}$$

where ν = Poisson's ratio. E.g. assuming a typical drained ν of 0.2 (noting that M_{DMT} is a drained modulus), the *working strain shear modulus* may be obtained from Eq. 1 as $G_{DMT} = 0.375\ M_{DMT}$. It should be noted that correlations between the DMT parameters (E_D and K_D) and M_{DMT} proposed by Marchetti (1980) are based on the assumption that M_{DMT} represents a reasonable estimate of the "operative" or drained *working strain* modulus (*i.e.* the modulus that, when introduced into the linear elasticity formulae, provides realistic estimates of the settlement of a shallow foundation under working loads). This assumption is supported by the good agreement observed in a large number of well documented comparisons between measured and DMT-predicted settlements or moduli (see Monaco *et al.*, 2006; Marchetti *et al.*, 2008).

The use of the SDMT to assess the *in situ* decay of stiffness at various test sites is explored in the following sections using data obtained in different soil types and where both SDMT data and "reference" stiffness decay curves were available. Such stiffness decay curves were: (a) back-figured from the observed behavior under a full-scale test embankment (Treporti) or footings (Texas), (b) obtained by laboratory tests (L'Aquila, Fucino plain, Po plain), or (c) reconstructed by the combined use of different *in situ*/laboratory techniques (Western Australia). The procedure adopted in all cases is as follows, and is shown schematically on Fig. 2:

1) Using SDMT data obtained at the same depth of each available reference stiffness decay curve, a *working strain* modulus G_{DMT} (or E_{DMT}) is derived from M_{DMT} and normalized by its *small strain* value G_0 (or E_0) derived from V_S.
2) The G_{DMT}/G_0 (or E_{DMT}/E_0) horizontal ordinate line is superimposed to the same-depth experimental stiffness decay curve, in such a way that the data point ordinate matches the curve;
3) The "intersection" of the G_{DMT}/G_0 (or E_{DMT}/E_0) horizontal ordinate line with the stiffness decay curve provides a shear strain value referred to here as γ_{DMT}.

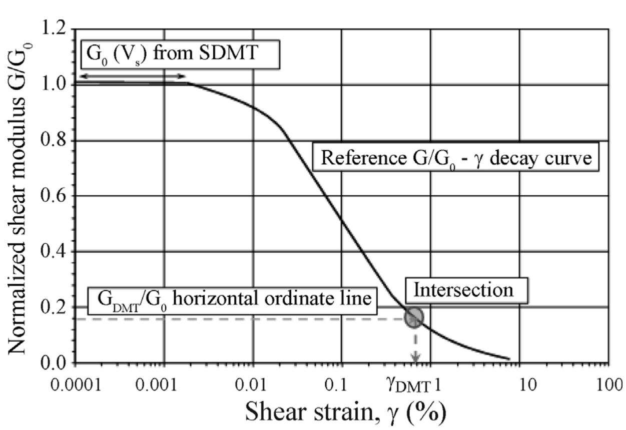

Figure 2 - Procedure to derive *in situ* G-γ decay curves from SDMT.

5. Stiffness Decay by SDMT at Various Test Sites

5.1. Treporti, Venice (Italy)

A full-scale vertically-walled cylindrical test embankment (40 m diameter, 6.7 m height, applied load 106 kPa) was constructed at the site of Treporti, Venice (Italy) where ground conditions are typical of the highly heterogeneous, predominantly silty deposits of the Venice lagoon. Pore pressures, surface settlements, horizontal movements and vertical displacements were monitored continuously and at various depths; see Simonini (2006). The Treporti test site was investigated extensively by means of piezocone tests (Gottardi & Tonni, 2004), flat dilatometer tests (Marchetti *et al.*, 2004), seismic piezocone tests and seismic dilatometer tests (McGillivray & Mayne, 2004), continuous coring boreholes and high quality laboratory tests (Simonini *et al.*, 2006). Significant results of the experimental program at Treporti have already been published by various research groups.

Figure 3 shows the profiles of the DMT parameters at Treporti, namely the material index I_D, the constrained modulus M_{DMT}, the undrained shear strength s_u and the horizontal stress index K_D from DMT 14 at the centre of the embankment, as well as the profiles of V_S obtained from SDMT 14 (McGillivray & Mayne, 2004), before starting the construction of the embankment (2002).

The Treporti embankment research has provided a unique opportunity to investigate the decay of soil stiffness *in situ* (Monaco *et al.*, 2014). Besides the moduli at the end of construction, moduli were also back-calculated in the elements on the centerline from local vertical strains ε_v measured during construction, under each load increment (from *small* to *working strains*). The stiffness considered in this section is the Young's modulus E.

In situ secant Young's moduli E were back-calculated at the mid-height of each 1 m soil layer as $E = (\Delta\sigma_v - 2\nu\ \Delta\sigma_r)/\varepsilon_v$, assuming vertical and radial stress increments $\Delta\sigma_v$ and $\Delta\sigma_r$ according to the theory of elasticity, ε_v obtained from extensometer data at the centre of the embankment under each load increment during construction (Marchetti *et al.*, 2006). Figure 4a shows the moduli corresponding to the first construction step (H = 0.5 m), to half-bank (H = 3.5 m) and to the construction end (H = 6.7 m). In the same figure, the small strain modulus E_0, derived from V_S

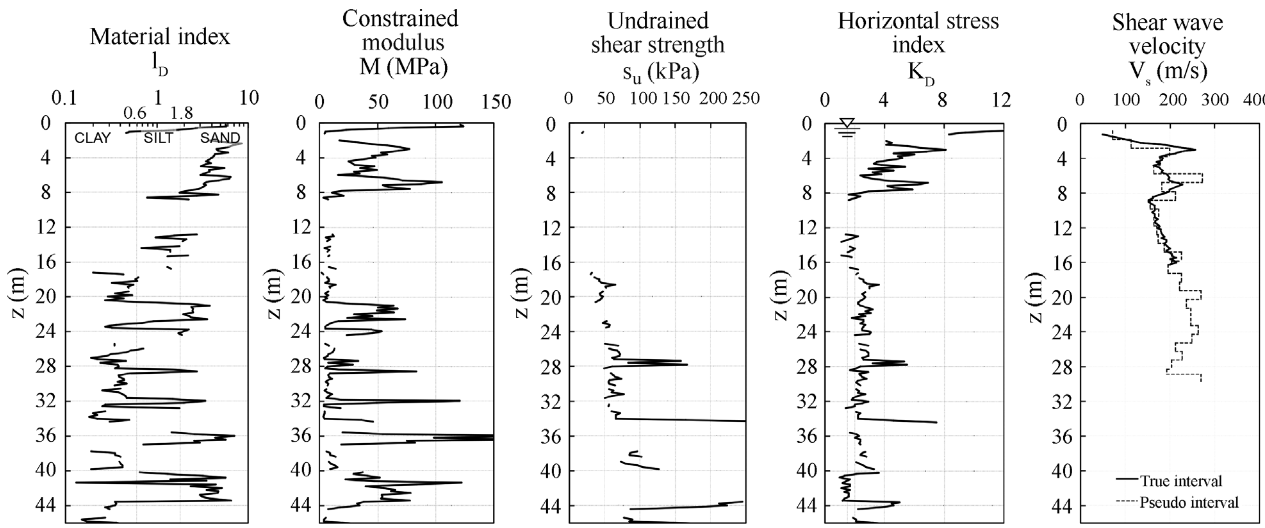

Figure 3 - Profiles of soil parameters from DMT 14 at the bank center (Marchetti *et al.*, 2004) and V_s profiles from SDMT 14 (McGillivray & Mayne, 2004) before embankment construction.

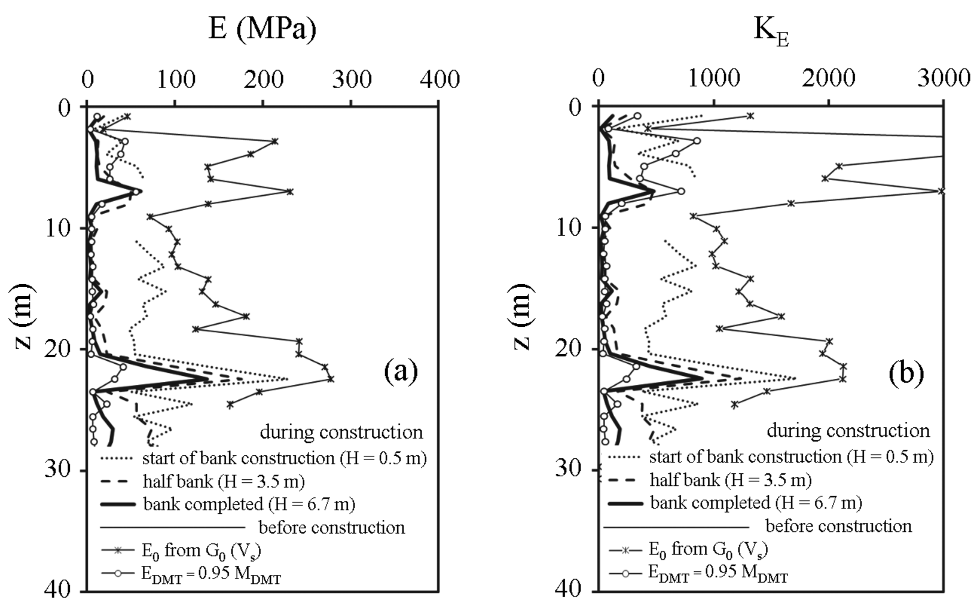

Figure 4 - Variation of (a) secant Young's modulus E, and (b) corresponding modulus number K_E (Eq. 2), back-calculated from local ε_v measured at the center under various embankment loads throughout construction (Monaco *et al.*, 2014, with permission from ASCE).

measured by SDMT, and the modulus E_{DMT} derived from M_{DMT} are shown for comparative purposes, assuming elasticity theory and a Poisson's ratio ν = 0.15 for both cases (hence E_{DMT} = 0.95 M_{DMT}). Figure 4a shows the progressive reduction of the back-calculated moduli E under increasing load. Such reduction should reflect the combined effects of the increase in stiffness with stress level and the reduction in stiffness with strain level.

In order to separate the two effects, the dependence of E on current stress level was taken into account, as a first approximation, by use of the Janbu's relation:

$$E = K_E p_a \left(\frac{\sigma'_v}{p_a} \right)^n \qquad (2)$$

where K_E = modulus number, p_a = reference atmospheric pressure (100 kPa), σ'_v = current vertical effective stress, and n = exponent, generally varying between 0.5 to 1 and assumed here to equal 0.5, following the observations of Cola & Simonini (2002). The variation of the modulus number K_E in Eq. 2 corresponding to E back-calculated under each load increment is represented in Fig. 4b, which even more clearly shows the decay of stiffness, normalized for the effect of stress level, with increasing strain.

In situ decay curves of soil stiffness with strain level (Fig. 5) were reconstructed from the back-calculated moduli at the mid-height of each 1 m soil layer. To account for the effect of varying stress level, such *in situ* curves are expressed in terms of variation of the ratio K_E/K_{E0}, where K_E and K_{E0} are respectively the modulus number corresponding to E back-calculated for each load increment and to the initial modulus E_0 (K_{E0} is obtained by Eq. 2 for $E = E_0$ and $\sigma'_v = \sigma'_{v0}$). The two sets of curves in Fig. 5 are representative of two distinct soil layers: (a) the sand layer between 2 to 8 m depth, and (b) the low plasticity (plasticity index PI = 8-12%, Simonini *et al.*, 2006) silt layer between 8 to 20 m depth (which contributed most of the observed settlement). Note that the initial part of the curves in Fig. 5 at small strains is missing, since the extensometers did not provide reliable measurements of ε_v less than about 0.01-0.5%.

At Treporti test site, using SDMT results obtained at the depth of each back-figured *in situ* stiffness decay curve in Fig. 5, Young's moduli E_{DMT} were derived from M_{DMT} using elasticity theory and normalized by their small strain values E_0 derived from V_S. The E_{DMT} moduli were derived from the constrained moduli M_{DMT}, using the theory of elasticity, by Eq. 3:

$$E_{DMT} = \frac{M_{DMT}(1+\nu)(1-2\nu)}{(1-\nu)} \tag{3}$$

assuming ν = 0.15, hence $E_{DMT} = 0.95\ M_{DMT}$.

The dots in Fig. 5 are the intersection between the *in situ* decay curve at a given depth and the horizontal line having as ordinate the ratio K_E/K_{E0} corresponding to E_{DMT}/E_0 at the same depth. Such "intersections" provided the values of the associated abscissas, i.e. the vertical strains ε_v in this case. The rectangular shaded areas in Figs. 5a and 5b denote, for each soil layer, the range of values of the ratio K_E/K_{E0} corresponding to E_{DMT}/E_0 and the associated range of vertical strains: $\varepsilon_v \approx 0.01$ to 0.1% in sand, $\approx$ 0.3 to 1% in silt (Monaco *et al.*, 2014).

Hence, the ratio G_{DMT}/G_0 was calculated by using the theory of elasticity (Eq. 4), while the corresponding shear strain γ_{DMT} was obtained by Eqs. 5, 6, as introduced by Atkinson (2000):

$$G_{DMT} = \frac{E_{DMT}}{2(1+\nu)} \tag{4}$$

assuming ν = 0.15, hence $G_{DMT} = 0.43\ E_{DMT}$.

$$\varepsilon_s = (1+\nu)\varepsilon_v \tag{5}$$

$$\gamma_{DMT} = \frac{3}{2}\varepsilon_s \tag{6}$$

where ε_s = shear strain for the individual soil elements.

The values of the *normalized working strain shear modulus* G_{DMT}/G_0 range from 0.18 to 0.24 in sand and 0.02 to 0.12 in silt, while the range of values of the shear strain γ_{DMT} are 0.02% to 0.14% in sand, 0.50% to 1.65% in silt.

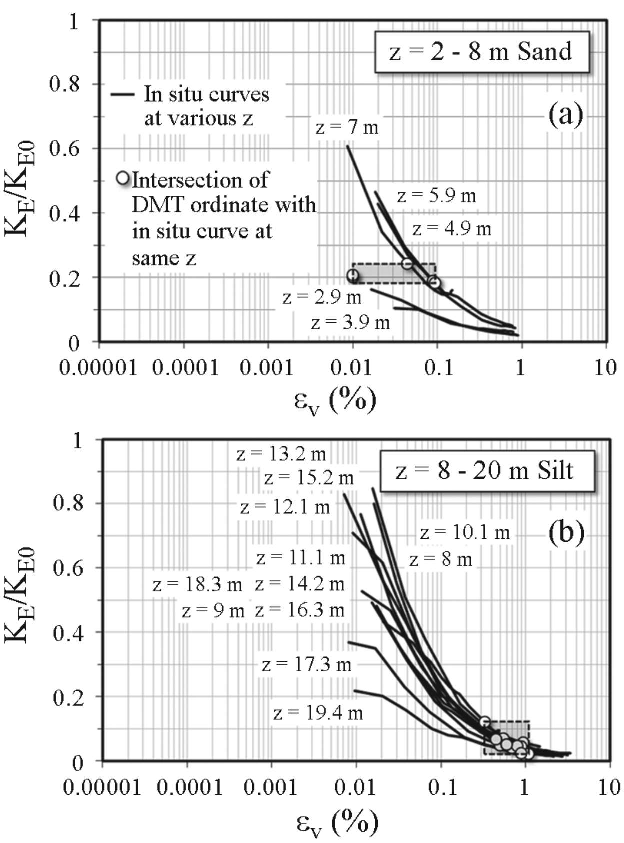

Figure 5 - Curves of decay of soil stiffness with vertical strain back-calculated from local ε_v measurements (curves labeled "*In situ* curves") in the sand layer 2 to 8 m depth (box a) and in the silt layer 8 to 20 m depth (box b). The dots are the intersection between the curve at a given depth and the horizontal line having as ordinate the ratio K_E/K_{E0} corresponding to E_{DMT}/E_0 at the same depth. Such "intersections" provided the values of the associated abscissas ε_v (Monaco *et al.*, 2014, with permission from ASCE).

5.2. Texas A&M University National Geotechnical Experimentation Site (U.S.A.)

In 1994 a Spread Footing Prediction Symposium was conducted at the Texas A&M University National Geotechnical Experimentation Site, as part of the ASCE Geotechnical Specialty Conference Settlement '94. Five square footings, ranging in size from 1 to 3 m, were constructed and tested to obtain the complete load-settlement curves (Gibbens & Briaud, 1994a). The test site, composed of medium dense silty fine sand, was extensively investigated by several *in situ* tests (SPT, CPTU, DMT, borehole pressuremeter, Cross-Hole, borehole shear test and step blade test). Laboratory triaxial and resonant column tests were executed on reconstituted samples (Gibbens & Briaud, 1994b). Figure 6 plots the DMT profiles (DMT 1, DMT 2),

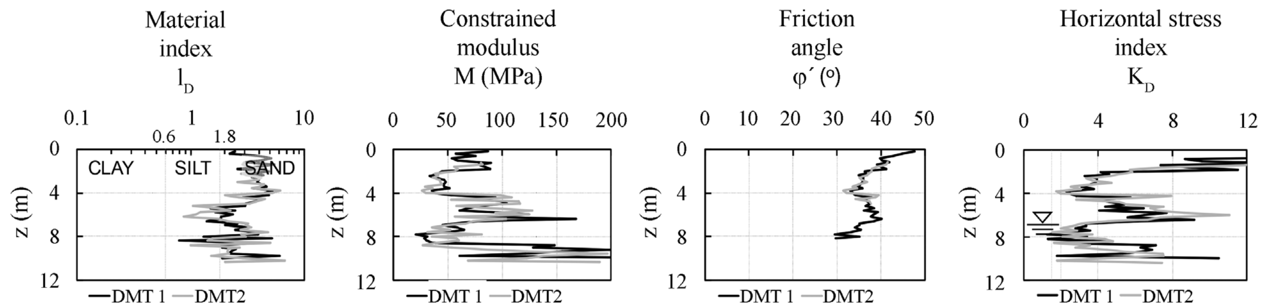

Figure 6 - DMT profiles at Texas A&M University National Geotechnical Experimentation Site (after Gibbens & Briaud, 1994b).

in terms of the material index I_D, the constrained modulus M, the friction angle φ' and the horizontal stress index K_D.

Figure 7 shows the *in situ* stiffness decay curve reconstructed by Berardi (1999) based on the observed performance of the footings. The Young's modulus E was back-figured from the observed load-settlement curves by use of a non linear iterative approach. The influence of current stress level was considered "implicit" in the E values determined over a limited influence depth, assumed within B and $2B$ (B = footing width). In Fig. 7 the decay of E, normalized to its initial value E_0, is plotted as a function of the relative displacement $w/B\%$ (footing settlement $w/$ width B).

From the results of two DMTs executed at the Texas A&M University test site, Young's moduli E_{DMT} (average values over an influence depth assumed within B and $2B$) were derived from M_{DMT} by Eq. 3, assuming ν = 0.2. The initial values of E_0 over the same depth interval were derived from V_S measured by Cross-Hole via elasticity theory (for ν = 0.2). In Fig. 7 the data points corresponding to E_{DMT}/E_0 for each footing size (3 m, 2 m, 1.5 m and 1 m) are superimposed to the E/E_0 - w/B curve reconstructed by Berardi (1999). The "intersection" of the DMT data points with the

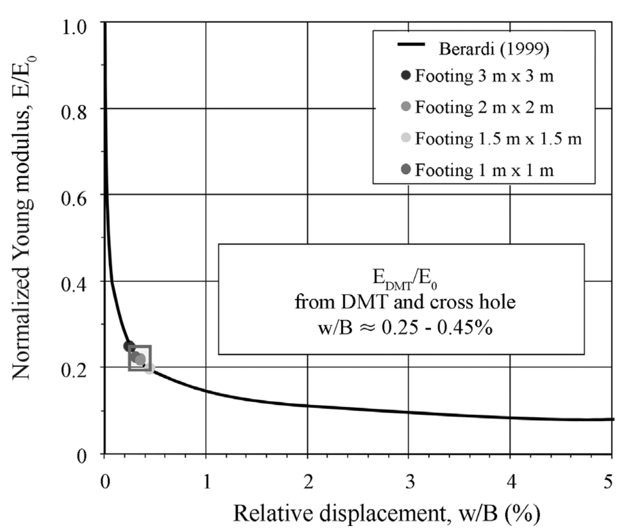

Figure 7 - Stiffness decay curve at Texas A&M University National Geotechnical Experimentation Site (Berardi, 1999) and superimposed E_{DMT}/E_0 data points (Amoroso *et al.*, 2012).

observed *in situ* decay curve indicates that the moduli estimated from DMT are located in a range of relative displacement $w/B \approx 0.25$ to 0.45%.

Hence, the ratio G_{DMT}/G_0 was calculated by using the theory of elasticity (Eq. 4), while the corresponding shear strain γ_{DMT} was obtained by Eqs. 6, 7, as introduced by Atkinson (2000):

$$\varepsilon_v \approx \frac{w}{3B} \tag{7}$$

The values of the *normalized working strain shear modulus* G_{DMT}/G_0 range from 0.20% to 0.25%, while the range of values of the shear strain γ_{DMT} are 0.02 to 0.14% in sand, 0.13 to 0.23% in silt.

5.3. L'Aquila (Italy)

Following the destructive April 6, 2009 earthquake (moment magnitude $M_w = 6.3$), the area of L'Aquila was extensively investigated by a variety of geotechnical and geophysical testing techniques, involving several working groups. Soon after the earthquake site investigations, including Down-Hole, surface wave tests and SDMT, were concentrated at a number of sites selected for the construction of new temporary houses for the homeless people (C.A.S.E. Project). Advanced cyclic/dynamic laboratory tests, including resonant column/torsional shear tests (RC-CTS) and double sample direct simple shear tests (DSDSS), were carried out on undisturbed samples from several C.A.S.E. sites, in medium- to fine-grained soils, by a network of Italian soil dynamics laboratories. Details and data are reported in Monaco *et al.* (2012); Santucci de Magistris *et al.* (2013); Monaco *et al.* (2013). The availability of both SDMT and laboratory test results at three C.A.S.E. sites (Cese di Preturo, Pianola, Roio Piano) permitted some calibration of empirical estimates of non-linear parameters from SDMT (Amoroso *et al.*, 2012).

Coupled data from SDMT and resonant column/torsional shear tests were also obtained from an extensive geotechnical investigation performed in the Southern part of the city centre of L'Aquila for the reconstruction of several damaged buildings (Totani *et al.*, 2012; Amoroso *et al.*, 2015).

Table 1 reports the values of the shear wave velocity V_S measured by SDMT, the small strain shear modulus G_0 *in situ* obtained from V_S, the constrained modulus M_{DMT} obtained from the SDMT at the depth of the samples tested in the laboratory, the *working strain shear modulus* G_{DMT} calculated using Eq. 1, assuming ν = 0.2, and the plasticity index *PI*. The values of the *normalized working strain shear modulus* G_{DMT}/G_0, also reported in Table 1, result 0.10 to 0.23 in silt and clay, 0.37 in silty sand. Figure 8 plots the SDMT profiles, in terms of the material index I_D, the constrained modulus *M*, the undrained shear strength s_u, the horizontal stress index K_D and the shear wave velocity V_S at the four mentioned sites. In Fig. 9 each G_{DMT}/G_0 data point (grey symbols) is superimposed on the corresponding same-depth laboratory G/G_0 curve (RC tests by University of Napoli Federico II, DSDSS tests by University of Roma La Sapienza). The range of values of the shear strain γ_{DMT} resulting from the "intersection" of the G_{DMT}/G_0 data points with the laboratory curves (rectangular areas in Fig. 9) are γ_{DMT} = 0.24 to 0.52% in silt and clay, γ_{DMT} = 0.16% in silty sand; these are also reported in Table 1.

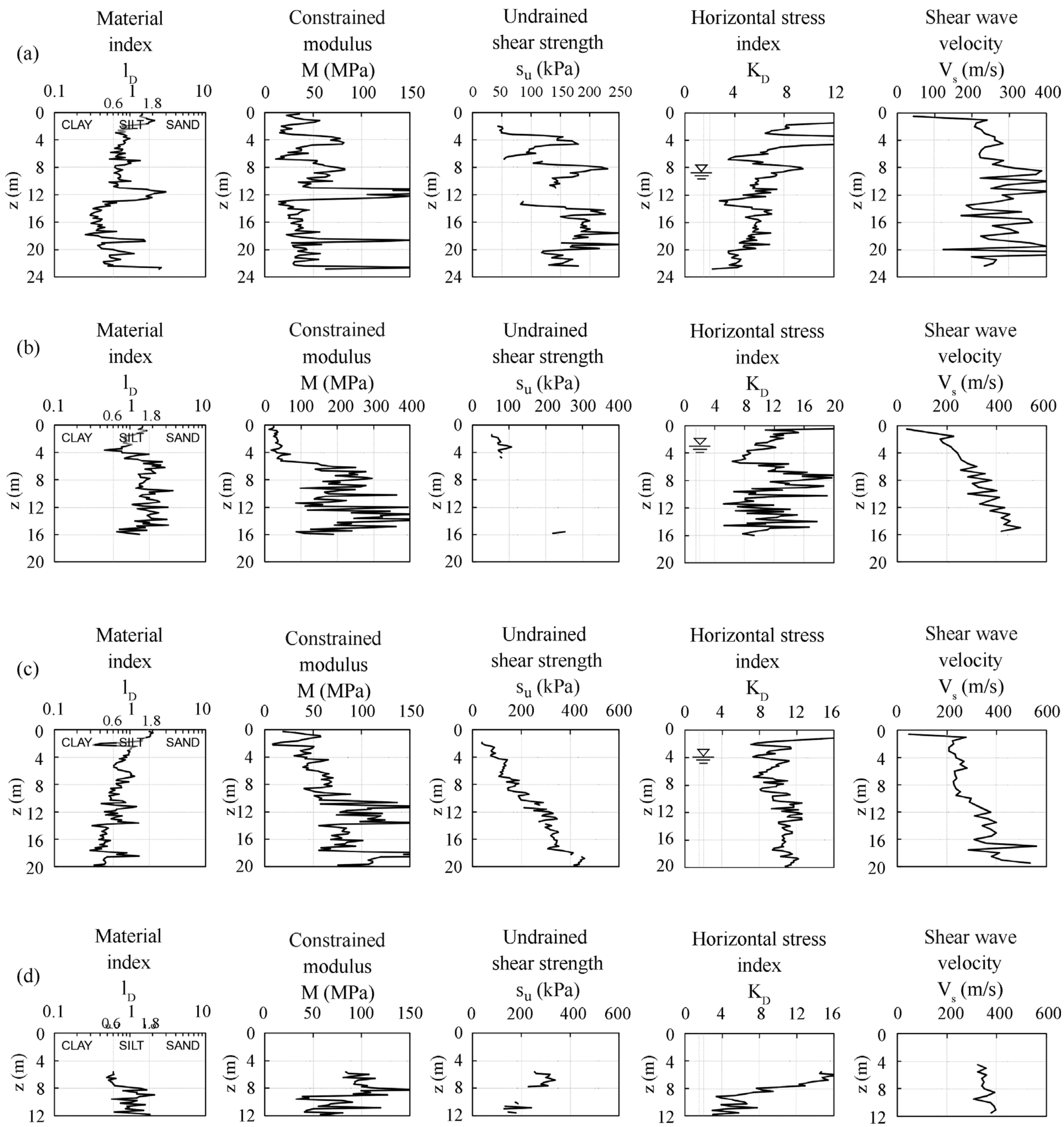

Figure 8 - SDMT profiles at L'Aquila basin: (a) Cese di Preturo, (b) Pianola, (c) Roio Piano, (d) L'Aquila (after Monaco *et al.*, 2012).

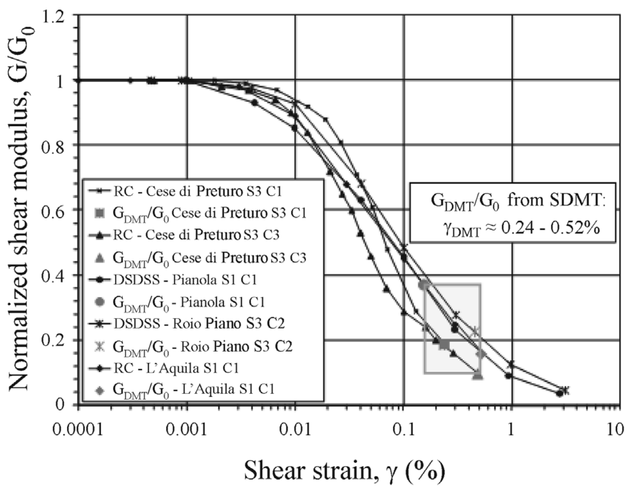

Figure 9 - Laboratory G/G_0-γ curves and superimposed G_{DMT}/G_0 data points at L'Aquila (after Amoroso *et al.*, 2012).

5.4. Fucino plain (Italy)

In 1986 a comprehensive investigation, involving static and dynamic loading effects, was carried out in the national research site of Fucino, Italy (Burghignoli *et al.*, 1991). *In situ* tests (SPT, CPT, DMT, self-boring pressumeter, vane test, Down-Hole, Cross-Hole, Spectral Analysis of Surface Waves) and laboratory tests (static and dynamic) were carried out to investigate the homogeneous lacustrine clay deposit to a depth of 40 m. Resonant column/torsional shear tests (RC-CTS) were executed on twelve undisturbed samples recovered from depths ranging between 3 and 37 m (effective vertical stress between 30 and 250 kPa). Although the data points pertain to a wide range of consolidation stresses, the results define, within a narrow band, the strong dependence of the stiffness on the strain level (Burghignoli *et al.*, 1991). In 2004 the same site in the Fucino plain was investigated by seismic dilatometer (Marchetti *et al.*, 2008) and the results are illustrated in Fig. 10.

Table 2 reports the values of the shear wave velocity V_S measured by SDMT, the small strain shear modulus G_0 *in situ* obtained from V_S, the constrained modulus M_{DMT} obtained by SDMT at the depth of the samples tested in the laboratory, the *working strain shear modulus* G_{DMT} calculated by Eq. 1, assuming $\nu = 0.2$, and the plasticity index *PI*. The values of the *normalized working strain shear modulus* G_{DMT}/G_0, also reported in Table 2, result 0.04 to 0.13 in clay. In Fig. 11 each G_{DMT}/G_0 data point (grey symbols) is superimposed on the corresponding same-depth laboratory G/G_0 curve (RC tests). The range of values of the shear strain γ_{DMT} resulting from the "intersection" of the G_{DMT}/G_0 data points with the laboratory curves (rectangular areas in Fig. 11) are γ_{DMT} = 1.10 to 1.70% in clay; these are also reported in Table 2.

Table 1 - L'Aquila - Values of G_{DMT}/G_0 obtained from SDMT and corresponding shear strain γ_{DMT} determined from the intersection with the G/G_0-γ laboratory curves (after Amoroso *et al.*, 2012).

Test site	Sample	Depth (m)	Soil type	V_S (m/s)	G_0 (MPa)	M_{DMT} (MPa)	ν	G_{DMT} (MPa)	G_{DMT}/G_0	γ_{DMT} (%)	PI (%)
Cese di Preturo	S3-C1	4.0-4.8	Silty clay	261	133	67	0.2	25	0.19	0.24	37
Cese di Preturo	S3-C3	17.5-18.0	Clayey silt	274	149	39	0.2	15	0.1	0.48	37
Pianola	S1-C1	6.0-6.5	Silty sand	303	195	193	0.2	72	0.37	0.16	31
Roio Piano	S3-C2	7.0-7.5	Clayey silt	233	105	64	0.2	24	0.23	0.46	19
L'Aquila	S1-C1	3.5-4.0	Clayey-sandy silt	344	232	97	0.2	36	0.16	0.52	31

Table 2 - Fucino plain - Values of G_{DMT}/G_0 obtained from SDMT and corresponding shear strain γ_{DMT} determined from the intersection with the G/G_0-γ laboratory curves.

Test site	Sample	Depth (m)	Soil type	V_S (m/s)	G_0 (MPa)	M_{DMT} (MPa)	ν	G_{DMT} (MPa)	G_{DMT}/G_0	γ_{DMT} (%)	PI (%)
Telespazio	-	5.0	Clay	70	14.7	1.4	0.2	0.5	0.04	1.70	30-70
Telespazio	-	10.0	Clay	101	15.7	1.8	0.2	0.7	0.04	1.70	30-70
Telespazio	-	15.0	Clay	98	17.7	2.2	0.2	0.8	0.05	1.60	30-70
Telespazio	-	20.0	Clay	124	16.7	4	0.2	1.5	0.09	1.40	30-70
Telespazio	-	25.0	Clay	156	16.7	5.6	0.2	2.1	0.13	1.10	30-70
Telespazio	-	30.0	Clay	183	17.7	5.9	0.2	2.2	0.13	1.10	30-70

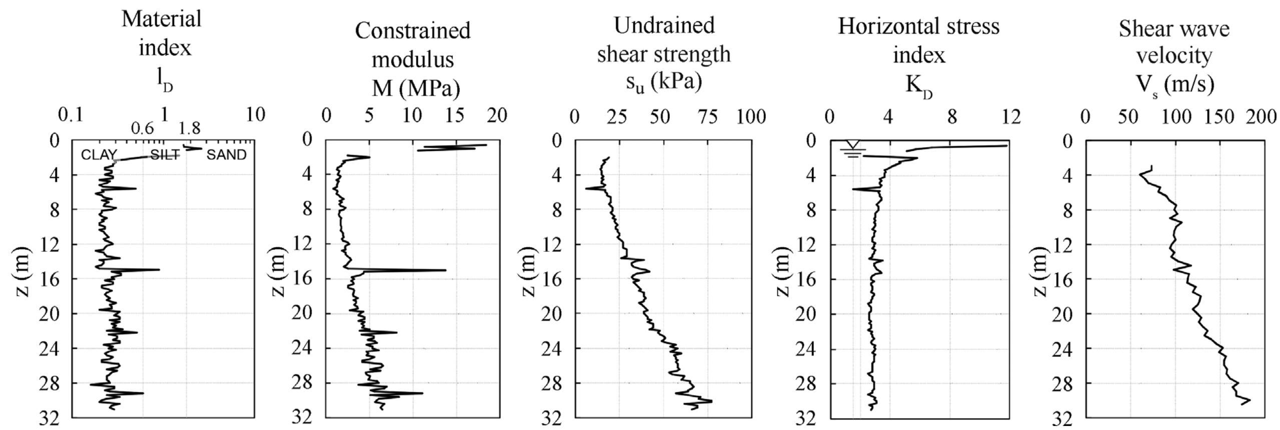

Figure 10 - SDMT profiles at Fucino plain (Marchetti *et al.*, 2008).

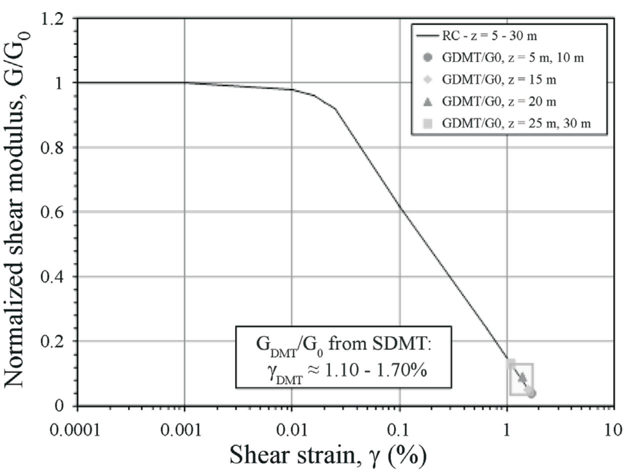

Figure 11 - Laboratory G/G_0-γ curve (Burghignoli *et al.*, 1991) and superimposed G_{DMT}/G_0 data points at Fucino plain.

5.5. Po plain (Italy)

The seismic sequence which affected northern Italy in May 2012, in particular the two main shocks that occurred on May 20, 2012 (M_w = 5.8) and May 29, 2012 (M_w = 5.6), induced several cases of liquefaction and related ground deformations.

An extensive site investigation program was subsequently planned by the "Liquefaction Working Group" promoted by the Emilia Romagna regional government and by the national Department of Civil Protection, in addition to the existing soil investigation data base, to characterize the soils and to define the input data necessary for site seismic response analyses and for assessment of liquefaction hazard (Regione Emilia Romagna - Liquefaction Working Group, 2012). The available results of this investigation programme, illustrated in various reports and papers (*e.g.* Facciorusso *et al.*, 2012, Fioravante *et al.*, 2013), include borehole logs, results of piezocone/seismic piezocone penetration tests (CPTU/SCPTU) and laboratory tests on samples, including resonant column/torsional shear tests (RC-CTS). An additional investigation involving seismic dilatometer (SDMTs), as illustrated in Fig. 12, as well as resonant column tests (RC) was carried out by the Working Group S2-UR4 (2013) and focused only on the area of San Carlo; see also Romeo *et al.* (2015). The town of San Carlo was constructed above the abandoned channel of the Reno River, and sand is the prevailing lithology in the band near this paleo-channel. Part of the town was built on the ancient banks of the Reno River.

The availability of results from both SDMT and laboratory resonant column (RC) tests on undisturbed samples taken in nearby boreholes in the area of San Carlo permitted some calibration of empirical estimates of non-linear parameters from SDMT.

Table 3 reports the values of the shear wave velocity V_S measured by SDMT, the small strain shear modulus G_0 *in situ* obtained from V_S, the constrained modulus M_{DMT} obtained from SDMTs performed at the depth of the samples tested in the laboratory, the *working strain shear modulus* G_{DMT} calculated by Eq. 1, assuming ν = 0.2, and the plasticity index *PI*. The values of the *normalized working strain shear modulus* G_{DMT}/G_0 range from 0.07 to 0.10 in silt and clay, and 0.06 to 0.32 in silty sand; see Table 3. In Fig. 13 each G_{DMT}/G_0 data point (black and grey symbols) is superimposed on the corresponding same-depth laboratory G/G_0 curve (RC tests). The range of values of the shear strain γ_{DMT} resulting from the "intersection" of the G_{DMT}/G_0 data points with the laboratory curves (rectangular areas in Fig. 13) are γ_{DMT} = 0.32% to 0.47% in silt and clay, γ_{DMT} = 0.07 to 0.30% in silty sand; see Table 3.

5.6. Western Australia

The G/G_0-γ decay curves presented in this section were obtained at five different test sites in Western Australia (Shenton Park, Ledge Point, Perth CBD, East Perth, Margaret River). Such curves were constructed based on the results of several *in situ* tests, including flat/seismic dilatometer tests (DMT/SDMT), seismic cone penetration tests (SCPT), self-boring pressuremeter tests (SBP) and

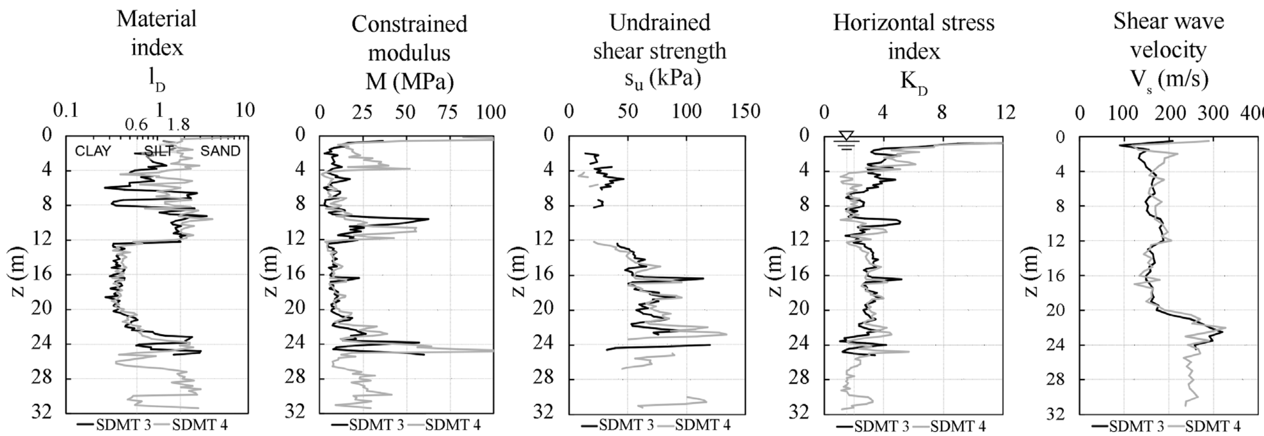

Figure 12 - SDMT profiles at Po plain (Working Group S2-UR4, 2013).

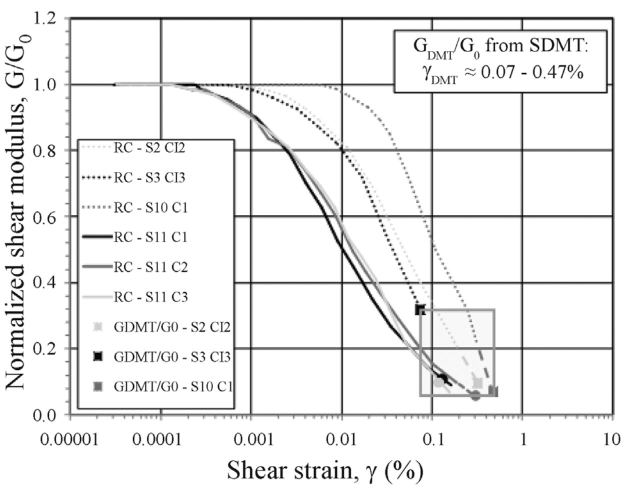

Figure 13 - Laboratory G/G_0-γ curves (after Fioravante *et al.*, 2013) and superimposed G_{DMT}/G_0 data points at Po plain.

laboratory triaxial tests. Details can be found in Amoroso (2011), Fahey *et al.* (2003, 2007), Lehane *et al.* (2007), Lehane (2010), Lehane & Fahey (2004), Schneider *et al.* (2008), Schneider & Lehane (2010).

Figure 14 shows the SDMT profiles, in terms of the material index I_D, the constrained modulus M_{DMT}, the inferred friction angle φ' or the undrained shear strength s_u, the horizontal stress index K_D and the shear wave velocity V_S at the three mentioned sites.

The *in situ* normalized G/G_0-γ decay curves shown in Fig. 15 (Shenton Park, silica sand), Fig. 16 (Ledge Point, calcareous sand) and Fig. 17 (Perth CBD, alluvial silty clay) were reconstructed by combining the information resulting from SCPT and SBP. In particular:

- the initial part of the curves ($\gamma \le 0.001\%$) was characterized by the small strain shear modulus G_0 obtained from V_S measured by SCPT (no SDMT data were available at these sites);
- the non-linear G/G_0-γ decay at medium to large shear strains ($\gamma \ge 0.01\%$) was estimated based on SBP data, according to the procedure proposed by Jardine (1992);
- the central part of the curves ($0.001\% > \gamma > 0.01\%$) was defined by simply connecting the initial part obtained from SCPT (G_0) and the final part obtained from SBP.

The *working strain shear modulus* G_{DMT} was calculated from M_{DMT} obtained by DMT at the same depths of the SCPT and SBP data used to define the G/G_0-γ curve, by use of Eq. 1, assuming ν = 0.2 in sand in silty clay. The values

Table 3 - Po plain - Values of G_{DMT}/G_0 obtained from SDMT and corresponding shear strain γ_{DMT} determined from the intersection with the G/G_0-γ laboratory curves (after Working Group S2-UR4, 2013).

Test site	Sample	Depth (m)	Soil type	V_S (m/s)	G_0 (MPa)	M_{DMT} (MPa)	ν	G_{DMT} (MPa)	G_{DMT}/G_0	γ_{DMT} (%)	PI (%)
San Carlo	S3 CI3	9.5-9.6	Silty sand	181	64	54	0.2	20	0.32	0.07	-
San Carlo	S10 CI1	13-13.6	Silty clay	159	46	8	0.2	3	0.07	0.47	49
San Carlo	S2 CI2	7.3-7.4	Sandy silt	175	53	14	0.2	5	0.10	0.32	12-17
San Carlo	S11 CI1	2.0-2.6	Silty sand	205	75	23	0.2	9	0.11	0.13	-
San Carlo	S11 CI2	6.0-6.6	Silty sand	157	42	7	0.2	3	0.06	0.30	-
San Carlo	S11 CI3	9.0-9.6	Silty sand	170	53	14	0.2	5	0.10	0.12	-

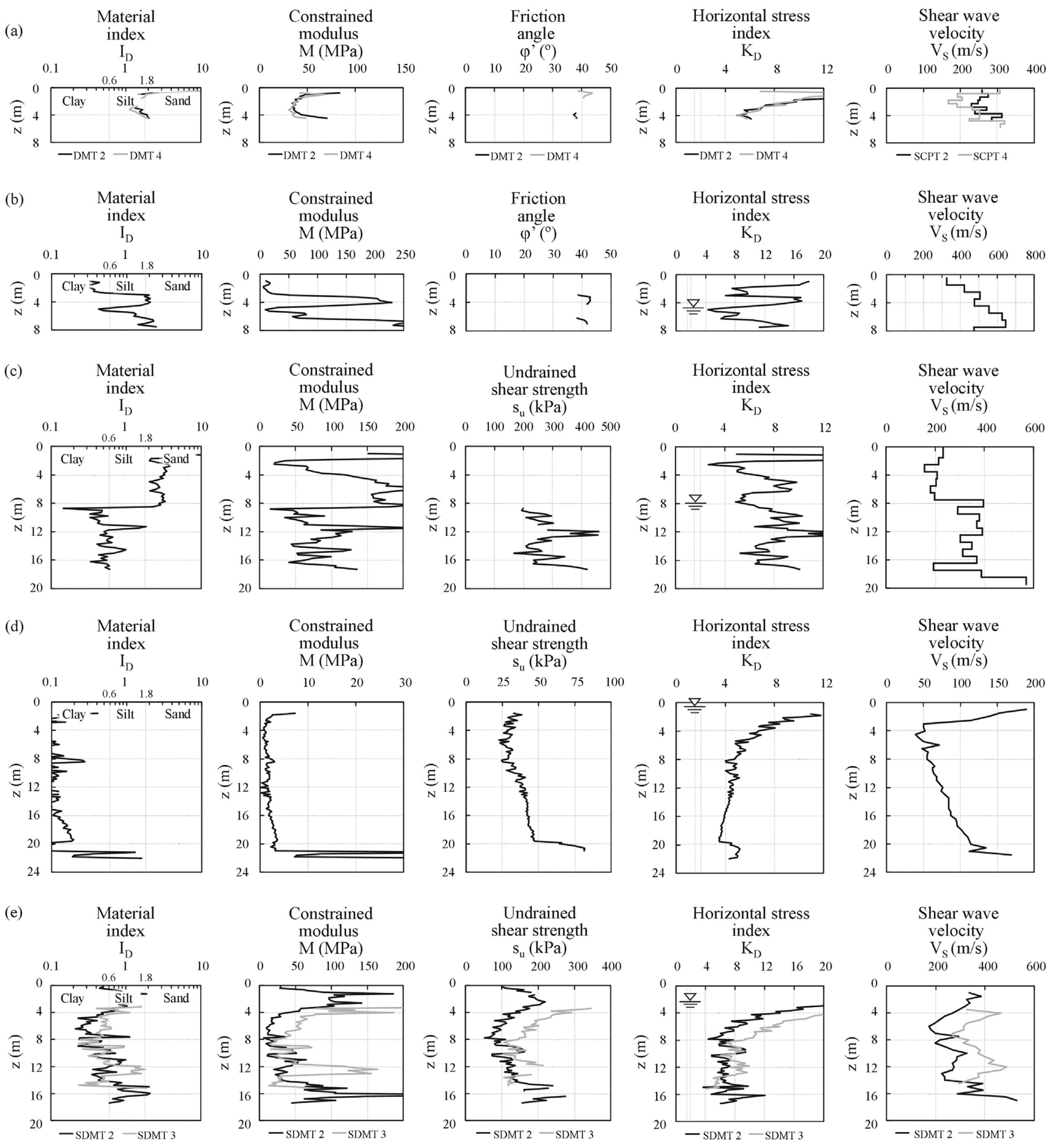

Figure 14 - DMT profiles and V_S profiles at different sites in Western Australia: (a) Shenton Park, (b) Ledge Point, (c) Perth CBD, (d) East Perth, (e) Margaret River (Amoroso, 2011).

of G_{DMT}/G_0 range from 0.10 to 0.20 in silica sand, 0.08 to 0.31 in calcareous sand, 0.09 to 0.30 in silty clay; see Table 4. The black and grey symbols in Figs. 15, 16 and 17 represent the position of the G_{DMT}/G_0 data points on the corresponding *in situ* reference G/G_0-γ decay curves. The range of values of the shear strain γ_{DMT} resulting from the "intersection" with the *in situ* G/G_0-γ curves (rectangular shaded areas in Figs. 15, 16 and 17), also reported in Table 4, are γ_{DMT} = 0.04-0.15% in sand and γ_{DMT} = 0.23-1.50% in silty clay.

The G/G_0-γ decay curves shown in Fig. 18 (East Perth, soft clay) and Fig. 19 (Margaret River, silty clay) were reconstructed by combining the information resulting

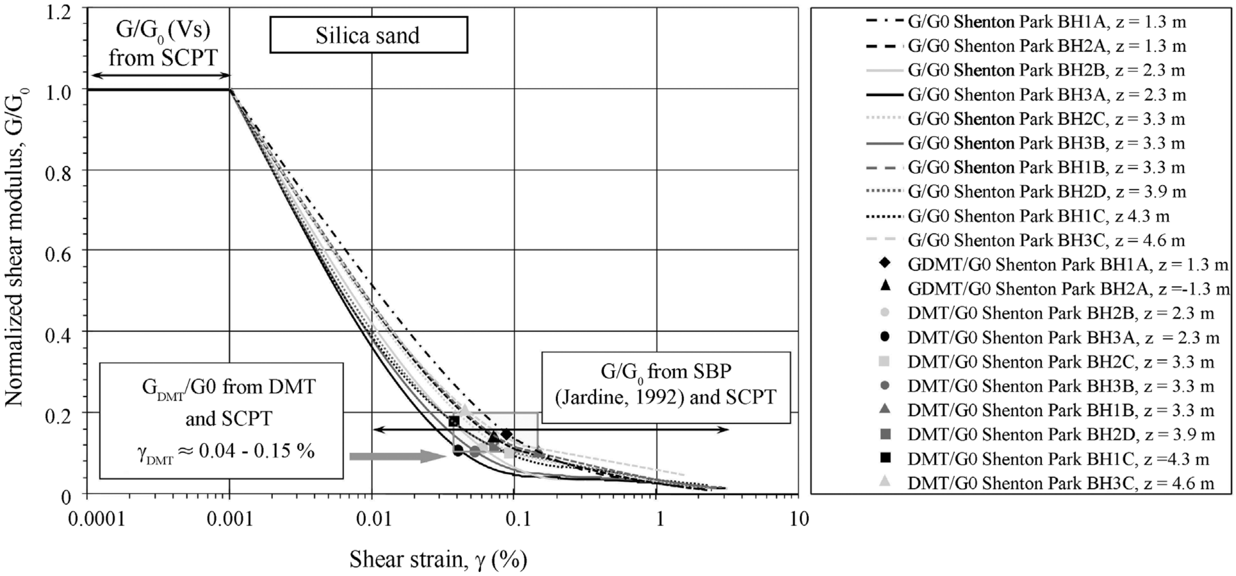

Figure 15 - *In situ* G/G_0-γ decay curves and superimposed G_{DMT}/G_0 data points at Shenton Park (silica sand), Western Australia (Amoroso *et al.*, 2012).

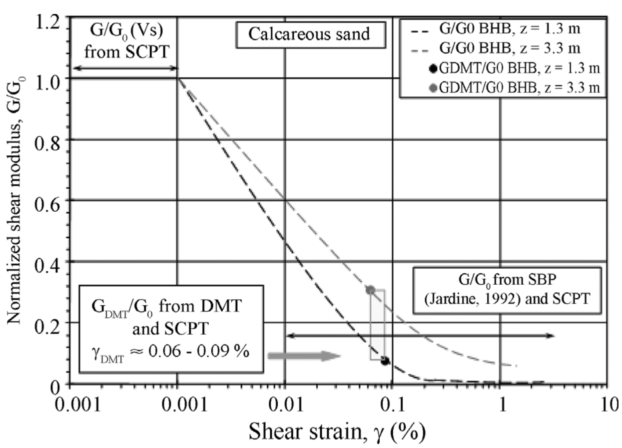

Figure 16 - *In situ* G/G_0-γ decay curves and superimposed G_{DMT}/G_0 data points at Ledge Point (calcareous sand), Western Australia (Amoroso *et al.*, 2012).

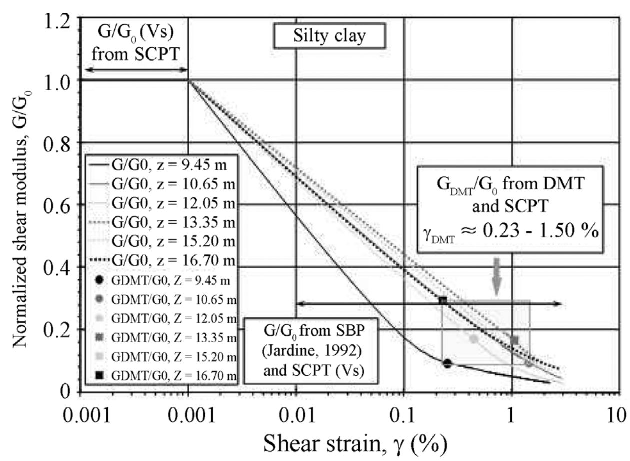

Figure 17 - *In situ* G/G_0-γ decay curves and superimposed G_{DMT}/G_0 data points at Perth CBD (silty clay), Western Australia (after Amoroso *et al.*, 2012).

from *in situ* SDMT and laboratory triaxial tests. In this case:

- the initial part of the curves (γ ≤ 0.001%) was characterized by G_0 derived from V_S measured by SDMT;
- the non-linear G/G_0-γ decay at medium to large shear strains (γ ≥ 0.1% at Margaret River, γ ≥ 0.5% at East Perth) was estimated from triaxial tests according to Atkinson (2000);
- the central part of the curves (0.001% > γ > 0.5% at East Perth, 0.001% > γ > 0.1% at Margaret River) was defined by simply connecting the initial part obtained from SDMT (G_0) and the final part obtained from triaxial tests.

The *working strain shear modulus* G_{DMT} was calculated from M_{DMT} obtained by SDMT at the same depths of the samples tested in the laboratory by use of Eq. 1, assuming ν = 0.2 at both sites. The values of G_{DMT}/G_0 vary from 0.04 in soft clay to 0.07 in silty clay; see Table 4. The values of the shear strain γ_{DMT} resulting from the "intersection" of the G_{DMT}/G_0 data points with the reconstructed reference G/G_0-γ decay curves (dot symbols in Figs. 18 and 19) are 5.5% in soft clay and vary from 0.23% to 1.50% in silty clay; see Table 4.

6. Discussion

6.1. Summary of results at various test sites

Over the past decades, numerous studies have been conducted regarding the dynamic soil properties and the

Table 4 - Western Australia - Values of G_{DMT}/G_0 obtained from SDMT (or DMT + SCPT) and corresponding shear strain γ_{DMT} determined from the intersection with the G/G_0 - γ reference curves at five test sites (Amoroso *et al.*, 2012).

Test site	Sample	Depth (m)	Soil type	V_S (m/s)	G_0 (MPa)	M_{DMT} (MPa)	ν	G_{DMT} (MPa)	G_{DMT}/G_0	γ_{DMT} (%)	PI (%)
Shenton Park	BH1A	1.3	Silica sand	252	105	42	0.2	16	0.15	0.09	-
Shenton Park	BH2A	1.3	Silica sand	252	105	40	0.2	15	0.14	0.07	-
Shenton Park	BH2B	2.3	Silica sand	267	118	35	0.2	13	0.11	0.06	-
Shenton Park	BH3A	2.3	Silica sand	267	118	33	0.2	12	0.11	0.04	-
Shenton Park	BH2C	3.3	Silica sand	280	129	36	0.2	14	0.11	0.15	-
Shenton Park	BH3B	3.3	Silica sand	280	129	36	0.2	13	0.10	0.09	-
Shenton Park	BH1B	3.3	Silica sand	280	129	35	0.2	13	0.10	0.05	-
Shenton Park	BH2D	3.9	Silica sand	282	132	42	0.2	16	0.12	0.07	-
Shenton Park	BH1C	4.3	Silica sand	283	132	63	0.2	23	0.17	0.04	-
Shenton Park	BH3C	4.6	Silica sand	283	132	72	0.2	27	0.20	0.05	-
Ledge Point	BHB	1.3	Calcareous sand	217	78	16	0.2	6	0.08	0.09	-
Ledge Point	BHB	3.3	Calcareous sand	361	215	176	0.2	76	0.31	0.06	-
Perth CBD	NML4	9.45	Silty clay	334	212	52	0.2	20	0.09	0.25	20
Perth CBD	NML4	10.65	Silty clay	373	264	67	0.2	25	0.10	1.45	20
Perth CBD	NML4	12.05	Silty clay	388	286	130	0.2	49	0.17	0.45	20
Perth CBD	NML4	13.35	Silty clay	319	193	86	0.2	32	0.17	1.05	20
Perth CBD	NML4	15.2	Silty clay	324	199	56	0.2	21	0.11	1.5	20
Perth CBD	NML4	16.7	Silty clay	260	128	101	0.2	38	0.30	0.23	20
East Perth	BH6	15.8-16.0	Soft clay	87	12	1.8	0.2	0.5	0.04	5.5	45-50
Margaret R.	BH3	6.0	Silty clay	174	55	13	0.2	4	0.07	1.75	43
Margaret R.	BH5	9.0	Silty clay	362	256	68	0.2	20	0.07	0.36	13

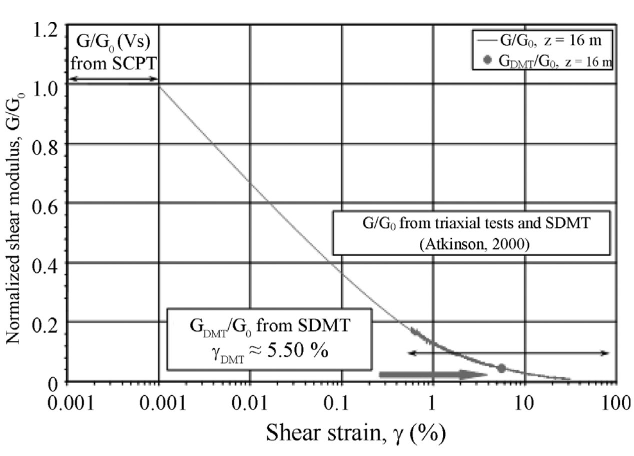

Figure 18 - *In situ* G/G_0-γ decay curves and superimposed G_{DMT}/G_0 data points at East Perth (soft clay), Western Australia (Amoroso *et al.*, 2012).

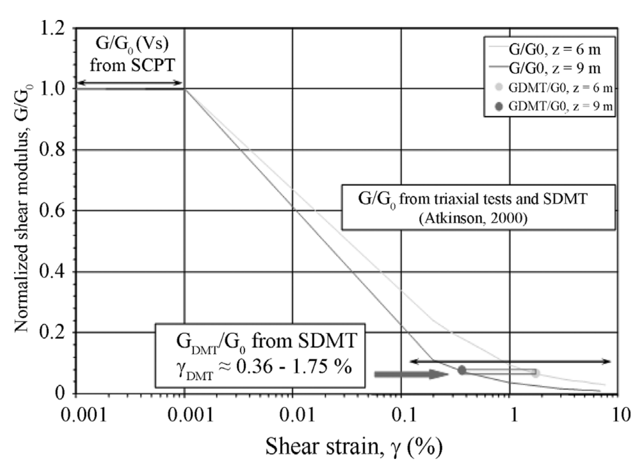

Figure 19 - *In situ* G/G_0-γ decay curves and superimposed G_{DMT}/G_0 data points at Margaret River (silty clay), Western Australia (Amoroso *et al.*, 2012).

parameters affecting them, such as the mean effective confining pressure, the soil type and the plasticity. Various investigators have proposed non linear curves for sands (for example Darendeli, 2001; Seed *et al.*, 1986; Iwasaki *et al.*, 1978; Kokusho, 1980), clays and silts with different plasticity (for example Darendeli 2001; Vucetic & Dobry, 1991; Sun *et al.*, 1988). Figure 20 summarizes the upper and lower ranges of these typical curves, obtained for different values of the mean effective confining pressure, assumed between 25 and 1600 kPa, and a plasticity index *PI* ranging between 0% and 100%. Figure 20 shows that the curves proposed by Darendeli (2001) including all the other reference curves.

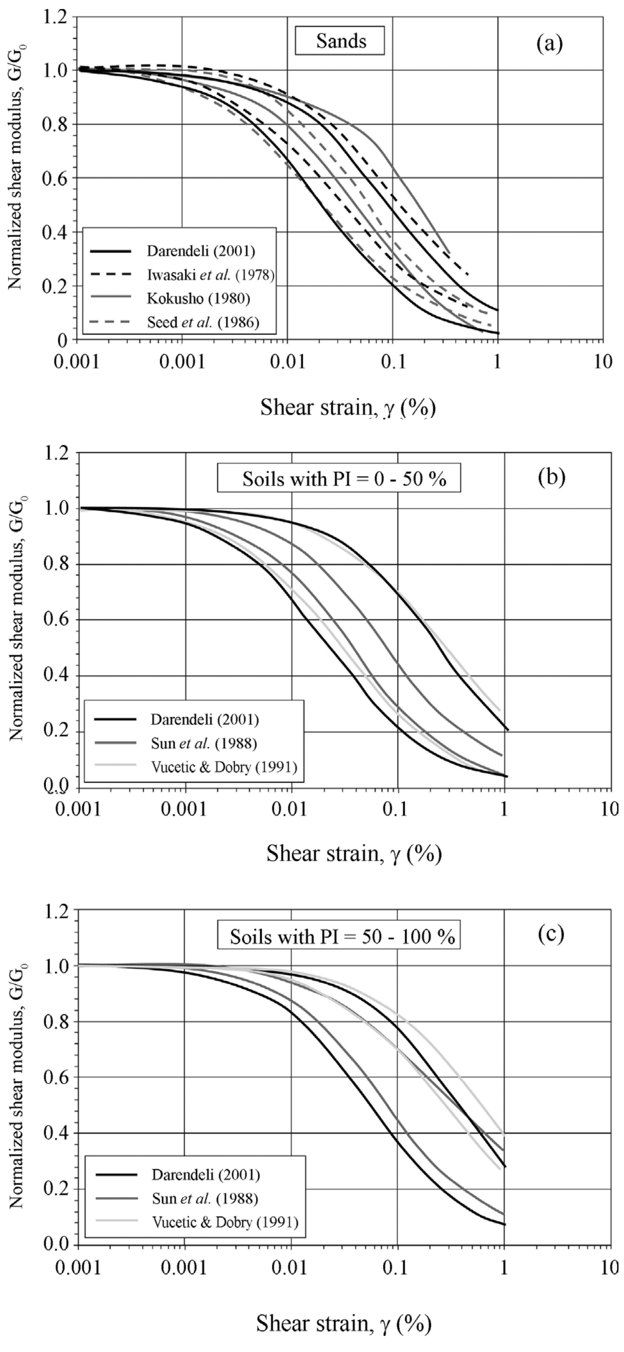

Figure 20 - Reference G/G_0-γ decay curves: (a) sands, (b) silts and clays with plasticity index *PI* = 0-50%, (c) silts and clays with plasticity index *PI* = 50-100%.

Figure 21 depicts the possible use of the SDMT for calibrating the selection of *in situ* G/G_0-γ decay curves in various soil types. The results obtained at all the test sites previously described were superimposed on the Darendeli (2001) G/G_0-γ stiffness decay curves. The rectangular shaded areas in Fig. 21 represent the range of values of the *normalized working strain shear modulus* G_{DMT}/G_0 determined in different soil types (sand, silt and clay) and the corresponding shear strain γ_{DMT} determined by the "intersection" procedure. Based on the available information, the "typical range" of shear strain associated to the working strain moduli G_{DMT} can be approximately assumed as: $\gamma_{DMT} \approx$ 0.01-0.45% in sand, $\gamma_{DMT} \approx$ 0.1-1.9% in silt and clay. In soft clay the values of $\gamma_{DMT} > 2\%$ (not shown in Fig. 21) are too high to attempt an interpolation using a reference stiffness decay curve.

These observations are in agreement with preliminary literature indications (Mayne, 2001; Ishihara, 2001). Moreover, the calculated values of the ratio G_{DMT}/G_0 - which could be regarded as the shear modulus decay factor at *working strains* - are in line with the trends observed by Marchetti *et al.* (2008), who investigated the experimental interrelationship between *small strain* and *working strain* stiffness using SDMT in sand, silt and clay. In particular, the diagrams of the ratio G_{DMT}/G_0 vs. the DMT horizontal stress index K_D (related to OCR) constructed by Marchetti *et al.* (2008) using the SDMT results at 34 different sites, in a variety of soil types, indicated that the *G* decay in sands is more significant at lower strains than in silts and clays, and that the decay curves in silts and clays are very similar.

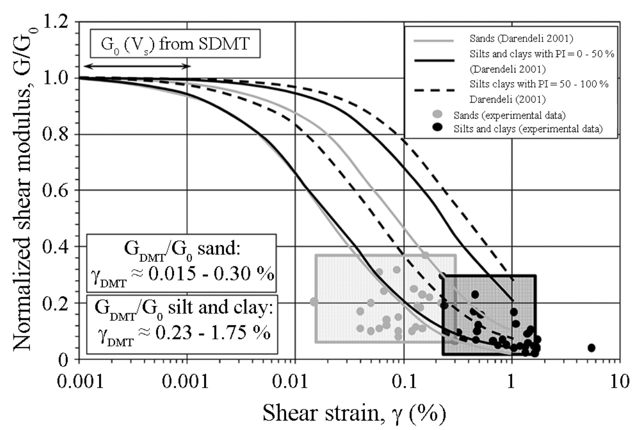

Figure 21 - Possible use of the SDMT for calibrating the selection of *in situ* G/G_0-γ decay curves in various soil types.

6.2. Proposed numerical G-γ decay curves from SDMT

Several authors (Hardin & Drnevich, 1972; Bellotti *et al.*, 1989; Byrne *et al.*, 1990; Fahey & Carter, 1993; Fahey, 1998) introduced a hyperbolic model to represent the non-linear stress-strain behaviour of soil in pressuremeter tests. In this respect, the SDMT experimental data determined at all the investigated test sites (Fig. 22) were used to assist the construction of a hyperbolic stress-strain equation (Eq. 8):

$$\frac{G}{G_0} = \frac{1}{1+\left(\dfrac{G_0}{G_{DMT}}-1\right)\dfrac{\gamma}{\gamma_{DMT}}} \tag{8}$$

Thus, the ratio G_{DMT}/G_0 obtained from SDMT and the estimated shear strain γ_{DMT} were used to plot the corresponding hyperbolic curve at each test site. In the examples shown in Fig. 23a (Shenton Park, sand) and 23b (Roio Piano, clayey silt), the curves obtained from SDMT, using Eq. 8 and the coupled values of G_{DMT}/G_0 - γ_{DMT} introduced in the tables (thick black lines in Figs. 23a and b), evidently provide a reasonable fit to the "measured" stiffness decay curves.

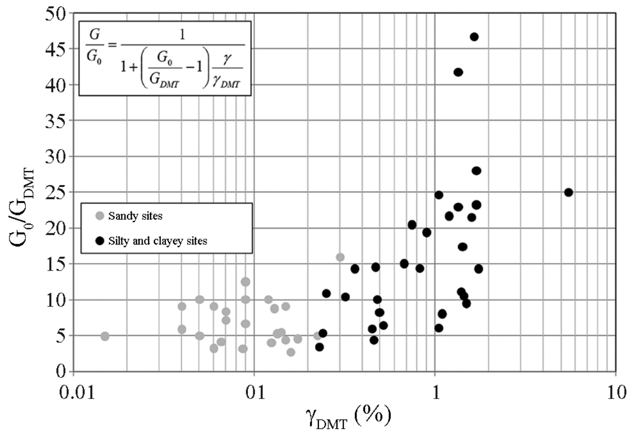

Figure 22 - SDMT experimental data used to assist the construction of a hyperbolic equation.

The estimated γ_{DMT} values for each case history examined are plotted on Fig. 23. It is apparent that γ_{DMT} values in clays are higher than those in sands; this trend is in keeping with that seen on Fig. 20. Combined with a measured G_{DMT}/G_0 value from the SDMT, Fig. 23 can be used in combination with Eq. 8 to provide a first order estimate of a given soil's elemental G vs γ curve. It is noted that hyper-

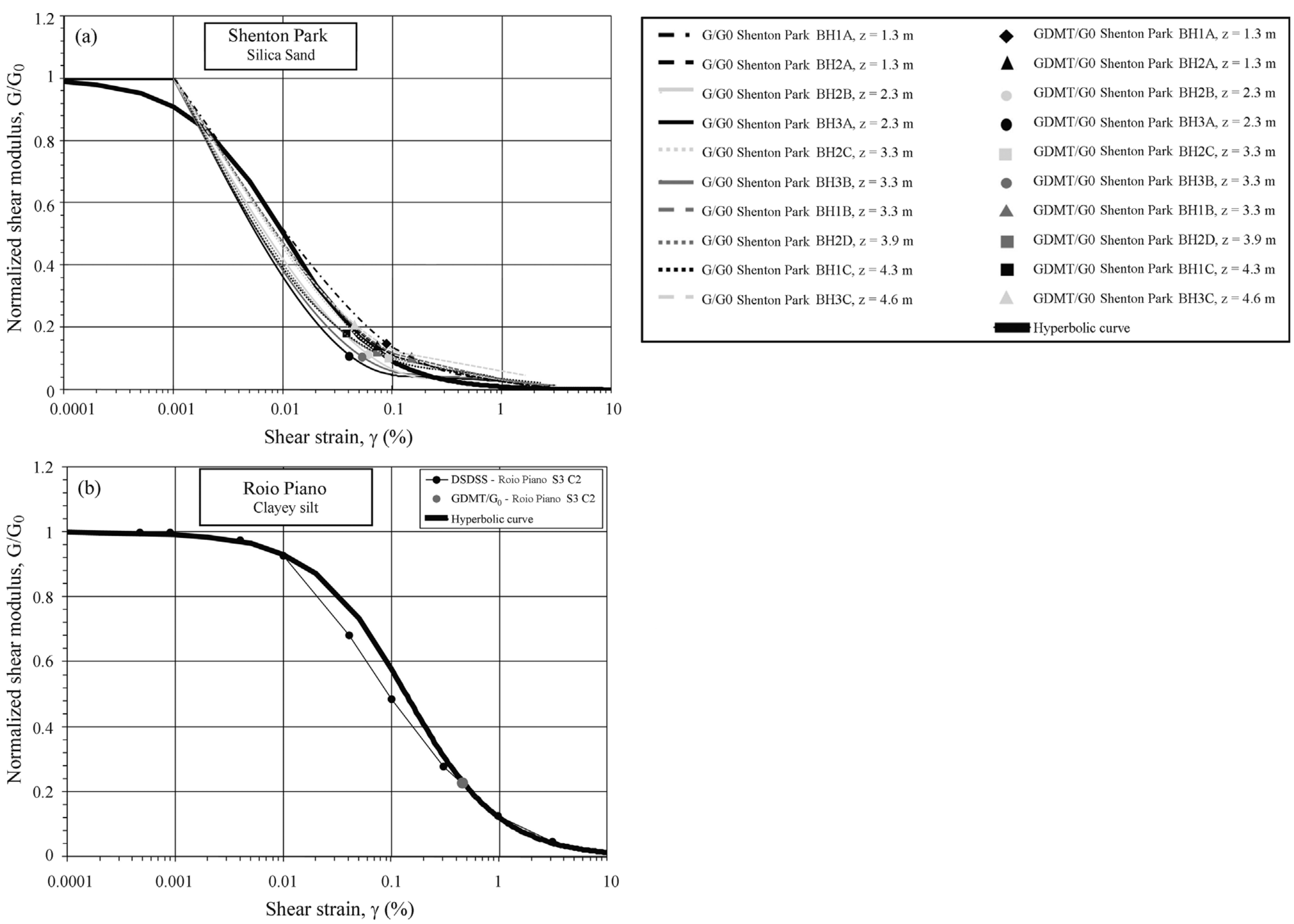

Figure 23 - Comparison between hyperbolic and "measured" stiffness decay curves at Shenton Park (a) and Roio Piano (b).

bolic G vs γ curves have been seen to be particularly relevant for dynamic/cyclic applications.

7. Conclusions

The results presented in this paper support the possible use of the SDMT to assess the decay of *in situ* stiffness with strain level and to address the selection of elemental G-γ curves in various soil types. This potential stems from the ability of the SDMT to provide routinely, at each test depth, both a *small strain* stiffness (G_0 from V_S) and a *working strain* stiffness G_{DMT} (derived via standard DMT correlations). "Reference typical-shape" laboratory G-γ curves may be tentatively fitted through these two stiffness values. A significant premise of this approach is that, to locate the second point on the G-γ curve, it is necessary to know (at least approximately) the shear strain γ_{DMT} corresponding to *working strain modulus* G_{DMT}.

Typical ranges of γ_{DMT} in different soil types have been inferred from the "intersection" of the SDMT data points with same-depth reference stiffness decay curves - back-figured from the observed field behavior under full-scale loading, or obtained by cyclic/dynamic laboratory tests or reconstructed by the combined use of different *in situ*/laboratory techniques - at various test sites.

Based on the available information, γ_{DMT} is typically about 0.1% in sand, about 0.5 to 1.0% in silt and clay and greater than 2% in soft clay. The proposed hyperbolic relationship, together with an estimate of γ_{DMT} from Fig. 21, can provide a useful first order estimate of a soil's G-γ degradation curve.

Acknowledgments

Special thanks to Prof. Silvano Marchetti for providing the initial ideas for this study, and for his precious and continuous suggestions to support this research. Special thanks also to Prof. Martin Fahey for offering his knowledge and experience to critically approach the present study.

References

Amoroso, S. (2011) G-γ decay curves by seismic dilatometer (SDMT). PhD Dissertation, Department of Structural, Water and Soil Engineering, University of L'Aquila, L'Aquila, 480 p.

Amoroso, S.; Monaco, P. & Marchetti, D. (2012) Use of the Seismic Dilatometer (SDMT) to estimate *in situ* G-γ decay curves in various soil types. Coutinho, R. & Mayne, P.W. (eds) Proc. 4th Int. Conf. on Geotechnical and Geophysical Site Characterization, ISC'4, Porto de Galinhas, Brazil, v. 1, p. 489-497.

Amoroso, S.; Totani, F.; Totani, G. & Monaco, P. (2015) Local seismic response in the Southern part of the historic centre of L'Aquila. Engineering Geology for Society and Territory - Urban Geology, Sustainable Planning and Landscape Exploitation, Springer International Publishing, v. 5:XVIII, p. 1097-1100.

Atkinson, J.H. (2000) Non-linear soil stiffness in routine design. Géotechnique, v. 50:5, p. 487-508.

Bellotti, R.; Ghionna, V.; Jamiolkowski, M.; Robertson, P.K. & Peterson, R.W. (1989) Interpretation of moduli from self-boring pressumeter tests in sand. Géotechnique, v. 39, p. 269-292.

Berardi, R. (1999) Non linear elastic approaches in foundation design. Jamiolkowski, M.; Lancellotta R. & Lo Presti D.C.F. (eds) Pre-Failure Deformation Characteristics in Geomaterials. Balkema, Rotterdam, p. 733-739.

Burghignoli, A.; Cavalera, L.; Chieppa, V.; Jamiolkowski, M.; Mancuso, C.; Marchetti, S.; Pane, V.; Paoliani, P.; Silvestri, F.; Vinale, F. & Vittori, E. (1991) Geotechnical characterization of Fucino clay. Proc. X ECSMFE, Firenze, v. 1, p. 27-40.

Byrne, P.M.; Salgado, F.M. & Howie, J.A. (1990) Relationship between the unload shear modulus from pressumeter tests and the maximum shear modulus for sands. Proc. 3rd International Symposium on Pressumeters, ISP3, Oxford, p. 231-241.

Cola, S. & Simonini, P. (2002) Mechanical behaviour of silty soils of the Venice lagoon as a function of their grading properties. Can. Geotech. J., v. 39:4, p. 879-893.

Darendeli, M.B. (2001) Development of a New Family of Normalized Modulus Reduction and Material Damping Curves. PhD Dissertation, University of Texas.

Elhakim, A.F. & Mayne, P.W. (2003) Derived stress-strain-strength of clays from seismic cone tests. Proc. 3rd Int. Symp. Deform. Charact. Geomaterials, Lyon, v. 1, p. 81-87.

Facciorusso, J.; Madiai, C. & Vannucchi, G. (2012) Risposta sismica locale e pericolosità sismica di liquefazione a San Carlo e Mirabello (FE). University of Florence, 3 October 2012 (in Italian), http://ambiente.regione.emilia-romagna.it/geologia/temi/sismica/liquefazione-gruppo-di-lavoro/RAPPORTO_RSL_LIQ_ott_2012_UNIFI.pdf/at_download/file/RAPPORTO_RSL_LIQ_ott_2012_UNIFI.pdf.

Fahey, M. & Carter, J.P. (1993) A finite element study of the pressuremeter test in sand using a non-linear elastic plastic model. Can. Geotech. J., v. 30, p. 348-362.

Fahey, M. (1998) Deformation and *in situ* stress measurement. Robertson P.K. & Mayne P.W. (eds) Proc. 1st Int. Conf. on Site Characterization, Atlanta, v. 1, p. 49-68.

Fahey, M.; Lehane, B.M. & Stewart, D. (2003) Soil stiffness for shallow foundation design in the Perth CBD. Australian Geomechanics, v. 38:3, p. 61-90.

Fahey M.; Schneider, J.A. & Lehane, B.M. (2007) Self-boring pressuremeter testing in Spearwood dune sands. Australian Geomechanics, v. 42:4, p. 57-71.

Fioravante, V.; Giretti, D.; Abate, G.; Aversa, S.; Boldini, D.; Capilleri, P.P.; Cavallaro, A.; Chamlagain, D.; Crespellani, T.; Dezi, F.; Facciorusso, J.; Ghinelli, A.; Grasso, S.; Lanzo, G.; Madiai, C.; Massimino, M.R.; Maugeri, M.; Pagliaroli, A.; Rainieri, C.; Tropeano, G.; Santucci De Magistris, F.; Sica, S.;Silvestri, F. & Vannucchi, G. (2013) Earthquake geotechnical engineering aspects of the 2012 Emilia-Romagna earthquake (Italy). Proc. 7th Int. Conf. on Case Histories in Geotechnical Engineering, Chicago, Paper No. EQ-5.

Gibbens, R.M. & Briaud, J.L. (1994a) Test and prediction results for five large spread footings on sand. Geotechnical Special Publication, ASCE, v. 41, p. 92-128.

Gibbens, R.M. & Briaud, J.L. (1994b) Data and prediction request for the spread footing prediction event (at the occasion of the ASCE Spec. Conf. Settlement ‘94). Geotechnical Special Publication, ASCE, v. 41, p. 11-85.

Gottardi, G. & Tonni, L. (2004) A comparative study of piezocone tests on the silty soils of the Venice lagoon (Treporti Test Site). Viana da Fonseca A. & Mayne P.W. (eds) Proc. 2nd International Conference on Site Characterization, Porto, v. 2, p. 1643-1649.

Hardin, B. O. & Drnevich, V. P. (1972) Shear modulus and damping in soils: design equations and curves. J. Soil Mech. and Found. Div., ASCE, v. 98:SM7, p. 667-692.

Hepton, P. (1988) Shear wave velocity measurements during penetration testing. Proc. Penetration Testing in the UK, ICE, p. 275-278.

Ishihara, K. (2001) Estimate of relative density from in-situ penetration tests. Rahardjo P.P. & Lunne T. (eds). Proc. Int. Conf. on *In Situ* Measurement of Soil Properties and Case Histories, Bali, p. 17-26.

Iwasaki, T.; Tatsuoka, F. & Takagi, Y. (1978) Shear moduli of sands under cyclic torsional shear loading. Soils and Foundations, v. 18:1, p. 39-56.

Jardine, R.J. (1992) Non-linear stiffness parameters from undrained pressuremeter tests. Can. Geotech. J., v. 29:3, p. 436-447.

Kokusho, T. (1980) Cyclic triaxial test of dynamic soil properties for wide strain range. Soils and Foundations, v. 20:2, p. 45-60.

Lehane, B.M. & Fahey, M. (2004) Using SCPT and DMT data for settlement prediction in sand. Viana da Fonseca A. & Mayne P.W. (eds) Proc. 2nd Int. Conf. on Site Characterization, Porto, v. 2, p. 1673-1679.

Lehane, B.M.; Mathew, G. & Stewart, D. (2007) A laboratory investigation of the upper horizons of the Perth/Guildford formation in Perth CBD. Australian Geomechanics, v. 42:3, p. 87-100.

Lehane, B.M. (2010) Shallow foundation performance in a calcareous sand. Proc 2nd Int. Symposium on Frontiers in Offshore Geotechnics, ISFOG-2, Perth, p. 427-432.

Marchetti, S. (1980) *In Situ* Tests by Flat Dilatometer. J. Geotech. Engrg. Div., ASCE, v. 106:GT3, p. 299-321.

Marchetti, S.; Monaco, P.; Totani, G. & Calabrese, M. (2001) The Flat Dilatometer Test (DMT) in Soil Investigations - A Report by the ISSMGE Committee TC16. Proc. 2nd Int. Conf. on the Flat Dilatometer, Washington D.C., p. 7-48.

Marchetti, S.; Monaco, P.; Calabrese, M. & Totani, G. (2004) DMT-predicted vs measured settlements under a full-scale instrumented embankment at Treporti (Venice, Italy). Viana da Fonseca A. & Mayne P.W. (eds) Proc. 2nd Int. Conf. on Site Characterization, Porto, v. 2, p. 1511-1518.

Marchetti, S.; Monaco, P.; Calabrese, M. & Totani, G. (2006) Comparison of moduli determined by DMT and backfigured from local strain measurements under a 40 m diameter circular test load in the Venice area. Failmezger R.A. & Anderson J.B. (eds) Proc. 2nd Int. Conf. on the Flat Dilatometer, Washington D.C., p. 220-230.

Marchetti, S.; Monaco, P.; Totani, G. & Marchetti, D. (2008) *In Situ* tests by seismic dilatometer (SDMT). Laier, J.E.; Crapps D.K. & Hussein M.H. (eds) From Research to Practice in Geotechnical Engineering. Geotechnical Special Publication, ASCE, v. 180, p. 292-311.

Martin, G.K. & Mayne, P.W. (1997) Seismic flat dilatometer tests in Connecticut Valley Varved clay. Geotech. Testing J., ASTM, v. 20:3, p. 357-361.

Martin, G.K. & Mayne, P.W. (1998) Seismic flat dilatometer in Piedmont residual soils. Robertson P.K. & Mayne P.W. (eds) Proc. 1st Int. Conf. on Site Characterization, Atlanta, v. 2, p. 837-843.

Mayne, P.W.; Schneider, J.A. & Martin, G.K. (1999) Small- and large-strain soil properties from seismic flat dilatometer tests. Jamiolkowski, M.; Lancellotta R. & Lo Presti D.C.F. (eds) Pre-failure Deformation Characteristics in Geomaterials. Balkema, Rotterdam, p. 419-427.

Mayne, P.W. (2001) Stress-strain-strength-flow parameters from enhanced in-situ tests. Rahardjo P.P. & Lunne T. (eds), Proc. Int. Conf. on *In Situ* Measurement of Soil Properties and Case Histories, Bali, p. 27-47.

Mayne, P.W. (2003) Class “A” footing response prediction from seismic cone tests. Proc. 3rd Int. Symp. Deform. Charact. Geomaterials, Lyon, v. 1, p. 883-888.

McGillivray, A. & Mayne, P.W. (2004) Seismic piezocone and seismic flat dilatometer tests at Treporti. Viana da Fonseca A. & Mayne P.W. (eds) Proc. 2nd Int. Conf. on Site Characterization, Porto, v. 2, p. 1695-1700.

Monaco, P.; Totani, G. & Calabrese, M. (2006) DMT-predicted vs observed settlements: a review of the available experience. Failmezger R.A. & Anderson J.B. (eds) Proc. 2nd Int. Conf. on the Flat Dilatometer, Washington D.C., p. 244-252.

Monaco, P.; Totani, G.; Barla, G.; Cavallaro, A.; Costanzo, A.; D’Onofrio, A.; Evangelista, L.; Foti, S.; Grasso, S.;

Lanzo, G.; Madiai, C.; Maraschini, M.; Marchetti, S.; Maugeri, M.; Pagliaroli, A.; Pallara, O.; Penna, A.; Saccenti, A.; Santucci de Magistris, F.; Scasserra, G.; Silvestri, F.; Simonelli, A.L.; Simoni, G.; Tommasi, P.; Vannucchi, G. & Verrucci, L. (2012) Geotechnical aspects of the L'Aquila earthquake. Sakr M.A. & Ansal A. (eds) Special Topics in Advances in Earthquake Geotechnical Engineering, Chapter 1. Springer Science+Business Media B.V.

Monaco, P.; Totani, G.; Amoroso, S.; Totani, F. & Marchetti, D. (2013) Site characterization by seismic dilatometer (SDMT) in the city of L'Aquila. Rivista Italiana di Geotecnica, v. XLVII:3, p. 8-22.

Monaco P.; Amoroso S.; Marchetti S.; Marchetti D.; Totani G.; Cola S. & Simonini P. (2014) Overconsolidation and Stiffness of Venice Lagoon Sands and Silts from SDMT and CPTU. J. Geotech. Geoenviron. Eng., ASCE, v. 140:1, p. 215-227.

Regione Emilia Romagna - Liquefaction Working Group (2012) Primo rapporto sugli effetti della liquefazione osservati a S. Carlo, frazione di S. Agostino (Provincia di Ferrara). 25 June 2012 (in Italian), http://ambiente.regione.emilia-romagna.it/geologia/temi/sismica/liquefazione-gruppo-di-lavoro/rapporto_sancarlo.pdf/at_download/file/rapporto_sancarlo.pdf.

Robertson, P.K. & Ferrera, R.S. (1993) Seismic and pressuremeter testing to determine soil modulus. Predictive soil mechanics, Wroth Memorial Symposium, p. 562-580.

Romeo, R. W.; Amoroso, S.; Facciorusso, J.; Lenti, L.; Madiai, C.; Martino, S.; Monaco, P.; Rinaldis, D. & Totani, F. (2015) Soil liquefaction during the Emilia, 2012 seismic sequence: investigation and analysis. Engineering Geology for Society and Territory - Urban Geology, Sustainable Planning and Landscape Exploitation, Springer International Publishing, v. 5:XVIII, p. 1107-1110.

Santucci de Magistris, F.; d'Onofrio, A.; Evangelista, L.; Foti, S.; Maraschini, M.; Monaco, P.; Amoroso, S.; Totani, G.; Lanzo G.; Pagliaroli, A.; Madiai, C.; Simoni, G. & Silvestri, F. (2013) Geotechnical characterization of the Aterno valley for site response analyses. Rivista Italiana di Geotecnica, v. XLVII:3, p. 23-43.

Schneider, J.A.; Fahey, M. & Lehane, B.M. (2008) Characterization of an unsaturated sand deposit by *in situ* testing. Proc. 3rd Int. Conf. on Site Characterization, p. 633-638.

Schneider, J.A. & Lehane, B.M. (2010) Evaluation of cone penetration test data from a calcareous sand dune. Proc. 2nd Int. Symp. on Penetration Testing, Huntington Beach, CA.

Seed, H.B.; Wong, R.T.; Idriss, I.M. & Tokimatsu, K. (1986) Moduli and damping factors for dynamic analyses of cohesionless soils. Journal of the Soil Mechanics and Foundations Division, ASCE, v. 112:SM11, p. 1016-1032.

Simonini, P. (2004) Characterization of the Venice lagoon silts from in-situ tests and the performance of a test embankment. Viana da Fonseca A. & Mayne P.W. (eds) Proc. 2nd Int. Conf. on Site Characterization, Porto, v. 1, p. 187-207.

Simonini, P.; Ricceri, G. & Cola, S. (2006) Geotechnical characterization and properties of the Venice lagoon heterogeneous silts. Proc. 2nd Int Workshop on Characterization and Engineering Properties of Natural Soils, Singapore, v. 4, p. 2289-2328.

Sun, J.I.; Golesorkhi, R. & Seed H.B. (1988) Dynamic Moduli and Damping Ratio for Cohesive Soils. Report, UCB/EERC-88/15, University of California at Berkley, 48 p.

Totani, G.; Totani, F.; Monaco, P.; Tallini, M.; Del Monaco, F. & Zia, G. (2012) Site investigations and geotechnical problems in the Southern part of the historic centre of L'Aquila. Maugeri M. & Soccodato C. (eds) Proc. 2nd Int. Conf. on Performance-Based Design in Earthquake Geotechnical Engineering, Taormina, Italy, Paper No. 2.13, p. 315-328 (CD-ROM).

Vucetic, M. & Dobry, R. (1991) Effect of soil plasticityon cyclic response. Journal of Geotechnical Engineering, ASCE, v. 120:7, p. 585-594.

Working Group S2-UR4 (2013) Analysis of the liquefaction phenomena in the area of San Carlo by seismic dilatometer (SDMT). Project S2-2012 INGV-DPC, Deliverable D8.1 - Annex 3, Rev. 1.1, Sept. 2013 https://docs.google.com/file/d/0B60wsWaPpDL4RVMzb01ETU8zT2s/edit?usp=sharing.

An Approach to Derive Strength Parameters of Residual Soils from DMT Results

N. Cruz, C. Rodrigues, A. Viana da Fonseca

Abstract. Residual soils show a specific mechanical behaviour classified as non-conventional when compared with sedimentary transported soils, since the presence of a cemented matrix plays an important role on their strength and stiffness. Moreover, suction is frequent in natural profiles, which in residual soils creates several problems on the interpretation of *in-situ* test results. These two factors, cementation and suction, are contributing simultaneously as structuring factors. Correlations to deduce strength parameters in Portuguese granitic residual soils by Marchetti Dilatometer were previously established under a data base obtained in careful triaxial testing programs executed on "undisturbed" samples. However, the reference results were affected by sampling disturbance and space variability, and therefore somehow deviated from *in-situ* conditions. To solve these problems, a large calibration box was constructed to work with artificially cemented soils where DMT blades could be pre-installed and pushed-in. Water level, suction and seismic velocities were monitored during the experiment and a triaxial program was established in parallel on the same artificially cemented mixtures. As a result, specific correlations to derive the cohesion intercept value and the angle of shearing resistance in saturated and unsaturated conditions were developed and subsequently tested in a well characterized experimental site. Herein, the results of that experimental framework are presented and discussed.

Keywords: residual soils, Portuguese granitic formations, cohesion intercept, angle of shearing resistance, suction, *in-situ* characterization, DMT.

1. Introduction

Residual soils strength characterization is not an easy task to estimate from *in situ* tests, due to its cohesive-frictional nature (Viana da Fonseca & Coutinho, 2008). Having two components - friction and cohesion - a strength will have to be evaluated from laboratory triaxial tests over undisturbed samples, since the evaluation of strength through *in situ* tests is usually conveyed under pure frictional granular soils, under the bias of angle of shearing resistance (frictional and dilatant components) or under Tresca type shear strength when geomaterials are analysed in total stresses, as it is the case of undrained shear strength in clayey soils, or the maximum total shear strength in very hard soils and soft rocks. This will be approximate to the concept of "cohesive" soils, where the strength is mostly a property explicitly non-frictional.

In the case of residual soils, cohesive strength is related with the inter-particular bonding inherited from the parent rock that provided the cemented structure and with the contribution of suction, when this is present. On the other hand, the angle of shearing resistance comprises two portions, as stated above. One is related with the pure friction that is mobilized during the relative movement between the particles. The other concerning the resistance that is mobilized during this relative movement, required to destroy the natural inter-particular cementation and its spatial organization, that is, its fabric. It should be stressed that due to the usually low void ratio of these materials typically there is an increase in volume (positive dilatancy) during shear.

The most straightforward way to characterize this type of strength is through triaxial tests, but the process has to face the important disadvantage related with sampling disturbance (Ferreira *et al.*, 2011), where the partial loss of cementation structure is mostly unavoidable. The referred sampling disturbance and the discontinuous information related to laboratory tests leave an important role to *in-situ* tests on residual soil characterization for routine analysis, especially those that induce small disturbance during installation and allow the direct estimation of stress-strain response (Viana da Fonseca *et al.*, 2011), such as pressuremeters (self-boring pressuremeter, SBPT, in a first degree and, as a fair compromise, Ménard pressuremeter, PMT) and dilatometers (such as Marchetti Flat Dilatometer, DMT). Seismic tests may give relevant interpretation when associated to the more simple tools (seismic dilatometer SDMT, seismic piezocone SCPTu), as they give a reference value of the small strain shear modulus ($G_0 = \rho.V_s^2$). Some important works modelling *in-situ* tests in residual soils have been undergoing, such as the new cavity expansion model that incorporates the effects of structure and its degradation (Mantaras & Schnaid, 2002; Schnaid & Man-

Nuno Bravo de Faria Cruz, PhD, Department of Geology and Geotechnics, MOTA-ENGIL / University of Aveiro, Vila Nova de Gaia, Portugal. e-mail: nbdfcruz@gmail.com.
Carlos Manuel Gonçalves Rodrigues, PhD, Coordinator Professor, Department of Civil Engineering, Polytechnic Institute of Guarda, Guarda, Portugal. e-mail: crod@ipg.pt.
António Joaquim Pereira Viana da Fonseca, PhD, Associate Professor, Department of Civil Engineering, University of Porto, Porto, Portugal. e-mail: viana@fe.up.pt.
Submitted on March 20, 2014; Final Acceptance on December 15, 2014; Discussion open until April 30, 2015.

taras, 2003), the extension of the cavity expansion theory to unsaturated soils (Schnaid & Coutinho, 2005) and the overall fitting Self-Boring Pressuremeter pressure-expansion curve (Fahey & Randolph, 1984; Viana da Fonseca & Coutinho, 2008; Topa Gomes *et al.*, 2008; Topa Gomes, 2009). Viana da Fonseca (1996) had also highlighted the utility of plate load tests, by performing series of tests with different plate sizes allowing the determination of strength parameters (c' and ϕ') by multiple optimization of the results, although this procedure is time-consuming and the limitation of involving very superficial horizons makes it less attractive.

2. DMT Tests in Residual Soils

DMT tests can be seen as a combination of some features of both CPT/CPTu and PMT tests with some details that really make it a very interesting technique available in modern geotechnical characterization. The fundamental advantages of the test are related with the high level of precision measuring both the pressures and the displacements, the response supported by semi-spherical expansion theories, the quasi-continuous profiles that provide a reasonable amount of data adequate for statistical analysis, the numerical identification of soil type, the deduction of intermediate parameters that represent common geotechnical features (namely deformability and stress history) and its easy combination with any type of *in-situ* and laboratory tests.

In its essence, dilatometer is a stainless steel flat blade (14 mm thick, 95 mm wide and 220 mm length) with a flexible steel membrane (60 mm in diameter) on one of its faces. The equipment is pushed (or driven) into the ground, by means of a CPT rig or similar, and an expansion of the membrane is conventionally performed every 20 cm depth. At each depth, the penetration is stopped and the membrane is expanded to lift-off the diaphragm (reading A, corresponding to a deflection of 0.05 mm), followed by a deflection of 1.10 mm (reading B). After this expansion sequence an additional pressure, designated by "C-reading" (closing pressure), may be taken by slowly deflating the membrane soon after the B position is reached until the membrane comes back to the 0.05 mm position (A position). These pressures must then be corrected by the values ΔA and ΔB, determined by calibration, to take into account the membrane stiffness and thus converted into the three basic pressures p_0, p_1 and p_2. Four intermediate parameters are deduced from these basic test parameters, namely Material Index (I_D), Dilatometer Modulus (E_D), Horizontal Stress Index (K_D) and Pore Pressure Index (U_D), having some recognizable physical meaning and some engineering usefulness (Marchetti, 1980), as discussed below. Current geotechnical soil parameters are obtained from these intermediate parameters (and not directly from the basic p_0, p_1 and p_2 parameters), independently or combined together, covering a wide range of possibilities.

The I_D parameter is one key parameter for DMT interpretations, due to its ability to identify soils throughout a numerical value, which can be easily introduced in specific formulae for deriving geotechnical parameters. Although I_D is not a result of a sieve analysis but just a mechanical behaviour parameter (a kind of rigidity index) from which soil stratigraphy is deduced (Marchetti, 1997), the numerical result representing soil types undoubtedly offers a lot of extra possibilities to develop constitutive laws to be applied to wide ranges of different soils, with particular emphasis to Intermediate Geomaterials (IGM).

The horizontal stress index (Marchetti, 1980) was defined to be related to the at rest earth pressure coefficient, K_0, and thus its determination is obtained by the effective lift-off pressure (p_0 - u_0, where u_0 is the equilibrium pore pressure) normalized by the *in-situ* effective vertical stress. The parameter can be regarded as a K_0 amplified by penetration, with normally consolidated (NC) deposits with no ageing and/or cementation structure represented by the value $K_D \approx 2$ (in clays) (Marchetti, 1980). Furthermore, the typical K_D profile is very similar in shape to the OCR profile giving useful information not only about stress history but also on the presence of cementation structures (Cruz *et al.*, 2004a; Cruz 2010). In general the evolution of K_D profiles follows some typical trends, (Marchetti, 1980):

a) K_D profiles tend to follow the classical shape of the OCR profile;
b) Normally-consolidated (NC) soils tend to present values of K_D around 2;
c) Over-consolidated (OC) soils show values of K_D above 2, decreasing with depth and converging to NC values;
d) Normally consolidated soils affected by cementation or ageing structures show values of K_D higher than 2, remaining fairly stable with depth.

The theory of elasticity is used to derive the dilatometer modulus, E_D (Marchetti, 1980), by considering that membrane expansion into the surrounding soil can be associated to the loading of a flexible circular area of an elastic half-space, from which the outward movement of the membrane centre under a normal pressure variation, $\Delta p = p_1 - p_0$, can be calculated. Considering the characteristics of the test, the dilatometer modulus is represented by the equation:

$$E_d = \frac{E}{1-\nu^2} = 34.7\Delta p \quad (1)$$

where E represents the Young's modulus and represents the Poisson's ratio.

At last, the pore pressure index, U_D, (Lutenegger & Kabir, 1988) is related to pore pressure condition, which is quite similar to B_q of CPTu tests.

DMT tests have been mostly used in sedimentary soils, where the test has shown his remarkable usefulness in estimating stress history, strength and stiffness characteristics in soft/loose to medium soils. However, the application of the test to residual soils characterization is still beginning, mostly within research programs. In general practice, is rather common to see applying correlations developed for sedimentary to residual soils characterization, which frequently leads to erroneous interpretations. In the case of Portuguese residual sandy soils, the angle of shearing resistance is clearly overestimated because it incorporates the cohesive component of strength due to cementation, while this (cohesive) parcel cannot be calculated since is not considered in sedimentary approaches for the test interpretations. Since at least two basic parameters (p_0 and p_1) are obtained, DMT offers a good via to separate cohesive from friction/dilatancy components.

Previous research using DMT alone or combined with CPTu tests in residual soil characterization (Cruz, 1995; Cruz *et al.*, 1997, 2004a, b; Cruz & Viana da Fonseca, 2006a, 2006b) has shown that the test could be efficiently used to derive strength parameters of residual soils from Porto Granites. Firstly, Cruz *et al.* (1997) based their hypotheses on two well documented cases (Cruz, 1995; Viana da Fonseca, 1996) following the proposal from Marchetti (1980) from which K_D may be a well adapted index parameter for detecting cementation and quantify its magnitude. The results showed that typical profiles were more or less stable with depth, within 5-7 interval, indicating cementation or ageing according to Marchetti's (1980) initial statements. However, the correlation with the values of the cohesive intercept obtained from triaxial testing in undisturbed samples revealed poor sensitivity of the parameter to be used with success. This is certainly related to the fact that K_D depends only on p_0, which is the parameter more affected by the blade penetration, so mostly associated to the horizontal stress state, more than natural interparticle cementation.

A second step was attempted by Cruz *et al.* (2004b) and Cruz & Viana da Fonseca (2006a), based on the OCR parameter derived from DMT. In fact, OCR correlates strongly with the range between p_0 and p_1 and is an amplification of K_D, thus bringing more sensitivity to small variations of cohesive intercept. Although the concept of overconsolidation does not have a meaning in residual soils and is very questionable in the case of sandy soils, the presence of a naturally cemented structure gives rise to some aspects of the mechanical behaviour, similar to those observed in overconsolidated clays, as it is sustained by Leroueil & Vaughan (1990). In short, the behaviour of a cohesive-frictional soil will show an important variation in the stress-strain behaviour when the cementation bonds start to break, which will be very similar to the response of overconsolidated soils, although with quite distinct pattern of the relative values of void ratios, namely under the classical critical state approaches (Viana da Fonseca *et al.*, 2011). In the case of cohesive-frictional materials, the pre-consolidation stress as defined in sedimentary clays would be directly associated to the magnitude of the cohesive component of strength related mainly to interparticle cementation and/or suction, but also to some contribution to dilatancy. For this reason, the concept is usually designated as "virtual", vOCR (Viana da Fonseca, 1996), or "apparent" overconsolidation, AOCR (Mayne, 2006), since it does not represent a pre-consolidation stress as in the true OCR, but only the strength arising from structural interparticle cementation. Having in mind that residual soils from Porto Granite are mostly sandy silts to silty sands, OCR derived from DMT in granular sedimentary soils (Marchetti & Crapps, 1981) was selected as reference parameter for correlation with the cohesive intercept in Mohr-Coulomb strength criteria. In parallel, the ratio between constrained modulus (M_{DMT}) and CPTu corrected tip resistance (q_t) was also studied as an index parameter, because it is also related to overconsolidation ratio in sandy soils (Baldi *et al.*, 1988; Jendeby, 1992) and could work as a control parameter of OCR derived from DMT. Based on a large quantity of *in-situ* information collected in Porto Granite Formation (40 boreholes with regular Standard Penetration Tests SPT, 36 DMT, 22 CPTu, 4 PMT, 5 Dynamic Probing Super-Heavy tests DPSH), specific correlations were proposed to deduce the effective cohesion intercept from vOCR and M_{DMT}/q_t. The obtained data clearly demonstrated parallel trends followed by both indexes and a similar good level of accuracy of the respective correlations to deduce cohesive component of strength (Cruz *et al.*, 2004a; Cruz & Viana da Fonseca, 2006a). Since they are independent evaluations, this convergence seems to confirm the adequacy of the proposed approach.

The presence of a cemented structure also creates a serious obstacle to derive angles of shearing resistance from *in-situ* tests (SPT, CPTu, PMT and, of course, DMT) when sedimentary soil correlations are used, because they were developed on the principle of a (unique) granular strength (Viana da Fonseca, 1996; Cruz *et al.*, 2004a; Cruz & Viana da Fonseca, 2006a; Viana da Fonseca *et al.*, 2009; Cruz, 2010). Resistance in cemented soils is then "assumed" in the same way as in granular materials, that is high values of strength associated to higher values of the angle of shearing resistance (peak value) incorporating the frictional component of a critical state value, plus dilatancy. In short, cohesive component of strength is "transformed" in an "equivalent" additional value on the angle of shearing resistance and once the cohesive intercept is obtained, it is reasonable to expect that it can be used to correct the over-estimation of that angle, derived from sedimentary correlations. Considering the low influence that sampling has on the evaluation of angle of shearing resistance (Viana da Fonseca, 2003), the observed difference between calculated φ_{DMT} (which represents the global strength) and $\varphi_{triaxial}$ (which represents solely the friction plus dilatants value) should correlate with the magnitude of cohesion, that is with vOCR (Cruz & Viana da Fonseca, 2006a).

Although the proposed correlations were established with careful triaxial testing programs, the results of reference cohesion were obviously affected in an unknown extent by sampling disturbance and space variability, and therefore the reference values used to define these correlations would be deviated from "*in-situ*" real conditions (Cruz *et al.*, 2004a; Cruz, 2010).

3. Experimental Framework

As a consequence of the effects of sampling on the derived correlations referred in the previous section, it became fundamental to develop an experimental programme in controlled conditions that could avoid those effects to settle more definitive correlations. To do so, a special large dimension container with diverse measuring systems (CemSoil Box) was created in order to work with large artificially cemented samples where DMT blades could be installed, remoulded in the same conditions as those that would be tested in triaxial apparatus. Moreover, it was also decided to pre-install blades, aiming to evaluate the static penetration influence in the loss of cementation strength, and the overall effects on stiffness. The whole experience (Cruz, 2010) relied on residual soils from Guarda Granitic Formation, characterized by patterns of behaviour identical to those observed in Porto Granite Formation (Viana da Fonseca, 1996, 2003), where the previous research (Cruz *et al.*, 2004a; Cruz & Viana da Fonseca, 2006a) had been performed. The natural spot from where the soil was collected is located in a very well characterized experimental site (Rodrigues, 2003), investigated by laboratory triaxial tests (within the same ranges of confining stresses and void ratios of the present experiment) and *in-situ* CPTu, PMT and DMT tests.

Four different compositions of soil-cement mixtures and one uncemented were prepared to be tested in CemSoil, followed by an exhaustive laboratory program, including uniaxial, tensile and triaxial testing at low to medium confining stresses, performed on samples prepared in the same conditions of CemSoil. As a consequence of these dispositions, it was possible to create comparable controlled conditions, namely in curing times, compaction procedures, final unit weights and void ratios. Therefore, the sampling problems were avoided and the effects of DMT blade insertion on naturally cemented residual soils could be reproduced and studied, aiming to correct the empirical correlations previously proposed by Cruz *et al.* (2004b). In summary, the most relevant issues considered in the preparation of the experiment were the following:

a) Artificially remoulded samples were used in the present experiment avoiding problems associated to sampling damage, by eliminating this dispersion factor;

b) CemSoil and triaxial samples had the same curing times, void ratios (or unit weights) and cementation levels when tested, thus space variability and microfabric differences were tentatively minimized;

c) Since CemSoil samples were prepared in one time with the water being introduced only after curing, then observed differences in strength above and below water level should be mainly due to suction effects;

d) The testing sequences in Cemsoil box were controlled by using piezometers, tensiometers and geophones for seismic wave velocities measurements;

e) The experiment was based in DMT measurements both in pre-installed and pushed-in blades, which allowed to compare the influence of its penetration.

3.1. Laboratory calibration program

As previously referred, four different compositions of soil-cement mixtures and one uncemented were prepared to be tested in CemSoil Box and in an exhaustive laboratory program. This program included uniaxial and diametral compressive tests performed in saturated and unsaturated conditions, as well as isotropically consolidated drained (CID) triaxial testing at low to medium confining stresses (25, 50, 75 and 300 kPa), in saturated conditions. On the whole, the laboratory program included 40 unconfined, diametral and triaxial compressive tests. Figure 1 illustrates some details of triaxial testing system.

a) b) c)

Figure 1 - Triaxial testing: a) Artificially cemented sample; b) LVDT installation; c) Test apparatus.

The mixtures were moulded to represent the geotechnical units existing in Porto and Guarda Granites, corresponding to identical ranges of uniaxial and tensile strengths, both of them used as cementation reference indexes. This indexation was supported by the extensive data collected for Porto Geotechnical Map (COBA, 2003) from which a global study on the mechanical degradation with weathering of Porto Granites was made (Cruz, 2010). Guarda Granites geotechnical information (Rodrigues, 2003) was compared and fitted within that data base.

Two types of cement have been used, namely SECIL CIM I/52.5R (Mixtures 1 and 3, corresponding respectively to 1% and 2% of cement) and CIMPOR CIM II/B-L 32.5N (Mixtures 2 and 4 corresponding respectively to 2% and 3% of cement). Detailed discussion about this combined use can be found in Cruz (2010), but it should be mentioned that the whole research program was based in considering exactly the same curing time for each pair of samples (laboratory and the corresponding CemSoil samples). Compressive and tensile strength were used for indexation, instead the percentage of cement. Therefore, as far as the accuracy of these index parameters and the similarity of CemSoil and laboratory samples were ensured, the combination of the both cement types could be considered acceptable.

3.2. CemSoil box

CemSoil box (Fig. 2) is a container (Large box) with 1.5 m height steel box with a square cross section of 1.0 m^2, with 3 mm thick steel walls, reinforced by metal bars placed at 1/3 and 2/3 of its height. Each panel was fixed to the adjacent with a profile of 5 screws (10 mm) with 150 mm of influence radius. Due to the panel-to-panel fixation system, in two of the faces this reinforcement system was in contact with the wall by a central 7 mm thick H beam (100 x 50 mm^2) placed vertically. This system aimed to reduce horizontal displacements during compaction processes. The inner surfaces (vertical walls) and bottom surface of the cell were covered with a plastic film, in contact with the steel wall, followed by 15 mm Styrofoam plates in order to create a smooth and flexible transition between the soil and the external border.

Figure 3 shows a plan view and a vertical cross-section of CemSoil box with the distribution of installed equipment. CemSoil block samples (1.0 x 1.0 x 1.5 m^3) were compacted in homogeneous layers of 70-80 mm, aiming to create homogeneous samples, with similar void ratios in CemSoil and triaxial testing, thus creating comparable conditions. The compaction in CemSoil box was handmade, using a round wood hammer of 40 cm diameter.

Considering the main objectives of the experiment, two DMT blades were positioned during the compaction processes, one being placed 20 cm above CemSoil base level and the other 25 cm below the surface upper level of the soil. Furthermore, since residual soils are commonly affected by suction phenomena, which clearly affect their strength and stiffness behaviour and mislead the interpretation of *in-situ* test results, block samples were only partially saturated to have the chance of studying the influence of suction on DMT results. For this purpose, two open tube PVC piezometers were installed, one located nearby the water entry in CemSoil and another in the opposite corner, which allowed to control the water level and its stabilization during the main experiment. To evaluate the generated suction profile, six tensiometers were placed at different locations in Cemsoil box. Finally, three pairs of geophones to evaluate compression (V_p) and shear (V_s) wave velocities were placed vertically and horizontally (Almeida *et al.*, 2012), respectively for suction and low energy seismic vibrational wave velocities determinations. Figure 4 illustrates this monitoring system.

The location and distribution of all these measuring tools within CemSoil box was chosen with reference to some available published works on the subject, namely those that studied the influence of DMT dimensions by

a) b)

Figure 2 - CemSoil Box: a) CemSoil sample ready for testing; b) View after testing.

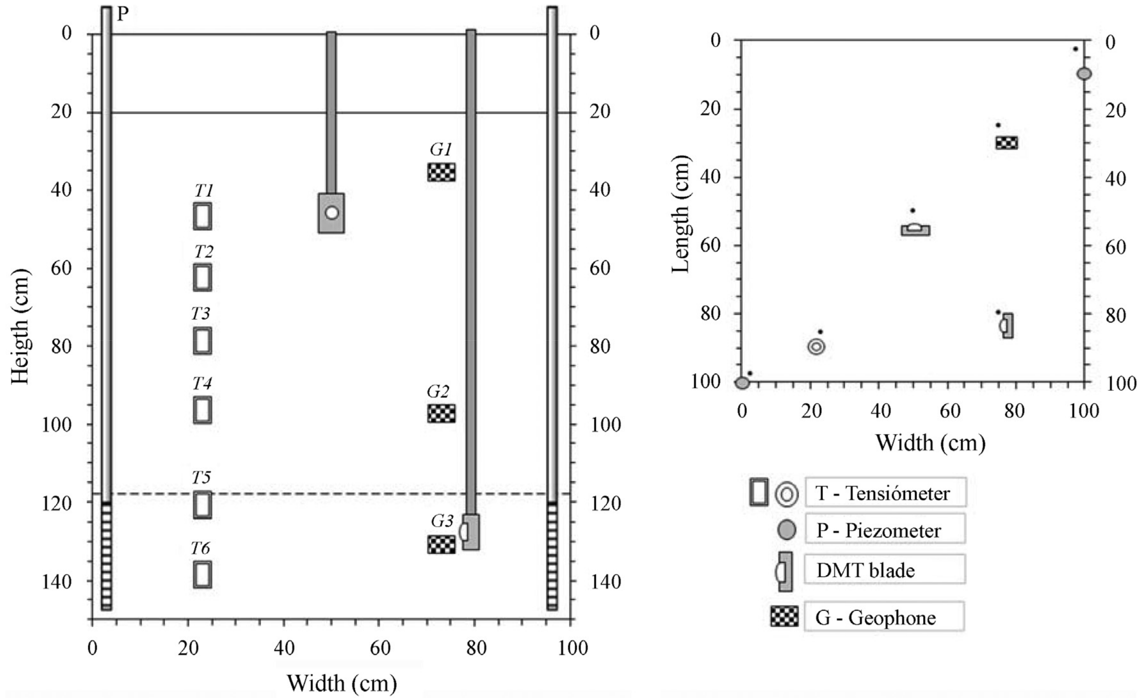

Figure 3 - Vertical cross section and plan view of Cemsoil instrumentation.

a) b)

Figure 4 - Testing devices: a) Tensiometers b) Geophones.

strain path analysis (Huang, 1989; Finno, 1993; Whittle & Aubeny, 1992) or flat cavity expansion analysis (Yu *et al.*, 1993; Smith & Houlsby, 1995). Numerical modelling of the penetration phase, using the strain path analysis (Whittle & Aubeny, 1992), pointed out some useful indications about the soil volume that may be influenced by the dilatometer insertion, which were considered in accordance.

The experiment with DMT in CemSoil box included pre-installed and pushed-in blades to analyse the effects of penetration on the final results. However, pushed-in tests were performed only in the destructured non-cemented sample and in Mixture 1 and Mixture 2, since due to its high resistance it was impossible to penetrate the equipment in the remaining mixtures. In all samples, regular measurements of suction pressures and seismic wave velocities were obtained during curing periods, before and after the saturation phase, which was concluded two days before each test. Finally, at each pre-selected testing day, DMT expansion tests of the first (below water level) and second (above water level) installed blades were made. After these tests, the second testing sequence with the blade being pushed-in down to the first blade depth was executed (details in Cruz, 2010). The respective results were then compared with triaxial test results in terms of strength and stiffness parameters, from where the correlations based in DMT parameters were developed.

4. Discussion of Results

4.1. Laboratory strength evaluation

Table 1 presents a summary of laboratory results obtained both in naturally and artificially cemented samples, indexed by the N_{SPT} (SPT blow count) ranges found in Porto and Guarda natural geotechnical units. These ranges were settled by considering the comparable ranges of uniaxial and tensile strengths found in Porto Geotechnical Map (COBA, 2003).

The reference strength parameters (*c*', φ') were obtained through CID triaxial testing, following the Mohr-Coulomb strength criterion, assuming the failure as corresponding to the maximum of the stress ratio *q*/*p*' (where q is the deviator stress and p' is the mean effective stress) mobilized during shear. The obtained failure envelopes in the artificially cemented mixtures and destructured uncemented samples are represented in Fig. 5, which clearly shows the non-linearity of the envelope, more evident with increasing cementation levels. As so, the envelopes deviate from the theoretical Mohr-Coulomb model, which assumes linearity between normal and shear stresses in the failure plane.

The aforementioned deviation should be understood as a consequence of complex phenomena that rules the shear strength mobilization in this type of cohesive-frictional materials. In fact, in order to allow the relative movement of particles, fabric interlocking creates an extra resistance during shear that commonly generates a volume increase (positive dilatancy), as a result of the usually medium to low void ratios of these soils. The higher is the interlocking, the higher will be the strength arising from this effect. On the other hand, although the ratio between friction forces that are mobilized in the surface of the particles and the installed normal forces is linear, the required forces to overcome interlocking vary with the magnitude of normal forces, which aggravates the non-linearity of failure envelope. Figure 6 gives a closer look of the relationships between dilatancy ($d = \delta\varepsilon_v/\delta\varepsilon_s$, where $\delta\varepsilon_v$ is the increment of volumetric strain and $\delta\varepsilon_s$ is increment of shear strain) and stress ratio, ($\eta = q/p'$) for the conventional drained tests. In order to simplify the analysis only some of the obtained results are plotted, namely the uncemented, the weakest (Mix 1) and the strongest cemented (Mix 4) samples, subjected to lower and higher confining stresses (p'_0 = 25 kPa and p'_0 = 300 kPa, respectively). The results show that for the uncemented sample the relationship *d*;*q*/*p*' is essentially linear, showing that the mobilized resistance is eminently frictional, while in cemented materials the increment of effective confining stress leads to a decreasing dilatancy and generates a higher punctual friction between particles as a result of the normal stress increase. Figure 6a reveals that there is a volume increase in shearing, being the strain levels related with maximum stress ratio (*q*/*p*') and maximum dilatancy very close.

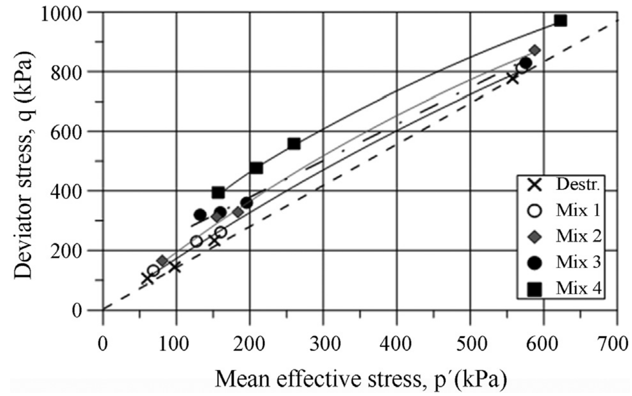

Figure 5 - Failure envelopes from triaxial tests performed in artificially cemented soils and natural de-structured soils.

Another characteristic highlighted by Fig. 6 is that the cementation structure is increasingly degraded with increasing confining stresses. In fact, the stress-dilatancy behaviour of Mix 4 (25 kPa) reveals a first part with an increasing volume reduction up to the coordinates [*d* = 0.7; *q*/*p*' = 0.9], which might be related with the readjustment to the initial conditions of the test. From this point on, the evolution is almost vertical up to the coordinates [*d* = 0.82; *q*/*p*' = 2.1], meaning that dilatancy remains fairly constant and corresponds to an elastic response of the soil. This suggests that cementation opposes to the volume increase. With the stress evolution, the cemented structure starts to

Table 1 - Laboratory test results related with CemSoil samples.

Strength	Naturally cemented	Destructured non-cemented	Mixture 1	Mixture 2	Mixture 3	Mixture 4
Ranges of N_{SPT} (blows/30 cm)	10-30	-	10-30	30-60	> 60 (ISRM W_5)	
Uniaxial compressive strength, q_u (kPa)	81.3	20.8	72.6	124.9	273.0	312.3
Diametral compressive strength, q_d (kPa)	12.3	1.5	7.2	15.3	33.2	39.4
Cohesion, *c*' (kPa)*	37.1	0.0	23.8	38.4	63.2	107.7
Angle of shearing resistance, φ' (°)*	34.0	35.0	33.0	34.0	30.0	30.0

*Results obtained in triaxial compression tests in saturated samples, cured in the same conditions of the set of tests, both in laboratory and in CemSoil box.

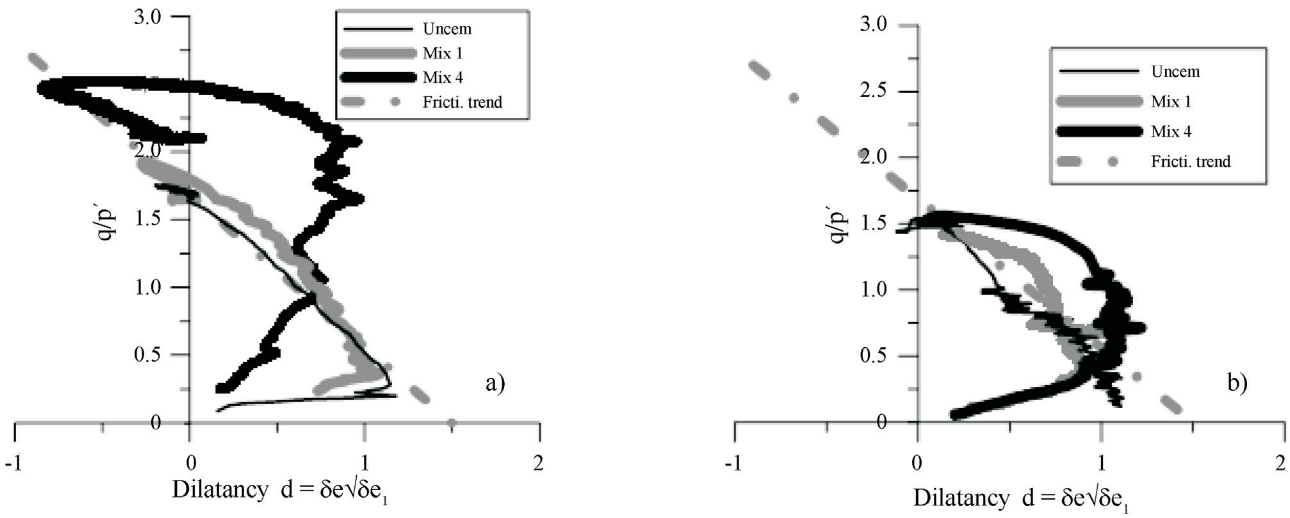

Figure 6 - Stress ratio dilation relation for uncemented and cemented samples subject to a confining effective stress of: a) 25 kPa, b) 300 kPa.

break generating a yield (Second yield, according to Coop & Willson, 2003) followed by a rapid evolution towards maximum dilatancy (close to peak resistance), when generalized failure occurs (Gross yield, according to Coop & Willson, 2003). This means that for the maximum stress ratio (assumed as the failure criterion) the strength resulting from cementation is already significantly affected. After peak strength, there is a decrease on dilatancy rates of evolution that follows the strength decrease towards the critical state (constant resistance with null dilatancy). The same sample (Mix 4), when subjected to higher confining stresses (300 kPa), shows a smoother pattern of variation with no signs of volume increase, evolving directly to critical state after generalized bond breakage. This may be related with the previous partial bond breakage during consolidation phase and also by the higher stress restraining the volume increase. Therefore, strain levels related to peak strength increase with effective confining stress, which will probably generate higher level of destructuration. The behaviour of the less cemented sample (Mix 1) is located within the behaviours of uncemented and more cemented sample (Mix 4). In conclusion, as the cementation level decreases, the stress-dilatancy behaviour approaches linearity revealing loss of importance of the cement portion.

From the practical point of view, which is at the base of the present research, this complex behaviour creates serious difficulties to establish a simple way to get mechanical parameters of these residual soils for design. Firstly, because design of foundations or retaining walls and slope stability analysis usually are based on limit equilibrium models that depend on the Mohr-Coulomb strength criterion, where the dilatancy is not an input parameter. In such case, to estimate the Mohr-Coulomb strength parameters (c', φ') it is necessary to linearize the failure envelope. For this purpose, when wide stress fields are considered the deviations will certainly be relevant, generating an overestimation of cohesive intercept for high mean stresses and the overestimation of angles of shearing resistance in the opposite situation. However, if the stress field in the characterization programme is somewhere close to those of the geotechnical problem under study, then the deviations will have small consequences on the final results.

On the other hand, the strength contributions differentiated by cohesion, dilatancy and friction, would be very difficult to get from DMT tests, as in any other geotechnical tests used in routine analysis. In such case, triaxial and DMT results could not be easily compared, since cohesion and friction incorporate the dilatancy contributions in the case of DMT, while in the triaxial case that influence could be identified independently (Viana da Fonseca *et al.*, 2014). As a consequence, and for simplicity, it was assumed to select comparable situations in the correlations definition, meaning that triaxial testing results were expressed in terms of a cohesive and a frictional contribution, which incorporate the influence of dilatancy and the effect of bonding that is still present when the maximum strength is mobilized. In other words, the strength parameters obtained by DMT tests from the correlations arising from this work can be directly applied in a Mohr-Coulomb based analysis, without losing the distinct contributions of the cohesive and frictional/dilatant strength that really will be present in the field.

4.2. DMT test results

4.2.1. Basic and intermediate parameters

From the basic pressures point of view, the comparison of pushed-in and pre-installed blades showed that penetration generates different disturbance consequences in non-cemented and cemented soils. In fact, in non-cemented soils the basic DMT parameters (p_0 and p_1) are higher in the case of pushed-in tests, revealing a somehow expected effect of densification around the blade, especially on the membrane where measurements are made. On the other hand, in cemented soil mixtures the same insertion procedure reduces the values of pressures monitored during the tests by local destructuration or interparticle debonding. Accordingly, under pushed-in conditions, p_0 and p_1 increase with cementing level (Fig. 7), confirming the previously mentioned sensitivity of DMT to cementation (Cruz *et al.*, 2004a). As a consequence of these trends, the intermediate parameters E_D and K_D increase with cementation, while I_D remains essentially the same (Cruz, 2010).

Aiming at an effective control of the experiment with external reference, DMT tests were also performed in the same spot of natural residual soils from where the soil was collected and remoulded. The obtained results revealed that local DMT basic and intermediate parameters were situated between those obtained in Mixtures 1 and 2, which is coherent with the results of uniaxial, diametral and triaxial (cohesive) strengths previously presented in Table 1.

4.2.2. The influence of suction on DMT parameters

The results obtained in unsaturated conditions revealed an increment of the global strength and stiffness, which must be related to the presence of suction. In fact, when unsaturated results are normalized in relation to pushed-in saturated values (Fig. 8), here designated by p_1*, E_D*, I_D*, K_D*, a decrease of the magnitude of each normalized parameter when approaching the water level is observed suggesting an adequate sensitivity of DMT to detect

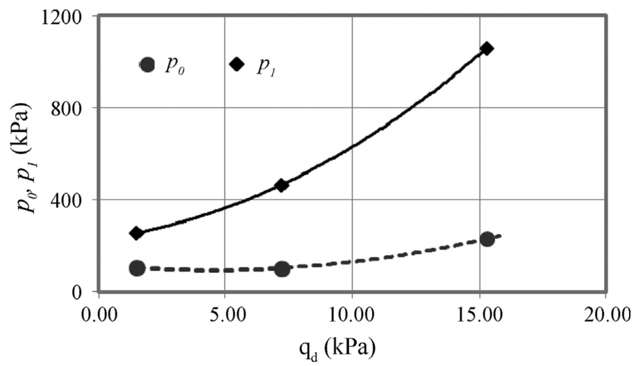

Figure 7 - Variation of DMT basic parameters with diametral compressive strength (q_d), in pushed-in conditions.

the effect of suction, somehow expected since DMT pressures are directly measured.

This conclusion is confirmed also by the non-cemented sample results in unsaturated conditions, considering that in this case the results should reflect suction alone. Data also reveal a decay of K_D and E_D with increasing cementation, apart from suction influence, which is explained by the clear increase of cohesion intercept, while suction remains essentially the same. Therefore, these results clearly put in evidence the high sensitivity of DMT to both suction and cementation in the cohesive component of strength.

A different behaviour is followed by I_D, revealing to be mostly independent from saturation levels in cemented soils, while in non-cemented samples suction influences notoriously the magnitude of the parameter. This is in accordance with recent evidences of such behaviour, pub-

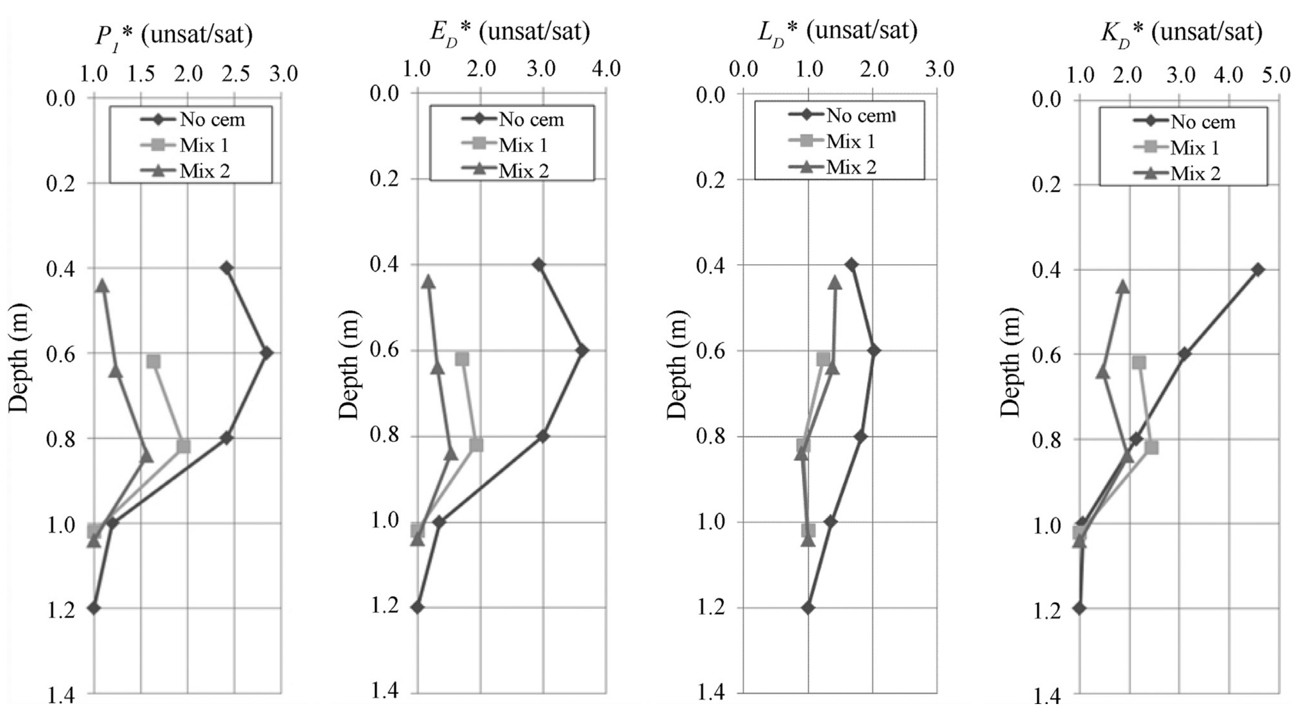

Figure 8 - Normalized (unsaturated/saturated) DMT parameters obtained in pushed-in conditions.

lished in Arroyo *et al.* (2013). In saturated conditions, the evaluation of soil type was found very accurate when compared with elemental soil classifications based on the percentage of clay, silt and sand, while unit weights obtained through I_D and E_D (Marchetti & Crapps, 1981) were confirmed by laboratory determinations on good quality extracted samples. Since the homogeneity in the large prototype (CemSoil) was carefully assessed, and differences between triaxial and CemSoil samples were minimized by the careful correspondence in the preparation of both void, moisture and cementation conditions, the above considerations strongly suggest that DMT is adequate to infer the cohesion components arising from suction and cementation, even after the blade penetration.

4.2.3. The virtual overconsolidation ratio (vOCR) and global cohesion (c'_g)

As previously stated by Cruz *et al.* (2004a) and Cruz & Viana da Fonseca (2006a), the DMT key parameter for evaluating the cohesive strength is the virtual overconsolidation ratio (vOCR) that represents the order of magnitude at which the stress-strain behaviour changes, expressed by the enlargement of yield locus due to cementation structure. The determination of vOCR follows the same formulations proposed by Marchetti & Crapps (1981) for sedimentary soils, as follows:

$$I_D < 1.2 \text{ (cohesive soils) } \mathrm{OCR} = (0.5\,K_D)^{1.56} \tag{2}$$

$$I_D > 2 \text{ (sandy soils) } \mathrm{OCR} = (0.67\,K_D)^{1.91} \tag{3}$$

$$1.2 < I_D < 2 \text{ (mixed soils) } \mathrm{OCR} = (m\,K_D)^n \tag{4}$$

where

$$m = 0.5 + 0.17\,P \tag{5}$$

$$n = 1.56 + 0.35\,P \tag{6}$$

with

$$P = (I_D - 1.2)/0.8 \tag{7}$$

The considerations presented in the previous subchapter revealed that above the water level the magnitude of the DMT intermediate parameters is clearly influenced by suction, and so will be vOCR. Considering the homogeneity and similarity of the triaxial and CemSoil samples, triaxial cohesion intercept can be assumed as representative of the whole sample moulded in CemSoil. Therefore the increase in the results obtained above the water level should be interpreted as a consequence of suction. If that is accepted, a global cohesive component (c'_g) due to both interparticular bonding and suction (when the latter is present), should be the reference parameter to correlate with DMT results.

The suction measurements taken during the CemSoil experiment make possible evaluating suction contribution to shear strength, from the third term in the model proposed by Fredlund *et al.* (1978):

$$\tau = c' + (\sigma - u_a)\tan\varphi' + (u_a - u_w)\tan\varphi^b \tag{8}$$

where u_a is the atmospheric pressure, u_w is the pore water pressure and φ^b is the "angle" of increase of cohesion with suction (similar to the concept of angle of shearing resistance in its dependence on stress).

The term $(u_a - u_w)$ corresponds to the suction measured on tensiometers, while for φ^b, a 14° reference value was obtained by Topa Gomes (2009) in Porto highly weathered granites (W_4 to W_5) and in the residual soil of ISC'2-CEFEUP (Arroyo *et al.*, 2013), which was assumed in this analysis given the similarity of Guarda and Porto granites, in what concerns to mineralogy, grain size distribution, plasticity and solids unit weight.

Expressing the global cohesion (c'_g) results as function of vOCR, a specific correlation to derive the global cohesive intercept is obtained, as presented in Eq. 9 and in Fig. 9. In this figure, the previous correlation presented by Cruz *et al.* (2004a) based on triaxial testing is also represented.

$$c'_g = 7.716\ln(\mathrm{vOCR}) + 2.9639 \tag{9}$$

It is important to note that the previous correlation was based on a narrower band of vOCR values and it was defined as a straight line, while the new data are better represented by a logarithmic function. Considering this new approach, the former data were incorporated and a new match fundamental function was defined. As it would be expected, the effect of sampling processes usually leads to a reduction of cohesion intercept, with an extent that seems to be dependent on the most appropriate equipment and convenient procedures. In this case, the differences between correlations lead to a general loss (mainly related to sampling) of around one third (1/3). For future interpretations, the previous correlations were based on statically pushed-in 70 mm Shelby tube samples.

Since the parameter φ^b is not usually available, thus it has to be estimated, it is important to analyse their influence on the final results. Taking into account the usual values for

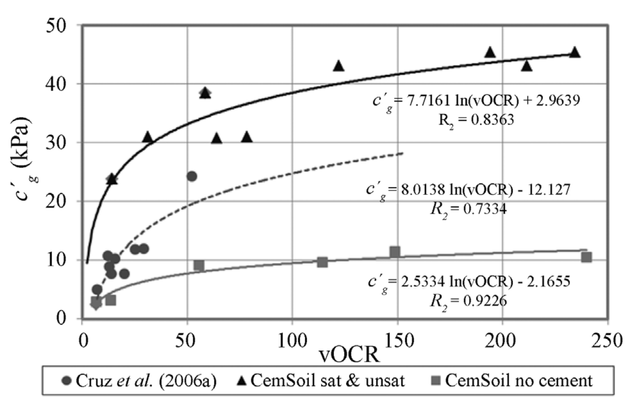

Figure 9 - Correlations of global cohesion intercept (c'_g) as a function of vOCR.

this parameter in the studies developed in Porto granite residual soils, as those reported in Topa Gomes *et al.* (2008), and in other international reference works (Futai, 1999), a variation of 5° around the considered value was found to be sufficient. Observed deviations resulting from variations of φ^b within 10° and 20° are insignificant, as shown in Fig. 10.

The evolution of the global cohesion intercept, c'_g, in CemSoil and *in-situ* test results obtained from direct application of the proposed correlation is presented in Figs. 11a and 11b, respectively. Figure 11a reveals once more the same trends observed in all other analysed parameters, with *in-situ* values falling between Mixtures 1 and 2, while the *in-situ* profile (Fig. 11b) shows a general decrease of the overall cohesion intercept until the water level is reached, remaining fairly constant after that depth with slightly lower values than those obtained in triaxial testing. It is also worth to note the convergence with the c'_g profile represented in the same figure, obtained by considering a theoretical linear evolution of suction as a function of the distance from the water level.

4.2.4. Corrected angle of shear resistance

Angles of shearing resistance in these residual soils can be derived by the approach proposed by Marchetti (1997) for sedimentary sandy soils, applying a correction factor that should be function of the result of cohesion intercept or the index DMT parameter used in cohesion correlation (vOCR), as proposed by Cruz *et al.* (2004a) and Cruz & Viana da Fonseca (2006a). The correlation for correcting the angle of shearing resistance, derived from the available data in the course of this framework, is presented in Fig. 12, where φ_{dmt} represents the angle of shearing resistance obtained from the correlations applied to sedimentary soils and φ_{ref} is the reference angle of shearing resistance obtained by triaxial tests on remoulded conditions. As a consequence, the corrected angle of shearing resistance (φ_{corr}) derived from DMT can be obtained as follows:

$$\varphi_{corr} = \varphi_{dmt} - 3.3483 \ln(OCR) + 5.4367 \qquad (10)$$

Using this correction, the CemSoil box (pushed-in tests) and *in-situ* test results are compared with the respective triaxial data, revealing a good reproduction of the experimental results. Figure 13 shows that CemSoil saturated results converge well with triaxial tests, while *in-situ* data slightly decrease with depth due to suction effects.

4.3. Procedure to evaluate strength parameters

As a consequence of this calibration work, it was possible to propose a procedure (Fig. 14), to derive strength parameters of Porto and Guarda granitic residual soils from DMT data. Its application in other granitic environments should be verified, although the authors believe that this method may be generalized in other granitic residual sapro-

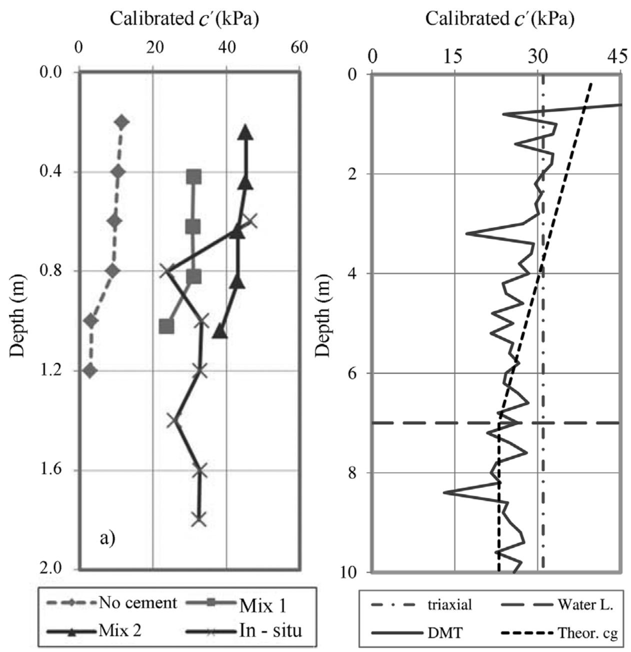

Figure 11 - Global cohesion intercept (c'_g) results in: a) Cemsoil; b) *In-situ*.

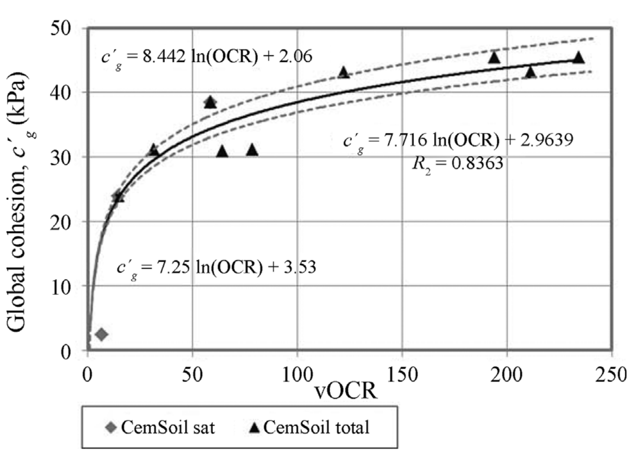

Figure 10 - Upper and lower expected limits for the cohesive intercept (c'_g) correlations.

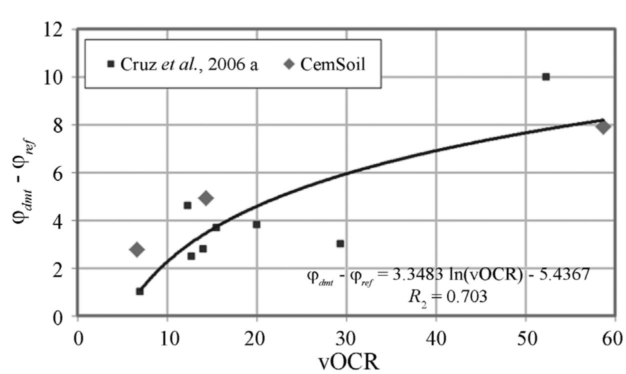

Figure 12 - Correction factor for evaluating angle of shearing resistance.

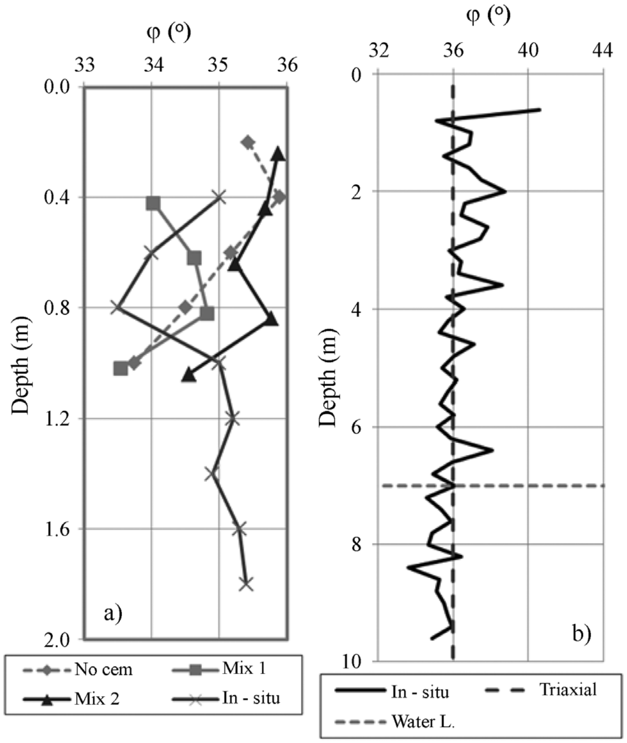

Figure 13 - Triaxial and deduced angles of shearing resistance in: a) Cemsoil; b) *In-situ*.

litic soils. For applications in other residual geomaterials (as for instance, in lateritic soils) with different genesis or different mineralogical/chemical compositions, specific correlations should be calibrated by tentatively using the same procedure followed in this work.

The procedure to get the parameters from DMT tests starts with the evaluation of global cohesion through the correspondent correlation. If the conditions are saturated, then the result represents both global and true cohesion, since suction is null. In the case of unsaturated conditions, the global cohesion incorporates both contributions and so suction related parameters (u_a - u_w, φ^b) are required for respective differentiation. An alternative way that may be helpful, when values of these parameters (measured or estimated) are not available, is to consider the mean value of cohesion obtained in the first results below water level ($c'_{(avg\ below)}$) as representative of the soil cohesion above water level. Considering this approach, it becomes possible to evaluate suction by subtracting the value of $c'_{(avg\ below)}$ from the value of the global cohesion (c'_g). Finally, the corrected angles of shearing resistance (φ_{corr}) are obtained by subtracting the correction factor (Fig. 12, in previous sub-section) to the angles of friction obtained by traditional sedimentary approach (φ_{DMT}).

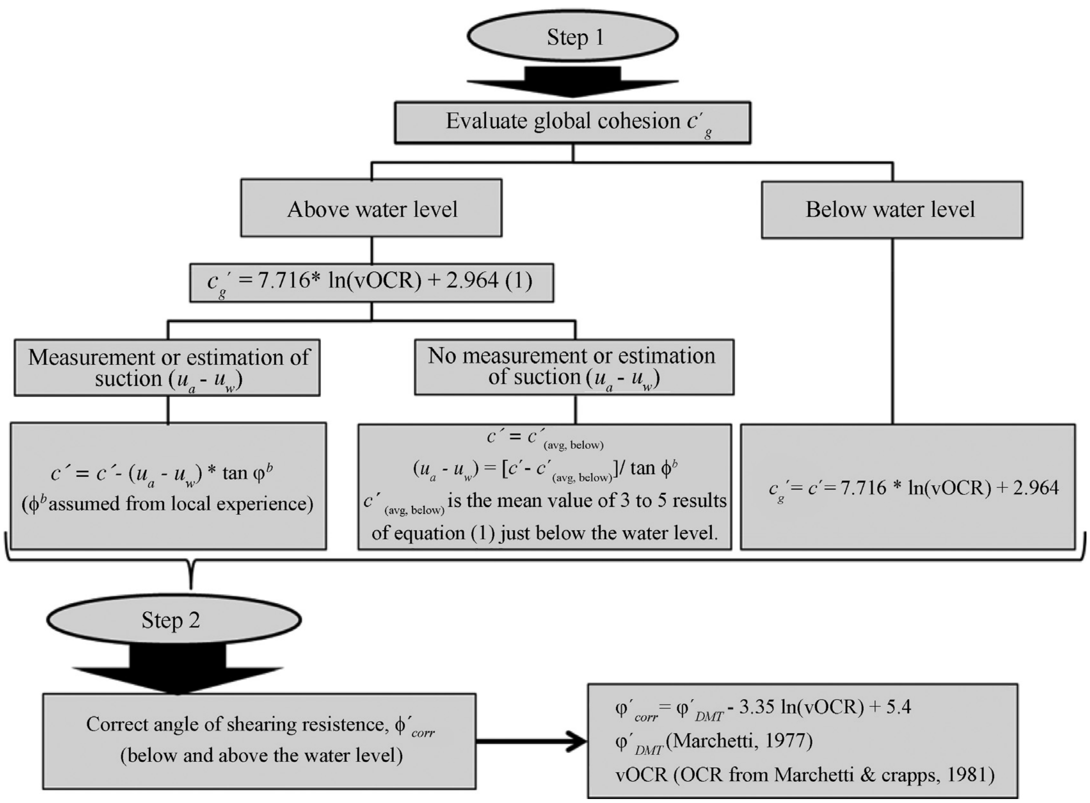

Figure 14 - Evaluation of strength parameters in residual soils.

5. Conclusions

In the context of this framework a model to interpret DMT results in residual soils from Portuguese granites was elaborated, followed by an experiment in controlled conditions to establish adequate correlations with the geotechnical strength parameters, namely the global cohesion intercept (arising from the cementation structure and suction) and the angles of shearing resistance corresponding to a linearized Mohr-Coulomb failure envelope. The obtained correlations were then applied to DMT tests performed in the IPG experimental site (Rodrigues, 2003; Cruz, 2010) and the consequent results showed an excellent convergence with the reference parameters, proving to be adequate for Porto and Guarda granites.

Previous correlations to obtain strength of the same materials (Cruz *et al.*, 2004a; Cruz & Viana da Fonseca, 2006) were affected by sampling disturbance and space variability of the triaxial testing that served as reference and did not take into account suction effects on cohesive intercept. To overcome these uncertainties a dedicated experimental facility was planned and realized, consisting of a large dimension prototype (CemSoil box), where artificially cemented soils were moulded with the purpose of executing DMT tests with pre-installed and pushed-in blades. Specimens for triaxial testing were also prepared following the same moulding process and state conditions. The obtained results confirmed that DMT parameters are influenced by both cementation and suction. Using as reference parameter a concept similar to overconsolidation ratio, designated by "virtual" (vOCR), it was possible to establish calibrated correlations for deriving a global cohesive intercept (c'_g) generated by cementation and suction effects. Moreover, when suction parameters (φ^b and u_a - u_w) are available, the cohesion resulting from cementation structure is easily obtained by subtracting the suction contribution, calculated by the third term of Fredlund *et al.* (1978) strength criterion. In cases where there is no information about suction, a novel procedure to separate cementation and suction contributions was also proposed. The experiment also proved that angles of shearing resistance could be derived with accuracy by the approach proposed by Marchetti (1997) for sedimentary sandy soils, as far as a correction factor based on vOCR is used. DMT tests performed in the same spot of Guarda Granitic Formation from where the artificial samples of the main experiment were moulded, showed high convergence with triaxial results, confirming the adequacy of the correlations developed in this framework for deriving the *in-situ* strength parameters. The presented correlations were tested only in Portuguese granites, and so its extension to other residual soils with different genesis or different mineralogic/chemical compositions should be confirmed in the first place. The presented work may represent a path to follow.

Acknowledgments

This research was developed under the activities of MOTA-ENGIL, namely "Geomechanic Modelling of Residual Soils, RESOIL, financed by European Community (QREN/UE/FEDER), under the activities of CEC (FEUP), PTDC/ECM/099475/2008, financed by the Operational Program for Competitive Factors, COMPETE.

References

Almeida, F.; Café. L.; Cruz, N. & Rodrigues, C. (2012) Laboratorial S-wave measurements with buried geophones in a large calibration box. Proc. Geotechnical and Geophysical Site Characterization ISC'4, v. 2, p. 1419-1426.

Arroyo, M.; Amaral, M.F. & Viana da Fonseca, A. (2013) Isotropic yielding of unsaturated cemented silty sand. Canadian Geotechnical Journal, v. 50:8, p. 807-819.

Baldi, G.; Bellotti, R.; Ghionna N. & Jamiolkowski, M. (1988) Stiffness of sands from CPT, SPT and DMT - a critical review. Penetration Testing. Institution of Civil Engineers, British Geotechnical Conference, Birmingham, paper n. 42, p. 299-305.

COBA (2003) Porto Geotechnical Map. Work performed by COBA with the collaboration of Faculty of Sciences of University of Porto. Porto City Hall (in Portuguese).

Coop, M.R. & Willson, S.M. (2003) Behavior of hydrocarbon reservoir sands and sandstones. Journal of Geotechnical and Geoenvironmental Engineering, ASCE, v. 129:11, p. 1010-1019.

Cruz, N. (1995) Evaluation of Geotechnical Parameters by DMT Tests. MSc Thesis, Faculty of Science and Technology, University of Coimbra.

Cruz, N. (2010) Modelling Geomechanics of Residual Soils by DMT Tests. PhD Thesis, University of Porto, Portugal.

Cruz, N.; Viana da Fonseca, A.; Coelho, P. & Lemos, J. (1997) Evaluation of geotechnical parameters by DMT in Portuguese soils. XIV Int. Conf. on Soil Mechanics and Foundation Engineering, Hambourg, Germany, v. 1, p. 77-80.

Cruz, N.; Viana da Fonseca, A. & Neves, E. (2004a) Evaluation of effective cohesive intercept on residual soils by DMT data. Proc. 2nd Int. Site Characterization - ISC'2, Porto, Portugal, Sept. 2004. Millpress, Rotterdam, v. 2, p. 1275-1278.

Cruz, N.; Figueiredo, S. & Viana da Fonseca, A. (2004b) Deriving geotechnical parameters of residual soils from granite by interpreting DMT+CPTU tests. Proc. 2nd Int. Site Characterization - ISC'2, Porto, Portugal, v. 2, p. 1799-1803.

Cruz, N. & Viana da Fonseca, A. (2006a) Portuguese experience in residual soil characterization by DMT tests. Proc. 2nd Int. Flat Dilatometer Conference, Washington D.C., v. 1, p. 359-364.

Cruz, N. & Viana da Fonseca, A. (2006b) Characterization of stiff residual soils by dynamically push-in DMT. ASCE Geotechnical Special Publication n. 149, p. 261-268.

Fahey, M. & Randolph, M.F. (1984) Effect of disturbance on parameters derived from self-boring pressuremeter tests in sands. Géotechnique, v. 34:1, p. 81-97.

Ferreira, C.; Viana da Fonseca, A. & Nash, D. (2011) Shear wave velocities for sample quality assessment on a residual soil. Soils and Foundations, v. 51:4, p. 683-692.

Finno, R. J. (1993) Analytical interpretation of dilatometer penetration trough saturated cohesive soils. Géotechnique, v. 43:2, p. 241-254.

Fredlund, D.G.; Morgenstern, N.R. & Widger, R.A. (1978) The shear strength of unsaturated soils. Canadian Geotechnical Journal, v. 15:3, p. 313-321.

Futai, M.M. (1999) Theoretical-Experimental Study of Non-Saturated Tropical Soils: Application to Slopes Ravine Processes. PhD Thesis, COPPE-UFRJ, Rio de Janeiro.

Huang, A.B. (1989) Strain path analysis for arbitrary three-dimensional penetrometers. Journal for Numerical and Analytical Methods in Geomechanics, v. 13:5, p. 551-564.

Jendeby, L. (1992) Deep compaction by vibrowing. Nordic Geot. Meeting, v. 1, p. 19-24.

Leroueil, S. & Vaughan, P.R. (1990) The general and congruent effects of structure in natural clays and weak rocks. Géotechnique, v. 40:3, p. 467-488.

Lutenegger, A. J. & Kabir, M.G. (1988) "Dilatometer C-reading to help determine stratigraphy". Proc. ISoPT-1, Orlando, FL, v. 1, p. 549-554.

Mantaras, F.M. & Schnaid, F. (2002) Cylindrical cavity expansion in dilatant cohesive-frictional materials. Géotechnique, v. 52:5, p. 337-348.

Marchetti, S. (1980) *In-situ* tests by flat dilatometer. J. Geotechnical, Eng. Div. ASCE, v. 106:3, p. 299-321.

Marchetti, S. (1997) The flat dilatometer design applications. III Geotechnical Engineering Conference, Cairo University. Keynote Lecture, v. 1, p. 421-448.

Marchetti, S. & Crapps, D.K. (1981) DMT operating manual. GPE Inc.Gainsville, Florida.

Mayne, P. W. (2006) Interrelationships of DMT and CPT in soft clays. Proc. 2nd Int. Conf. on Flat Dilatometer, Washington, DC, v. 1, p. 231-236.

Rodrigues, C. (2003) Geotechnical Characterization and Geomechanical Behaviour Analysis of a Saprolite from Guarda Granites. PhD Thesis, University of Coimbra. (in Portuguese).

Schnaid, F. & Mantaras, F.M. (2003) Cavity expansion in cemented materials: structure degradation effects. Géotechnique, v. 53:9, p. 797-807.

Schnaid, F. & Coutinho, R.Q. (2005) Pressuremeter tests in Brazil (National Report). International Symposium 50 Years of Pressuremeters, v. 2, p. 305-318.

Smith, M.G. & Houlsby, G.T. (1995) Interpretation of Marchetti's dilatometer in clay. Proc. 11th European Conf. on Soil Mechanics and Foundation Engineering. Copenhagen, Denmark. p. 1247-1253.

Topa Gomes, A., Viana da Fonseca, A. & Fahey, M. (2008) Self-boring pressuremeter tests in Porto residual soil: results and numerical modelling. Geotechnical Site Characterization. Huang and Mayne (eds). Proc. ISC'3. Taylors & Francis, v. 2, p. 1193-1021 (CD-Rom)

Topa Gomes, A. (2009) Elliptical Shafts by the Sequential Excavation Method. The Example of Metro do Porto. PhD Thesis, University of Porto. (in Portuguese).

Viana da Fonseca, A. (1996) Geomechanics of Porto Residual Soil from Granite. Design Criteria for Direct Foundations. PhD Thesis presented to Porto University.

Viana da Fonseca, A. (2003) Characterising and deriving engineering properties of a saprolitic soil from granite, from Porto. Tan, Phoon, Hight & Leroueil (eds) Characterisation and Engineering Properties of Natural Soils. Swets & Zeltlinger, Lisse, v. 2, p. 1341-1378.

Viana da Fonseca, A. & Coutinho, R. Q. (2008) Characterization of residual soils. Keynote paper. Proc. 3rd International Conference on Site Characterization, Taiwan.

Viana da Fonseca, A.; Silva, S. & Cruz, N. (2009) Geotechnical characterization by *in-situ* and lab tests to the back analysis of a supported excavation in Metro do Porto. Int. Geotechnical and Geological Engineering Journal, v. 28:3, p.251-264.

Viana da Fonseca, A.; Coop, M.R.; Fahey, M. & Consoli, N. (2011) The interpretation of conventional and non-conventional laboratory tests for challenging geotechnical problems. Keynote Lecture, 5th Int. Symp. on Deformation Characteristics of Geomaterials. IOS Press, Amsterdam, v. 1, p. 84-119.

Viana da Fonseca, A.; Amaral, M.F.; Panico, F. & Rios, S. (2014) Indexation of dynamic and static geomechanical properties of a cemented aggregate for transportation engineering. Journal of Transportation Geotechnics, v. 1, p. 1-14.

Whittle, A.J. & Aubeny, C.P. (1992) The effects of installation disturbance on interpretation of *in situ* tests in clay. Proc. Wroth Memorial Symp., Oxford, July, v. 1, p. 742-767.

Yu, H.S.; Carter, J.P. & Booker, J.R. (1993) Analysis of the dilatometer test in undrained clay. Predictive Soil Mechanics. Thomas Telford, London, v. 1, p. 783-795.

List of Symbols

c': cohesive intercept in Mohr-Coulomb criterion

c'_g: global cohesion due to cementation and suction in Mohr-Coulomb criterion

CID: triaxial test, isotropically consolidated drained

CPT: cone penetration test

CPTu: piezocone test

d: rate of dilatancy = $\delta\varepsilon^p_v/\delta\varepsilon^p_s$, where $\delta\varepsilon^p_v$ is the increment of volumetric strain and $\delta\varepsilon^p_s$ is increment of shear strain
DMT: Marchettis flat dilatometer test
DPSH: dynamic probing super-heavy test
E_D: dilatometer modulus (DMT)
E_D*: ratio between unsaturated/saturated values of E_D
I_D: material index (DMT)
I_D*: ratio between unsaturated/saturated values of I_D
K_D: horizontal stress index (DMT)
K_D*: ratio between unsaturated/saturated values of K_D
NC: normally consolidated soil
N_{SPT}: number of blows to penetrate 30 cm in SPT
OC: overconsolidated soil
OCR: overconsolidation ratio
p': mean effective stress
p_0: DMT first pressure reading (lift-off)
p_1: DMT second pressure reading (membrane expansion)
p_1*: ratio between unsaturated/saturated values of p_1
p_2: DMT third pressure reading (closing pressure)
p_a: atmospheric pressure (101.3 kPa)
PMT: Ménard pressuremeter test
q: deviator stress
q_c: cone tip resistance (CPT/CPTu)
q_d: diametral compression strength
q_t: corrected cone tip resistance (CPTu)
q_u: uniaxial compression strength
q_u*: ratio between unsaturated/saturated values of q_u
SCPTu: seismic piezocone test
SDMT: seismic dilatometer test
SPT: standard penetration test
u, u_w: pore water pressure
u_0: at rest pore water pressure
u_a: pore air pressure
U_D: pore pressure index (DMT)
U_D*: ratio between unsaturated/saturated values of U_D
vOCR/AOCR: virtual OCR/apparent OCR
V_P: compression wave velocity
V_S: shear wave velocity
z: depth
φ': effective angle of shearing resistance
φ'_{DMT}: angle of shearing resistance derived from DMT
φ'_{ref}: reference angle of shearing resistance
φ^b: suction angle of shearing resistance
η: stress ratio (q/p').

A View of Pressuremeter Testing in North America

J. Benoît, J.A. Howie

Abstract. The pressuremeter was introduced to North America by Ménard in 1957. It consists of a cylindrical probe which is inserted into the ground in a borehole, by self-boring or by pushing, and is expanded against the soil or rock to obtain a pressure-expansion curve. Interpretation methods based on cavity expansion theory applied to realistic models of soil behavior allow derivation of *in situ* lateral stress, stiffness, strength and volume change characteristics of the material being tested. Since its introduction, the pressuremeter test (PMT) has been a popular topic of research but has not gained wide acceptance in geotechnical engineering site characterization practice which, in North America, is still dominated by the Standard Penetration Test (SPT) and more recently by the piezocone (CPTu). Over the same period, the PMT has become the dominant tool for site investigation and foundation design in France. There, the PMT is used empirically based on a very large amount of load testing and experience. This paper examines the use of the PMT in North American practice, discusses its strengths and weaknesses, identifies trends in its use for site characterization and geotechnical design and identifies possible reasons for its lack of adoption by industry. We conclude that the PMT is not competitive with other techniques such as the CPTu and SPT for general site characterization where such tests are possible but that the PMT offers great potential to provide geotechnical design parameters in problematic materials such as hard, very dense or gravelly soils, residual, saprolitic or lateritic soils, soft and fractured rocks, frozen ground and ice. The PMT also has application in all soils where high consequences of failure require very detailed analysis and design. We also emphasize the need for improvements in the education of geotechnical practitioners on the use of the pressuremeter.

Keywords: Ménard, pressuremeter, self-boring, prebored, pressuremeter design.

1. Introduction

The original concept of the pressuremeter dates back to Kögler in 1933 who developed a device consisting of a rubber bladder clamped at both ends and lowered in a pre-bored hole. The expansion of the device against the sides of the borehole allowed the determination of the stress-strain characteristics of the soil. Without knowledge of Kögler's work, Ménard (1957) developed a much improved pressuremeter (PMT), which has been widely used in engineering practice for more than half a century. In spite of the simplicity of this concept, there are a number of inherent problems associated with inserting an instrument in a pre-bored hole. The pre-drilling of a borehole inevitably induces disturbance due to the drilling process and also allows unloading due to pre-boring the hole. When used in relatively stiff soils and soft rocks, these problems are easily overcome, but in soft clays and cohesionless soils such as sands, these problems are more difficult to circumvent. However, under the assumptions that disturbance and stress relief are minimal when using careful borehole preparation techniques, the cavity expansion measurements and interpreted results can be used directly in a set of design rules, derived empirically but based on theory. The results can also be used indirectly by obtaining soil and rock strength and deformation parameters which can be used in conventional design of geotechnical structures.

Recognizing the effects of pre-boring on the parameters obtained and the corresponding necessity of using empirical correlations, French and English research groups (Baguelin *et al.*, 1972; Wroth & Hughes, 1972) independently developed a self-boring pressuremeter (SBPM) which could be inserted into the ground with minimal disturbance. The SBPM probe is similar in testing concept to the prebored pressuremeter except that it is advanced into the ground through a balanced process of pushing while cutting the soil which enters a sharp cutting shoe located at the bottom of the probe. The cuttings are flushed above the probe in the annular space inside the probe body. Results from SBPM tests have been used primarily to obtain soil parameters such as strength and deformation properties for use in conventional design or analytical methods such as finite element analysis. Other types of pressuremeters have been introduced, mostly in an effort to increase productivity especially offshore. Such techniques include push-in and full displacement devices. These methods also induce a consistent and repeatable amount of disturbance and consequently are not as operator dependent.

Regardless of the type of probe used or method of placement into the ground, once the appropriate depth is reached, a pressuremeter test is conducted as follows. The membrane is expanded against the sides of the borehole and the pressure, displacement and, in some cases, porewater pressures are monitored and recorded. Either stress or strain

Jean Benoît, Ph.D., Professor, Department of Civil Engineering, University of New Hampshire Kingsbury Hall, Durham, New Hampshire, USA. e-mail: jean.benoit@unh.edu.
John A. Howie, Ph.D., Associate Professor, Department of Civil Engineering, University of British Columbia, BC, Canada. e-mail: jahowie@civil.ubc.ca.
Submitted on March 28, 2014; Final Acceptance on December 15, 2014; Discussion open until April 30, 2015.

controlled expansion tests may be carried out. Each test may generally be conducted in 10 to 30 min depending on the type of material and test procedure.

This paper will review the current use of the pressuremeter as an *in situ* testing tool in North America, highlight its benefits and discuss why its use has been limited compared to other field techniques such as the Standard Penetration Test (SPT) and the Cone Penetration Test (CPT). While emphasis will be placed on the prebored pressuremeter test, other pressuremeter tests will be discussed in terms of applicability and acceptability to engineering practice.

2. Background

The prebored pressuremeter as we know it today is the product of the vision and ingenuity of Louis Ménard while a student at Ecole Nationale des Ponts et Chaussées in Paris. As part of his final project, Ménard and his two colleagues (Gauthier *et al.*, 1954) described the pressuremeter shown in Fig. 1, its use, and a theoretical study governing the interpretation of the test curve. Although the manuscript was only 20 pages, it covered stresses and displacements around the expanding cylindrical cavity for cases of cohesive soils, saturated sands and clays, unsaturated soils and inelastic soils followed by numerical examples for dry and saturated soil. They concluded that the principal advantage of pressuremeter use was to allow the study of pressure-deformation characteristics of soils and that their study was to shed light on the interpretation of those results. At that stage of their study, they also assumed that no remolding of soil occurs as a result of borehole preparation. Ménard's patent application followed and was submitted in Paris on January 19, 1955. The schematic of his probe described in his patent application is as previously shown in Fig. 1.

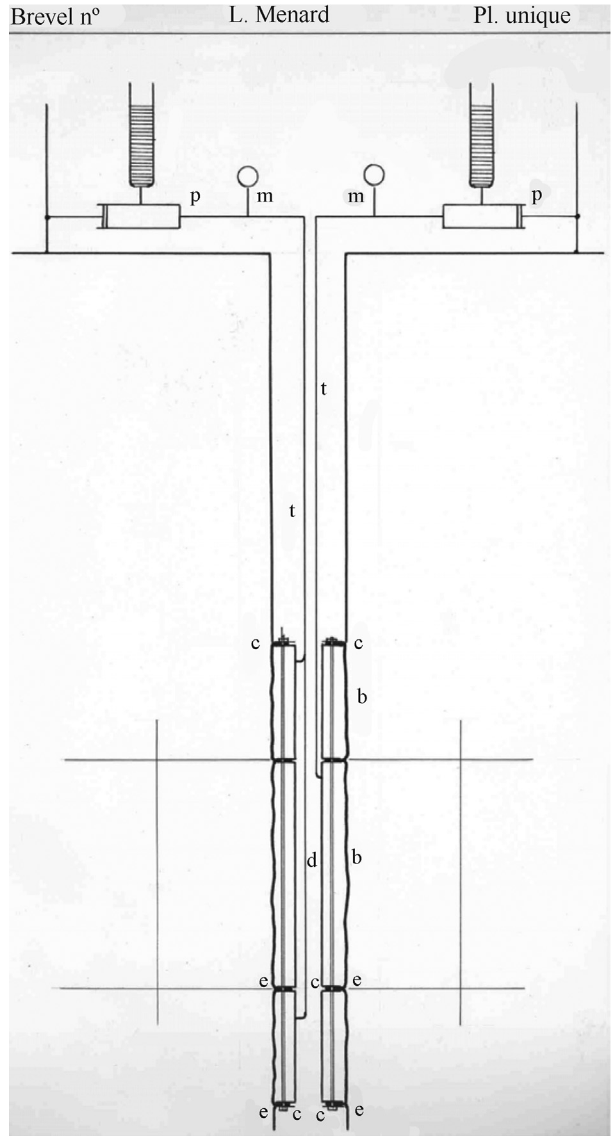

Figure 1 - Schematic description of the original pressuremeter (Gauthier *et al.*, 1954).

Following his studies in Paris, he travelled to the USA to do a Master's thesis under Dr. Ralph Peck. His thesis entitled "An Apparatus for Measuring the Strength of Soils in Place" was completed in 1957 at the University of Illinois. Ménard recognized that his invention, which he coined the "pressiometer" had competition from other field tools such as the field vane in clays and the standard penetration test in sands. However, he recommended his tool because "A theoretical interpretation of the curve "strain versus stress" gives immediately the values of the cohesion, the friction angle and the modulus of elasticity." From his work he concluded the following:

a) The pressiometer is a very precise method of subsurface exploration;

b) The bearing capacity increases with the modulus of elasticity of the soil.

Part of his research work included testing in various soils such as glacial till, fluvial and compacted clays and sand. Figure 2 shows pressuremeter tests done in Chicago clays at shallow depth in an investigation designed to evaluate the remolding due to the driving of H-piles and decompression from the excavation for the Island Steel Building. The test labeled 42 was performed 1 m away from the pile while test 44 was done at the same depth but only 0.3 m away. The results from the tests indicated a decrease in undrained strength of about 40% due to the driving of the piles and unloading from the excavation while the modulus of elasticity varied from 41 kg/cm^2 (4 MPa) for the undisturbed clay compared to only 6 kg/cm^2 (0.6 MPa) for the remolded clay. Through testing at two other sites, Ménard was able to demonstrate good agreement between his theoretical derivations and the experimental results.

According to Ladanyi (1995), Ménard recognized some limitations in his initial theoretical approach to interpretation of the test and began to develop empirical rules governing the use of the pressuremeter results for founda-

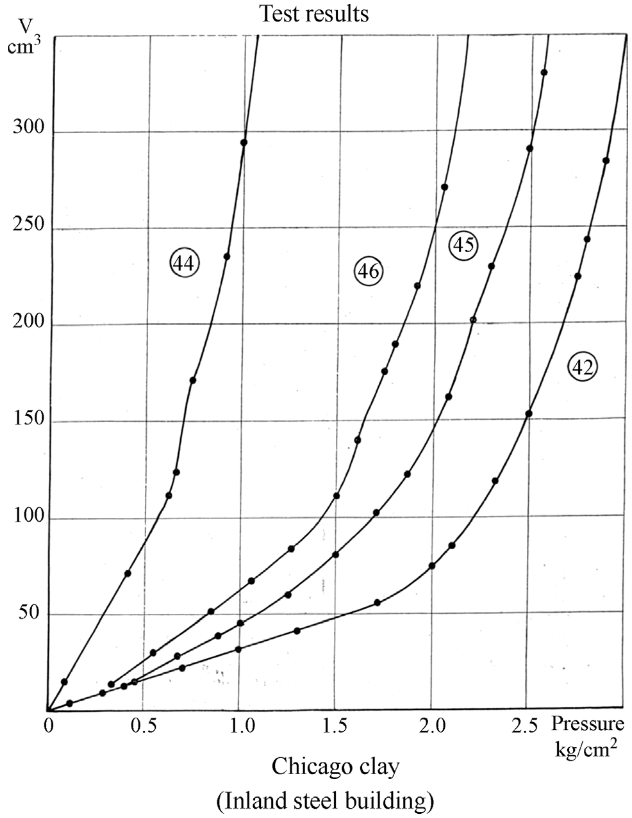

Figure 2 - Pressuremeter tests performed by Ménard in Chicago clays (Ménard, 1957).

tion design. The approach was validated initially by comparison to full-scale load tests and has been improved and extended by research and practice in the years since, particularly in France where it has become the dominant tool for site investigation and foundation design. Although the original pressuremeter shown in Fig. 1 required a borehole diameter of 140 mm, the second prototype was reduced to 50 mm (Cassan, 2005). A series of improvements and modifications in the guard cells' design and pressurization, volume and pressure measurement systems, membrane protection, and control unit for conducting and recording the test were continuously implemented in an effort to make the pressuremeter a more reliable and accurate test method. These changes also allowed the pressuremeter to be used at greater depths and higher pressures. Dimensions of the pressuremeter also evolved to improve on the length to diameter ratio. Other groups outside France have also modified the details of the pressuremeter and the system used to measure expansion of the pressuremeter membrane by using various displacement sensors instead of volume measurements.

The prebored pressuremeter has been successfully used in hard soils and soft or weak rocks where other *in situ* tools cannot penetrate these materials or lack the capacity to measure geotechnical parameters in these formations. Special probes with rugged membranes can acquire pressure-expansion curves which can be interpreted to estimate material stiffness properties and, in some cases, strength parameters in carefully prepared boreholes.

Ménard protected his invention from outside influence for 10 years through patent protection but in 1969 began to sell and license its use to others (Ladanyi, 1995). This opened the pressuremeter concept to much research. In an effort to eliminate the disturbance effects of preboring, the self-boring pressuremeter was developed by research groups in France (Baguelin *et al.*, 1972) and England (Wroth & Hughes, 1972). Differences exist between the French system (PAFSOR) and the British system (CamKoMeter) but the objectives are the same. Insertion of the probe into the ground occurs using a cutter system located inside a cutting or driving shoe to minimize disturbance. As the probe is pushed into the ground, the soil which enters the cutting shoe is cut by the rotating cutter and flushed to the ground surface through the annular space inside the probe body. Other systems of advance have been successfully used, *e.g.* jetting (Benoît *et al.*, 1995) and have proved to often be more time-effective in soils. Once the testing depth is reached, the membrane is expanded against the sides of the borehole and the pressure, displacements (or volume) and, in some cases, porewater pressures, are measured continuously and automatically. The SBPM test can be conducted in a stress or strain controlled manner. Because the SBPM is inserted with minimal disturbance, the cavity expansion measurements can be analyzed using basic continuum mechanics of cavity expansion and consequently engineers need not rely on empirical correlations to obtain soil parameters for use in foundation design.

Other types of pressuremeter were introduced in an effort to circumvent the requirements to produce a prepared hole for testing or to use an often time consuming method of advance in the case of self-boring by using pushing as the method of insertion. The need for pressuremeter testing offshore was the major catalyst for these innovations. One approach developed was the Push-in Pressuremeter (Reid *et al.*, 1982) which comprised an expansion unit mounted around a tube similar to a sample tube. However, Bandis & Lacasse (1986) showed that the insertion of this unit caused considerable disturbance and the fact that the probe had to be withdrawn from the hole between tests did not offer significant improvement in productivity. Another development aimed at the offshore market was the Cone Pressuremeter which was also known as the Full-Displacement Pressuremeter (Hughes & Robertson, 1985; Withers *et al.*, 1986). The Pencel Pressuremeter was an adaptation of the pavement evaluation tool described by Briaud & Shields (1979) which was also pushed into place for testing. These tools were based on the concept that it was better to create a consistent, repeatable degree of disturbance in the soil adjacent to the expansion unit. An additional advantage of this method is an increased production rate.

3. Approaches to Analysis and Interpretation of Test Curves

In a report by the ISSMGE Committee TC 16 on pressuremeter testing in onshore ground investigations, Clarke & Gambin (1998) noted that two approaches to interpretation and use of pressuremeter results had evolved. One was based on analytical methods used to derive basic soil properties (strength, stiffness etc.) from the test curves and the other was based on the development of a set of empirical design rules based on measurements made in a very standard way with a standard instrument. They also hinted at a strong diversity of opinion between proponents of the two approaches but regarded such differences as healthy.

Figure 3 from Clayton *et al.* (1995) shows schematic pressuremeter curves obtained using the three principal methods of insertion. The differences are readily seen. For the prebored test, the wall of the test pocket has been unloaded by the drilling and will have relaxed inwards. The pressure increase and deflection required to re-establish contact between the probe and the cavity wall and to exceed the *in situ* lateral stress to begin expansion will depend on the material type and properties, the relative diameters of the borehole and the probe, the quality of the drilling and the expertise of the pressuremeter test field crew in installation of the probe. This results in an S-shaped expansion curve. For the full displacement probe, since it is pushed into the ground, the initial deformation results in the expansion curve starting at a higher stress. In principle, for the self-boring advance, the stresses *in situ* are theoretically unchanged by the probe insertion and thus the beginning of the expansion curve should represent the *in situ* lateral stress.

In reality, no probe can be installed without some disturbance of the soil. For example, a 0.5 mm expansion of a 76 mm diameter pressuremeter represents 1.3% cavity strain ($\Delta r/r_o$ where r_o is the initial cavity radius and Δr is the change in radius). With full scale expansion of a typical SBPM test being only 10% cavity strain, small movements induced during installation can have a large effect on the measured expansion curve. For most soils, such a deformation would lead to the formation of a zone immediately adjacent to the pressuremeter that has reached yield. For saturated fine grained soils, this will be a zone exhibiting excess pore pressure and in free-draining soils, will be a zone of volume change. From Fig. 3(b), it can be seen that there is the potential for disturbance to cause large stress changes from the *in situ* stress even for SBPM testing in relatively soft soils. In stiff soils, the potential stress changes are very large. Consequently, "lift-off" pressures are unreliable measures of *in situ* stress even in a test conducted after expert installation of the probe. Much research effort has been expended in an attempt to clarify the effects of such disturbance on subsequent test curves but the fundamental problem is that it is not possible to reliably assess from the measured test curve the degree of disturbance caused by installation of the probe.

The schematic test curves in Fig. 3 all include unload-reload loops. Palmer (1972) showed that the slope of the initial part of an ideal expansion curve is twice the shear modulus. To avoid the effects of disturbance on the initial part of the expansion curve, unload-reload loops can be interpreted to give the elastic shear modulus of the soil or rock. Such loops are considered to be little affected by disturbance as is shown in Fig. 3 where the slopes of the unload-reload loops are similar in all three cases.

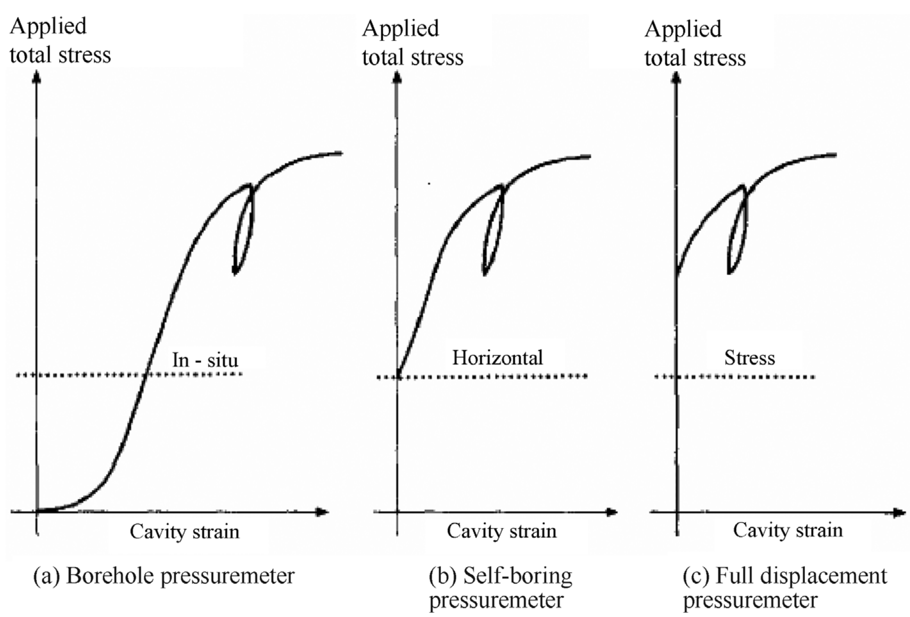

Figure 3 - Schematic differences in stress-strain curves as a result of pressuremeter installation procedures (Clayton *et al.*, 1995).

3.1. Interpretation to derive soil properties

The analysis of pressuremeter test results based on theory requires the following assumptions:

- The probe can be installed without disturbing the soil to be deformed by the test (or in the case of the cone pressuremeter, the degree of disturbance is consistent),
- The assumed soil model is representative of the stress-strain response of the soil being deformed by the pressuremeter expansion,
- Deformation occurs under plane strain conditions.

The analysis is dependent on the type of soil and whether the cavity expansion is conducted drained or undrained. If the test is undertaken in a saturated fine-grained soil and the test is conducted fast enough to prevent drainage, then the soil will deform at constant volume and all elements surrounding the probe will have the same stress-strain behavior. However, if the soil is a free draining granular material, the stress-strain curve will no longer be unique with radius but rather a function of the stress level. In other words, near the walls of the cavity the stresses will be high and hence the shear resistance will be high. Both stresses and strength will decrease with radial distance. Furthermore, because the volume is allowed to change during the test, as the sand shears, the material will expand or dilate depending on its initial stress level and initial density. If the material is a rock then the interpretation becomes even more complex because of the tensile strength of the rock, the presence of discontinuities and planes of weakness and the determination of a suitable failure criterion.

In general, from a pressuremeter test, it is possible to obtain, empirically, theoretically or analytically, the lateral stress in the ground, the stress-strain behavior, the strength and in some cases the consolidation characteristics. Several interpretation techniques are available to evaluate these various parameters.

The early approaches to pressuremeter interpretation based on cavity expansion theories used graphical manipulations of the test curves to derive soil parameters. Table 1 from Yu (2004) gives examples of available methods to interpret fundamental soil parameters from *in situ* testing. In the initial attempts at interpretation, parameters were treated separately. The total lateral stress was taken to be the stress at first movement of the membrane (“lift-off” pressure), the shear modulus was derived from unload-reload loops or from an inferred stress-strain curve and shear strength was obtained from graphical manipulation of the test curve. As noted by Ladanyi (1995), with the advent of the PC-age, the whole pressuremeter curve could be analyzed using computer-aided modeling. Shuttle & Jefferies (1995) refer to the process as Iterative Forward Modeling. The ability to simulate complete pressuremeter curves, both loading and unloading, using realistic soil models has led to attempts to use comparisons between simulated and measured pressuremeter curves to obtain estimates of geotechnical parameters. Both expansion and contraction curves can be modeled. To use the approach, a group of relevant parameters is selected based on the assumed constitutive model and is used to predict a theoretical curve. The parameters are adjusted until good agreement is achieved between the measured and calculated curves. Figure 4(a) shows an example of curve fitting for a clay soil from Jefferies (1988) and Fig. 4(b) is an example for sand from Roy *et al.* (2002). Both of these examples are based on SBPM data. However, modeling can also be applied to prebored or full-displacement pressuremeter test data, provided the curve-matching focuses on the latter part of the expansion curve or the unloading curve (*e.g.* Ferreira & Robertson, 1992). Schnaid *et al.* (2000) suggested that in a lightly structured granite saprolite, the curve fitting technique applied to the loading curve of a SBPM test provided

Table 1 - Examples of the capabilities of *in situ* tests for measuring soil properties (Yu, 2004).

Test	Measured Properties	Selected References
Cone penetration tests (CPT/CPTU)	Soil profiling; Stress history (OCR); Consolidation coefficient; In situ state parameter for sand; Undrained shear strength; Hydrostatic pore pressure	Robertson (1986), Wroth (1984), Mayne (1993), Baligh and Levadoux (1986), Teh (1987), Been *et al.* (1987), Yu and Mitchell (1998), Lunne *et al.* (1997)
Self-boring pressuremeter tests (SBPMT)	Horizontal in situ stress; Shear modulus; Shear strength; Stress-strain curve; In situ state parameter for sand; Consolidation coefficient; Small strain stiffness	Jamiolkowski *et al.* (1985), Wroth (1982), Gibson and Anderson (1961), Hughes *et al.* (1977), Palmer (1972), Manassero (1989), Yu (1994, 1996, 2000), Clarke *et al.* (1979), Byrne *et al.* (1990), Jardine (1992), Fahey and Carter (1993), Bolton and Whittle (1999)
Cone pressuremeter tests (CPMT)	Horizontal in situ stress; Shear modulus; Shear strength; In situ state parameter for sand	Houlsby and Withers (1988), Schnaid (1990), Yu (1990), Yu *et al.* (1996)
Flat dilatometer tests (DMT)	Soil profiling; Horizontal in situ stress; Stress history (OCR); Shear strength; In situ state parameter for sand	Marchetti (1980), Mayne and Martin (1998), Finno (1993), Huang (1989), Yu (2004)

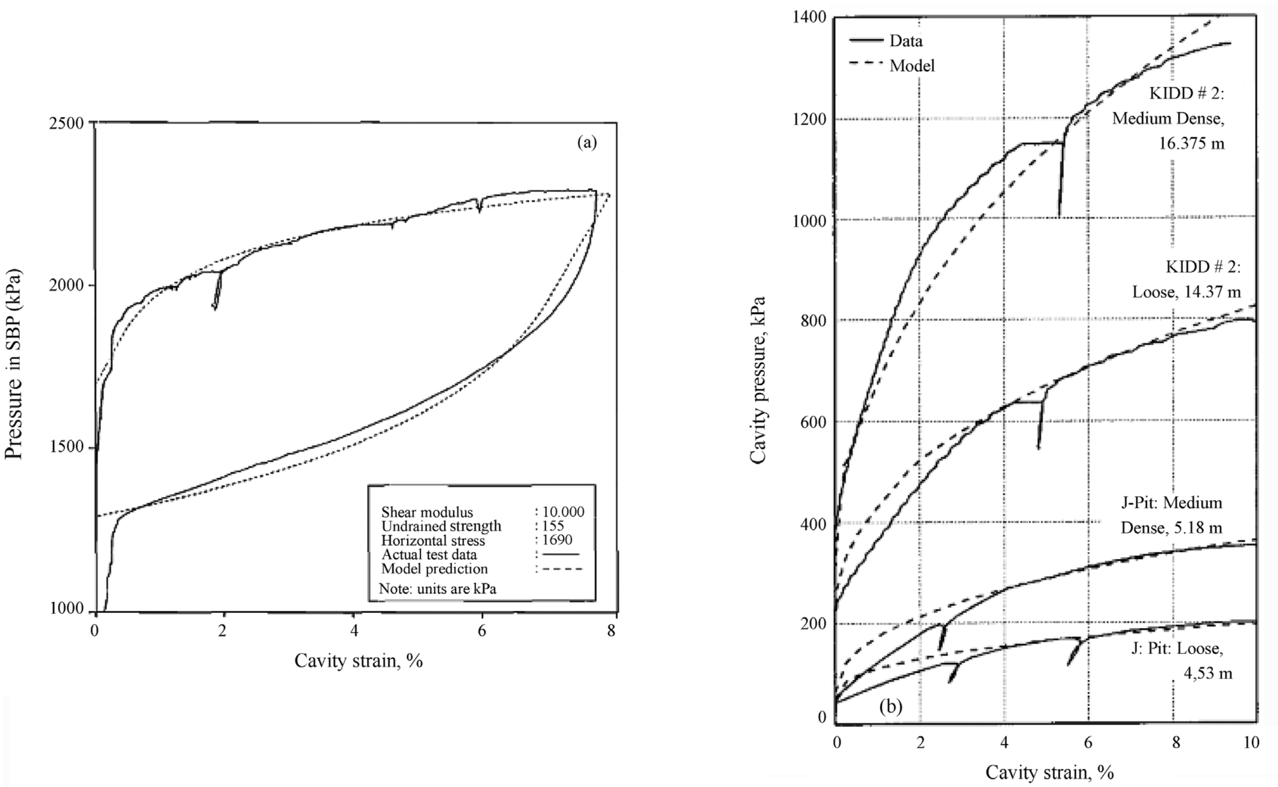

Figure 4 - (a): Example of curve fitting in clay (after Jefferies 1988). (b): Example of curve fitting in sand (Roy *et al.*, 2002).

properties typical of peak shear strength parameters, whereas those obtained from the unloading portion were more typical of the critical state behavior.

This approach has the advantage that parameters are related to each other and can be checked for consistency with those of soils that are typical of the soil being tested. For example, for a linear elastic, perfectly plastic soil, the parameters assumed would be the total horizontal stress, shear modulus (G) and undrained shear strength (s_u). Whether the resulting derived soil parameters are typical of the soil being tested can be assessed. Similarly, the estimated total lateral stress and equilibrium pore pressure can be used to derive the coefficient of earth pressure at-rest, K_o. This value can be assessed against values typical of soils with similar geological history. As the soil models increase in complexity, the number of soil parameters that have to be adjusted may become large.

Numerical analysis also allows the influence of departures from the ideal case to be assessed. For example, Yeung & Carter (1990), Houlsby & Carter (1993) and Jefferies & Shuttle (1995) discuss the effect of the finite length of the probe on the shear strength and rigidity index derived from approaches based on assumption of an infinitely long cavity and linear elastic, perfectly plastic soil behavior. These authors show that the effects of the finite length should be considered in the interpretation of the pressuremeter curves and indicate that such effects could result in errors in interpreted undrained shear strength of up to 40%.

It is clear that computer aided modeling provides great potential for the interpretation of pressuremeter test curves to determine the characteristic behavior of the soil tested. However, the interpretation must be considered together with other available geotechnical and geological information about the material and requires the application of engineering judgment based on an appreciation of the factors affecting the results.

3.2. Interpretation by Ménard rules

The alternative to interpreting the curves to obtain fundamental properties and the attendant problems arising from the many uncertainties in both the test curve and the interpretation is the one followed by Ménard and developed by his collaborators and successors. A prebored pressuremeter test is conducted using a standard probe, installed according to restrictive drilling requirements governing the formation of the test pocket, and expanded according to a standard test procedure. The resulting test curves are analyzed in a prescribed way and specific parameters are derived from them.

From a conventional pressuremeter expansion, three basic parameters are obtained: the creep pressure p_f, the Ménard modulus E_M and the limit pressure p_{LM}. Figure 5 shows the analysis procedure from the current international draft standard, ISO 22476 4, which is used to define the three main pressuremeter parameters: p_f, E_M, and p_{LM}. The quality of the test is evaluated using the number of data points available to define each portion of the expanding cavity as well as the scatter of the test points. The test curve shown in Fig. 5 is an ideal test. The first part of the curve is a recompression zone, followed by a quasi-linear zone which transforms to a non-linear third portion as the cavity volume approaches twice its initial volume. The test curve has been corrected for pressure and volume losses per standard calibration procedures outlined in the standard.

A test where test points are found in the first two groups only may indicate that the test hole was too large while a test with only the last two groups of points is generally indicative of the hole being too small or the presence of swelling ground. This approach has been in existence for decades as previously reported by Kastman (1978) using PMT tests carried out in the USA. Below the test curve is the corrected creep curve resulting from the differences in volume between the 30 s and 60 s readings from each pressure increment. This creep curve is used to define the various sections of the test. For example, the creep pressure is

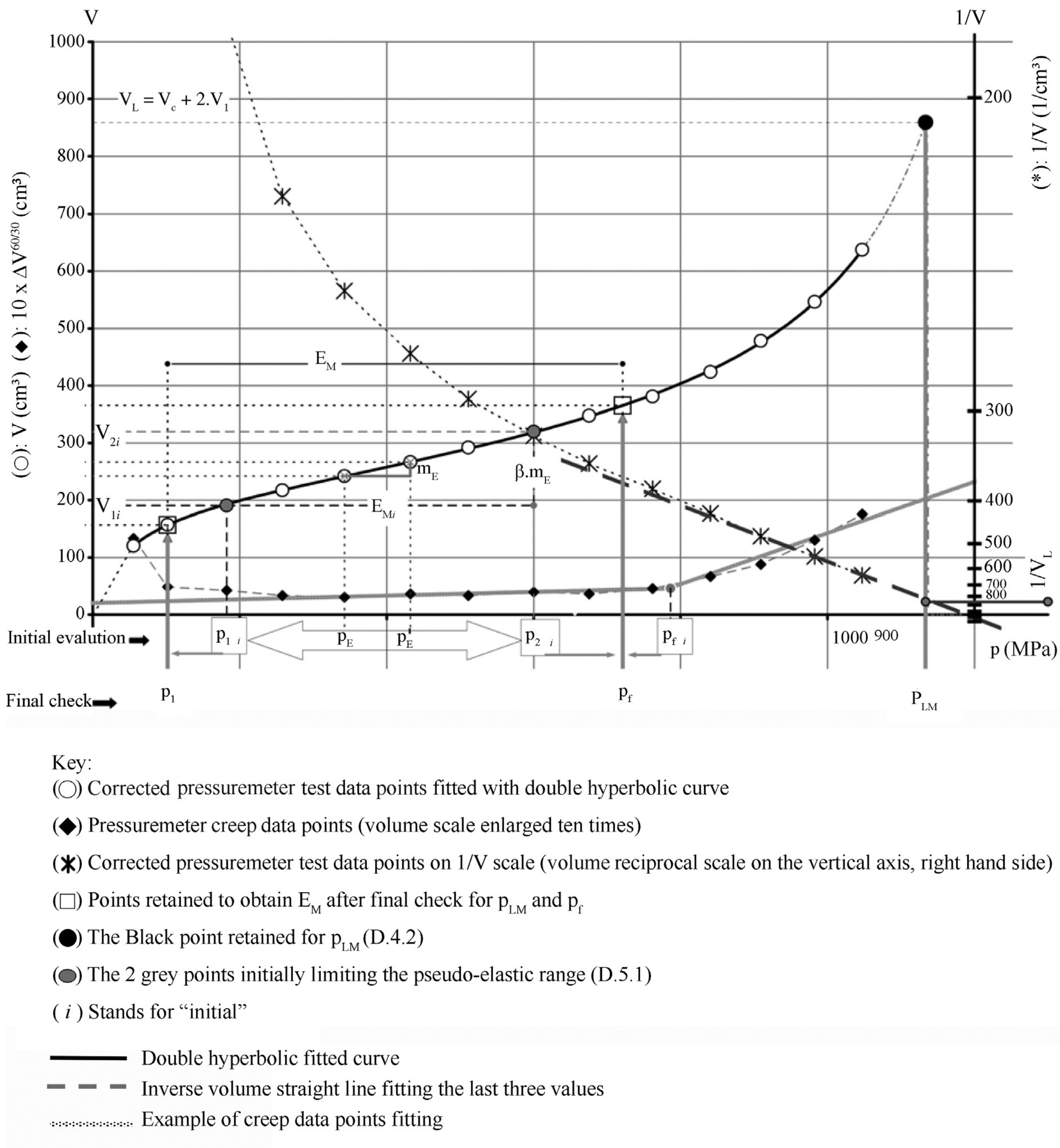

Figure 5 - Pressuremeter test curve analysis (ISO/FDIS 22476-4:2009 (E)).

located between the values p_{2i} and p_{fi} which are estimated using a graphical procedure. It has been shown that the quality of the test is reflected in the closeness of those two values.

The limit pressure is also obtained from the test but typically using an extrapolation technique. The limit pressure is defined as the pressure required for doubling the initial borehole cavity. In practice, this pressure is rarely attained because of the risk of membrane burst at higher expansion. Consequently, the limit pressure is obtained by extrapolation using a variety of methods. Often the value is obtained visually using the test curve. However, more reproducible methods should be used such as the reciprocal method (1/V from ASTM and ISO 22476-4) or the double hyperbolic method. Figure 5 illustrates both techniques.

Finally, the pressuremeter modulus, often referred to as the Ménard modulus, is generally defined as the slope of the linear portion of the expansion curve prior to the creep pressure. This pseudo-elastic range is defined by points p_{1i} and p_{2i} in Fig. 5. The modulus obtained using the pressuremeter test is often quoted as being an elastic modulus equal to Young's modulus since it is obtained from Eq. 1 which is based on the theory of linear elasticity (Gambin *et al.*, 1996).

$$E_M = 2(1+\nu)\left[V_c + \left(\frac{V_1 + V_2}{2}\right)\right]\frac{(p_2 - p_1)}{(V_2 - V_1)} \quad (1)$$

with Poisson's ratio ν = 0.33, where E_M = pressuremeter modulus and V_c = volume of initial cavity.

However, as stated by Gambin *et al.* (1996), Ménard recognized that the modulus of the soil was dependent on the stress path and strain level. It is clear from Gambin *et al.* (1996) and Briaud (1992) that the slope of the curve used to derive the modulus E_M obtained using the pressuremeter is influenced by the various parameters and conditions including the coefficient of earth pressure at-rest, K_o, the friction angle, soil stiffness, the length to diameter ratio of the pressuremeter probe, the stress path, the disturbance of the borehole wall and the test expansion strain rate. The pressuremeter modulus, E_M, is more appropriately referred to as a modulus of deformation. Gambin *et al.* (1996) conclude that in analyses of deformation based on linear elasticity where a modulus is required, E_M should likely be multiplied by a factor of 5 to 10 if it is going to be used as a Young's modulus.

Interpretation of the pressuremeter test is well-detailed in the standard but is still subject to variability. Reiffsteck (2009) reports that pressuremeter test curves provided to 9 individuals as part of a pile prediction exercise during the International Symposium on Pressuremeters (ISP5) yielded an acceptable range of pressuremeter modulus and limit pressure. Figure 6 shows the results in terms of limit pressure for a total of 42 PMT tests. Reiffsteck states that the mean error is in the order of 24% which is consistent with errors observed with other *in situ* tests such as the CPT as reported by Long (2008).

Because these parameters are obtained by a standard procedure in all materials, their values can be used in a similar manner to the standard parameters measured in the CPTu (tip, friction and pore pressure), *i.e.* by comparison with data from other similar materials, it is possible to make qualitative assessments of the likely soil characteristics. The parameters can also be used to design foundations by following strict design rules. From the onset, design rules have been devised in France using the pressuremeter results directly in the assessment of bearing capacity of shallow foundations, deep foundations including lateral loading, settlement evaluation of shallow and deep foundations as

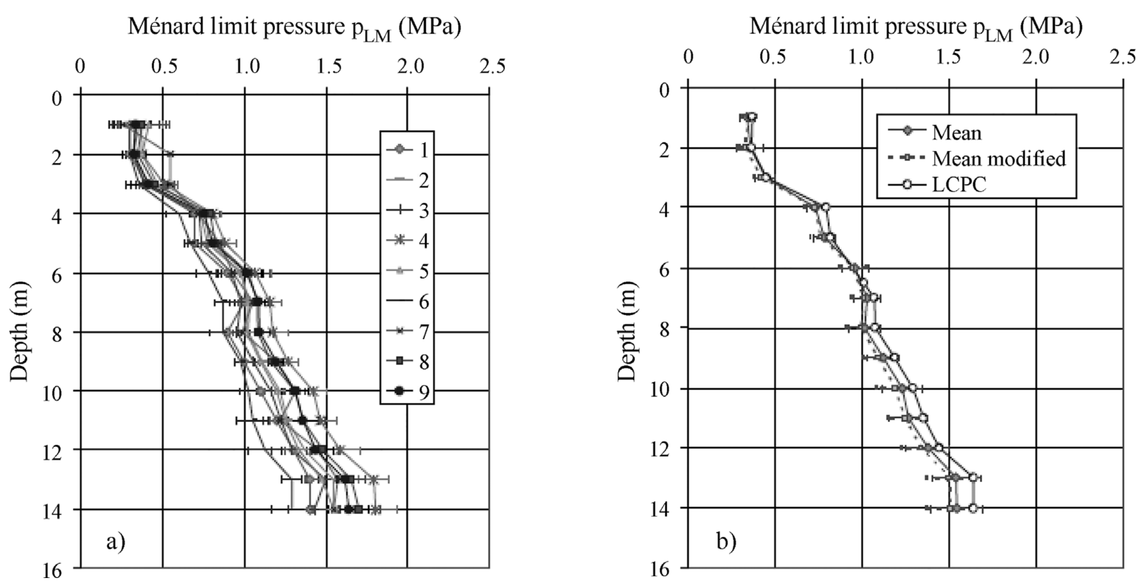

Figure 6 - Limit pressure from 9 participants on 3 boreholes for a total of 42 tests (Reiffsteck, 2009).

well as a panoply of applications to geotechnical structures and methods. From the pressuremeter deformation modulus, it is possible to assess settlement of foundations and displacement of laterally loaded piles while with the limit pressure, the bearing capacity can be evaluated for shallow and deep foundations. These rules are based on theory as well as observations and measurements of numerous instrumented experiments carried out at well documented test sites located in a variety of geological materials. The rules are not described in this paper but can be found in numerous documents (Briaud, 1992). However, many are in French. Work is ongoing to incorporate these design rules into the Eurocode which would make them significantly more accessible.

The majority of design work in France is done using the PMT and the well-established design rules. With improvements in testing techniques, equipment, additional observations and advanced numerical modeling, the rules are constantly revised to provide more versatile, accurate and safe design procedures. Expanding these rules through the Eurocode will also lead to improvements.

Some examples are provided herein to illustrate the efforts undertaken by various French research groups to advance the Ménard design rules. For example, Bustamante *et al.* (2009) in a paper describing pile design using the PMT, states that the current method is based on 561 pile load tests on more than 400 piles instrumented to measure skin friction and end bearing. These piles have been installed using more than 26 different techniques. They also show that the PMT is often more versatile than other *in situ* tests such as the CPT, the SPT and coring for laboratory testing as shown in Table 2. The tests were carried out in various materials including weathered or fragmented rock and cemented or very fine cohesionless formations. Their results led to improvements in design charts for unit skin friction, q_s, and a simplification of tip bearing factors, k_p, for 26 pile types. The work was further simplified as part of the drafting of the French standard for deep foundations for implementation in Eurocode 7 (AFNOR, 2012; Reiffsteck & Burlon, 2012). Using results from 159 load tests, a chart as shown in Fig. 7 was developed for determining the unit skin friction, q_s. Each curve represents a different pile type and installation method and was validated using, on average, 30 load tests. The values for f_{sol}, equivalent to the normalized unit frictional resistance, f_s, are given in tabular form in the standard NF P94-262 as a function of soil type. The unit skin friction, q_s, is then determined using f_{sol} multiplied by a soil-structure coefficient which is a function of pile type and installation method as well as soil type. The standard also provides limiting values for q_s for each case. The methods are straightforward, reliable considering the number of load tests used in their development, and useful especially for cases with similar geological conditions.

4. Pressuremeter Testing in North America

Based on a review of North American literature, it seems that most pressuremeter testing has been of the prebored variety. Early SBPM research was conducted in soils conducive to the installation of the SBPM with minimal disturbance which are also the soils that are suited to investigation by other *in situ* tests such as the SPT, the CPTu, the field vane and the flat plate dilatometer (DMT). In such soils, the pressuremeter offers no significant advantages for

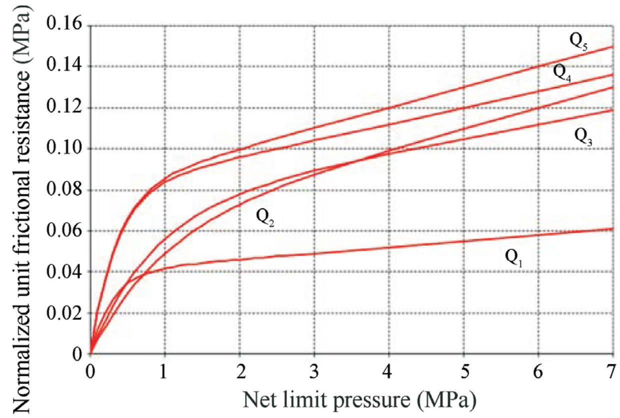

Figure 7 - Design chart for evaluating the unit skin friction q_s from pressuremeter test limit pressure (in Reiffsteck & Burlon, 2012; AFNOR (2012) Standard NF P94-262).

Table 2 - Comparison of *in situ* test and coring feasibility at 204 sites (Bustamante *et al.*, 2009).

Type of test	Number of sites as a function of test feasibility[1]			
	Tests completed[2]	Insufficient no. of tests[3]	Tests possible but curtailed	Tests inadequate[4]
PMT (p_{LM})	155 Sites (76%)	3 Sites (1.5%)	46 Sites (22.5%)	0 Site (0%)
CPT (q_c)	60 Sites (29.4%)	79 Sites (38.7%)	23 Sites (11.3%)	42 Sites (20.6%)
SPT (N)	26 Sites (12.7%)	54 Sites (26.5%)	72 Sites (35.3%)	52 Sites (25.5%)
Coring for laboratory (c' and φ')	21 Sites (10.3%)	67 Sites (32.8%)	69 Sites (33.8%)	47 Sites (23.1%)

[1]It is assumed that a PMT or an SPT log includes a test every meter. [2]Throughout the whole pile depth at least. [3]Insufficient No. of tests (PMT), premature refusal (CPT), excessive blow count (SPT) or sample badly recovered. [4]Tests deemed inadequate beforehand due either to soil type or to soil resistance.

geotechnical characterization over these other tests and so the other tools dominate. In the research sphere, the PMT has continued to be of great interest. The PMT has also found use in what Ladanyi (1995) termed "non-standard" materials. He was primarily referring to testing in frozen soils, ice and in soft and hard rock but there has also been considerable testing in other hard-to-investigate soils such as glacial tills, hard clays, residual soils and municipal wastes.

4.1. ASTM standards

The only ASTM standard related to pressuremeter testing in North America is ASTM Standard D4719. The current version was published in 2007 and is concerned with prebored pressuremeter testing. The scope of this standard is summarized in the following excerpts from ASTM:

> *This test method covers pressuremeter testing of soils. A pressuremeter test is an in situ stress-strain test performed on the wall of a borehole using a cylindrical probe that is expanded radially. To obtain viable test results, disturbance to the borehole wall must be minimized.*
>
> *This test method includes the procedure for drilling the borehole, inserting the probe, and conducting pressuremeter tests in both granular and cohesive soils, but does not include high pressure testing in rock. Knowledge of the type of soil in which each pressuremeter test is to be made is necessary for assessment of (1) the method of boring or probe placement, or both, (2) the interpretation of the test data, and (3) the reasonableness of the test results.*

It goes on to state that the method does not cover the self-boring pressuremeter and is limited to the pressuremeter which is inserted into predrilled boreholes or, under certain circumstances, is inserted by driving. There is no current ASTM Standard for versions of the test focused on the derivation of basic soil parameters.

Elsewhere, pressuremeter testing and test interpretation are provided by the international draft standard ISO 22476-4 prepared by the Technical Committee ISO/TC 182 (*Geotechnics*, Subcommittee SC 1, and by Technical Committee CEN/TC 341, *Geotechnical investigation and testing*) which provides a more complete set of procedures. The international standard is not limited to using the PMT in soils only but includes weak rocks. It is interesting to note that this standard refers to the prebored pressuremeter as the Ménard Pressuremeter Test (MPT). Figure 8 shows a schematic of the MPT.

The ASTM standard outlines the test procedures as well as making suggestions on best practices for borehole preparation based on soil types as shown in Table 3. In Table 4 are the recommendations from the international stan-

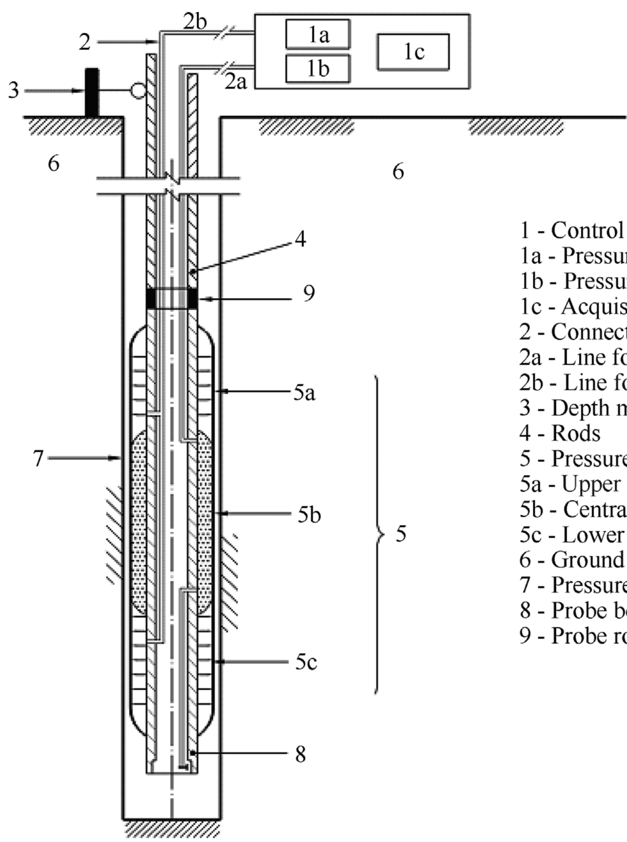

1 - Control unit (CU)
1a - Pressurization, differential pressurization and injection devices
1b - Pressure and volume measuring devices
1c - Acquisition, storage and printing out of the data (required for procedure B)
2 - Connecting lines
2a - Line for liquid injection
2b - Line for gas injection
3 - Depth measurement system
4 - Rods
5 - Pressuremeter probe
5a - Upper guard cell
5b - Central measuring cell
5c - Lower guard cell
6 - Ground
7 - Pressuremeter test pocket
8 - Probe body, hollow
9 - Probe rod coupling

Figure 8 - Schematic of the prebored or Ménard pressuremeter (ISO, 2009).

Table 3 - Guidelines for Selection of Borehole Preparation Methods and Tools (ASTM D4719).

Soil	Type	Rotary Drilling with bottom discharge of prepared mud	Pushed thin wall sampler	Pilot hole drilling and subsequent sampler pushing	Pilot hole drilling and simultaneous shaving	Continuous flight auger	Hand auger in the dry	Hand auger with bottom discharge of prepared mud	Driven or vibro-driven sampler	Core barrel drilling	Rotary percussion	Driven vibro-driven or pushed slotted tube
Clayey soils												
	Soft	2[B]	2[B]	2	2	NR	NR	1	NR	NR	NR	NR
	Firm to stiff	1[B]	1	2	2	1[B]	1	1	NR	NR	NR	NR
	Stiff to hard	1	2	1	1	1[B]	NA	NA	NA	1[B]	2[B]	NR
Silty soils												
	Above GWL[C]	1[B]	2[B]	2	2[B]	1	1	2	2	NR	NR	NR
	Under GWL[C]	1[B]	NR	NR	2[B]	NR	NR	1	NR	NR	NR	NR
Sandy soils												
	Loose and above GWL[C]	1[B]	NR	NR	2	2	2	1	2	NA	NR	NR
	Loose and below GWL[C]	1[B]	NR	NR	2	NR	NR	1	NR	NA	NR	NR
	Medium to dense	1[B]	NR	NR	2	1	1	1	2	NR	2[B]	NR
Sandy gravel or gravely sands below GWL												
	Loose	2	NA	NA	NA	NA	NA	NA	NR	NA	2	2
	Dense	NR	NA	NA	NA	NR	NA	NA	NR	NA	2	1[D]
Weathered rock		1	NA	2[B]	NA	1	NA	NA	1	2	2	NR

[A] 1 is first choice; 2 is second choice; NR is not recommended; and NA is nonapplicable.
[B] Method is applicable only under certain conditions (see text for details).
[C] GWL is groundwater level.
[D] Pilot hole drilling required beforehand.

dard. The international standard also defines the maximum time allowed between formation of the test pocket and the actual testing as well as the length of opened borehole permitted between tests to avoid further disturbance of the soil or rock. Table 5 shows these recommendations.

The ASTM specifications were originally developed using the French standards as a template. The new international standard includes contributions from several countries and users with diverse experiences making the document more useable and consistent. The ASTM standard often lags behind where updates are required only every 7 years and is revised by a smaller pool of users. Using the international standard as a working document for North American practice would help promote exchange of information and results that could be used in developing improved methods of insertion, testing and interpretation.

A difference between ASTM and the ISO 22476-4 standards should also be pointed out. The international committee does not mention the use of unload-reload loops as part of the Ménard pressuremeter test while ASTM indicates that such a loop is acceptable and that the resulting modulus should be clearly identified as an unload-reload modulus. However, D4719 gives little guidance as to how such an unload-reload loop should be conducted and interpreted. In his Ménard lecture, Briaud (2013) states that he "would strongly discourage the use of the reload modulus" in the prebored PMT because it is not a "standard modulus" and "is not precisely defined".

However, one of the most significant benefits of pressuremeter testing in soils and rocks is the ability to evaluate a modulus *in situ* from the resulting stress-strain measurement during expansion of the test cavity and unload-reload cycles. As shown in Table 6 from Clarke (1995), the moduli obtained from pressuremeter tests are quoted several different ways, making it difficult to arrive at consistent and pertinent use of the pressuremeter moduli in analyses of deformation. It has been shown that the unload-reload modulus appears to be relatively unaffected by the method of insertion since this unloading and reloading is essentially elastic. However, it is necessary to perform the unload-reload loops carefully to ensure that they can be interpreted reliably. For example, Wroth (1984) argued that the stress decrement in an unload-reload loop should be limited to twice the undrained shear strength in undrained PM tests. In sands, the stress decrement should be limited to approximately 40% of the initial effective stress at the start of unloading (Fahey, 1991). In addition, the strain increment level associated with the modulus needs to be reported since the modulus reduces with increasing strain increment level (Clarke, 1995). In drained expansion, the effect of stress level at the start of unloading also needs to be considered as stiffness increases with stress level.

Table 4 - Guidelines for pressuremeter probe placement techniques (adapted from ISO, 2009).

	Probe placing without soil displacement										Probe placing by direct driving
	$1 < dt/dc \leq 1.15$										($dt/dc \approx 0$)
	Rotary drilling				Rotary percussion			Tube pushing, driving or vibrodriving			Driven slotted tube
	OHD *	HA/HAM*	CFA	CD	RP	RPM	STDTM	PT	DT	VDT	DST
Sludge and soft clay	S°	R°	-	-$		-	-$	R TWT	-		A$
Soft to firm clayey soils	R°	R°	S$	S$	-	A$ °	A°	A$	A	-	
Stiff clayey soils	R°	S$ °	R	R °	A$	S°	S$ °	-	A$	-	
Silty soils:											
- above water table	S°	R°	S	S$ °	-	A°	S°	A$	A	A	-
- below water table	A$ °	S$ °	-	A$ °	-	A°	S$°	-	-	-	A$
Loose sandy soils:											
- above water table	S°	R$ °	S	A	-	A°	A°	-$	-	-	-
- below water table	A$ °	S°	-	-$	-	A°	A$°	-$	-	-	A$+
Medium dense and dense sandy soils	R°	R°	R	A °	A	S°	S$°	-	A	A	S$+
Gravels, cobbles	S °	-$°	-$	-$	A	R°	A$°		A	A	R$+
Cohesive non homogeneous soils (*e.g.* boulder clay)	S°	A°	A	S$ °	A	R°	A$ °		A	A	
Loose non homogeneous soils, other soils not specified above (e.g. tills, some alluvial deposits, manmade soils, treated or untreated fills)	S°	A°	A	A °	A	S°	S$ °	-	A	A	S$+
Weathered rock, weak rock	R°	S°	S	S$ °	A $	S°	S$ °		A$	A$	

R	Recommended	OHD	Open hole drilling.	PT	Pushed tube
S	Suited	HA	OHD performed with a hand auger	TWT	Thin wall tube, pushed
A	Acceptable	HAM	OHD performed with a hand auger and mud	DT	Driven tube
-	Not suited	CFA	Continuous flight auger	VDT	Vibro driven tube
(grey)	Not covered by this standard	CD	Core drilling	DST	Driven slotted tube
dt	drilling tool diameter	RP	Rotary percussion		
dc	probe outside diameter	RPM	Rotary percussion with mud		
		STDTM	Slotted tube with inside disintegrating tool and mud circulation		

$ Depending on the actual site conditions and on the evaluation of the operator -

* Rotation speed should not exceed 60rpm and tool diameter not be more than 1.15dc

° Slurry circulation: pressure should not exceed 500kPa and the flow rate 15l/min. The flow can be temporarily interrupted if necessary

\+ Pilot hole with possible preboring techniques: DST, RP and RPM

4.2. Examples of pressuremeter testing

Although Ménard carried out his first pressuremeter tests in the USA, acceptance and utilization of the test has been overall relatively slow compared to other *in situ* tools and techniques such as the cone penetration test. Nevertheless, several firms make use of the PMT either as soil testing services for various clients or directly by geotechnical consultants for site characterization and design of foundations. The use of the PMT in the USA and Canada appears to be localized and is highly dependent on historical use and experience.

One of the early uses of the prebored PMT was in the Chicago area as shown in the original work of Ménard and then later in publications by Kastman (1978), Baker (2005) and Lukas (2010). A paper by Kastman (1978) uses the ratio between the Ménard modulus and the net limit pressure E_M/p_{LM} as an indicator of test quality (or disturbance) and for identifying soils. Figure 9 shows results from Kastman (1978) for a variety of soils tested using the PMT in the USA using the ratio E_M/p_{LM} as a function of the logarithm of the pressuremeter modulus. The summary of results clearly shows a strong linear relationship for each soil type. The ratio was found to be in the range of 8 to 12 for normally consolidated soils and 12 to 20 for overconsolidated soils.

Lukas (2010) discusses his experience with the PMT in Chicago clays which are heavily overconsolidated and cannot be penetrated by the CPT or by sampling with thin walled Shelby tubes. Up to the 1970's, properties were obtained from the SPT where penetration values N were generally greater than 50 to 100. The use of the pressuremeter was well-received as it was easily deployed in the field and far less expensive than full scale load tests. Bearing capacity and settlement predictions in 35 years of experience have correlated reasonably well. In his paper he discusses two cases. Settlement of a sixty-one story building founded on drilled piers in "hardpan" was estimated using pressure-

Table 6 - Terms used to define moduli taken from pressuremeter tests (Clarke, 1995).

Symbol	Definition
G_i	Initial secant shear modulus
E_M	Ménard modulus
G_{ur}	Secant shear modulus from an unload/reload cycle
G_u	Secant shear modulus from an unloading curve
G_r	Secant shear modulus from a reloading curve
E_m	Secant elastic modulus from an unloading curve
E_{m^*}	Secant elastic modulus from a reloading curve
E_{mo}	Maximum elastic modulus from an unloading curve
E_{ro}	Maximum elastic modulus from a reloading curve
G_n	Secant shear modulus measured over strain range n%
G_o	Maximum shear modulus
G_s	Equivalent element modulus
G_{uro}	Equivalent shear modulus at the in-situ effective stress

Table 5 - Maximum continuous drilling or driving stage length before testing (adapted from ISO, 2009).

Soil type	Maximum continuous drilling or tube driving stage length (m)		
	Adapted rotary drilling[b]	Rotary percussive drilling[b]	Tube pushing, driving and vibrodriving[c]
Sludge and soft clay, soft clayey soil	1[a]	-	1[a]
Firm clayey soils	2	2	3
Stiff clayey soils	5	4	4
Silty soils: above ground water table	4	3	3
Silty soils: below water table	2[a]	1[a]	-
Loose sandy soils: above ground water table	3	2	-
Loose sandy soils: below water table	1[a]	1[a]	-
Medium dense and dense sandy soils	5	5	4
Coarse soils: gravels, cobbles	3	5	3
Coarse soils with cohesion	4	5	3
Loose non homogeneous soils, other soils not specified above (*e.g.* tills, etc.)	2	3	2
Weathered rock, weak rock	4	5	3

[a]: Or the required interval between two successive tests.
[b]: Refer to Table C.2 for acceptable techniques.
[c]: Not applicable to STDTM technique (see C.2.6.3).

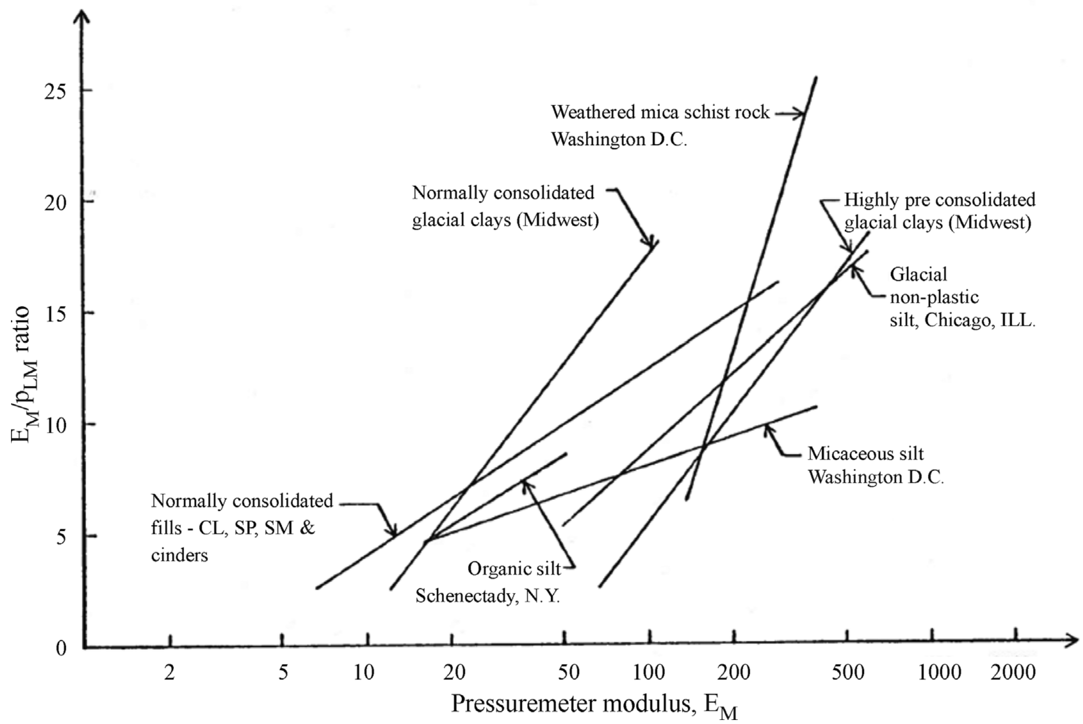

Figure 9 - Pressuremeter ratio E_M/p_{LM} as a function of the pressuremeter modulus E_M (Kastman, 1978).

meter data. The estimated movements agreed well with the measurements in the field when the bearing pressures were below the creep pressure and the pressuremeter modulus was used in settlement calculations. The second case dealt with bearing capacity of a mat foundation for a high rise to be founded on the overconsolidated clay. Using the pressuremeter results, the calculated bearing capacity agreed well with that obtained by more conventional approaches to design when using undrained shear strengths derived from the PM test.

Similarly to Lukas (2010), Baker (2005) describes his experience with the pressuremeter in the Chicago area soils as well as in other parts of the world. The PMT has been used in Chicago since 1969 and has allowed less conservative design of drilled piers and caissons than is obtained using parameters derived from SPT and unconfined compression tests, increasing allowable pressures by more than 50%. From his experiences in highly consolidated glacial tills and medium dense to dense deposits, using the pressuremeter theory and appropriate PMT results allows reliable predictions of settlement magnitudes of deep foundations under working load. The confidence in reliably predicting settlements has afforded them to be more innovative in their designs. Baker suggests that for reliable settlement predictions, the dead load bearing stress plus the overburden pressure should not exceed the average creep pressure. However, there are cases where such an approach is not applicable, *e.g.* weakly cemented sandstone. Their settlement evaluation is done either using the Ménard rules or elastic theory with an equivalent Young's modulus derived from the PMT. Their approach has been based on local experience and performance monitoring of other similar foundations in similar soils. This often leads to company-specific empirical relationships.

Pressuremeter testing has also been carried out extensively in the Miocene clay in the Richmond, Virginia area (Martin & Drahos, 1986). This clay is highly preconsolidated and hard in consistency. This material is also sensitive and highly plastic. From their work they developed a relationship between the constrained modulus from the reload portion of their consolidation tests and the pressuremeter modulus, E_M. The results shown in Fig. 10 were found to be much different than what was previously published by Lukas & DeBussy (1976) for Chicago clays. They also developed a correlation between the PMT creep pressure and the preconsolidation pressure (p_c) and recommended a conservative estimate of p_c could be obtained from the expression: $p_c = 0.6\ p_f$.

Based on the technical literature and geotechnical reports reviewed by the authors, a number of different versions of the pressuremeter are in use as outlined in Table 7. By far the most common encountered was the Texam pressuremeter. This is a monocellular version of the prebored PM developed by Briaud and his co-workers (Briaud, 1992). There is also a high capacity version of this probe, the Probex, designed for testing in rock. According to Briaud (2005), the Texam was designed:

"to simplify and make safer (no pressurized gas bottle) the operation and the repairing of the Ménard

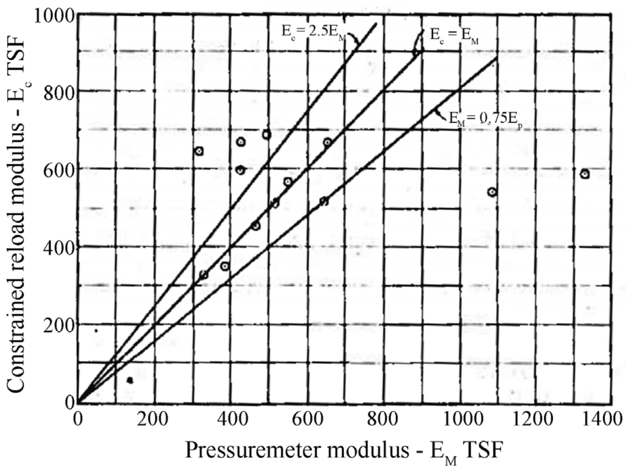

Figure 10 - Relationship between Constrained Reload Modulus from consolidation tests and Pressuremeter Modulus (after Martin & Drahos, 1986) (Note: 1 TSF = 95.76 kPa).

pressuremeter while allowing for more versatility in the types of possible PMT tests (e.g.: cyclic tests).”

Briaud (1992) stated that comparison testing between the Texam and the triple cell Ménard probes showed that the results were comparable provided the length to diameter ratio (*L*/*D*) of the monocell probe exceeded 6. Since then, the Texam probe appears to have become the most common version of the probe in published case histories of prebored testing. However, the standard GAM model series is the preferred tool in Europe and complies with European standards. The Pencel probe has also been the subject of considerable research, particularly in Florida (Cosentino *et al.*, 2006; Messaoud & Nouaouria, 2010; Messaoud *et al.*, 2011). At 35 mm diameter, it is much smaller than most other probes. A major focus of this work has been the derivation of p-y curves for the design of piles under lateral loads.

Some testing has also been done using a Cambridge style monocell probe installed in a prebored hole which is inflated by gas and has strain feeler arms at 120 degree intervals at mid-height of the probe. Test curves obtained with this probe only expand to 10% to 15% cavity strain and so cannot be continued to sufficient cavity strain to achieve a doubling of the cavity volume. Consequently, Ménard-type limit pressures also have to be obtained by extrapolation for this tool. However, most of the cases involving this approach to pressuremeter testing were based on test procedures that did not follow ASTM D4719 and were analyzed and interpreted using computer aided modelling (CAM) based on simple constitutive models of soil behavior. The tests were interpreted to obtain the fundamental properties of the materials tested which were then considered in conjunction with other geotechnical and geological information collected by the site characterization.

Jefferies *et al.* (1987) used CAM and SBPM testing to determine a profile of effective stress in Beaufort Sea clays. They argued that the lateral stress profile did not agree with estimates based on overconsolidation ratios obtained from consolidation tests and emphasized the importance of field testing. A similar recent example of such an approach is presented in Hoopes & Hughes (2014) in which pressuremeter test results were used in the estimation of the *in situ* lateral stress profile of glacially over-ridden glaciolacustrine clay by seeking a pressure during unloading at which no expansion or contraction occurred.

In a paper on the use of *in situ* tests for design of drilled shafts in coarse granular deposits, Rabab’ah *et al.* (2012) described an ingenious solution developed by Durkee *et al.* (2007) to the preparation of a test pocket in such challenging soil conditions. They drilled an oversized hole (127 mm) using a down-hole air hammer and left a casing in place. They then tremie-grouted the hole with a weak grout placed through a central tube while withdrawing the casing. After a curing period of 2 weeks, they drilled a 76 mm diameter hole through the grout which left a 20 mm annulus around the wall of the pocket in which the PM was installed. The cement grout was designed to be brittle and to fracture early in the expansion of the pressuremeter. The test pocket preparation sequence is illustrated in Fig. 11. A total of 45 pressuremeter tests carried out in this way using a Cambridge-style monocell probe were considered to be of good to excellent quality and were interpreted to give geotechnical properties of the soil. The interpretation took ac-

Table 7 - Most common pressuremeters encountered in north american document review.

Model	Design	Method of insertion	Method of inflation	Method of strain measurement
Menard	Triple cell	Prebored	Hydraulic	Volume
Texam	Monocell	Prebored	Hydraulic	Volume
Probex*	Monocell	Prebored	Hydraulic	Volume
Cambridge type	Monocell	Prebored (some self-boring)	Gas	3/6 strain arms
Pencel	Monocell	Driven or pushed	Hydraulic	Volume
Oyo elastometer 100	Monocell	Prebored	Gas	2 feeler arms

*High capacity version of Texam.

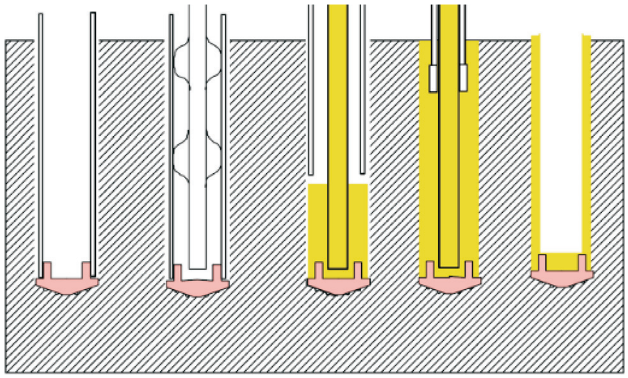

Figure 11 - Schematic of drilling procedure in gravelly soils (After Durkee *et al.*, 2007).

count of the presence of the grout. Despite the likelihood of some disturbance of the soil tested, this procedure allowed some assessment of soil properties which would have otherwise been impossible given the difficulty of drilling and sampling in such soils.

The pressuremeter continues to be of interest to researchers. Dafni (2013) presents a study of pressuremeter testing in weak rock using a Cambridge-type monocell instrument in which he applies CAM based on representative constitutive models for rock. A comparison of measured data and a curve simulated using the Hoek-Brown model initiated by Yang and Zou (2011) is shown in Fig. 12. Jacobs (2003) carried out Ménard-style PMTs to study the use of the pressuremeter for estimating the side shear capacity of drilled shafts in Florida limestone. An example of his test results is shown in Fig. 13. The existing approach was based on laboratory testing of intact rock core and there was interest in determining whether the PMT would give data more representative of the rock mass. He found that an empirical design method for side shear capacity by the Laboratoire Central des Ponts et Chaussées (LCPC) performed reasonably well and recommended that it be studied further. He observed that the method required further calibration by comparison with load testing before design use in Florida.

5. Discussion

Pressuremeter testing has not yet attained widespread acceptance in North American geotechnical engineering practice. It tends to be seen as being too expensive for routine practice. A common view of the test is expressed by the Nevada Department of Transportation as follows:

> *The pressuremeter test is a delicate tool, and the test is very sensitive to borehole disturbance. The data may be difficult to interpret for some soils, but it provides the advantage that due to the large size of the pressuremeter cell it is less likely to be adversely affected by gravel in the soil. This test requires a high level of technical expertise to perform, and is time consuming.*

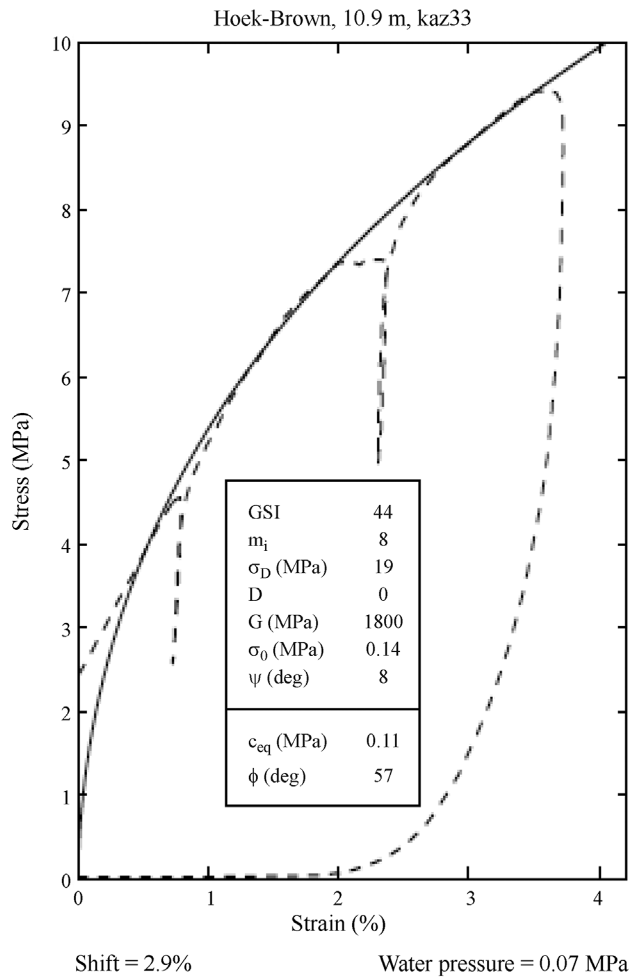

Figure 12 - Measured and simulated PMT curves in Weak Rock (Dafni, 2013).

The situation is complicated by the fact that a range of instruments and test procedures are in use. The shape of the pressuremeter test curve in any soil or rock is affected by the insertion method, the geometry of the instrument and by details of the test procedures. Consequently, tests carried out with different instruments and procedures will obtain different test curves in a given material, with the magnitude of the variation being material-dependent. There is evidence that engineers continue to interpret their test results using the Ménard rules despite their test data not being obtained by instruments and procedures conforming to those rules.

For conventional foundation engineering in sands and finer soils which are normally to moderately overconsolidated, the pressuremeter offers no advantage over faster and more robust *in situ* tests such as the seismic CPTu and DMT except in unusual cases where pressuremeter data can provide additional insight. However, the prebored PMT is better-suited than conventional penetration tests or drilling and sampling to the characterization of the mechanical behavior of hard or very dense soils, coarse grained soils, re-

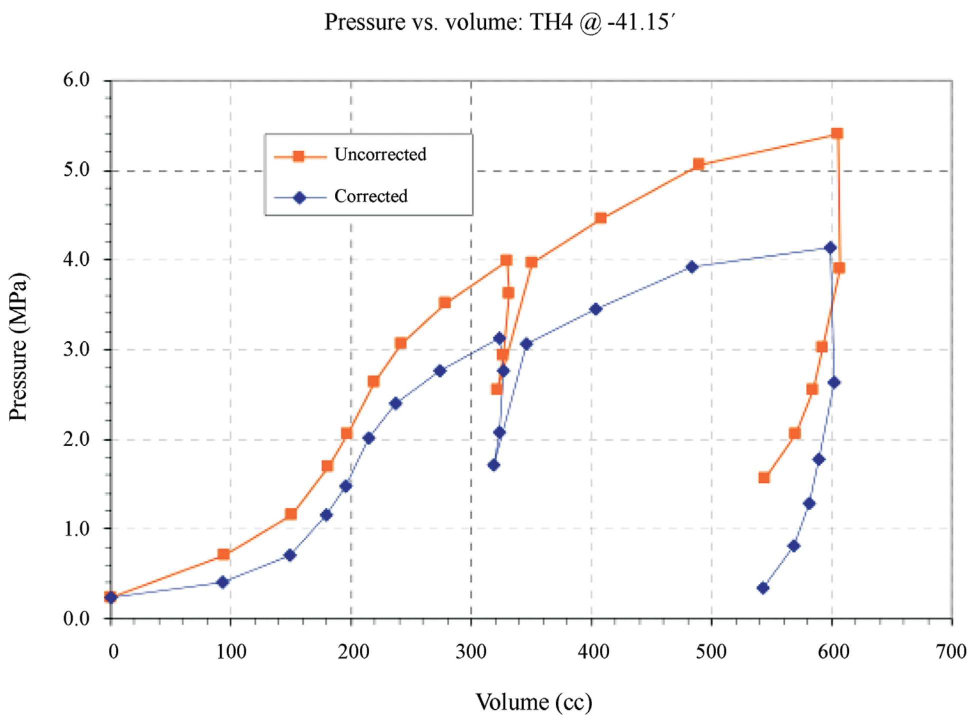

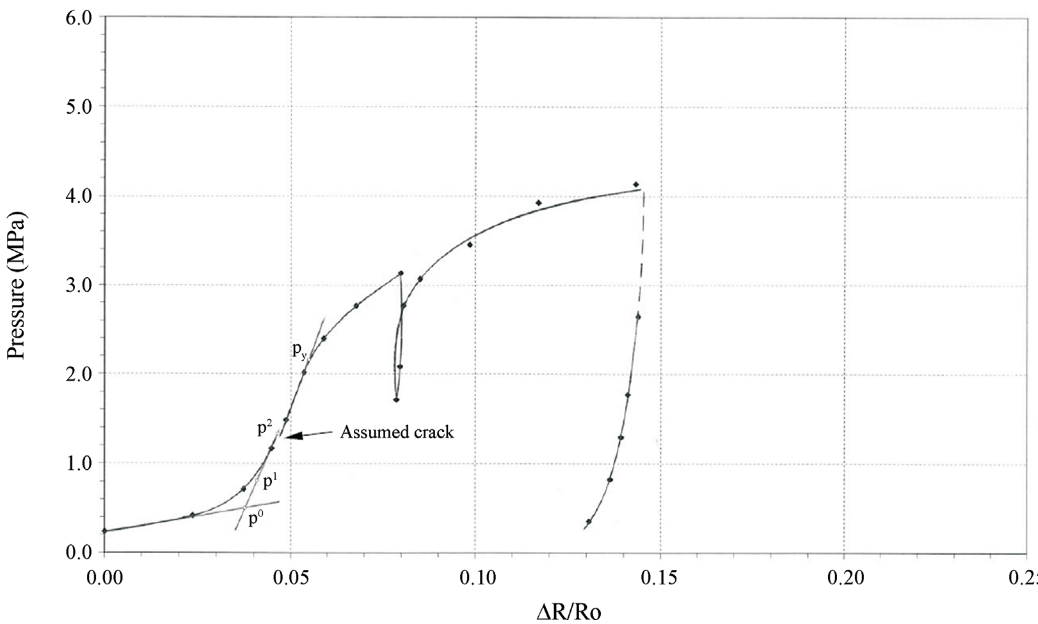

Figure 13 - Example of PMT in Limestone (Jacobs, 2003).

sidual, saprolitic or lateritic soils, soft and fractured rocks, frozen ground and ice.. The challenge then becomes to drill a suitable test pocket to allow pressuremeter tests to be carried out successfully. Briaud (2013) emphasizes that this is "the most important and most difficult step in a quality pressuremeter test".

Where pressuremeter testing is carried out, the procedures set out in the current version of the ASTM standard on prebored pressuremeter testing are not consistent with those of the European standard. The major difference is the option to include an unload-reload loop at some stage of the expansion. The latter guidelines are based on the decades of experience in France of successful use of PMT parameters directly for foundation design. This difference compromises the ability of engineers in North America to benefit from that experience.

One reason for the slow adoption of the PMT in North America is the lack of familiarity with the test and its interpretation and use. This can in part be traced to the education system. Benoît (2013), using a questionnaire distributed to members of the United States Universities Council on Geotechnical Education and Research (USUCGER), discussed the status of current pressuremeter activities in the United States of America. A questionnaire was widely distributed to academics to assess the level and type of activities in research and teaching. One of the questions asked how much lecture time was devoted to each *in situ* test in graduate courses. The results from this question are shown in Fig. 14. For the SPT and CPT, 25% of the programs spend less than 30 min while another 25% dedicate 1-2 h and about 13% cover the material in greater detail, using over 3 h. For the DMT, PMT and geophysical methods, approximately 40% of the programs spend only 10 to 30 min on these topics while about 15% of them use an hour or more. It was somewhat surprising that as much as 20% of the programs spend less than 10 min on the FVT, DMT, PMT and geophysical methods.

In this survey, the perception was that certain tools such as the pressuremeter are time consuming and too complex. However, if future and current geotechnical engineers are not taught the basic use and interpretation of the various test methods, opportunities to improve the efficiency and safety of our designs are likely to continue their slow progress and, of course, more sophisticated tests are unlikely. Proper training and understanding of more sophisticated test methods will lead to greater use of field methods such as the PMT.

6. Conclusions

While the PMT has been available in North America since the late 1950's, it has not achieved wide acceptance in geotechnical engineering practice. In sandy and finer soils which have not been subject to heavy overconsolidation or other processes of densification, the PM is slower and more expensive for routine use and cannot compete with more conventional tests such as the CPTu, DMT or SPT. It does find use in such soils for design problems where the consequences of poor geotechnical performance justify more extensive design and analysis. Examples of such uses would be in the derivation of p-y curves for the design of laterally loaded piles and the estimation of stiffness for detailed assessment of differential settlement. Where fundamental properties are derived from a Cambridge-style approach to PM testing, input parameters for detailed numerical analysis can be derived.

The PMT has been used extensively in areas of the US and Canada where hard or very dense soils are encountered such as in glacial tills and heavily overconsolidated clays, dense/hard residual soils, and very coarse granular soils. It has also been used in soft and fractured rock, frozen soils and ice and as a tool for quality control of ground improvement. Where the test has found favor, it has generally been where conventional approaches to site characterization yield uncertain or insensitive results (what is the difference in soil parameters between an SPT blow count of 50 for 1 inch and 100 for 1 inch?). As the methods of interpretation have a basis in theory, it is possible to derive meaningful strength and deformation parameters for all materials in which a PMT expansion curve can be obtained. It is also possible to relate the measured parameters to the extensive body of experience gained with the use of the PM for foundation design in Europe and elsewhere.

In order for the test to gain wider acceptance in engineering practice in North America, the following measures are required:

- the teaching of the theory and principles of PM testing at graduate schools must be improved. This will increase

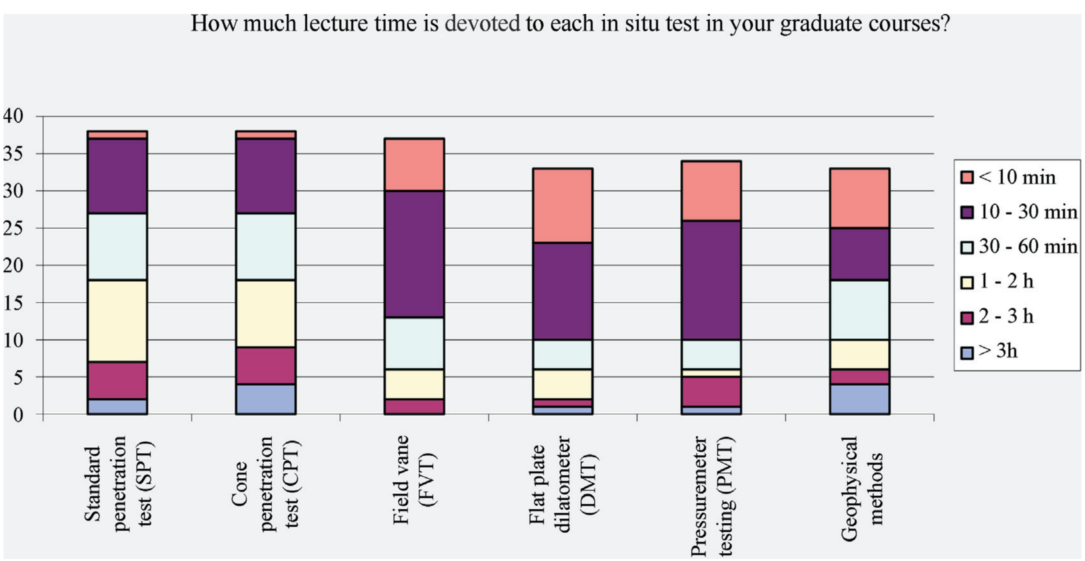

Figure 14 - *In Situ* tests lecture time in us graduate geotechnical courses (based on 40 respondents) (Benoît, 2013).

the likelihood that the PMT will be used appropriately and will result in a positive experience.

- equipment and test procedures should be more strictly standardized so that they produce data that are consistent with the design methods being employed. If the Ménard rules are to be invoked, then the test should be carried out according to the Ménard rules, *i.e.* no unload-reload cycles. If the Cambridge-type approach is to be used, then the ASTM D4719 test procedures are inapplicable and alternative equipment and procedures should be followed.
- it should be recognized that the PMT is most applicable in difficult ground conditions provided a suitable test pocket can be prepared.
- more full scale load testing and monitoring of foundations of North American projects are required to verify and promote the applicability of PM based design methods.

As stated by Casagrande (1966) when dealing with projects and subsurface conditions in Richmond, Virginia, an effort had to be made to "collect and evaluate systematically information on the subsoil conditions, and on the design and performance of buildings, in Richmond. This would eventually lead to a set of relatively simple and reliable guide rules for the design of building foundations in this city." The Ménard rules have essentially been derived and improved following this philosophy. The pressuremeter is a tool that has been insufficiently used in North America and, at times, has been used inappropriately. A revival of the use of the pressuremeter is essential, especially as numerical tools require more sophisticated parameters for analysis.

References

AFNOR (2012) Justification des Ouvrages Géotechniques - Normes d'Application Nationale de l'Eurocode 7 - Fondations Profondes, norme NF P94-262.

ASTM D4719 (2007) Standard Test Methods for Prebored Pressuremeter Testing in Soils. Annual Book of ASTM Standards, Section 4, v. 04.08.

Baguelin, F.; Jézéquel, J.-F.; Le Mée, H. & Le Méhaute, A. (1972) Expansions of Cylindrical Probes in Soft Soils. Journal of Soil Mechanics and Foundation Design, ASCE, v. 98:SM11, p. 1129-1142.

Bandis, C. and Lacasse, S. (1986) Interpretation of Self-Boring and Push-In Pressuremeter Tests in Holmen Sand. NGI Report No. 40019-21, Oslo.

Baker, C.N. (2005) The use of the Menard Pressuremeter in innovative foundation design from Chicago to Kuala Lumpur. Proceedings of the International Symposium 50 Years of Pressuremeters, Gambin, Magnan and Mestat, Editors, Presses de l'ENPC/LCPC, 22-24 August, Paris, France, v. 2, p. 63-95.

Benoît, J. (2013) Current status of pressuremeter testing education in the USA. Parallel International Symposium on Pressuremeters, 18th International Conference on Soil Mechanics and Geotechnical Engineering, Paris, France.

Benoît, J.; Atwood, M.J.; Findlay, R.C. & Hilliard, B.D. (1995) Evaluation of jetting insertion for the self-boring pressuremeter. Canadian Geotechnical Journal, v. 32, p. 22-39.

Briaud, J.-L. (2013) Ménard Lecture: The pressuremeter Test: Expanding its use. Proceedings of the 18th International Conference on Soil Mechanics and Geotechnical Engineering, Paris, France, p. 107-126.

Briaud, J.-L. (2005) The pre-boring pressuremeter: some contributions. Proceedings of the International Symposium 50 Years of Pressuremeters, Gambin, Magnan and Mestat, Editors, Presses de l'ENPC/LCPC, 22-24 August, Paris, France, v. 2, p. 103-124.

Briaud, J.-L. (1992) The Pressuremeter. A.A. Balkema Publications, Rotterdam, 322 p.

Briaud, J.-L. & Shields, D.H. (1979) A special pressuremeter and pressuremeter test for pavement evaluation and design. Geotechnical Testing Journal, v. 2:3, p. 143-151.

Bustamante, M.; Gambin, M. & Gianeselli, L. (2009) Pile Design at Failure Using the Ménard Pressuremeter: An Up-Date. French contributions to International Foundation Congress & Equipment Expo '09 Contemporary Topics in In Situ Testing, Analysis, and Reliability of Foundations, ASCE Geotechnical Special Publication No. 186, Orlando, Florida, p. 127-134.

Casagrande, L. (1966) Subsoils and Foundation Design in Richmond, VA. Journal of the Soil Mechanics and Foundation Design, SM5, September, p. 109-126.

Cassan, M. (2005) Historique des Pressiomètres. Proceedings of the International Symposium 50 Years of Pressuremeters, Gambin, Magnan and Mestat, Editors, Presses de l'ENPC/LCPC, 22-24 August, 2005, Paris, France, v. 2, p. 125-200.

Clarke, B.G. (1995) Pressuremeters in Geotechnical Design. Blackie Academic & Professional, city, 364 p.

Clarke, B. & Gambin, M.P. (1998) Pressuremeter testing in onshore ground investigations. A report by the ISSMGE Committee 16, International Conference on Site Characterization, Atlanta.

Clayton, C.R.I.; Matthews, M.C. & Simons, N.E. (1995) Site Investigation. Blackwell Science, city, 584 p.

Cosentino, P.; Kalajian, E.; Stansifer, R.; Anderson, J.B.; Kattamuri, K.; Sundaram, S.; Messaoud, F.; Misilo, T. & Cottingham, M. (2006) Standardizing the pressuremeter test for determining p-y curves for laterally loaded piles. FDOT Research Report, Contract BD 658.

Dafni, J. (2013) The Analysis of Weak Rock Using the Pressuremeter. M.Sc. Thesis, Department of Civil Engineering, University of Washington, Seattle.

Drahos, E.G. (2014) Personal communication.

Durkee, D.; Ackerman, F.; Smith, D. & Rucker, M. (2007) Borehole preparation technique for pressuremeter testing in sand gravel and cobbles. Geotechnical Special Publication No. 162, Geo-Denver 2007, February 18-21, 2007, Denver, Colorado.

Fahey, M. (1991) Measuring shear modulus in sand with the self-boring pressuremeter. deformation of soils and displacements of structures. Proc. X Eur. emif. SMFE, Florence,Italy, Balkema, Rotterdam, v. 1, p. 73-76.

Ferreira, R.S. & Robertson, P.K. (1992) Interpretation of undrained self-boring pressuremeter test results incorporating unloading. Canadian Geotechnical Journal, v. 29:6, p. 918-928.

Gambin, M.; Flavigny, E. & Boulon, M. (1996) Le module pressiométrique: Historique et modélisation. XI Colloque Franco-Polonais en Mécanique des Sols et des Roches Appliquée, Gdansk, Poland.

Gauthier, A.; Gonin, H. & Ménard, L. (1954) Travail de fin d'étude. Ecole Nationale des Ponts et Chaussées, Paris, France.

Hoopes, O. & Hughes, J. (2014) In Situ Lateral Stress Measurement in Glaciolacustrine Seattle Clay Using the Pressuremeter. Journal of Geotechnical and Geoenvironmental Engineering, 10.1061/(ASCE)GT.1943-5606.0001077, 04013054.

Houlsby, G.T. & Carter, J.P. (1993) The Effects of Pressuremeter Geometry on the Results of Tests in Clay. Géotechnique, v. 43, p. 567-576.

Houlsby, G.T. & Withers, N.J. (1988) Analysis of Cone Pressuremeter Test in Clay. Géotechnique, v. 38:4, p. 575-587.

Hughes, J. M. O. and Robertson, P. K. (1985). Full-Displacement Pressuremeter Testing in Sand. Canadian Geotechnical Journal, v. 22, p. 298-307.

ISO/FDIS 22476-4:2009(E) - ISO/TC 182/SC 1 (2009) Geotechnical Investigation and Testing - Field Testing - Part 4: Ménard Pressuremeter Test.

Jacobs, S.A. (2003) Insitu Measurement of Florida Limestone Modulus and Strength Properties, M. Eng. Thesis, University of Florida.

Jefferies, M.G. (1988) Determination of Horizontal Geostatic Stress in Clay with Self-Bored Pressuremeter. Canadian Geotechnical Journal, v. 25, p. 559-573.

Jefferies, M.G.; & Shuttle, D.A. (1995) Disturbance does not prevent obtaining reliable parameters from sbp tests, the pressuremeter and its new avenues. Proceedings of the Fourth International Symposium on Pressuremeters (ISP4), G. Ballivy (ed) Sherbrooke, Québec, Canada, May 17-19, A.A. Balkema, Publisher, p. 177-183.

Jefferies, M.G.; Crooks, J.H.A.; Becker, D.E. & Hill, P.R. (1987) Independence of geostatic stress from overconsolidation in some beaufort sea clays. Canadian Geotechnical Journal, v. 24:3, p. 342-356.

Kastman, K. (1978) In-Situ testing with the Ménard pressuremeter. Proceedings of a Symposium on Site Exploration in Soft Ground using In Situ Techniques, Alexandria, Virginia, Final Report, p. 206-223.

Ladanyi, B. (1995) A Brief History of Pressuremeter. Proceedings of the 4th International Symposium on the Pressuremeter and its New Avenues, Sherbrooke, Québec, Canada. Edited by G. Ballivy, A.A. Balkema, p. 5-23.

Long, M. (2008) Design Parameters from In Situ Tests in Soft Ground - Recent Developments. Proceedings of the Third International Conference on Geotechnical and Geophysical Site Characterization ISC-3, Taipei, Taiwan, p. 89-116.

Lukas, R.G. (2010) Pressuremeter Testing for Foundation Design. Art of Foundation Engineering Practice, ASCE Geotechnical Special Publication No. 198, Geo-Florida, p. 392-400.

Lukas, R.G. & De Bussy, B.L. (1976) Pressuremeter and Laboratory Test Correlations for Clays. ASCE Journal of Geotechnical Engineering, v. 102:9, p. 945-962.

Martin, R.E. & Drahos, E.G. (1986) Pressuremeter Correlations for Preconsolidated Clays. Proceedings of In Situ '86, ASCE, June, Blacksburg, Virginia, p. 206-220.

Ménard, L. (1957) An Apparatus for Measuring the Strength of Soils in Place. Thesis submitted in partial fulfillment of the requirements for the degree of Master of Science in Civil Engineering, University of Illinois, 50 p.

Messaoud, M.S.M.F. & Cosentino, P.J. (2011) PENCEL pressuremeter test evaluation for developing p-y curves for driven piles. ACEE International Journal on Transportation and Urban Development, v. 1:2, p. 14-18.

Messaoud, F. & Nouaouria, M.S. (2010) The use of PENCEL pressuremeter test for underground structures. International Journal of Civil Engineering, v. 8:1, p. 33-43.

Palmer, A.C. (1972) Undrained Plane-Strain Expansion of a Cylindrical Cavity in Clay: a Simple Interpretation of the Pressuremeter Test. Geotechnique, September, v. 22:3, p. 451-457.

Rabab'ah, S.R.; Niedzielski, J.C. & Durkee, D.B. (2012) Use of in-situ tests for design of drilled shafts in coarse granular deposits. GeoCongress 2012, p. 265-274.

Reid, W.M.; St. John, H.D.; Fyffe, S. & Rigden, W.J. (1982) The push-in pressuremeter. Proceedings of the Symposium on the Pressuremeter and its Marine Applications, Paris, France.

Reiffsteck, P. (2009) ISP5 Pile Prediction Revisited. French contributions to International Foundation Congress & Equipment Expo '09, Contemporary Topics in In Situ Testing, Analysis, and Reliability of Foundations, ASCE Geotechnical Special Publication No. 186, Orlando, Florida, p. 50-57.

Reiffsteck, P. & Burlon, S. (2012) Traitement des Incertitudes dans le Calcul Géotechnique avec la Nouvelle Norme Fondations Profondes NF P 94 262, Tunisia.

Roy, D.; Campanella, R.; Byrne, P.; & Hughes, J. (2002) Undrained Anisotropic Monotonic Behavior of Sand from In Situ Tests. Journal of Geotechnical and Geoenvironmental Engineering, v. 128:1, p. 85-91.

Schnaid, F.; Ortigao, J.A.R.; Mántaras, F.M.; Cunha, R.P. & MacGregor, I. (2000) Analysis of self-boring pressuremeter (SBPM) and Marchetti dilatometer (DMT) tests in granite saprolites. Canadian Geotechnical Journal, v. 37:4, p. 796-810,

Shuttle, D.A. & Jefferies, M.G. (1995) A practical Geometry Correction for Pressuremeter Tests in Clay. Géotechnique, v. 45:3, p. 549-553.

Withers, N.J.; Schaap, K.H.J. & Dalton, J.C.P. (1986) The Development of a Full Displacement Pressuremeter. Proceeding of the Symposium on Pressuremeter and its Marine Applications, ASTM STP 950, p. 38-56.

Wroth, C.P. (1984) The Interpretation of In-Situ Soil Tests. 24th Rankine Lecture, Géotechnique, v. 34:4, p. 449-489.

Wroth, C.P. & Hughes, J.M.O. (1972) An Instrument for the In Situ Measurement of the Properties of Soft Clays. Report of the Department of Engineering, University of Cambridge, CUED/C, Soils TR 13.

Yang. X.-L. & Zou, J.-F. (2011) Cavity Expansion Analysis with Non-linear Failure Criterion. Proceedings of the Institution of Civil Engineers - Geotechnical Engineering, v. 164, p. 41-49.

Yeung, S.K. & Carter, J.P. (1990) Interpretation of the Pressuremeter Test in Clay Allowing for Membrane End Effects and Material Non-homogeneity. Pressuremeters, London, Thomas Telford Limited, p. 199-208.

Yu, H.S. (2004) James K. Mitchell Lecture: In Situ Soil Testing: from Mechanics to Interpretation. Proceedings ISC-2 on Geotechnical and Geophysical Site Characterization. Millpress, Rotterdam.

Penetration Rate Effects on Cone Resistance: Insights From Calibration Chamber and Field Testing

R. Salgado, M. Prezzi

Abstract. Cone penetration in mixed or intermediate soils (soils containing mixtures of sand, silt and clay) is neither fully drained nor fully undrained at the standard cone penetration rate of 20 mm/s. Considerable research, mainly relying on centrifuge tests, has been undertaken to quantify the effects of penetration rate (and thus partial drainage) on cone resistance. In this paper, the effects of penetration rate on cone resistance in saturated clayey soils were investigated by performing field tests and miniature cone penetration tests in a calibration chamber. The field tests were performed at sites especially selected to span the range of drainage conditions from fully drained to fully undrained. The calibration chamber tests, using both conical and flat-tip penetrometers, were performed at different penetration rates in two specimens prepared by mixing kaolin clay and sand with different mixing ratios and one-dimensionally consolidateding the mixtures. A correlation between cone resistance and drainage conditions is established based on the cone penetration test results. The transitions from no drainage to partial drainage and from partial drainage to full drainage are defined as a function of penetration rate normalized with respect to the penetrometer diameter and the coefficient of consolidation.
Keywords: cone penetration, CPT, penetration rate, mixed soils.

1. Introduction

The cone penetration test (CPT) has become one of the preferred methods of site characterization partly due to its simplicity, partly as a result of the development of cone resistance-based correlations for footing design (Schmertmann, 1970; Mayne & Poulos, 1999; Lee & Salgado, 2002; Lee *et al.*, 2005; Foye *et al.*, 2006; Lee *et al.*, 2008; O'Loughlin & Lehane, 2010), pile design (Lee & Salgado, 1999; Lee *et al.*, 2003; Jardine *et al.*, 2005; Kolk *et al.*, 2005; Xu *et al.*, 2008; Seo *et al.*, 2009; Foye *et al.*, 2009; Niazi & Mayne, 2013) and liquefaction resistance estimation (Seed & De Alba, 1986; Stark & Olson, 1995; Salgado *et al.*, 1997; Robertson & Wride, 1998; Carraro *et al.*, 2003). The apparent simplicity of the CPT, however, hides considerably complex mechanics (Salgado, 2013). One source of complexity is possible partial drainage during cone penetration.

The standard rate of penetration in a CPT is 20 ± 5 mm/s according to ISO 22476-1 and ASTM D 5778. This standard penetration rate is specified regardless of soil type. Cone penetration at the standard rate is fully drained for clean sand and fully undrained for pure clay. For soils consisting of mixtures of silt, sand and clay, cone penetration may take place under partially drained conditions at the standard penetration rate, depending on the ratios of these three broad particle size groups. This means that use of correlations developed for sand (in which tests would be drained at standard rates of penetration) or clay (in which tests would be undrained at standard rates of penetration) will not work for soil in which penetration at the standard rate takes place under partially drained conditions.

Physically, drainage conditions during penetration are important because, if the penetration rate is sufficiently low for a given clayey soil, the soil ahead and around the advancing cone partially consolidates during penetration, thereby developing greater shear strength and stiffness than it would have under undrained conditions. The closer the conditions are to fully drained during penetration, the higher the value of q_c. Another physical process that is at play for soils with large clay content for penetration under fully undrained conditions is the effect of the rate of loading on shear strength due to the "viscosity" (rate dependence of the shear strength) of clayey soils. The higher the penetration rate is, the larger the undrained shear strength s_u (and therefore q_c) is. These two physical processes - drainage and loading rate effects - have opposite effects on q_c.

A number of studies (Bemben & Myers, 1974; Campanella *et al.*, 1983; Kamp, 1982; Powell & Quarterman, 1988; Rocha Filho & Alencar, 1985; Roy *et al.*, 1982; Tani & Craig, 1995) have considered rate effects in CPT testing for both clays and sands. Results of some field cone penetration tests and centrifuge test results indicated that cone resistance increases and excess pore pressure drops as the penetration rate decreases (Campanella *et al.*, 1983; House *et al.*, 2001; Randolph & Hope, 2004; Rocha Filho & Alencar, 1985; Mahmoodzadeh & Randolph, 2014).

The degree of consolidation during penetration depends on the cone penetration rate, cone diameter, and consolidation coefficient of the soil (Finnie & Randolph, 1994;

Rodrigo Salgado, Ph.D., Professor, Lyles School of Civil Engineering, Purdue University, West Lafayette, IN, USA. e-mail: rodrigo@purdue.edu.
Monica Prezzi, Ph.D., Professor, Lyles School of Civil Engineering, Purdue University, West Lafayette, IN, USA. e-mail: mprezzi@purdue.edu.
Submitted on May 30, 2014; Final Acceptance on December 15, 2014; Discussion open until April 30, 2015.

House *et al.*, 2001; Randolph & Hope, 2004; Mahmoodzadeh & Randolph, 2014). These factors can be used to obtain a normalized penetration rate V:

$$V = \frac{vd_c}{c_v}$$

where v = cone penetration rate; d_c = cone diameter; and c_v = coefficient of consolidation that would be obtained from a one-dimensional consolidation test performed on a sample with the same fabric orientation as it would have in the field. As pore pressure is generated during cone penetration, the generated hydraulic gradients in the soil around the cone will determine flow direction. Therefore, normalization with respect with c_v is not necessarily correct. Most results reported in the literature were normalized with respect to c_v, so this normalization will also be used in the present paper. Conceptually, penetration resistance would vary with rate of penetration, as illustrated in Fig. 1, which shows that penetration resistance is highest at low penetration rates, when penetration is drained, and then transitions to its lowest value at sufficiently high rates of penetration. The research questions in connection with this are:

1) Is there a single backbone curve if cone resistance is normalized in some manner, for all soil types?
2) For increasing penetration rates, what are the values of normalized penetration rates V_d and V_u at which penetration transitions to partially drained and then to fully undrained penetration?
3) If V_u is seen, alternatively, as the rate at which penetration resistance stabilizes at its lowest value, how does soil viscosity affect its value?

The centrifuge has been the primary tool used to study these questions. Figure 2 shows results from a few previous studies (Oliveira *et al.*, 2011; Randolph & Hope, 2004; Schneider *et al.*, 2007; Mahmoodzadeh & Randolph, 2014). The soil tested by Randolph & Hope (2004), Schneider *et al.* (2007) and Mahmoodzadeh & Randolph (2014) was a kaolin clay, while the soil tested by Oliveira *et al.* (2011) was silty mine tailings. The plot shows the ratio of normalized cone resistance ($q_{c,p}$ under drained, partially drained or undrained conditions divided by the undrained value of cone resistance $q_{c,u}$) *vs.* the normalized rate $V = vd_c/c_v$ of penetration, discussed earlier. The values of this ratio range between roughly 2.7 and 3.7. The limiting normalized penetration rate for drained penetration varies in a range of roughly 0.01 to 1, but the limiting normalized penetration rate for transitioning from partially to fully undrained penetration varies within a much wider range, from as little as 1 to over 100.

In this paper, the effect of rate on cone resistance is assessed through a series of CPTs performed using a miniature cone in a large calibration chamber and field tests especially designed to investigate rate effects. These experiments complement the body of work developed through centrifuge testing and shed some additional light on the three research questions posed earlier.

2. Field Testing

Kim *et al.* (2008) investigated the effects of penetration rate on cone resistance at two field test sites in the state of Indiana. The advantage of studying rate effects in the field is that the shortcomings of laboratory testing are avoided. The coefficient of consolidation c_v was obtained from consolidation tests performed for two loading stages close to the vertical effective stresses of the corresponding CPT test layers considered in the field. The values of the normalized cone resistance q_t / σ'_v obtained for the two test sites considered are plotted as a function of log V in Fig. 3. With the normalization, the values of q_t / σ'_v drop with increasing V until $V \approx 4$ and then increase only slightly as V increases further. The effect of the cone penetration rate on the excess pore pressure measured is shown in the same figure as a function of log V. The excess pore pressure is nor-

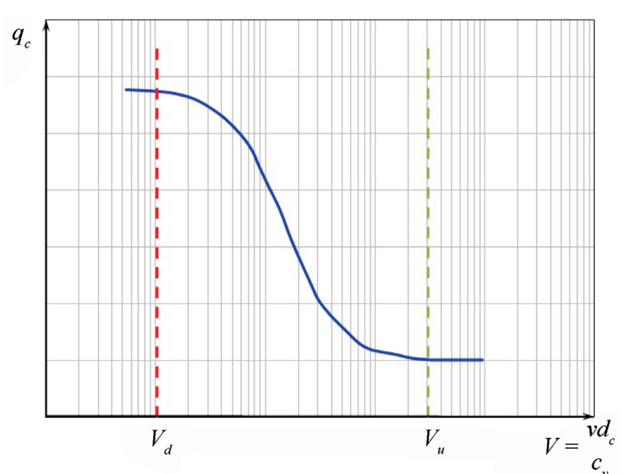

Figure 1 - Conceptual backbone curve for cone penetration resistance *vs.* rate of penetration.

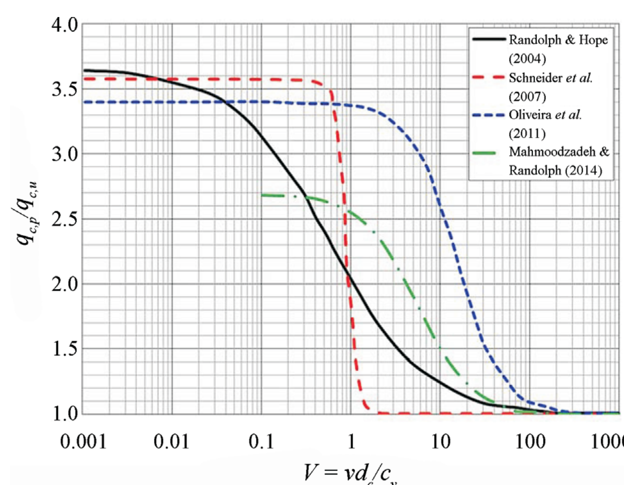

Figure 2 - Backbone curve for CPTs performed in centrifuges (modified after Oliveira *et al.*, 2011).

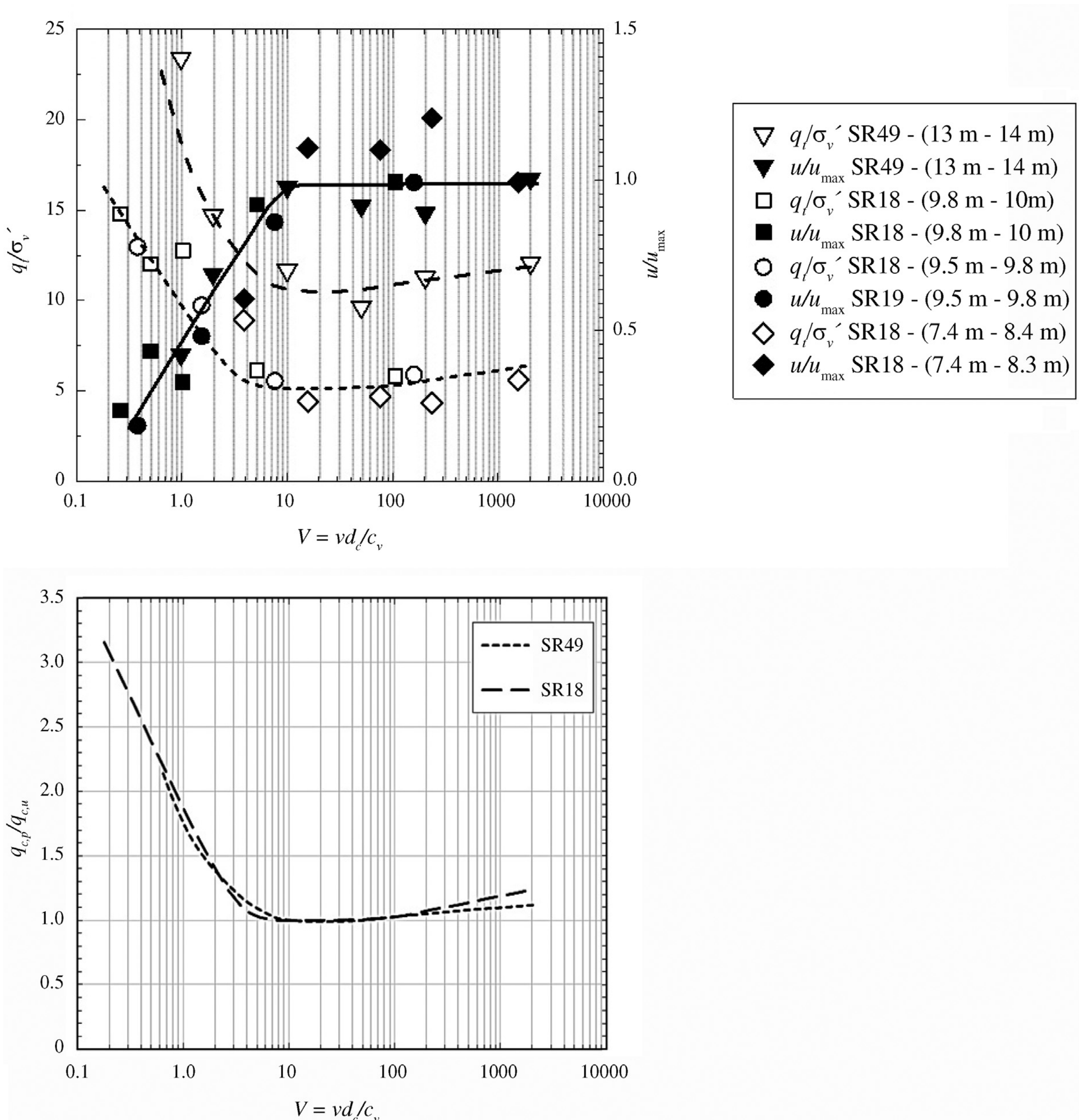

Figure 3 - Field results showing (a) cone penetration resistance *vs.* normalized rate of penetration and (b) backbone curve for CPTs performed in the field.

malized with respect to the maximum value of excess pore pressure measured in a given soil layer. The transition from undrained to partially drained penetration occurs at about $V = 10$.

Since the undrained shear strength s_u (and thus cone resistance measured under undrained conditions) depends on the rate of loading, the value of penetration rate at which penetration transitions from undrained to partially drained penetration (which should be based on pore pressure observations) does not coincide with the point at which the plot of cone resistance *vs.* penetration rate transitions from a range where it is flat to one in which it increases. According to Fig. 3(a) and (b), this transition occurs for $V \approx 10$. In the range between the minimum q_t in Fig. 3 (observed at $V \approx 4$) and $V \approx 10$, q_t would tend to drop because it approaches undrained conditions but would tend to increase because loading rate effects on the soil shear strength start becoming significant. From a practical standpoint, if the goal is to determine the value of V at which penetration resistance stops dropping, then the $V \approx 4$ read from the q_t plot may be of greater interest, but penetration may not be fully undrained at that value of V.

3. Calibration Chamber Cone Penetration Tests

3.1. Overview

Calibration chamber tests are useful in the development of empirical correlations between soil properties and *in situ* test methods such as the CPT. Homogeneous samples can be prepared in the calibration chamber, and the stress state of the soil sample in the chamber can be controlled.

Calibration chamber penetration tests with a miniature cone were performed at the Korea University Calibration Chamber Laboratory in Seoul, Korea (see Fig. 4). The chamber has an inside diameter of 1.2 m and a height of 1.0 m. The top plate of the chamber has 9 holes to provide access for the cone penetrometer. The chamber has a double-wall system, which permits the simulation of K_0 consolidation.

3.2. Normalization of penetration rate and discussion of chamber specimens

In order to evaluate CPT rate effects in clayey soils, cone penetration rates in the calibration chamber tests must cover the whole range of expected drainage conditions (from undrained to fully drained conditions). The normalized penetration rate V is useful to accommodate results obtained from different test conditions, penetrometer sizes, and samples. Results of CPTs performed in the field discussed earlier indicated that the values of V that correspond to the transition from fully undrained to partially drained conditions were between 4 and 10 (Kim *et al.*, 2008). Regarding the other end of the range, centrifuge test results discussed earlier showed that the value of V corresponding to the transition from partially to fully drained conditions could be as low as 0.01.

The range of the penetration rate possible in the chamber tests, based on equipment limitations, was between 20 mm/s and 0.01 mm/s. In planning the experiments, the target range for normalized penetration rate V was $0.01 < V < 30$ in order to fully cover the entire range of drainage conditions. Since the miniature cone diameter is 11.3 mm and the range of cone velocities is constrained by equipment limitations, the variable left to control was c_v.

3.3. Coefficient of consolidation and mixing ratios

A total of 16 flexible-wall permeameter tests were performed in general accordance with ASTM D 5084: ten tests with mixtures of Ottawa sand (ASTM C778 Graded) and kaolin clay (10%, 14.5%, 15%, 16.6%, 19%, 21%, 21.8% 24%, and 29.1% of kaolin clay), and six tests with mixtures of Jumunjin sand and kaolin clay (16%, 17.5%, 18.5%, 22%, 22.2%, and 25% of kaolin clay). Figure 5 shows the grain size distribution curves of Ottawa sand, Jumunjin sand and kaolin clay.

Figure 6 shows the percentage of clay of the soil mixtures studied *vs.* c_v in log scale for an isotropic confining stress of 150 kPa. From this graph, it can be seen that the log c_v has an approximately linear relationship with the clay content of the soil mixtures. Based on the c_v values shown in Fig. 6, values of V were calculated for $v = 20$ mm/s and $D = 11.3$ mm (the miniature cone diameter). For the target value of 60 for V (twice as high as the upper limit of 30 suggested in the literature) required to allow fully undrained conditions at a penetration rate of 20 mm/s, a soil with $c_v \leq 3.8 \times 10^{-6}$ m^2/s was found to be needed. Based on the flexible-wall test results, a mixing ratio of 25% kaolin clay and 75% Jumunjin sand ($c_v = 3.45 \times 10^{-6}$ m^2/s) was selected for the first calibration chamber sample. This sample al-

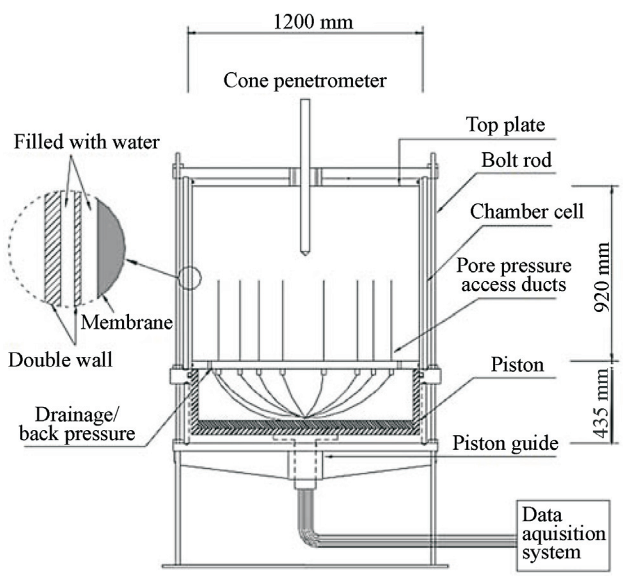

Figure 4 - Schematic view of the flexible wall calibration chamber (Kim *et al.*, 2006).

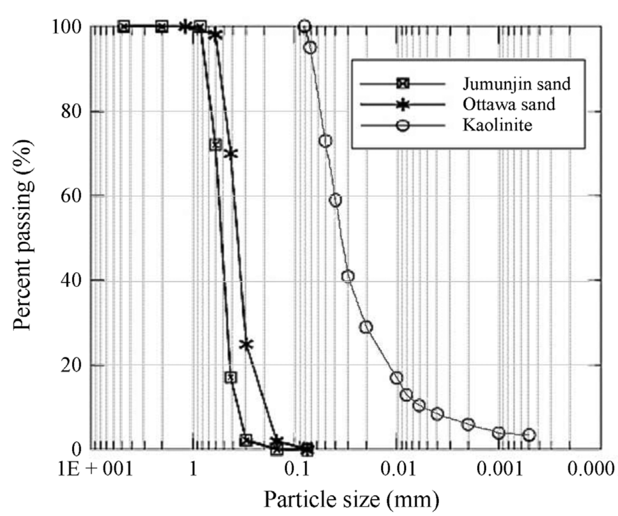

Figure 5 - Grain size distribution of Jumunjin sand, Ottawa sand, and kaolin clay (modified after Kim *et al.*, 2006).

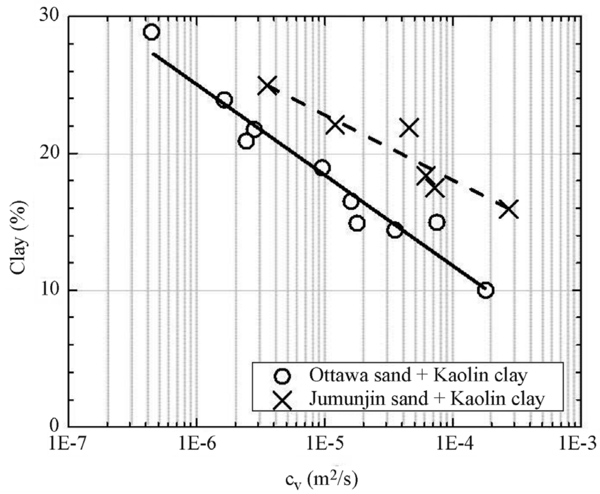

Figure 6 - Percentage of clay of soil mixtures *vs.* c_v.

lowed tests at $V = 0.033$ to $V = 66$ for $D = 11.3$ mm and v between 0.01 mm/s and 20 mm/s.

As previously discussed, a V as low as 0.01 was believed to be required to allow penetration under fully drained conditions. In order to achieve that value of V, the other chamber specimen was prepared with a mixing ratio of 18% clay and 82% Jumunjin sand ($c_v = 6.9 \times 10^{-5}$ m^2/s). The value of V for this soil mixture was equal to 0.0016 for $v = 0.01$ mm/s and $D = 11.3$ mm.

3.4. Cone penetration test program

The miniature piezocone penetrometer used in the calibration chamber tests has a diameter of 11.3 mm (projected cone area = 100 mm^2), a cone apex angle of 60° and a net area ratio of 0.62. The miniature cone, which was borrowed from Fugro B.V., Netherlands, is equipped with a friction sleeve and a porous stone to measure pore pressure just behind the tip. All pore pressure measurements should be considered to be related to where the porous stone is located, so comparison of results across experiments should be done carefully. A flat tip was manufactured specially for the minicone and used to investigate the effect of the tip shape on penetration test results.

Minicone penetration tests were performed at nine different penetration rates, ranging from 20 mm/s to 0.01 mm/s, in the specimen made with 25% kaolin clay and 75% Jumunjin sand by weight (referred to as P1), which had a floating fabric (Carraro *et al.*, 2009, Carraro *et al.*, 2003; Salgado *et al.*, 2000). Eight different penetration rates, ranging from 20 mm/s to 0.05 mm/s, were used in the tests in the specimen made with 18% kaolin clay and 82% Jumunjin sand (referred to as P2), which has a non-floating fabric. The CPTs were performed down to a depth of around 750 mm (out of the 950 mm specimen height). This penetration depth was sufficient to obtain stable cone resistance values for more than two different penetration stages. Therefore, the penetration test in each hole was done in two stages with two different penetration rates.

4. Results of Miniature Cone Penetration Tests

4.1. Penetration tests in specimen P1

Results of tests performed with both the conical and flat tips in specimen P1 are presented in Fig. 7. The cone resistance q_t is the corrected cone resistance for the pore pressure acting on the shoulder area behind the cone tip. Figure 7(a) shows that q_t for v of 20 mm/s and 8 mm/s is almost the same, around 0.7 MPa, and the corresponding excess pore pressures are 295 kPa and 270 kPa, respectively. These results show that, for v of 20 mm/s and 8 mm/s, cone penetration occurred under undrained conditions. The values of q_t started to increase slowly as v decreased from 8 mm/s to 0.25 mm/s. The measured average q_t values showed an increase of 30% (from 0.7 MPa to 0.91 MPa) for a reduction in v from 8 mm/s to 0.25 mm/s, whereas the pore pressure decreased about 20% for the same change in v. The values of q_t increased from 0.91 MPa to 3.14 MPa (or about 3.5 times) for a change in v from 0.25 mm/s to 0.02 mm/s. For the same change in v, the excess pore pressure dropped from 222 kPa to 8 kPa. The decrease in excess pore pressure to practically zero indicates that the drainage conditions changed from partially drained to drained. The values of q_t and excess pore pressure for $v = 0.01$ mm/s (for which conditions are also drained) are almost the same as the values measured for $v = 0.02$ mm/s.

The miniature penetration tests with a flat tip were performed to investigate the impact of the shape of the tip on penetration resistance. The results obtained using both a cone tip and a flat tip under the same conditions provide insights into the relationship between cone resistance and limit unit pile base resistance. The average values of flat-tip resistance and pore pressures are also presented in Fig. 7.

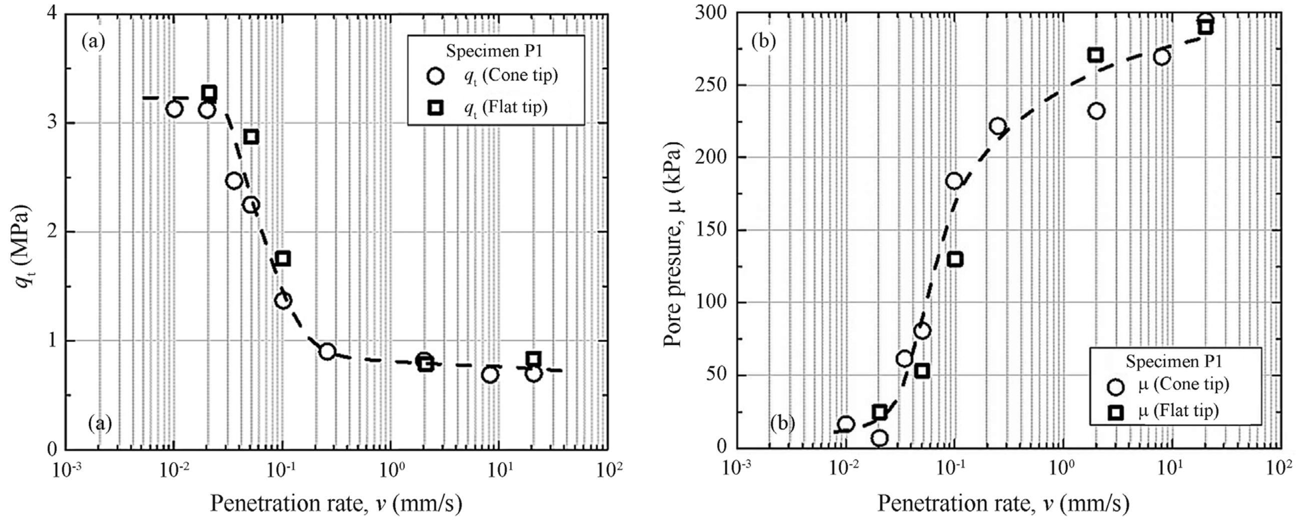

Figure 7 - Effect of penetration rate on (a) q_t and (b) pore pressure u for specimen P1.

The overall flat tip resistances obtained in P1 for the entire penetration rate range are similar to the corresponding cone resistances. The transition points indicating change in drainage conditions seem to be identical for the two tip shapes.

4.2. Penetration tests in specimen P2

The penetration tests performed in P2 focused on identifying the transition between partially drained and fully drained conditions. The steady-state values of q_t and excess pore pressure *vs.* penetration rate for specimen P2 are shown in Fig. 8(a) and Fig. 8(b). While the penetration rate decreased from 20 mm/s to 2 mm/s, the values of q_t increased from 1.28 MPa to 1.65 MPa, and the excess pore pressure decreased by about 40%. This drop in excess pore pressure indicates that the penetration was likely not fully undrained even with the 20 mm/s maximum v, and it certainly was not so for 2 mm/s. The transition from partially drained to fully drained conditions took place for a penetration rate of about 0.1 mm/s. The average q_t at fully drained conditions was approximately 4 MPa.

The shape of the tip influenced the values measured in the penetration tests performed in P2. For v = 20 mm/s, the resistance of the flat tip was 2.1 MPa, 64% higher than the cone resistance measured at the same speed. Over the whole range of penetration rates, the flat tip resistance values were higher than the corresponding cone resistance values, but this difference reduced as drainage increased. Under fully drained conditions, for v = 0.1 mm/s, the flat tip resistance was 4.4 MPa, and the cone resistance was 4.0 MPa, a more modest difference, practically justifying an assumption often made for sands that $q_c \approx q_{bL}$, where q_{bL} is the limit unit base resistance of a pile in sand under the

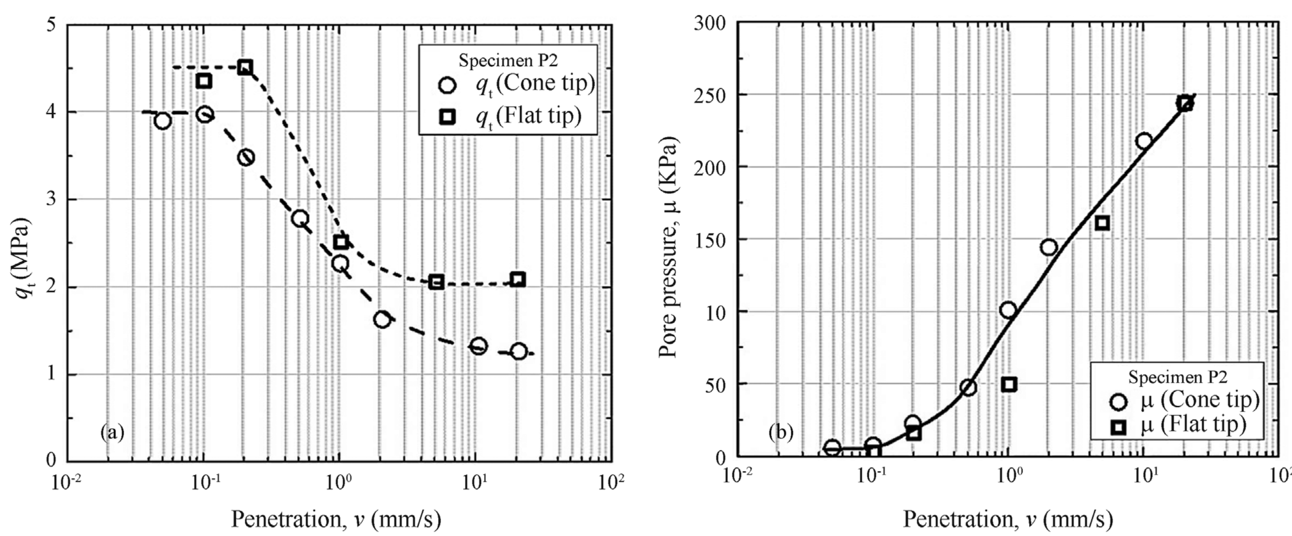

Figure 8 - Effect of penetration rate on (a) q_t and (b) pore pressure u for specimen P2.

same conditions as those under which q_c was measured, so long as the ratio of pile to particle size is sufficiently large (a ratio as low as 20 might be sufficient). Only a small difference in the excess pore pressure measurements was observed.

4.3. Normalized cone resistance *vs.* normalized penetration rates

The results of the penetration tests in the two different specimens can be plotted in terms of the cone resistance normalized by vertical effective stress and the normalized penetration rate *V*. The values of c_v used for normalization were calculated using the data obtained from the calibration chamber specimen consolidation, which was conducted under perfect 1D conditions, without sidewall resistance. The measured values of c_v are equal to 3.5 x 10^{-6} m^2/s for P1 and 3.1 x 10^{-5} m^2/s for P2.

The normalized results for P1 and P2 are shown in Fig. 9 as a function of log *V*. The plots in Fig. 9 (a) suggest that the cone resistance increases when *V* drops below approximately 1, with the transition between partially drained and fully drained conditions occurring around $V \approx 0.05$. According to the normalized excess pore pressure shown in Fig. 9 (a), the transition from undrained to partially drained penetration occurs around $V \approx 10$, and the transition from partially drained to fully drained conditions occurs around $V \approx 0.05$. The reason for the discrepancy between the penetration rate at which q_t stabilizes and that at which the excess pore pressure stabilizes can be explained by the superposition of the two main rate effects. In the penetration range between $V \approx 1$ and $V \approx 10$, q_t would tend to drop because it approaches partially drained conditions but would tend to increase because loading rate effects due to viscosity effects start taking place. From a practical standpoint, if the goal is to determine the value of *V* at which penetration resistance is stable, then the $V \approx 1$ read from the q_t plot may be of greater interest. The backbone curves in Fig. 9 (b) show the effect of fabric on the normalized cone resistance values. The maximum ratio of $q_{c,p}/q_{c,u}$ for specimen P1, which has a floating fabric, is about 4.7, while that for specimen P2, which has a non-floating fabric, is about 2.5. This is likely related to the different distribution of excess pore pressure developing ahead of the advancing cone, with the specimen with floating fabric experiencing greater excess pore generation [see Fig. 7(b) and Fig. 8(b)], and thus offering relatively less resistance to the penetration of the cone under partially drained conditions. These results highlight the difficulty in assessing partial drainage effects for *in situ* soils consisting of mixtures of sand, silt and clay, where fabric effects can affect the measured cone resistances.

The results presented in this paper may be used to obtain the limiting values of c_v that clayey soils would have to have for penetration to take place under drained and undrained conditions for given values of penetration rate and

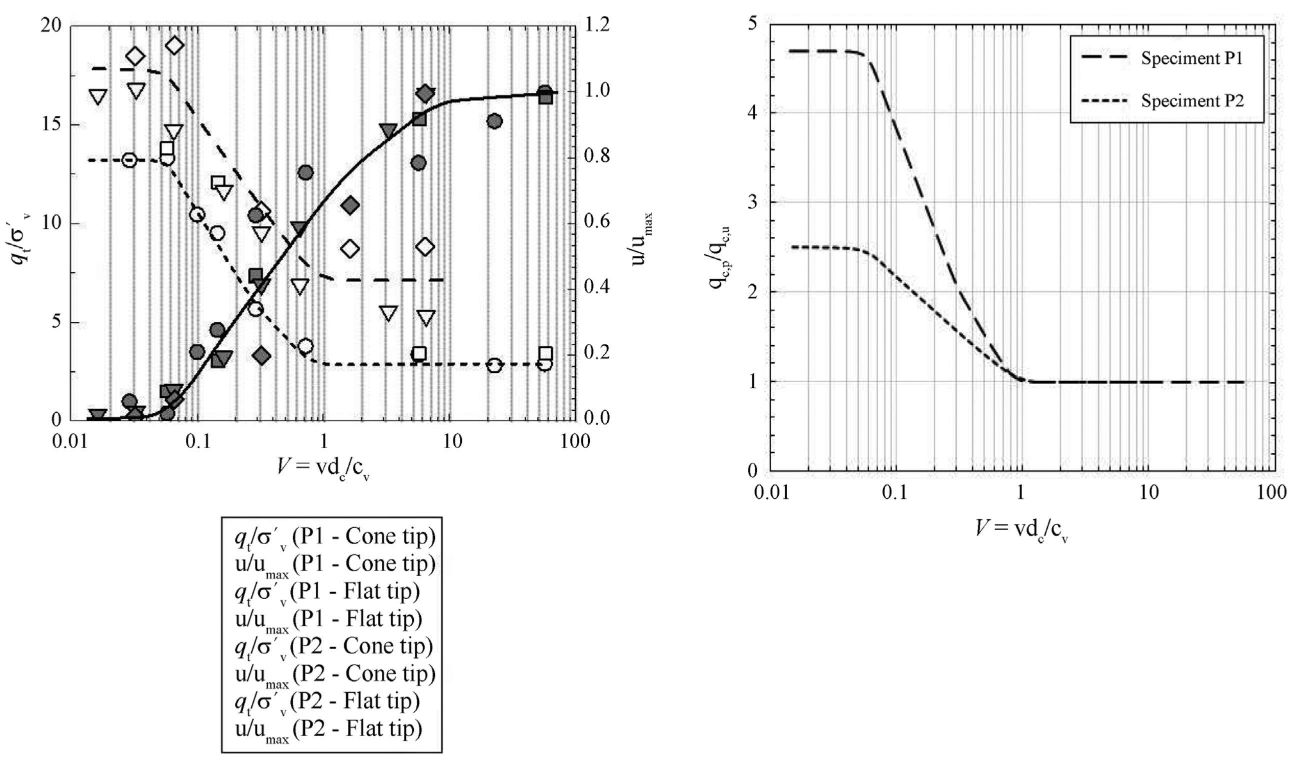

Figure 9 - Results for specimens P1 and P2: (a) cone resistance normalized with respect to vertical effective stress and excess pore pressure normalized with respect to its maximum observed value *vs.* normalized penetration rate *V* and (b) backbone curves (in terms of ratio of q_c at any rate of penetration to q_c under undrained conditions) for specimen P1 and P2.

cone diameter. As discussed previously, the drainage conditions change from undrained to partially drained at a value of $V \approx 10$, which corresponds to a $c_v \approx 7.1 \times 10^{-5}$ m^2/s for the standard cone penetration rate (20 mm/s) and diameter (35.7 mm). However, because of the offsetting effect of rate-dependent shear strength, cone resistance starts to plateau for $V > 1$, which corresponds to a $c_v \approx 7.1 \times 10^{-4}$ m^2/s. Therefore, we can conclude that undrained cone resistance is expected to be measured in CPTs performed with the standard cone at the standard rate in soils having c_v values less than roughly 10^{-3} to 10^{-4} m^2/s. At the other end of the spectrum, the test results suggest that a value of c_v larger than about 1.4×10^{-2} m^2/s (or roughly 10^{-2} m^2/s) is necessary for fully drained conditions to be achieved with a standard CPT.

5. Discussion

Table 1 summarizes what has been learned so far in connection with the dependence of cone resistance on rate of penetration for soils tested so far (kaolinite, clay, sandy clay, silty mine tailings) in the centrifuge, calibration chamber and field. V_d is the rate below which penetration is drained. V_u is the rate above which the cone resistance stabilizes at its lowest value. The value approximates, but not necessarily coincides with, the rate above which penetration is undrained, as discussed previously. It is apparent from the table that there are differences in the values observed for the limiting rates between centrifuge on the one hand and chamber and field tests on the other. The centrifuge test results also appear to suggest that these rates could vary within relative wide ranges.

The relatively wide ranges observed in centrifuge results may be due to fundamental differences in soil behavior as well as details of the penetration boundary-value problem. The centrifuge tests that led to the backbone curves in Fig. 2 were performed in a kaolinite sample and a silty soil. A clear difference between clay and silt, both of which have been used in research on this topic, is that clay develops planes of failure with aligned particles and has a residual shear strength less than critical, but silt does not. Differences in fabric between test models also would have an effect on the gradients of strength and drainage around the advancing cone. Spatial variation of rates of loading and degree of consolidation around the advancing cone also place limits on achievement of a single backbone curve, as well as on normalization of rates of penetration with respect to c_v. The backbone curves are likely to depend not only on the nature of the soil but also its state (void ratio, effective stress state, over-consolidation ratio and fabric), and generalizations may not be achievable before significant amount of testing is done for soils spanning the whole range of particle sizes and soil state.

Table 1 - Approximate values of the rates at which penetration transitions from drained to partially drained and partially drained to drained penetration and ratio of drained to undrained penetration resistance for the field, chamber and centrifuge testing.

Key quantities	Field	Chamber	Centrifuge
V_d	< 1	0.05	0.01-1
V_u	10	1	2-100
$q_{c,\,drained}/q_{c,\,undrained}$	undefined	2.5-4.7	2.7-3.7

The lesson to CPT performance and interpretation in practice from research done on this topic so far is clear and relatively straightforward: the use of the standard 20 mm/s should no longer be the norm. Every effort should be made to perform CPTs under either fully drained or fully undrained penetration whenever feasible. The alternative is to interpret tests performed under partially drained penetration, which is still very challenging. In order to avoid penetration under partial drainage and the more challenging interpretation of such tests, CPTs in sand-controlled soils should be performed as slowly as possible to guarantee full drainage, while CPTs in clay-controlled soils should be performed as fast as required to ensure fully undrained penetration.

6. Summary and Conclusions

The main focus of the research presented in this paper was to evaluate and quantify the factors affecting the results of cone penetration testing performed at penetration rates leading to drainage conditions ranging from fully drained to fully undrained. Rate effects and the effects of drainage conditions around the cone tip during penetration were studied. Results from a series of penetration tests performed in the centrifuge, the calibration chamber and the field conducted at various penetration rates were presented, and the transition from undrained to partially drained and then to fully drained penetration was investigated in terms of a normalized penetration rate.

The ratio of cone resistance measured under drained to that under undrained conditions observed in the calibration chamber tests in clay samples was 2.5 to 4.7. The transition from undrained to partially drained conditions occurred for V values approximately equal to 10. For V between approximately 10 and 1, cone resistance was fairly stable because of the offsetting effects on shear strength of loading rate and drainage rate. The transition from partially drained to fully drained conditions occurred at $V \approx 0.05$. From these limiting V values, it is possible to obtain limiting values of c_v required for fully drained and fully undrained penetration for a given cone and penetration rate for the test soil. For soils like the soil tested in the calibration chamber tests reported here having c_v values less than about 7.1×10^{-5} m^2/s ($V = 10$), standard penetration ($v = 20$ mm/s and $D = 35.7$ mm) takes place under undrained conditions, whereas for c_v values greater than about 1.4×10^{-2} m^2/s ($V = 0.05$), standard penetration takes place under drained conditions.

The fact that results from centrifuge tests on clay and silt are not in agreement and that no agreement can be found between the centrifuge test results and the calibration chamber test results on clay and a sandy clay tested in the calibration chamber suggests that a single backbone curve that would apply to all soils likely does not exist. Significant further testing with a variety of soils in a variety of conditions is required to advance understanding of penetration rate and its relationship to drainage rate. In order to avoid the challenges that the limited understanding of this relationship presents to interpretation of CPT results, it may be advantageous to vary the rate of penetration during a test, where possible, to guarantee either full drainage or no drainage during penetration.

References

ASTM (2013) Standard Specification for Standard Sand - C778-13. ASTM International, West Conshohocken, Pennsylvania, USA

ASTM (2012) Standard Test Method for Electronic Friction Cone and Piezocone Penetration Testing of Soils - D5778-12. ASTM International, West Conshohocken, Pennsylvania, USA

ASTM (2010) Standard Test Methods for Measurement of Hydraulic Conductivity of Saturated Porous Materials Using a Flexible Wall Permeameter, ASTM International - D5084-10. West Conshohocken, Pennsylvania, USA

Bemben, S.M.; & Myers, H.J.; (1974) The influence of rate of penetration on static cone resistance in Connecticut river valley varved clay, in: Proceedings of the European Symposium on Penetration Testing, Stockholm, p. 33-34.

Campanella, R.G.; & Robertson, P.K.; Gillespie, D. (1983) Cone penetration testing in deltaic soils. Can. Geotech. J. v. 20, p. 23-35.

Carraro, J.; Bandini, P.; & Salgado, R. (2003) Liquefaction resistance of clean and nonplastic silty sands based on cone penetration resistance. J. Geotech. Geoenvironmental Eng. v. 129, p. 965-976.

Carraro, J.; Prezzi, & M.; Salgado, R. (2009) Shear strength and stiffness of sands containing plastic or nonplastic fines. J. Geotech. Geoenvironmental Eng. v. 135, p. 1167-1178.

Carraro, J.A.H.; Bandini, P.; & Salgado, R. (2003) Liquefaction resistance of clean and nonplastic silty sands based on cone penetration resistance. J. Geotech. Geoenvironmental Eng. v. 129, p. 965-976.

Finnie, I.M.S.; & Randolph, M.F. (1994) Punch-through and liquefaction induced failure of shallow foundations on calcareous sediments, in: Proc. 17th Int. Conf. on the Behavior of Offshore Structures. assachusetts Institute of Technogology, Boston, p. 217-230.

Foye, K.C.; Abou-Jaoude, G.; Prezzi, M.; & Salgado, R. (2009) Resistance factors for use in load and resistance factor design of driven pipe piles in sands. J. Geotech. Geoenvironmental Eng. v. 135, p. 1-13.

Foye, K.C.; Salgado, R.; & Scott, B. (2006) Resistance factors for use in shallow foundation LRFD. J. Geotech. Geoenvironmental Eng. v. 132, p. 1208-1218.

House, A.R.; Oliveira, J.R.M. ; & Randolph, M.F. (2001) Evaluating the coefficient of consolidation using penetration tests. Int. J. Phys. Model. Geotech. v. 1, p. 17-26.

Jardine, F.M.; Chow, F.C.; Overy, R.F.; & Standing, J.R. (2005) ICP design methods for driven piles in sands and clays. Thomas Telford, London, UK.

Kamp, W.G.B. Te (1982) The influence of the rate of penetration on the cone resistance "qc" in sand, in: Proceedings of the Second European Symposium on Penetration Testing, ESOPT-II, Amsterdam, p. 627-633.

Kim, K., Prezzi, M.; & Salgado, R. (2006) Interpretation of cone penetration tests in cohesive soils. Report FHWA/IN/JTRP-2006/22, Joint Transportation Research Program.

Kim, K., Prezzi, M.; Salgado, R.; & Lee, W. (2008) Effect of penetration rate on cone penetration resistance in saturated clayey soils. J. Geotech. Geoenvironmental Eng. v. 134, p. 1142-1153.

Kolk, H.J.; Baaijens, A.E.; & Senders, M. (2005) Design criteria for pipe piles in silica sands, in: The 1st International Symposium on Frontiers in Offshore Geotechnics. Taylor & Francis, London, UK, Perth, Australia, p. 711-716.

Lee, J.; Eun, J., Prezzi, M.; & Salgado, R. (2008) Strain influence diagrams for settlement estimation of both isolated and multiple footings in sand. J. Geotech. Geoenvironmental Eng. v. 134, p. 417-427.

Lee, J.; & Salgado, R.; (2002) Estimation of footing settlement in sand. Int. J. Geomech. v. 2, p. 1-28.

Lee, J.; Salgado, & R.; Kim, S.; (2005) Bearing capacity of circular footings under surcharge using state-dependent finite element analysis. Comput. Geotech. v. 32, p. 445-457.

Lee, J.; Salgado, R.; & Paik, K. (2003) Estimation of load capacity of pipe piles in sand based on cone penetration test results. J. Geotech. Geoenvironmental Eng. v. 129, p. 391-403.

Lee, J.H.; & Salgado, R. (1999) Determination of pile base resistance in sands. J. Geotech. Geoenvironmental Eng. v. 125, p. 673-683.

Mayne, P.W.; & Poulos, H.G. (1999) Approximate displacement influence factors for elastic shallow foundations. J. Geotech. Geoenvironmental Eng. v. 125, p. 453-460.

Niazi, F.S.; & Mayne, P.W. (2013) Cone Penetration Test Based Direct Methods for Evaluating Static Axial Capacity of Single Piles. Geotech. Geol. Eng. v. 31, p. 979-1009.

O'Loughlin, C.D.; & Lehane, B.M.; (2010) Nonlinear cone penetration test-based method for predicting footing settlements on sand. J. Geotech. Geoenvironmental Eng. v. 136, p. 409-416.

Oliveira, J. R. M. S.; Almeida, M.S.S.; Motta, H.P.G.; & Almeida, M.C.F.; (2011) Influence of penetration rate on penetrometer resistance. J. Geotech. Geoenvironmental Eng. v. 137, p. 695-703.

Powell, J.J.M.; & Quarterman, R.S.T. (1988) The interpretation of cone penetration tests in clays, with particular reference to rate effects, in: Proceedings of the International Symposium on Penetration Testing, Orlando, p. 903-909.

Randolph, M.F.; & Hope, S. (2004) Effect of cone velocity on cone resistance and excess pore pressures, in: Kogisha, Y. (ed) Proc., Int. Symp. On Eng. Practice and Performance of Soft Deposits. Osaka, p. 147-152.

Robertson, P.K.; & Wride, C. (Fear). (1998) Evaluating cyclic liquefaction potential using the cone penetration test. Can. Geotech. J. v. 35, p. 442-459.

Rocha Filho, P.; & Alencar, J.A. (1985) Piezocone Tests in the Rio de Janeiro soft clay deposit, in: Proceedings of the 11th International Conference on Soil Mechanics and Foundation Engineering, San Francisco, p. 859-862.

Roy, M.; Tremblay, M.; Tavenas, F.; & Rochelle, P.L. (1982) Development of pore pressure in quasi-static penetration tests in sensitive clay. Can. Geotech. J. v. 19, p. 124-138.

Salgado, R.; (2013) The mechanics of cone penetration?: Contributions from experimental and theoretical studies, in: Proceedings of Geotechnical and Geophysical Site Characterization 4, ISC4. CRC Press (Keynote paper), p. 131-153.

Salgado, R.; Bandini, P.; & Karim, A. (2000) Shear strength and stiffness of silty sand. J. Geotech. Geoenvironmental Eng. v. 126, p. 451-462.

Salgado, R.; Boulanger, R.W.; & Mitchell, J.K. (1997) Lateral stress effects on CPT liquefaction resistance correlations. J. Geotech. Geoenvironmental Eng. v. 123, p. 726-735.

Schmertmann, J.H. (1970) Static cone to compute static settlement over sand. J. Soil Mech. Found. Div. v. 96, p. 1011-1043.

Schneider, J.A.; Lehane, B.M.; & Schnaid, F. (2007) Velocity Effects on Piezocone Measurements in Normally and Over Consolidated Clays. Int. J. Phys. Model. Geotech. v. 7, p. 23-34.

Seed, H.B.; & De Alba, P. (1986) Use of SPT and CPT tests for evaluating the liquefaction resistance of sands, in: Use of in Situ Tests in Geotechnical Engineering, Geotech. Spec. Publ, No.6. ASCE, New York City, N.Y.

Seo, H.; Yildirim, I.Z.; & Prezzi, M. (2009) Assessment of the Axial Load Response of an H Pile Driven in Multilayered Soil. J. Geotech. Geoenvironmental Eng. v. 135, p. 1789-1804.

Stark, T.D.; & Olson, S.M. (1995) Liquefaction resistance using CPT and field case histories. J. Geotech. Eng. v. 121, p. 856-869.

Tani, K.; & Craig, W.H., 1995. Bearing capacity of circular foundations on soft clay of strength increasing with depth. Soils Found. v. 35, p. 21-35.

Xu, X.; Schneider, J.A.; & Lehane, B.M. (2008) Cone penetration test (CPT) methods for end-bearing assessment of open- and closed-ended driven piles in siliceous sand. Can. Geotech. J. v. 45, p. 1130-1141.

Energy Measurement in the Brazilian SPT System

C.M. Santana, F.A.B. Danziger, B.R. Danziger

Abstract. This paper presents results of the instrumentation of 373 blows from two SPT deployments performed in the Sarapuí II Test Site, located in Duque de Caxias, Rio de Janeiro. In these blows the hammer drop height, its velocity at impact, the rate of blows and also the energy transferred to the rod stem have been measured. It is therefore possible to know the loss of energy for the SPT process (and the corresponding efficiency factors), since the hammer is delivered at zero velocity up to the time the transmitted energy reaches the rod stem.

Keywords: SPT, energy, efficiency.

1. Introduction

Despite the existing problems associated with the reliability and repeatability of the Standard Penetration Test, Campanella & Sy (1994) emphasize that the SPT continues to be the most used in situ test for foundation design, evaluation of liquefaction potential and compaction control of sands and sandy silts. Many authors associate the widespread use of the test to the simplicity of the test procedure, robustness of the equipment and low operational cost (*e.g.*, Broms & Flodin, 1988; Décourt, 1989).

Some factors influencing the N value obtained from SPT have been discussed in several papers (*e.g.*, Fletcher, 1965; Ireland *et al.*, 1970; De Mello, 1971; Serota & Lowther, 1973; Kovacs *et al.*, 1977, 1978; Palacios, 1977; Schmertmann & Palacios, 1979; Kovacs, 1979, 1980, 1994; Kovacs & Salomone, 1982; Riggs *et al.*, 1983; Belincanta, 1985, 1998; Skempton, 1986; Belincanta & Cintra, 1998; Décourt *et al.*, 1988; Tokimatsu, 1988; Décourt, 1989; Clayton, 1990; Matsumoto *et al.*, 1992; Morgano & Liang, 1992; Teixeira, 1993; Abou-matar & Goble, 1997; Aoki & Cintra, 2000; Fujita & Ohno, 2000; Cavalcante, 2002; Odebrecht, 2003; Daniel *et al.*, 2005; Youd *et al.*, 2008; Santana *et al.*, 2012).

One of these papers, by Schmertmann & Palacios (1979), has shown that the number of blows N varies inversely with the energy delivered to the rod stem, to N equal at least 50. After some discussions concerning the need to standardize and the choice of the proper energy to be used as a reference for the N value (*e.g.*, Kovacs & Salomone, 1982; Robertson *et al.*, 1983; Seed *et al.*, 1985; Skempton, 1986), ISSMFE (1989) has established 60% of the theoretical free fall energy (or nominal potential energy) as the international reference. Therefore the corresponding N_{60} is obtained as

$$N_{60} = N \frac{E}{E_{60}} \tag{1}$$

where N = measured number of blows, E = energy corresponding to N and E_{60} = 60% of the international reference energy E^*, E^* = 474 J.

Décourt (1989) and Kulhawy & Mayne (1990) have summarized the factors affecting the energy transmission from the hammer to the rods. According to Décourt (1989), the energy entering the rod stem (or enthru energy, E_i) can be obtained as

$$E_i = e_1 e_2 e_3 E^* \tag{2}$$

where e_1, e_2 and e_3 are efficiency (or correction) factors. The efficiency factor e_1 relates the kinetic energy just before the impact to the free fall energy and is mainly dependent on the way the hammer is lifted and released. A number of studies have been carried out on this subject (*e.g.*, Kovacs *et al.*, 1977, 1978; Kovacs, 1979, 1980; Kovacs & Salomone, 1982; Skempton, 1986; Tokimatsu, 1988; Décourt, 1989). The factor e_2 is associated to the loss of energy due to the presence of the anvil (*e.g.*, Skempton, 1986; Décourt, 1989). The efficiency factor e_3 is related to the rod length and e_3 values smaller than 1 have been proposed (*e.g.*, Schmertmann & Palacios, 1979; Skempton, 1986) to take into account the separation between hammer and anvil for rod lengths smaller than 10 m, due to the upcoming stress wave. However, recent research (Cavalcante, 2002; Odebrecht, 2003; Daniel *et al.*, 2005; Odebrecht *et al.*, 2005; Danziger *et al.*, 2006) has shown that a number of impacts may occur in a single blow, each impact being responsible for part of the energy delivered to the rod stem. Thus, e_3 should be taken as 1. The e_1, e_2 and e_3 values are discussed below together with the corresponding values obtained herein.

The efficiency factors are related to the theoretical (or nominal) free fall energy, thus they are not the real ones. Instead, the efficiency factors are influenced by the errors associated with the non-use of the real free fall energy during

Christian Matos de Santana, D.Sc., Civil Engineer, Departamento Nacional de Infraestrutura de Transportes, Aracaju, SE, Brazil. e-mail: christianmatoss@gmail.com.
Fernando Artur Brasil Danziger, D.Sc., Full Professor, COPPE e Escola Politécnica, Universidade Federal do Rio de Janeiro, Rio de Janeiro, RJ, Brazil. e-mail: danziger@coc.ufrj.br.
Bernadete Ragoni Danziger, D.Sc., Associate Professor, Escola de Engenharia, Universidade Estadual do Rio de Janeiro, Rio de Janeiro, RJ, Brazil. e-mail: bernadeterd@hotmail.com.
Submitted on June 27, 2014; Final Acceptance on December 15, 2014; Discussion open until April 30, 2015.

the test. To the authors' knowledge, very few studies have been conducted regarding the potential energy actually used in the test (*e.g.*, Riggs *et al.*, 1983; Cavalcante *et al.*, 2011), the latter only relating to the hand lifted pinweight hammer system regularly used in Brazil. However, a very experienced crew performed the SPTs in the study carried out by Cavalcante *et al.* (2011), and the obtained results cannot be considered typical but rather a benchmark for the best results possible to be obtained with this system.

This paper presents research to measure the potential energy of the regular Brazilian system in regular operational conditions, *i.e.* with a crew with regular experience. Also, the impact velocity of the hammer has been evaluated. The blow count rate was also measured, provided that there are recommendations for the rate to be used in liquefaction analysis (Seed *et al.*, 1985). The energy reaching the rod stem has been measured and used to evaluate the efficiency factors, which have been therefore evaluated based both on the nominal free fall energy and on the measured energy.

2. Equipment

2.1. SPT analyzer

The SPT Analyzer measures the energy transmitted to the rod stem, besides other quantities. It is composed of a data acquisition unit, instrumented rods and connection cables, as can be seen in Fig. 1.

The acquisition data unit has two channels for the force signal and other two for the acceleration signal. Its maximum sample frequency is 20 kHz. The maximum reading interval is 102.4 ms.

Rods 1 m in length have been instrumented, each with a pair of force measuring devices and a pair of accelerometers. Electric strain-gauges have been used for monitoring the force in the instrumented rods, forming a Wheatstone bridge directly fixed to the rods. Piezoelectric accelerometers, with 0.02 g resolution and capacity of 5000 g, have been used to record the rod acceleration. The accelerometers can be fixed to the rods in diametrically opposite positions and between the force sensors. The data acquisition system transforms the acceleration records into velocity upon integration with time.

2.2. High speed camera

A Casio EX-FH20 high speed camera, capable of recording up to 1000 pictures per second, was used to record the hammer drop height and impact velocity.

The images recorded by the camera were digitized and analyzed picture by picture in order to enable identification of the maximum height drop during hammer raise and the moment the hammer hit the anvil. To help determine the hammer position, an Invar ruler is positioned beside the SPT set. Figure 2 shows the system employed in the instrumentation of the SPT.

3. Tests Performed

3.1. Test characteristics

Two SPT deployments have been monitored in Sarapuí II Test Site, situated at the margin of the Washington Luiz Highway, in the area of the Navy Radio Station in the municipality of Duque de Caxias/RJ. Geotechnical characteristics of the test site have been provided by Jannuzzi (2009, 2013).

According to Jannuzzi (2009) the soil profile in the region is formed by a very soft clay layer with a typical thickness of 7.5 m to 8.0 m, followed by minor layers of clay, sands and silts and clays once more. The water table is at ground level.

The same crew including a chief-operator and three auxiliary-operators were in charge of the two SPT borings.

An anvil with a mass of 977 g was used (see Fig. 3). It should be pointed out that although the Brazilian standard NBR-6484/2001 states that the anvil should have a mass

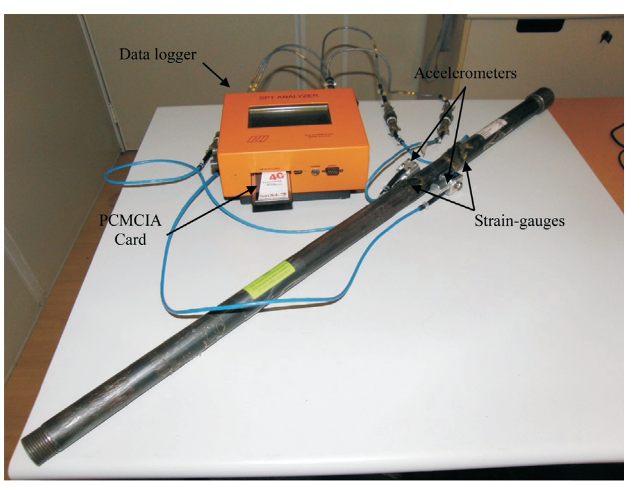

Figure 1 - SPT analyzer.

Figure 2 - System employed in SPT energy monitoring.

Figure 3 - Anvil employed in Sarapuí II SPTs.

ranging from 3.5 kg to 4.5 kg, anvils with a mass of around 1 kg are very often used all over Brazil. Reference must be made to, for example, Skempton 1986, Décourt 1989, Belincanta 1998 and Belincanta & Cintra 1998 for the influence of the anvil mass on the energy transmitted to the rod stem.

A sisal rope was used for lifting and releasing the hammer. The pinweight hammer with a wood cushion is shown in Fig. 4. No measurement was made of the hammer mass in the present study. However the SPT company in charge of the tests has informed that the hammer mass is verified periodically and is equal to 65 kg. Measurements made in previous research (Cavalcante, 2002) indicate that this information may be considered reliable, and errors in the hammer mass may be generally considered negligible. The hammer drop height has been visually controlled, as in the usual procedure, with the aid of a mark at the pinweight hammer.

Figure 4 - Equipment employed in the tests in Sarapuí II Experimental Test Site.

The rods employed in the tests had an external diameter of 33 mm, 3.2 kg per meter, as recommended in the Brazilian standard NBR-6484/2001.

In the first boring, named Boring 1, 141 blows have been monitored. The rod stem length (including the sampler) varied from 10.80 to 22.80 m (nominal test depths varying from 9 to 21 m).

In the second boring, named Boring 2, 232 blows have been monitored. The rod stem length (including the sampler) varied from 11.70 to 25.70 m (nominal test depths varying from 10 to 23 m).

3.2. Instrumentation results

In order to avoid significant loss of image quality, a rate of 210 pictures per second was used, corresponding to a maximum resolution of 480 x 360 pixels. The records obtained by the high speed camera have been transferred to a computer, separated picture by picture, and analyzed by *AutoCAD* software in a way that it would be possible to define the hammer height during drop by the action of each blow. An Invar ruler acted as a reference.

The height measured in the picture just before hammer release is defined as the hammer drop height. The hammer impact velocity has been obtained by the analysis of the hammer height picture by picture, since the instant of its release up to the imminence of impact (last picture before hammer contact with the anvil). Thus it has been possible to adjust a function that describes the relation between the height drop of the hammer and the time, according to Fig. 5.

The derivation of the hammer drop height in relation to time, when the height drop tends to zero is the impact velocity.

Different polynomial functions of two and three degrees have been tested in various blow counts that produced good agreement. The difference observed in the velocity during impact selecting one or other polynomial function has been of very low significance. The option has been then to try to adjust a second-degree polynomial function in order to simplify the numerical estimation.

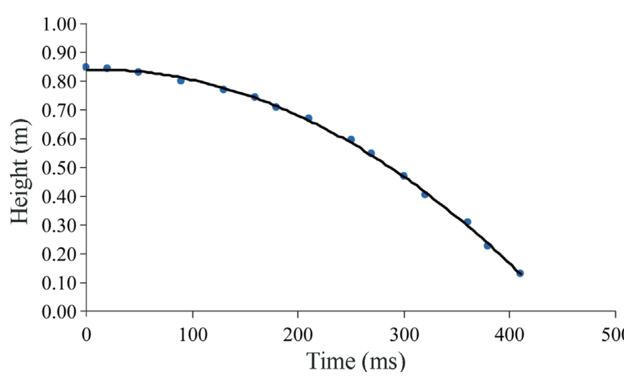

Figure 5 - Hammer drop height *vs.* time (obtained during filming).

Cavalcante *et al.* (2011) used polynomial functions of fourth degree to describe hammer drop height function with time.

The hammer acceleration in time is the second derivative of the hammer drop height in time. In this way, the use of a second-degree polynomial function implies the consideration of constant hammer acceleration during the hammer release.

The hammer acceleration during its release is influenced by the gravitational force (which is approximately constant) and by friction forces. In this way, the resultant from the friction forces is considered constant during the hammer release.

Considering that the second or third degree polynomial functions did not produce significant change in the adjustments, it is reasonable to consider that the friction *vs.* time function, in the analyzed cases, is approximately constant.

The average values of hammer drop height (h_d), hammer velocity at impact (v_i), potential energy of hammer at release (E_p) and kinetic energy at impact (E_k) in each blow sequence of borings 1 and 2 are presented in Tables 1 and 2, respectively. The potential energy and kinetic energy at impact have been calculated as:

$$E_p = m.g.h_d \tag{3}$$

$$E_k = 0.5.m.v_i^2 \tag{4}$$

where m = hammer mass, considered as 65 kg and g = gravity acceleration, considered as 9.81 m/s^2.

In the three first blow sequences of Boring 2 no filming has been carried out. Furthermore, in a significant number of blows from deployments 1 and 2 (152), it has not been possible to determine the impact velocity due to problems with the video. In a smaller number of blows (102) video problems prevented the determination of hammer drop height in both deployments.

Due to errors in the SPT Analyzer operation, the rod energy in six blows from sequences 6 and 9 from Boring 2 has not been monitored. However, the hammer drop height and impact velocity of these blows have been measured.

Figures 6 and 7 show the frequency distribution of the SPT hammer drop height in borings 1 and 2, respectively. Figures 8 and 9 illustrate the percentage of blows applied in different ranges of hammer drop height in borings 1 and 2, respectively.

Figures 10 and 11 show the hammer drop height blow by blow in each sequence from borings 1 and 2, in all available cases.

Tables 1 and 2 present, for each blow sequence, the following measurements: the number of blow counts for 45 cm sampler penetration (N_{45}), the average frequency of blow count application, the working shift when the blows have been applied (see definition below), the nominal depth of the test and the length of the rod stem, the hammer drop height, the impact velocity and the energies measured, as well as energy ratios.

The average frequency of the blows has been calculated considering the interval from the initial lifting of the hammer, in the first blow of each sequence, up to the final of the hammer impact for the last blow. Figure 12 shows the hammer drop height *vs.* the frequency of blows.

In order to evaluate the variation in hammer drop height during the day, the working period of the boring crew was divided in four shifts, namely: first shift, from 8 and 10 AM; second shift, from 10 to 12 AM; third shift, from 14 to 16 PM and fourth shift, from 16 to 18 PM. Figure 13 shows the corresponding variation.

The energy reaching the rod stem (enthru energy) (E_i) has been calculated from Eq. 5. The values of force (F) and velocity (v) have been obtained through the measurements from the strain-gauges and accelerometers installed on the rods. Tables 1 and 2 present the measured values.

$$E_i = \int F \cdot v \cdot dt \tag{5}$$

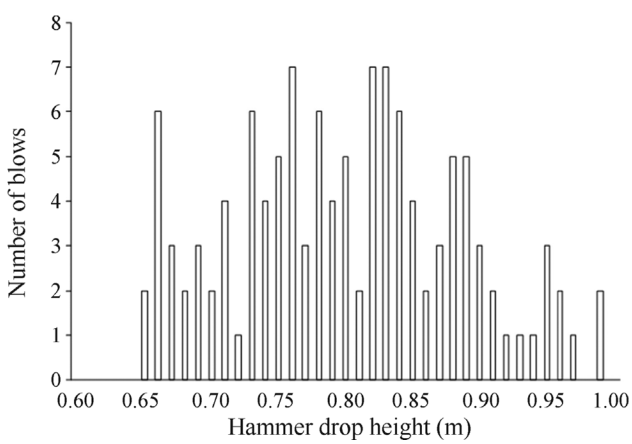

Figure 6 - Frequency distribution of the hammer drop height from Boring 1.

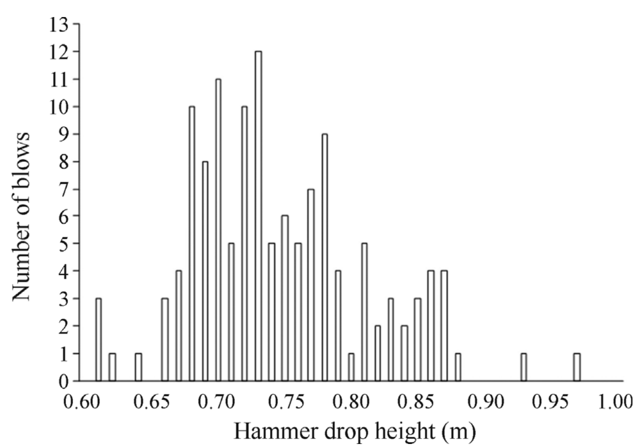

Figure 7 - Frequency distribution of the hammer drop height from Boring 2.

Table 1 - Measured values for Boring 1.

Sequence	N_{45}[1]	Frequency (Blows/min)	Shift	Depth[2] (m)	L[3] (m)	h_d[4] (m)		v_i[7] (m/s)		E_p[8] (J)		E_k[9] (J)		E_i[10] (J)		E_p/E^*[11]	E_k/E^* (e_1)	E_i/E^*	E_k/E_p (e_1*)	E_i/E_p	E_i/E_k (e_2)
						A[5]	SD[6]	A	SD	A	SD	A	SD	A	SD						
1	5	32.1	4	9.00	10.80	0.87	0.07	3.83	0.16	554.0	47.5	478.2	40.5	429.6	63.4	1.16	1.00	0.90	0.86	0.78	0.90
2	2	31.3	2	10.00	11.79	0.71	0.07	3.53	-	451.9	41.5	405.7	-	366.7	65.2	0.94	0.85	0.77	0.90	0.81	0.90
3	8	22.8	2	11.00	12.80	0.77	0.06	3.61	0.08	492.8	35.9	423.9	18.6	382.1	27.1	1.03	0.89	0.80	0.86	0.78	0.90
4	15	29.0	3	12.00	13.80	0.87	0.06	4.02	0.15	553.4	37.8	525.8	40.0	493.5	34.3	1.16	1.10	1.03	0.95	0.89	0.94
5	3	-	3	13.00	14.81	0.69	0.05	3.41	0.27	437.4	32.8	380.2	60.7	328.6	41.8	0.91	0.80	0.69	0.87	0.75	0.86
6	4	39.7	3	15.00	16.83	0.67	0.03	3.38	0.03	429.1	20.0	371.6	5.9	318.1	22.7	0.90	0.78	0.67	0.87	0.74	0.86
7	18	27.2	2	19.00	20.68	0.69	0.03	3.67	0.09	441.1	18.4	436.9	21.7	411.4	18.4	0.92	0.91	0.86	0.99	0.93	0.94
8	19	24.0	3	20.00	21.76	0.83	0.06	3.75	0.14	529.4	39.0	458.0	33.5	431.5	18.1	1.11	0.96	0.90	0.87	0.82	0.94
9	26	26.1	4	21.00	22.77	0.86	0.08	3.93	0.18	547.3	47.9	502.9	46.1	447.1	35.4	1.14	1.05	0.93	0.92	0.82	0.89
10	41	19.4	4	22.00	23.80	0.78	0.05	3.68	0.11	497.8	29.1	441.3	25.5	409.6	22.6	1.04	0.92	0.86	0.89	0.82	0.93

[1]N_{45} = number of blows for 45 cm sampler penetration;
[2]Depth = nominal depth of the SPT (m);
[3]L = length of the rod stem, including the sampler length (m);
[4]h_d = SPT hammer drop height;
[5]A = average value;
[6]SD = standard deviation;
[7]v_i = SPT hammer impact velocity;
[8]E_p = actual potential energy of the SPT hammer at the release moment;
[9]E_k = kinetic energy of the SPT hammer at the imminence of impact;
[10]E_i = energy measured just below the anvil;
[11]E^* = theoretical potential energy of SPT hammer from Brazilian system (478.2 J).

Table 2 - Measured values for Boring 2.

Sequence	N_{45}	Frequency (Blows/min)	Shift	Depth (m)	L (m)	h_d (m)		v_i (m/s)		E_p (J)		E_k (J)		E_i (J)		E_p/E^*	E_k/E^* (e_1)	E_i/E^*	E_k/E_p (e_1^*)	E_i/E_p	E_i/E_k (e_2)
						A	SD	A	SD	A	SD	A	SD	A	SD						
1	7	-	-	10.00	11.70	-	-	-	-	-	-	-	-	451.7	29.7	-	-	0.94	-	-	-
2	8	-	-	11.00	12.70	-	-	-	-	-	-	-	-	449.3	34.2	-	-	0.94	-	-	-
3	5	-	-	12.00	14.70	-	-	-	-	-	-	-	-	472.2	42.7	-	-	0.99	-	-	-
4	5	27.1	3	13.00	15.70	0.75	0.04	3.69	0.12	477.4	28.2	442.5	29.5	408.1	15.1	1.00	0.93	0.85	0.93	0.85	0.92
5	11	26.6	3	14.00	16.70	0.78	0.06	3.78	0.16	497.9	41.1	466.2	39.2	463.9	31.2	1.04	0.97	0.97	0.94	0.93	0.99
6	9	28.6	4	15.00	17.70	0.85	0.13	3.92	0.27	541.2	80.8	501.8	68.0	551.4	15.0	1.13	1.05	1.15	0.93	-	-
7	7	33.3	4	16.00	18.70	0.74	0.05	3.71	0.12	471.2	32.3	448.2	28.1	427.2	19.6	0.99	0.94	0.89	0.95	0.91	0.95
8	15	29.8	1	17.00	19.70	0.78	0.06	3.78	0.16	496.5	39.3	465.1	38.8	445.5	41.7	1.04	0.97	0.93	0.94	0.90	0.96
9	5	25.7	2	18.00	20.70	0.74	0.01	3.64	0.08	470.4	8.8	430.3	18.2	481.8	44.9	0.98	0.90	1.01	0.91	-	-
10	16	32.9	2	19.00	21.70	0.80	0.06	3.86	0.14	512.4	39.3	484.9	35.5	465.9	28.4	1.07	1.01	0.97	0.95	0.91	0.96
11	25	28.3	2	20.00	22.70	0.87	0.06	3.98	0.12	553.0	36.5	516.2	32.1	482.2	35.6	1.16	1.08	1.01	0.93	0.87	0.93
12	46	27.6	2	21.00	23.70	0.75	0.07	3.70	0.18	475.8	41.7	446.5	43.3	445.6	42.2	1.00	0.93	0.93	0.94	0.94	1.00
13	51	24.0	3	22.00	24.70	0.72	0.04	3.67	0.11	457.8	22.7	438.9	26.7	441.0	18.1	0.96	0.92	0.92	0.96	0.96	1.00
14	28	20.5	4	23.00	25.70	0.69	0.04	3.57	0.09	440.8	22.8	414.3	21.4	403.5	26.8	0.92	0.87	0.84	0.94	0.92	0.97

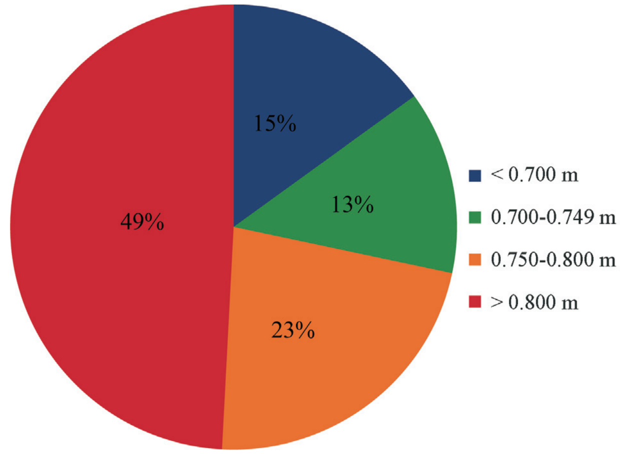

Figure 8 - Percentage of blow counts applied in different ranges of hammer drop height from Boring 1.

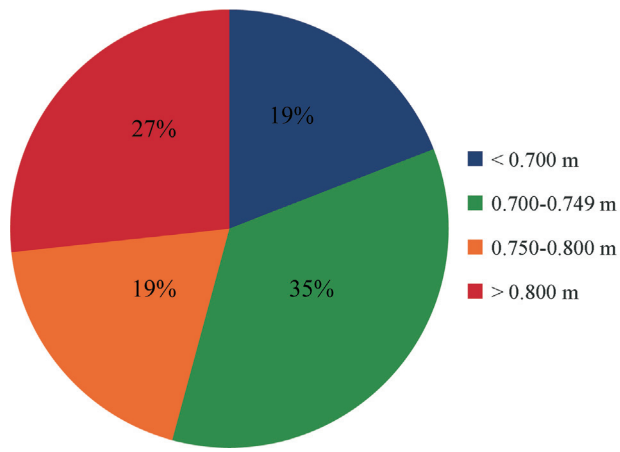

Figure 9 - Percentage of blow counts applied in different ranges of hammer drop height from Boring 2.

Figure 14 shows typical force and velocity signals measured just below the anvil. Figure 15 shows typical values of energy *vs.* time.

Figure 16 illustrates values of E_i normalized by the actual potential energy (E_p), as a function of the rod length, for borings 1 and 2.

3.3. Analysis of the results

The average hammer drop height of sequences from Boring 1 varied from 67 to 87 cm, with actual potential energy in the range 429.1 - 554.0 J, reaching a difference of 29%. The hammer has been lifted higher than 80 cm, or lower than 70 cm (difference higher than 5 cm from the standard value) in 64% of the blows. The average hammer drop height of the whole data from Boring 1 is 80 cm, with a standard deviation of 9 cm.

The scatter in hammer drop height values was smaller in Boring 2. The average hammer drop height varied from 69 to 87 cm, with potential energies in the range 440.8-553.0 J, reaching a difference of 25%. The hammer has

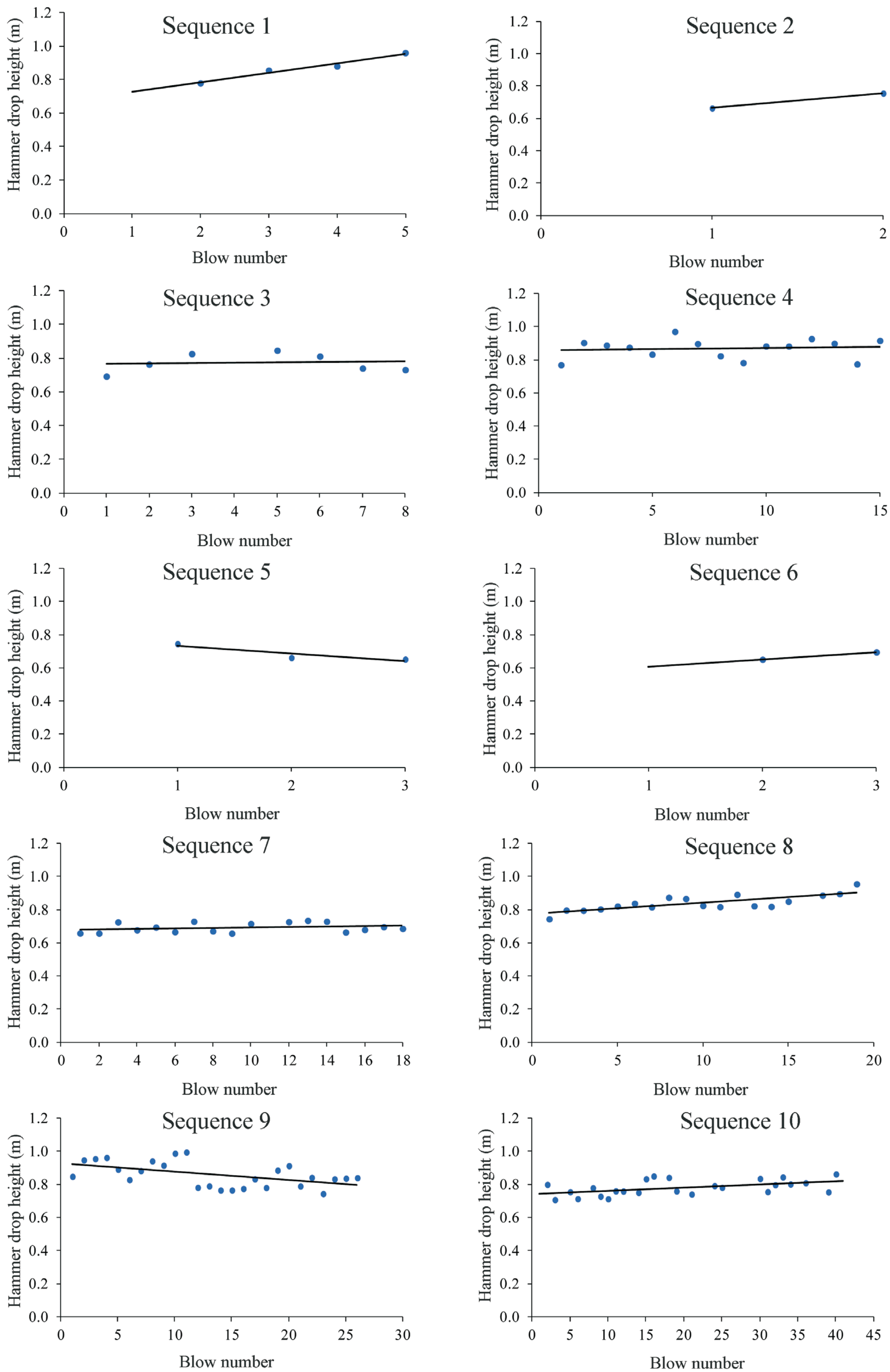

Figure 10 - Hammer drop height measured in Boring 1.

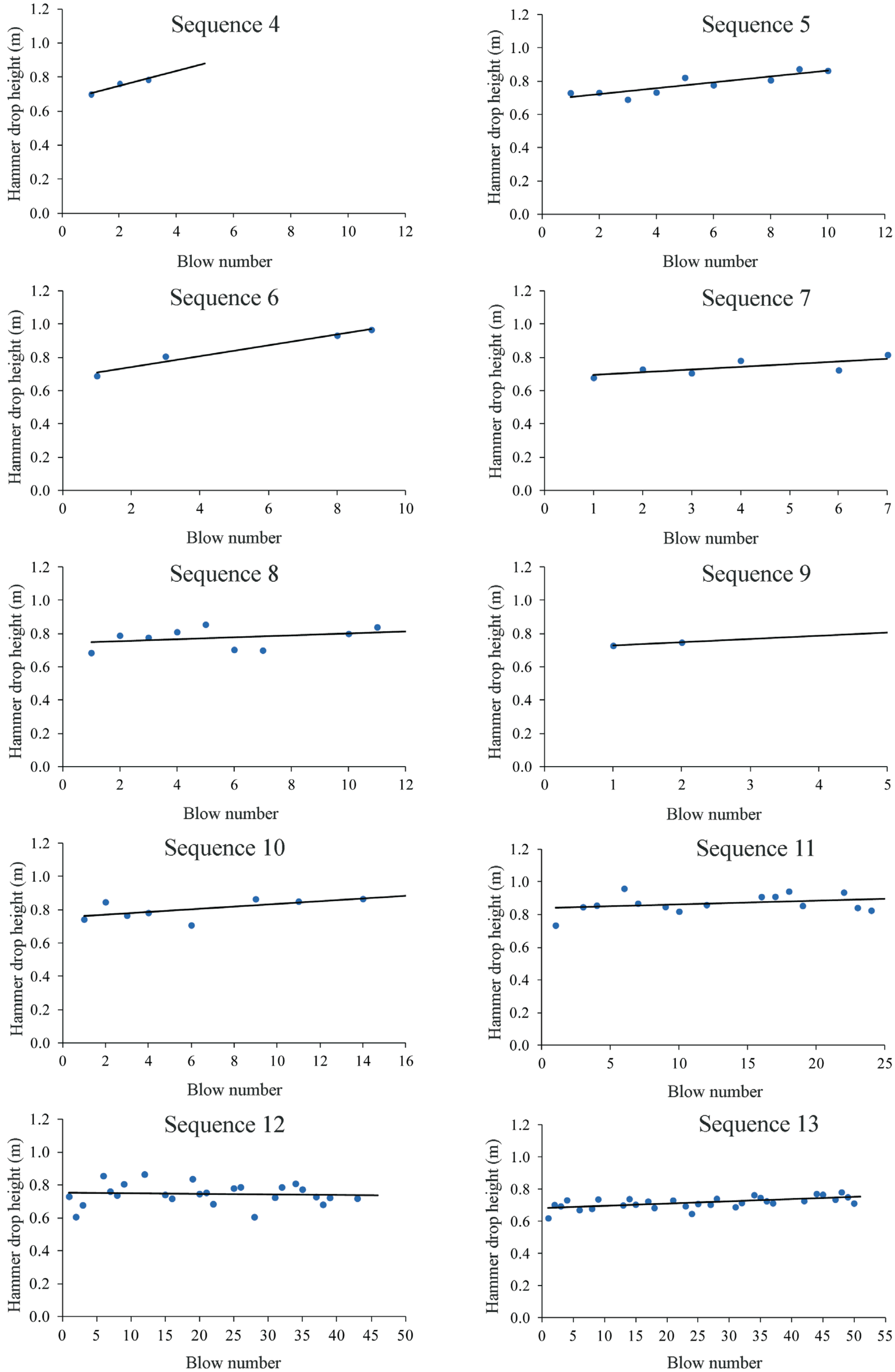

Figure 11a - Hammer drop height measured in Boring 2 (sequences from 4 to 13).

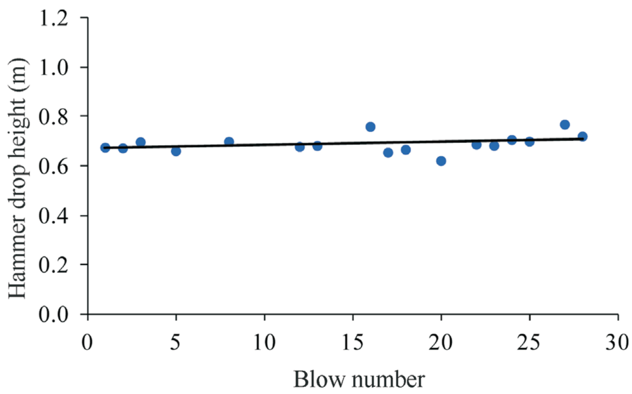

Figure 11b - Hammer drop height measured in Boring 2 (sequence 14).

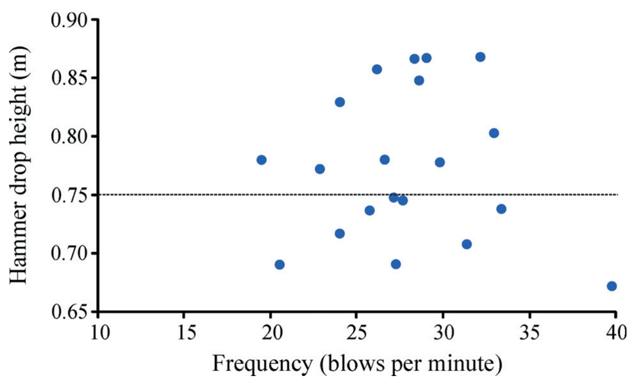

Figure 12 - Hammer drop height *vs.* frequency of blows per minute.

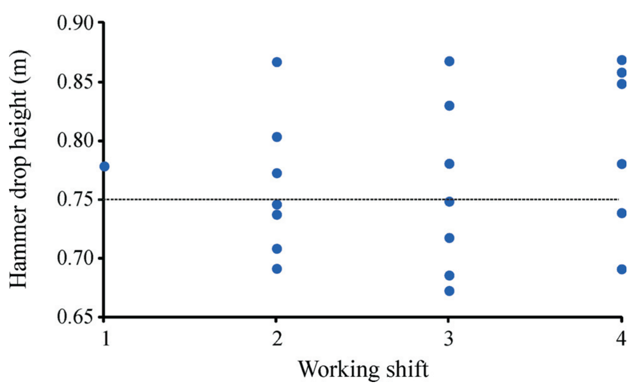

Figure 13 - Hammer drop height *vs.* shift (first shift, from 8 and 10 AM; second shift, from 10 to 12 AM; third shift, from 14 to 16 PM and fourth shift, from 16 to 18 PM).

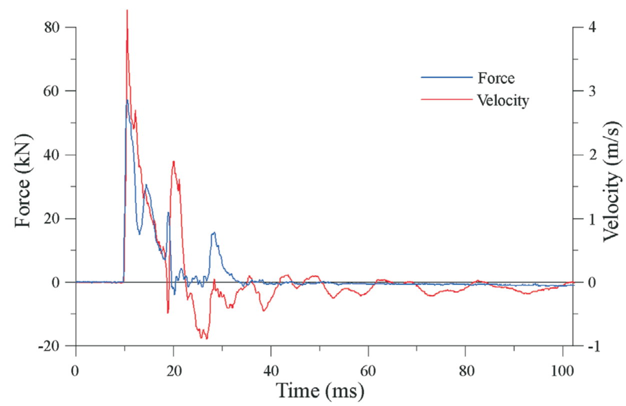

Figure 14 - Typical signals of force and velocity measured just below the anvil (Blow 21 of Sequence 9, Boring 1).

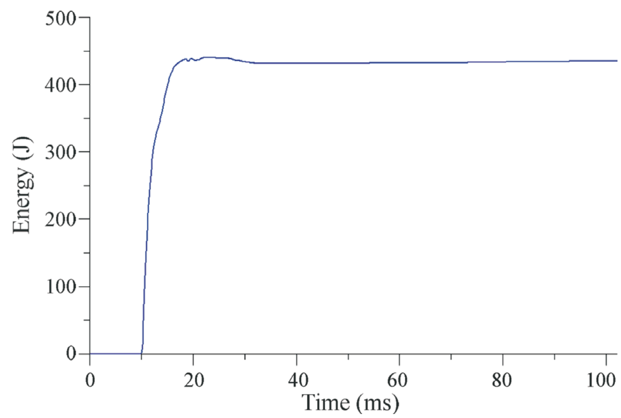

Figure 15 - Typical values of energy (just below the anvil) *vs.* time (Blow 21 of Sequence 9, Boring 1).

been lifted to heights greater than 80 cm or lower than 70 cm in 46% of the blows. The average hammer drop height is 76 cm, with a standard deviation of 8 cm.

Therefore, in spite of both borings had been performed by the same crew, using the same equipment and on the same site, under the same conditions, a difference on the average hammer drop height in Borings 1 and 2 was verified (80 and 76 cm, respectively). Two other aspects observed in the tests: i) a variation in the hammer drop height in the same blow sequence; ii) a variation in the average hammer drop height from different sequences.

A tendency to increase the hammer drop height with the advance of the sequence was observed in both borings. Only in two out of 21 sequences the opposite behavior was verified. It was hypothesized that the increase in hammer drop height is caused by the fatigue of the crew, resulting in less care in the procedure, although the opposite should seem more probable. The average frequency of the blows was 19.4 and 39.7 blows per minute, in Borings 1 and 2, respectively, which is a significant difference. The smaller frequencies were observed in the longer sequences, with more than 25 blows, probably also caused by fatigue of the crew. The shorter sequences, with five or even fewer blows, presented the higher frequencies. The average frequency of blows for all sequences (Borings 1 and 2) was 27.8 blows/min with a standard deviation of 4.7 blows/min.

Many authors (*e.g.*, Kovacs, 1979; Seed *et al.*, 1985; Skempton, 1986; Décourt, 1989) discuss the influence of the frequency of blows on SPT results.

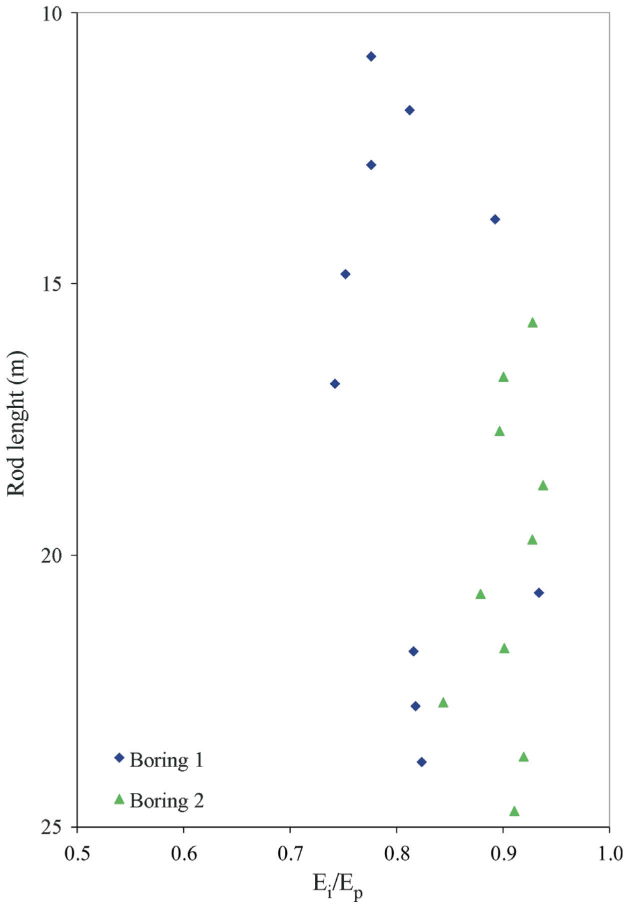

Figure 16 - Rod length *vs.* energy just below the anvil normalized by the actual potential energy (E_i/E_p).

In fact, the dynamic condition of SPT may generate excess pore water pressures that can influence the soil resistance to penetration, even in sands. These excess pore water pressures can be influenced by the driving frequencies. Tests submitted to different frequencies can result in different N values in the same soil. Seed *et al.* (1985) showed that the N values might be affected by the blow application frequency, depending on soil characteristics.

Danziger *et al.* (2009) and Souza *et al.* (2012a, 2012b) listed different values of the ratio q_c/N (where q_c is cone resistance) for loose and dense sands. Unlike the CPT, where the test is performed in drained conditions in the case of sands, SPT may generate positive excess pore pressures in loose sands and negative excess pore pressures in dense sands. This results in lower q_c/N values when tests are carried out in dense sands, and higher q_c/N values when tests are performed in loose sands.

Although not very pronounced, Fig. 12 shows a tendency of more scatter on the hammer drop height with the increase of the frequency of blows, not only above, but also below the standard value.

The work shift does not seem to have influenced the hammer drop height, as indicated by the data presented in Fig. 13, where a similar scatter was observed for all work shifts.

The average hammer velocity at impact varied from 3.38 to 4.02 m/s (kinetic energy of 371.6 and 525.8 J, respectively) in the sequences from Boring 1, whereas in the sequences from Boring 2 the average hammer velocity at impact varied from 3.57 to 3.98 m/s (kinetic energy of 414.3 and 516.2 J, respectively), see Tables 1 and 2. This variation is a consequence of the inadequate control in the hammer drop height.

The efficiency factor e_1 (E_k/E^*), defined by Décourt (1989), varied in Boring 1 from 0.78 to 1.10 and in Boring 2 from 0.87 to 1.08. These values are greater than those found by Cavalcante *et al.* (2011) and varied in a broader range than those presented by Décourt (1989), see Fig. 17. Values of e_1 greater than 1.00 are explained by the hammer drop height above the standard value in various sequences.

In order to avoid the influence of the hammer drop height on the efficiency factors, Santana *et al.* (2012) proposed the use of an efficiency factor e_1*, given by E_k/E_p. The values of e_1* varied from 0.86 to 0.99 in Boring 1 and from 0.91 to 0.96 in Boring 2. These values are greater than those presented by Décourt (1989) for the manual system and by Cavalcante *et al.* (2011), see Fig. 18. As expected, e_1* values have less scatter than e_1 values.

The average energy measured just below the anvil, E_i, varied from 318.1 J (efficiency of 67% in relation to the theoretical potential energy or nominal energy) to 493.5 J (efficiency of 103%) in Boring 1, whereas in Boring 2 varied from 403.5 J (efficiency of 84%) to 551.4 J (efficiency of 115%). This significant scatter in E_i values is mainly a consequence of the variation on the hammer drop height, see Tables 1 and 2.

These results indicate that even SPT performed by the same boring crew, in similar conditions, can result in N values with distinct significance. When the efficiency of the energy measured just below the anvil is calculated in relation to the actual potential energy, the range in efficiency is significantly lower, varying from 74% to 93% in Boring 1 and from 85% to 96% in Boring 2, see Tables 1 and 2.

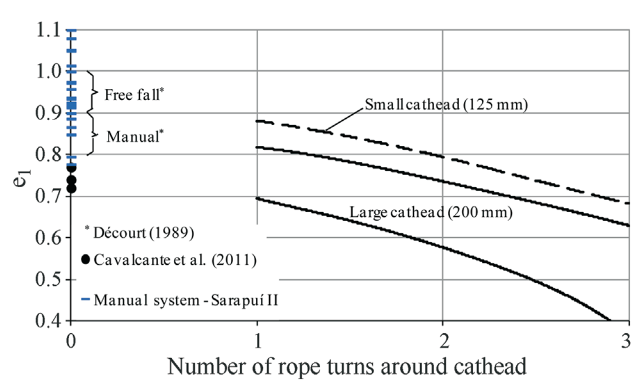

Figure 17 - Values of the efficiency factor e_1 (adapted from Skempton, 1986, Décourt, 1989 and Cavalcante *et al.*, 2011).

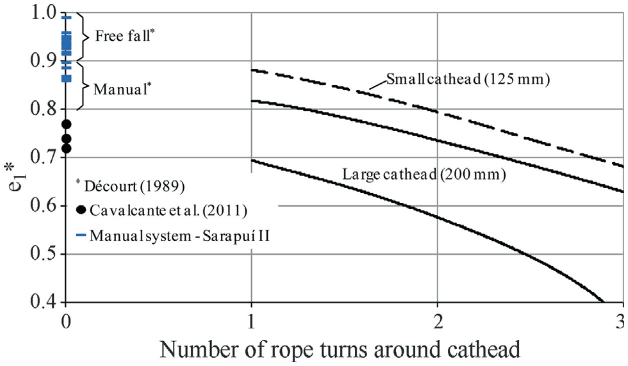

Figure 18 - Values of the efficiency factor e_1* (adapted from Skempton, 1986, Décourt, 1989 and Cavalcante *et al.*, 2011).

The efficiency factor e_2 (E_i/E_k) varied from 0.86 to 0.94 in Boring 1 and from 0.92 to 1.00 in Boring 2. These values are in the range - average line of Décourt (1989) data and Cavalcante *et al.* (2011) data -, considering the anvil of 977 g, see Tables 1 and 2 and Fig. 19.

It is possible that high values of factor e_2 are associated to the downward movement of the rod stem during hammer blow, generating an increase in potential energy that is transferred to the rods in subsequent hammer impacts of the same blow. This occurrence, described by Odebrecht (2003), is more relevant in low resistance soils. The SPT Analyzer is capable of measuring the whole energy transferred to the rod stem, only if the process occurs before 102 ms. However, the kinetic energy is calculated in relation to the first hammer impact with the anvil, so the e_2 value can be overestimated should other impacts occur.

The results of E_i/E_p as a function of the rod length measured in Borings 1 and 2 are presented in Fig. 16. This figure illustrates that the energy transferred to the rod stem is not significantly affected by its length, at least in the range of lengths analyzed, from 10.80 to 25.70 m. This is corroborated by previous studies (*e.g.*, Cavalcante, 2002; Odebrecht, 2003; Daniel *et al.*, 2005; Danziger *et al.*, 2008) indicating that the energy transmitted to the rod stem does not depend on its length and the e_3 factor should be considered equal to 1.00.

4. Conclusions

The paper presented the instrumentation results of two SPT deployments performed by the same crew, using the same procedures and equipment in the Sarapui II Experimental Test Site. The main conclusions are summarized as follows:

i) Although both borings had been performed by the same crew, using the same equipment and on the same site, under the same conditions, a difference was found in the average hammer drop height in Borings 1 and 2 (80 and 76 cm, respectively). Two other aspects observed in the tests: a variation in the hammer drop height in the same blow sequence; a variation in the average hammer drop height from different sequences.

ii) A tendency to increase the hammer drop height as the sequence advances was observed in both borings. The opposite behavior was verified in only two out of 21 sequences. It was hypothesized that the increase in hammer drop height is caused by the fatigue of the crew, resulting in the careless of the procedure, although the opposite should seem more probable.

iii) The average frequency of blows was 19.4 and 39.7 blows per minute in Borings 1 and 2, respectively. The smaller frequencies were observed in the longer sequences, with more than 25 blows, probably caused by the fatigue of the crew. The shorter sequences, with five or even less blows, presented the higher frequencies.

iv) A slight trend of higher scatter on the hammer drop height was observed when the rate of blows increased.

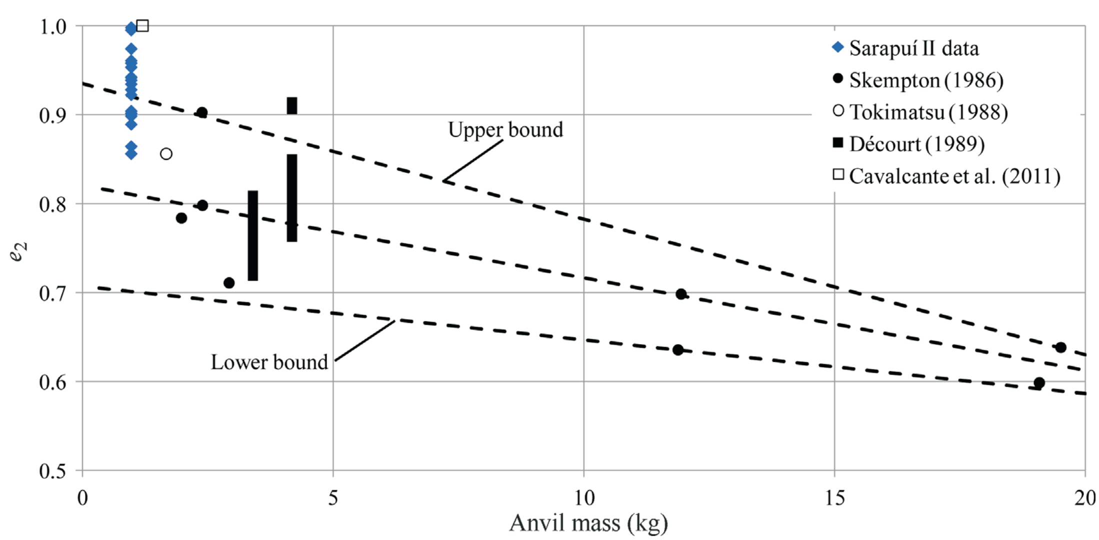

Figure 19 - Efficiency factor e_2 as a function of the anvil mass (adapted from Décourt, 1989 and Cavalcante *et al.*, 2011).

v) The work shift does not seem to have influenced the hammer drop height, since a similar scatter was observed for all work shifts.

vi) The efficiency factor e_1 (E_k/E^*) varied in Boring 1 from 0.78 to 1.10 and in Boring 2 from 0.87 to 1.08. These values are higher than those found by Cavalcante *et al.* (2011) and varied in a broader range than those presented by Décourt (1989). Values of e_1 greater than 1.00 are explained by the hammer drop height above the standard value in various sequences.

vii) The values of e_1* (E_k/E_p) varied in Boring 1 from 0.86 to 0.99 and in Boring 2 from 0.91 to 0.96, in a narrower range than the e_1 values.

viii) The average energy measured just below the anvil, E_i, varied from 318.1 J (efficiency of 67% in relation to the theoretical potential energy or nominal energy) to 493.5 J (efficiency of 103%) in Boring 1, whereas in Boring 2 varied from 403.5 J (efficiency of 84%) to 551.4 J (efficiency of 115%). The scatter in E_i values is mainly due to the variation in the hammer drop height. The obtained results indicate that even SPT performed by the same boring crew, in similar conditions, can result in *N* values with distinct significance.

ix) When the efficiency of the energy measured just below the anvil is calculated in relation to the actual potential energy, the range in efficiency is significantly lower, varying from 74% to 93% in Boring 1 and from 85% to 96% in Boring 2.

x) The efficiency factor e_2 (E_i/E_k) varied in Boring 1 from 0.86 to 0.94 and in Boring 2 from 0.92 to 1.00.

xi) The values of E_i/E_p *vs.* the rod length indicate that the energy transferred to the rod stem is not significantly affected by its length, and the efficiency factor e_3 should be considered as 1.00.

Acknowledgments

Roberto Marinho and Max Gomes de Souza, for their help in performing instrumented SPTs. Elvyn Marshall, who proofread the paper.

References

ABNT (2001) Soil - SPT - Test Method. Brazilian Standard NBR 6484, Brazilian Technical Standards Association (ABNT), 17 p. (in Portuguese).

Abou-Matar, H. & Goble, G.G. (1997) SPT Dynamics Analysis and Measurements. Journal of Geotechnical and Geoenvironmental Engineering, ASCE, v. 123:10, p. 921-928.

Aoki, N. & Cintra, J.C.A. (2000) The Application of Energy Conservation Hamilton's Principle to the Determination of Energy Efficiency in SPT Tests. Proc. 6th Int. Conf. on the Application of the Stress-Wave Theory to Piles, São Paulo, v.1, p. 457-460.

Belincanta, A. (1985) Dynamic Energy in SPT – Results from a Theoretical-Experimental Investigation. M.Sc. Thesis, EPUSP, São Paulo State University, São Paulo, 217 p. (in Portuguese).

Belincanta, A. (1998) Evaluation of Factors Affecting the Penetration Resistance in SPT. Ph.D. Thesis, EESC, São Paulo State University, São Carlos, 141 p. (in Portuguese).

Belincanta, A. & Cintra, J.C.A. (1998) Factors Affecting SPT: the Brazilian Experience. Solos e Rochas, v. 21:3, p. 119-133 (in Portuguese).

Broms, B.B. & Flodin, N. (1988) History of Soil Penetration Testing. Penetration Testing, ISOPT-1. J. De Ruiter Ed., Orlando, p. 178-186.

Campanella, R.G. & Sy, A. (1994) Recent Developments in Energy Calibration of Penetration Tests at UBC. Proc. XII Int. Conf. on Soil Mech. Found. Eng., New Delhi, p. 151-156.

Cavalcante, E. H. (2002) Theoretical-Experimental Investigation of SPT. Ph.D. Thesis, COPPE, Federal University of Rio de Janeiro, Rio de Janeiro, 430 p. (in Portuguese).

Cavalcante, E.H.; Danziger, B.R. & Danziger, F.A.B. (2011) Measurement of Drop Height and Impact Velocity in the Brazilian SPT System. Soils and Rocks, v. 34:3, p. 207-218.

Clayton, C.R.I. (1990) SPT Energy Transmission: Theory, Measurement and Significance. Ground Engineering, v. 23:10, p. 35-43.

Daniel, C.R.; Howie, J.A.; Jackson, R.S. & Walker, B. (2005) Review of Standard Penetration Test Short Rod Corrections. Journal of Geotechnical and Geoenvironmental Engineering, ASCE, v. 131:4, p. 489-497.

Danziger, B.R.; Souza, J.M.S. & Danziger, F.A.B. (2009) Comparison of Methods to Predict Mobilized Loads During SPT in Sand. Proc. Engenharia de Fundações: Passado Recente e Perspectivas, São Carlos, v. 1, p. 65-73 (in Portuguese).

Danziger, F.A.B.; Danziger, B.R. & Cavalcante, E.H. (2006) Discussion of Review of Standard Penetration Test Short Rod Corrections, by Chris R. Daniel, John A. Howie, R. Scott Jackson, & Brian Walker. Journal of Geotechnical and Geoenvironmental Engineering, ASCE, v. 132:12, p. 1634-1637.

Danziger, F.A.B.; Danziger, B.R. & Cavalcante, E.H. (2008) On the SPT Energy and the Meaning of N Value in Special Cases. Proc. XIV Braz. Conf. on Soil Mech. Geotech. Eng., Búzios, CD-rom, p. 2214-2224 (in Portuguese).

Décourt, L. (1989) General report / Discussion Session 2: SPT, CPT, Pressuremeter Testing and Recent Developments in In-Situ Testing – Part 2: The Standard Penetration Test, State-of-the-Art Report. Proc. XII Int. Conf. on Soil Mech. Found. Eng., Rio de Janeiro, v. 4, p. 2405-2416.

Décourt, L.; Muromachi, T.; Nixon, I.K.; Schmertmann, J.H.; Thorburn, S. & Zolkov, E. (1988) Standard Penetration Test (SPT): International Reference Test Procedure. Proc. ISSMFE Technical Committee on Penetration Testing – SPT Working Party, ISOPT-I, Orlando, v.1, p. 3-26.

De Mello, V.F.B. (1971) Standard Penetration Test. Proc. 4th Pan-American Conf. on Soil Mech. Found. Eng., Puerto Rico, v. l, p. 1-86.

Fletcher, G.F.A. (1965) Standard Penetration Test: Its Uses and Abuses. Journal of the Soil Mechanics and Foundations Division, ASCE, v. 91:SM4, p. 67-75.

Fujita, K. & Ohno, M. (2000) Stress Wave Application to Standard Penetration Test in Japan. Proc. 6th Int. Conf. on the Application of Stress-Wave Theory to Piles, São Paulo, v. 1, p. 469-475.

Ireland, H.O.; Moretto, O. & Vargas, M. (1970) The Dynamic Penetration Test: A Standard that is not Standardized. Géotechnique, v. 20:2, p. 185-192.

ISSMFE (1989) Report of the ISSMFE – Technical Committee on Penetration Testing of Soils – TC 16 With Reference Test Procedures – CPT – SPT – DP – WST. International Reference Test Procedure for the Standard Penetration Test (SPT), p. 17-19.

Jannuzzi, G.M.F. (2009) The Characterization of Sarapuí II Soft Clay Site by In-Situ Testing. M.Sc. Thesis, COPPE, Federal University of Rio de Janeiro, Rio de Janeiro, 195 p. (in Portuguese).

Jannuzzi, G.M.F. (2013) Innovative, Modern and Traditional Methods to Characterize the Sarapuí II Soft Clay. Ph.D. Thesis, COPPE, Federal University of Rio de Janeiro, Rio de Janeiro, 414 p. (in Portuguese).

Kovacs, W.D. (1979) Velocity Measurement of Free-Fall SPT Hammer. Journal of the Geotechnical Engineering Division, ASCE, v. 105:GT1, p. 1-10.

Kovacs, W. D. (1980) What Constitutes a Turn? Geotechnical Testing Journal, ASTM, v. 3:3, p. 127-130.

Kovacs, W.D. (1994) Effects of SPT Equipment and Procedures on the Design of Shallow Foundations on Sand. Proc. Settlement'94, ASCE, New York, v. 1, p. 121-131.

Kovacs, W.D.; Evans, J.C. & Griffith, A.H. (1977) Towards a More Standardized SPT. Proc. 9th Int. Conf. on Soil Mech. Found. Eng., Tokyo, v. 2, p. 269-276.

Kovacs, W.D.; Griffith, A.W. & Evans, J.C. (1978) An Alternative to the Cathead and Rope for the Standard Penetration Test. Geotechnical Testing Journal, ASTM, v. 1:2, p. 72-81.

Kovacs, W.D. & Salomone, L.A. (1982) SPT Hammer Energy Measurement. Journal of the Soil Mechanics and Foundations Division, ASCE, v. 108:GT4, p. 599-620.

Kulhawy, F.H. & Mayne, P.W. (1990) Manual on Estimating Soil Properties for Foundation Design. Prepared by Cornell University for Electric Power Research Institute (EPRI), 308 p.

Matsumoto, T.; Sikigushi, H. & Yoshida, H. (1992) Significance of Two Point Strain Measurement in SPT. Soils and Foundations, v. 32:2, p. 67-82.

Morgano, C.M. & Liang, R. (1992) Energy Transfer in SPT – Rod Length Effect. Proc. 4th Int. Conf. on the Application of Stress-Wave Theory to Piles, Netherlands, v. 1, p. 121-127.

Odebrecht, E. (2003) SPT Energy Measurement. Ph.D. Thesis, Federal University of Rio Grande do Sul, Porto Alegre, 230 p. (in Portuguese).

Odebrecht, E.; Schnaid, F.; Rocha, M.M. & Bernardes, G.P. (2005) Energy Efficiency for Standard Penetration Tests. Journal of Geotechnical and Geoenvironmental Engineering, ASCE, v. 131:10, p. 1252-1263.

Palacios, A. (1977) Theory and Measurements of Energy Transfer During Standard Penetration Test Sampling. Ph.D. Thesis, University of Florida, USA, 391 p.

Riggs, C.O.; Schmidt, O. N. & Rassieur, C.L. (1983) Reproducible SPT Hammer Impact Force with an Automatic Free Fall SPT Hammer System. Geotechnical Testing Journal, ASTM, v. 6:3, p. 201-209.

Robertson, P.K.; Campanella, R.G. & Wightman, A. (1983) SPT-CPT Correlations. Journal of Geotechnical Engineering, ASCE, v. 109:11, p. 1449-1459.

Santana, C.M.; Danziger, F.A.B. & Danziger, B.R. (2012) The measurement of Energy Reaching the Sampler in SPT. Proc. 4th Int. Conf. on Site Characterization, ISC-4, Porto de Galinhas, v. 1, p. 921-926.

Schmertmann, J.H. & Palacios, A. (1979) Energy Dynamics of SPT. Journal of the Geotechnical Engineering Division, ASCE, v. 105:GT8, p. 909-926.

Seed, H.B.; Tokimatsu, K.; Harder, L.F. & Chung, R.M. (1985) Influence of SPT Procedures in Soil Liquefaction Resistance Evaluations. Journal of the Geotechnical Engineering Division, ASCE, v. 111:12, p. 1425-1445.

Serota, S. & Lowther, G. (1973) SPT Practice Meets Critical Review. Ground Engineering, v. 6:1, p. 20-22.

Souza, J.M.S.; Danziger, B.R. & Danziger, F.A.B. (2012a) The Influence of the Relative Density of Sands in SPT and CPT Correlations. Soils and Rocks, v. 35:1, p. 99-113.

Souza, J.M.S.; Danziger, B.R. & Danziger, F.A.B. (2012b) The Influence of Sand Density on SPT x CPT Correlations. Proc. 4th Int. Conf. on Site Characterization, ISC-4, Porto de Galinhas, v. 1, p. 859-864.

Skempton, A.W. (1986) Standard Penetration Test Procedures and the Effects in Sands of Overburden Pressure, Relative Density, Particle Size, Ageing and Overconsolidation. Géotechnique, v. 36:3, p. 425-447.

Teixeira, A.H. (1993) An Improvement of the SPT. In Soils from São Paulo, ABMS-NRSP, chapter 4, p. 75-93 (in Portuguese).

Tokimatsu, K. (1988) Penetration Tests for Dynamic Problems. ISOPT-1, J. De Ruiter Ed., Orlando, p. 117-136.

Youd, T.L.; Bartholomew, H.W. & Steidl, J.H. (2008) SPT Hammer Energy Ratio *vs.* Drop Height. Journal of Geotechnical and Geoenvironmental Engineering, ASCE, v. 134:3, p. 397-400.

Geotechnical Characterization of Suape Soft Clays, Brazil

R.Q. Coutinho, M.I.M.C.V. Bello

Abstract. Comprehensive research has been carried out by the Geotechnical Group (GEGEP) of the Federal University of Pernambuco in the soft clay deposits in Northeastern Brazil near the city of Recife. This paper presents the results of important geotechnical investigations of soft clays in two areas within the Suape Port and Industrial Complex. The geotechnical parameters were obtained from laboratory (classification, compressibility and strength) and *in situ* (SPT, vane and CPTU) tests, and were compared with regional empirical correlations and proposals presented in literature. The vane tests were performed to obtain undrained strength and overconsolidation ratio parameters. The classifications for soil behavior, together with flow characteristics, strength and overconsolidation ratio parameters, were determined by piezocone tests. The results are compared with results from reference tests, and discussed with results from the literature, including the results of Recife and other Brazilian clays. This study confirms that parameters can be obtained by means of *in situ* tests with correlations suited to the local/regional experience and the importance of having a joint laboratory and *in situ* test program. This prediction is fundamental for a proper geotechnical site characterization in studies and engineering projects.

Keywords: geotechnical parameters, soft clays, laboratory and *in situ* testing.

1. Introduction

The Suape Port and Industrial Complex is a very complete and important industrial center in Northeast Brazil. The geographical location of Pernambuco State gives Suape Port an international status since it is located on the main international shipping routes. Large companies, a shipyard, refinery and other industries already exist or their facilities are under construction in this area.

The use of field tests to evaluate geotechnical parameters of soils has been increasing in recent years. Coutinho (2008) (see also Coutinho *et al.*, 2008) published a study about the geotechnical parameters obtained from *in situ* investigations for practical projects. The ability to obtain parameters by means of *in situ* tests with correlations suited to the local/regional experiment is fundamental for proper geotechnical site characterization in studies and engineering projects. Soil stratigraphy, compressibility and rate of consolidation parameters, undrained shear strength (Su) and the overconsolidation ratio (OCR) of soft clays can be estimated based on an investigation program including *in situ* and laboratory testing (Schnaid, 2009; Mayne, 2007; Lunne *et al.*, 1997).

This paper presents the results of important geotechnical investigations of soft clays carried out in two areas within the Suape Port and Industrial Complex. The geotechnical parameters were obtained from laboratory (classification, compressibility and strength) and *in situ* (SPT, water content measurement, vane and CPTU) tests, and then compared with regional and proposed correlations presented in literature. The vane tests were used for obtaining undrained strength and overconsolidation ratio parameters. The classifications concerning soil behavior, in addition to flow characteristics, strength and overconsolidation ratio parameters were determined by piezocone tests. The results were discussed after comparing the laboratory tests and regional and literature results. This study is part of a research program of the Geotechnical Research Group (GEGEP) of the Federal University of Pernambuco (UFPE).

2. Characteristics of the Study Area

The AE-1 and AE-2 study areas are within the Suape Industrial and Port Complex, in the town of Ipojuca, Pernambuco State, Brazil (Fig. 1). The coastal location is characterized by a complex geology, including low-lying plains, with soils featuring reduced load capacities, very soft organic clays, with the presence of peat, roots, shells and fine layers of sand and silt. This soft soil generally has a high water and organic content with very low penetration test values (N_{SPT}). Projects included construction of embankments of varying heights (some 17 m) on the subsoil of clays and peat material.

The AE-1 study area is part of an access route where a temporary embankment around 2.0 m in height, has been built. The AE-2 study area, which includes an important project, was divided into five (5) subdivisions, where 20 boreholes and 34 undisturbed Shelby samples were taken. Geotechnical site characterization included laboratory (characterization, oedometer and triaxial) and field (SPT, vane and CPTU) tests. Figures 2 and 3 illustrate typical soil parameter profiles for SUB-AREA A and C, respectively

Roberto Quental Coutinho, D.Sc., Professor, Departamento de Engenharia Civil, Universidade Federal de Pernambuco, Recife, PE, Brazil. e-mail: rqc@ufpe.br.
Maria Isabela Marques da Cunha V. Bello, D.Sc., Lecturer, Departamento de Engenharia Civil, Universidade Federal de Pernambuco, Caruaru, PE, Brazil. e-mail: isabelamcvbello@hotmail.com.
Submitted on April 30, 2014; Final Acceptance on December 15, 2014; Discussion open until April 30, 2015.

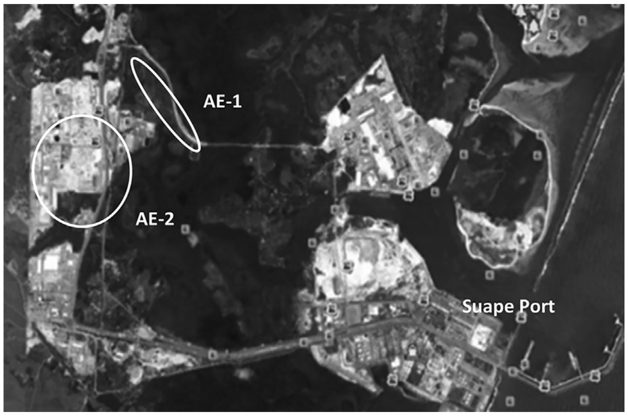

Figure 1 - Location of study areas: Suape, Ipojuca (Coutinho, 2010; Bello, 2011).

(AE-2 study area). Figure 4 presents a plasticity chart with laboratory test results on Suape soft soils, including organic soils. Results from two other Brazilian soft deposits are also presented (Recife-PE and Juturnaíba-RJ). Proposed ranges for inorganic and organic clays and peats are included. Further information about the geological and geotechnical characterization, together with parameters of the Suape study areas, can be found in Coutinho (2010) and Bello (2011).

3. Soil Classification Charts

Robertson & Campanella (1983), Robertson *et al.* (1986) and Sully *et al.* (1988) were the first to present charts based on piezocone tests that include measurements for cone resistance (q_t) corrected for pore pressure (Eq. 1).

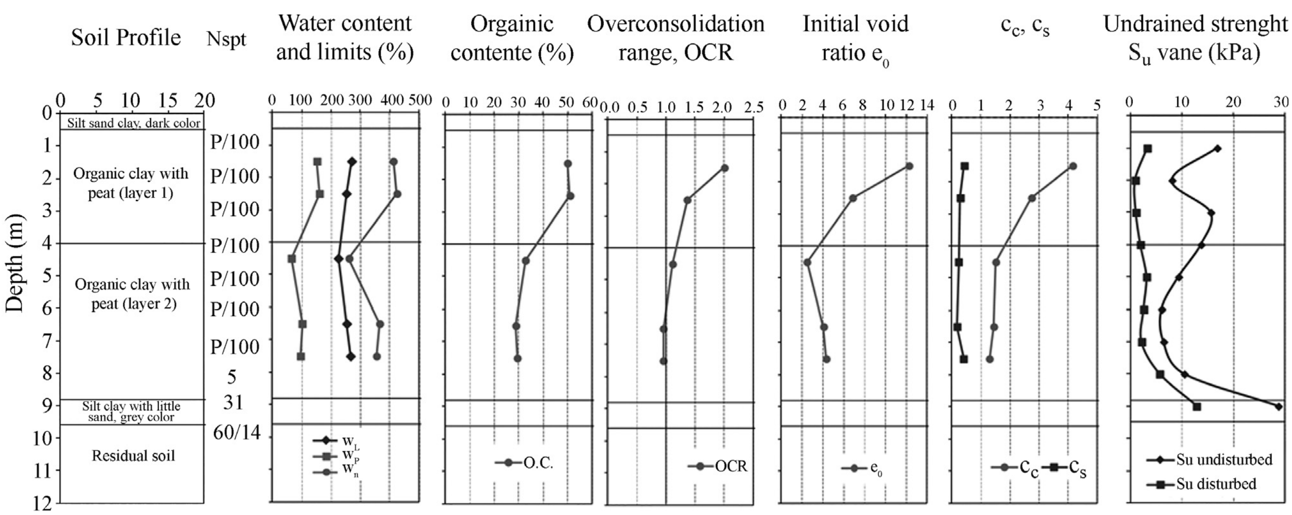

Figure 2 - Geotechnical profile of E106 (AE - 2 study area, SUB-AREA A), Suape (Coutinho, 2010; Bello, 2011).

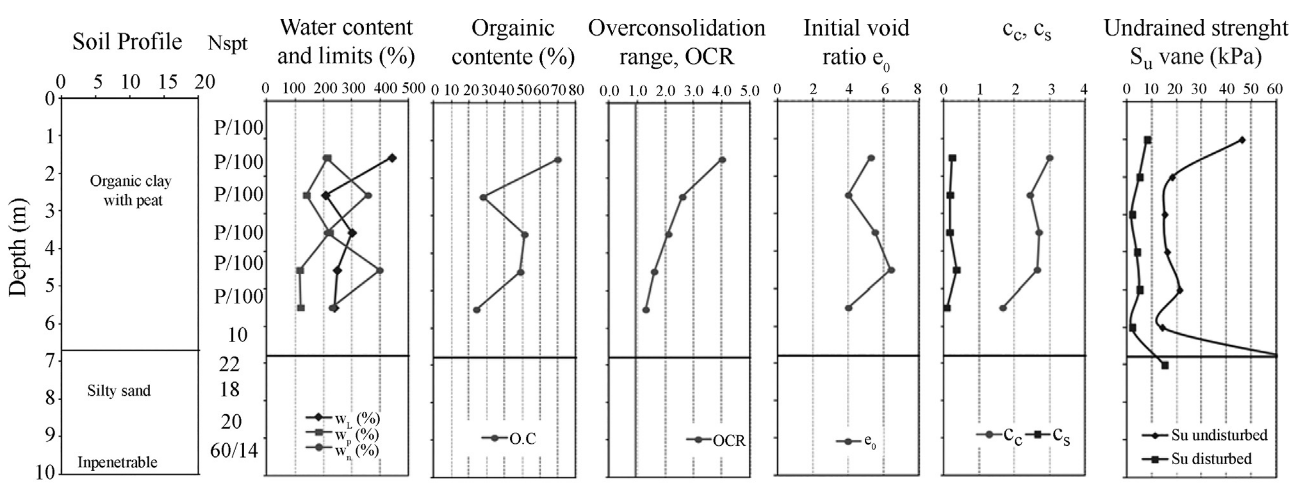

Figure 3 - Geotechnical profile of E121 (AE-2 study area, SUB-AREA C), Suape (Coutinho, 2010; Bello, 2011).

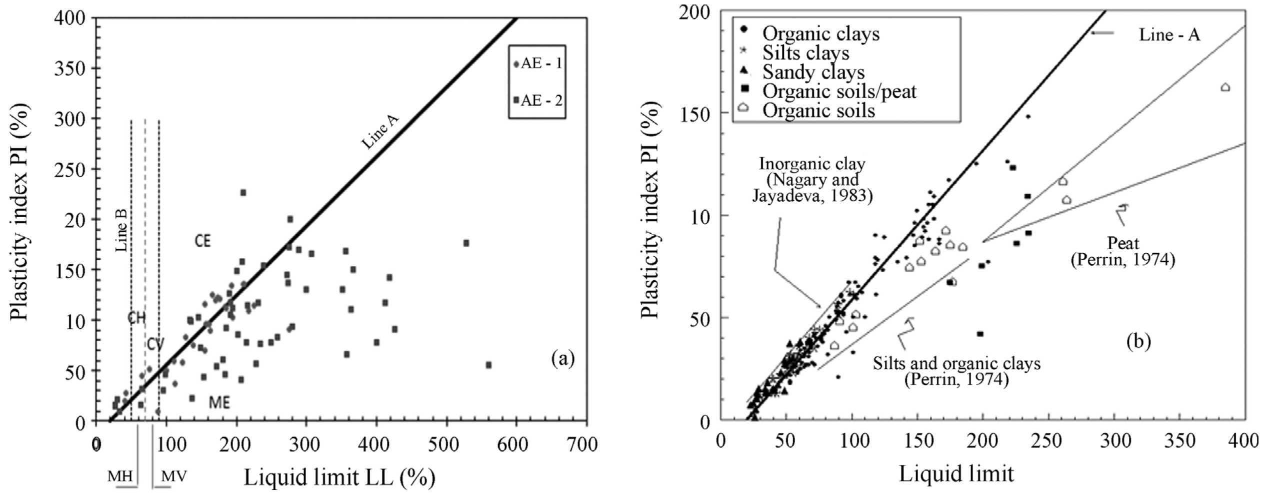

Figure 4 - Plasticity chart-soft soil results: (a) Suape (Bello, 2011); (b) Recife and Juturnaíba (Coutinho *et al.*, 1998).

Robertson *et al.* (1986) profiled a chart introducing the pore pressure ratio, *B*q (Eq. 2). This chart indicates 12 possible zones, or soil categories, obtained by plotting log q_t *vs.* F_r paired with sets of log q_t *vs.* B_q. Mayne (2007) shows 25 different CPT methods for soil classification, including the well-known methods from Begemann (1965), Schmertmann *et al.* (1978), and Robertson (1990).

$$q_t = q_c + u_2(1-a) \tag{1}$$

where u_2 = pore pressure measured at the cone shoulder; a = the ratio between the shoulder area unaffected by the pore water pressure and the total shoulder area.

$$B_q = \frac{u_2 - u_0}{q_1 - \sigma_v} \tag{2}$$

where B_q = pore pressure ratio; u_0 = *in-situ* pore pressure; σ_v = total vertical overburden stress at the depth z corresponding to the readings.

Robertson (1990) proposed a refinement of the Robertson *et al.* (1986) profiling chart, plotting "normalized cone resistance", Q_t, against "normalized friction ratio", F_r against pore pressure ratio B_q, and presented a nine-zone chart (Eqs. 3 and 4 respectively), (Fig. 5). Normalization was proposed to compensate for q_c dependency on the overburden stress, and when analyzing deep CPTU soundings (deeper than 30 m). Profiling charts developed for shallower soundings are not suitable for deeper sites.

$$Q_t = \frac{q_t - \sigma_{v0}}{\sigma'_{v0}} \tag{3}$$

$$F_r = \frac{f_s}{q_t - \sigma_{v0}} \times 100 \tag{4}$$

where f_s = sleeve friction.

Robertson (2010) suggested updating the charts supplied by Robertson *et al.* (1986), and Robertson (1990). The updated charts, which are dimensionless and color coded for improved presentation, define nine (9) SBT zones that are consistent.

Schneider *et al.* (2008) developed general soil classification charts using parametric studies (Fig. 6). The "zones" in the three charts are exactly the same, but the plots are shown in different formats: (1) coordinates log Q - log $\Delta u_2/\sigma'_{vo}$; (2) coordinates Q - $\Delta u_2/\sigma'_{vo}$; (3) coordinates semi-log Q - $\Delta u_2/\sigma'_{vo}$. These formats are best used in cases of: (1) clays, clayey silts, silts, sandy silts, and sands without negative penetration pore pressures; (2) sands and transitional soils with small negative excess penetration pore pressures, and (3) clay soils with large negative excess penetration pore pressure.

Long (2008) (see also Mollé, 2005; Coutinho, 2008) in a special study concluded that the Robertson *et al.* (1986) and Robertson (1990) charts for soil classification using CPTU data seem to work well in clays, clayey silts, silty sands and sands. They may have difficulties in using these charts in organic soils and peat, and in cases of complex stratigraphy.

Two proposals for soil classification from CPTU were utilized in Suape AE-2 study areas:

(a) Robertson (1990) charts:

(a.1) Coordinates log Q - B_q

(a.2) Coordinates log Q - F_r

(b) Schneider *et al.* (2008) charts:

(b.1) Case 1: Coordinates log Q - log $\Delta u_2/\sigma'_{vo}$

(b.2) Case 3: Coordinates semi log Q - $\Delta u_2/\sigma'_{vo}$

Eleven verticals were analyzed (six verticals in AE-2 SUB-AREA A, and five verticals in AE-2 SUB-AREA C). Figures 7 and 8 show results of CPTU classification from boreholes E104 (SUB-AREA A) and E121 (SUB-AREA C), respectively. For each borehole, classification of grain-

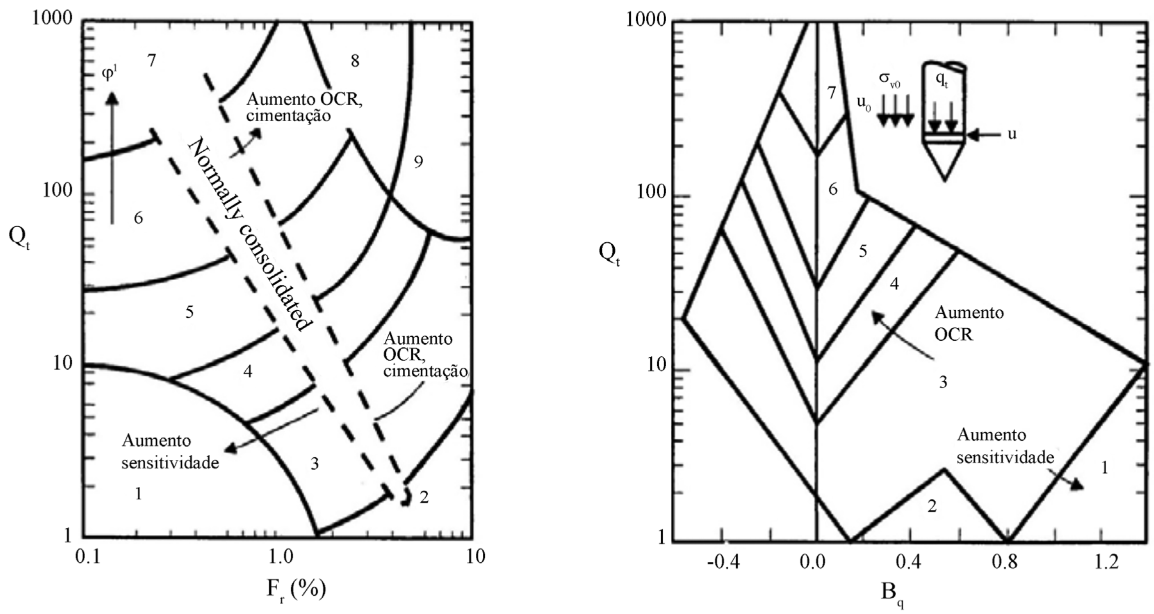

$$Q_t = \frac{q_t - \sigma_{v0}}{\sigma'_{v0}} \qquad B_q = \frac{u_2 - u_0}{q_t - \sigma_{v0}} \qquad F_r = \frac{f_s}{q_t - \sigma_{v0}} \times 100\%$$

Zone	Soil behaviour type:
1.	Sensitive, fine grained;
2.	Ogranic soils-peats;
3.	Clays-clay to silty clay;
4.	Silt mixtures clayey silt to silty clay;
5.	Sand mixtures; silty sand to sand silty;
6.	Sands: clean sands to silty sands;
7.	Gravelly sand to sand;
8.	Very stiff sand to clayey sanc
9.	Very stiff fine grained;

Figure 5 - Type of soil behavior (Robertson, 1990).

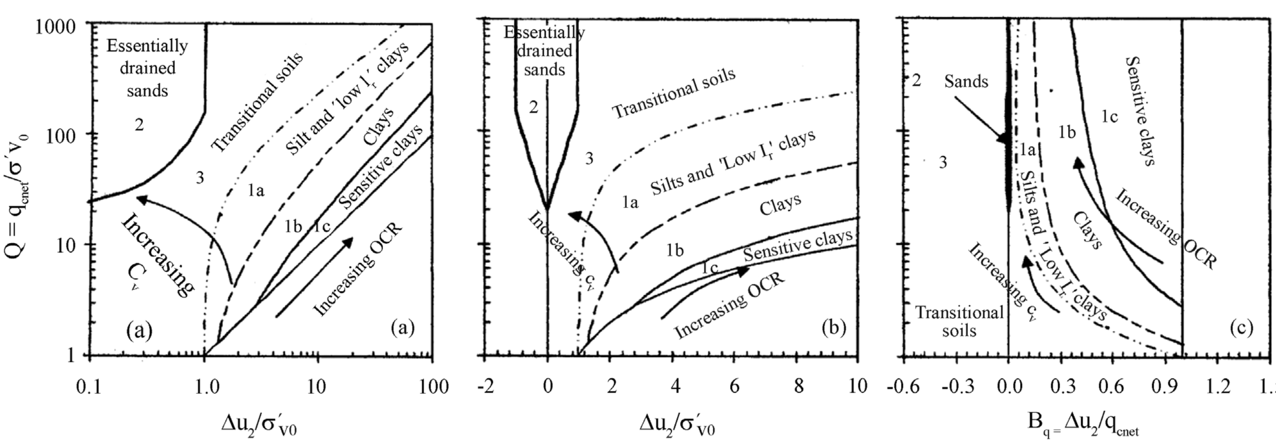

Figure 6 - Proposals for soils classification using CPTU testing for several forms of plotting (Schneider *et al.*, 2008).

size distribution and N_{SPT} values were compared with the CPTU classification.

3.1. Robertson (1990) charts results

In the Robertson (1990) chart (log Q - B_q), it was observed that the points tend to rise when the overconsolidation ratio (OCR) value increases (Figs. 7 and 8). These points are relative to the surface layer, and the layer below the clay layer, where silty and sandy material (bands 5, 6 and 7) can be found. These results were concordant with OCR and sensitivity (S_t) values obtained from oedometer and vane field tests, respectively. The points indicating clay soils are situated in bands 3 and 4.

In the Robertson (1990) chart (log Q - F_r), the points are situated in bands 3 and 4 (clay and silty clay). The F_r values were greater than 1.0.

The Robertson (1990) charts predict soil behavior, and are not directly related to soil classification criteria, using geological descriptions based on grain-size distribution. It has been verified that the greatest difference

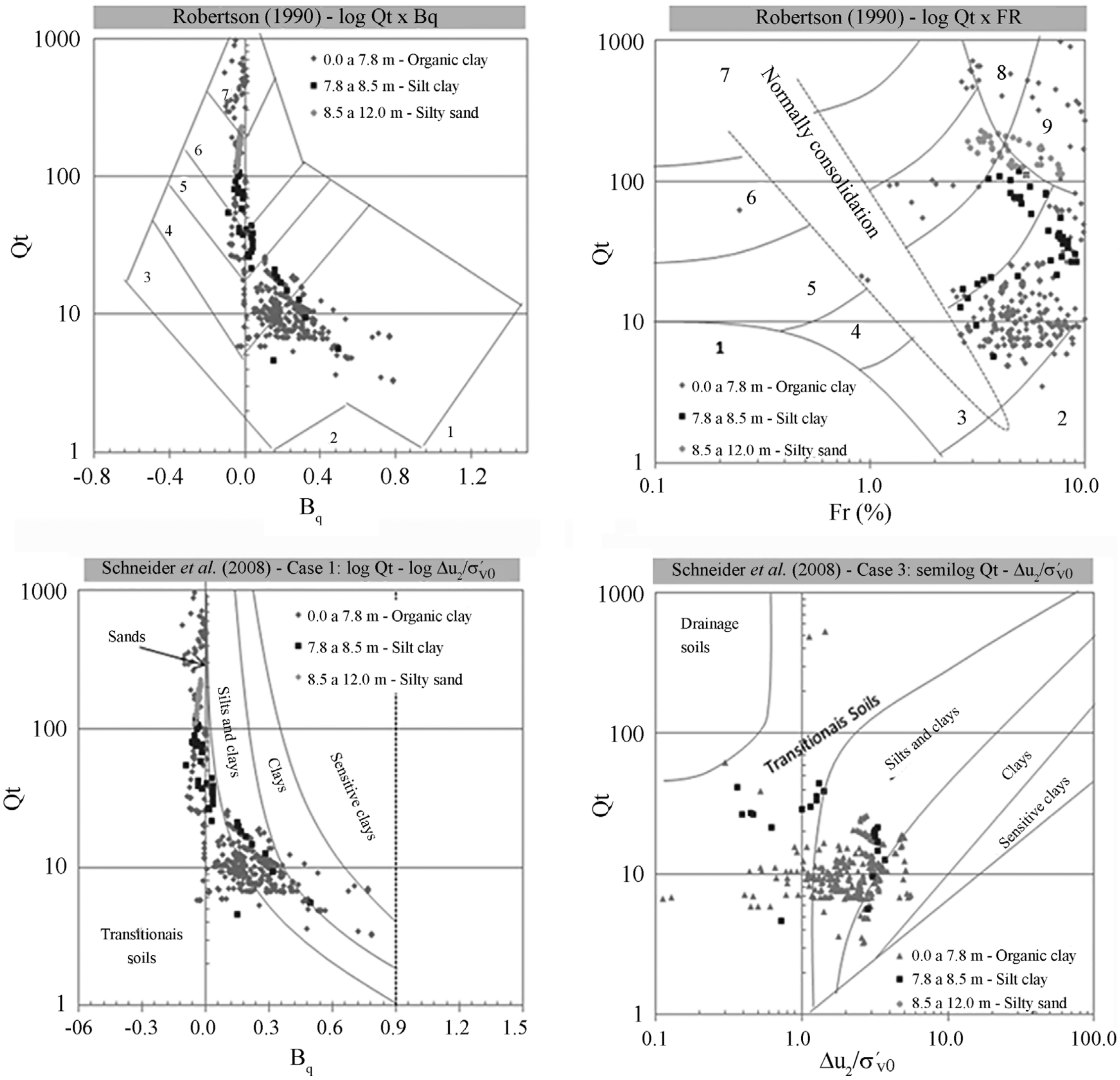

Figure 7 - Comparison between soil classification from grain-size, and piezocone tests - E104 (SUB-AREA A) (Bello, 2011; Bello & Coutinho, 2012).

between the results of classification from grain-size distribution and CPTU tests occurs in the mixed soil regions and in the transition zones between layers of the profile.

3.2. Schneider *et al.* (2008) charts results

The Schneider *et al.* (2008) chart - Case 1 (Coordinates log Q - log $\Delta u_2/\sigma'_{vo}$) features coordinates identical to the Robertson (1990) chart, allowing direct comparison of the results (Figs. 7 and 8). In general, soil classification of the study area by the Schneider *et al.* (2008) chart - Case 1 was in agreement with the classification from Robertson (1990).

In the Schneider *et al.* (2008) chart - Case 3 (Coordinates semi log Q - $\Delta u_2/\sigma'_{vo}$), the plotted results only took into consideration material with positive pore pressure values, since the horizontal coordinate is a semi-log scale. Therefore, this chart does not show materials with negative value of pore-pressure.

It is important to emphasize the care needed when identifying the points relating to SPT tests. Classification of layers indicating grain-size distribution can demonstrate differences in the values for N_{SPT} and water content, making it necessary to divide classification into sub-layers to be plotted into separate charts.

Another major concern is the presence of transitional soils. These soils are characterized as mixtures of different materials. In the Schneider *et al.* (2008) charts, these soils can be clearly observed inside the determined boundaries (Figs. 7 and 8). In general, results from the Schneider *et al.* (2008) charts were also satisfactory for the Suape soft soils, consistent with classification using grain-size distribution and N_{SPT} values.

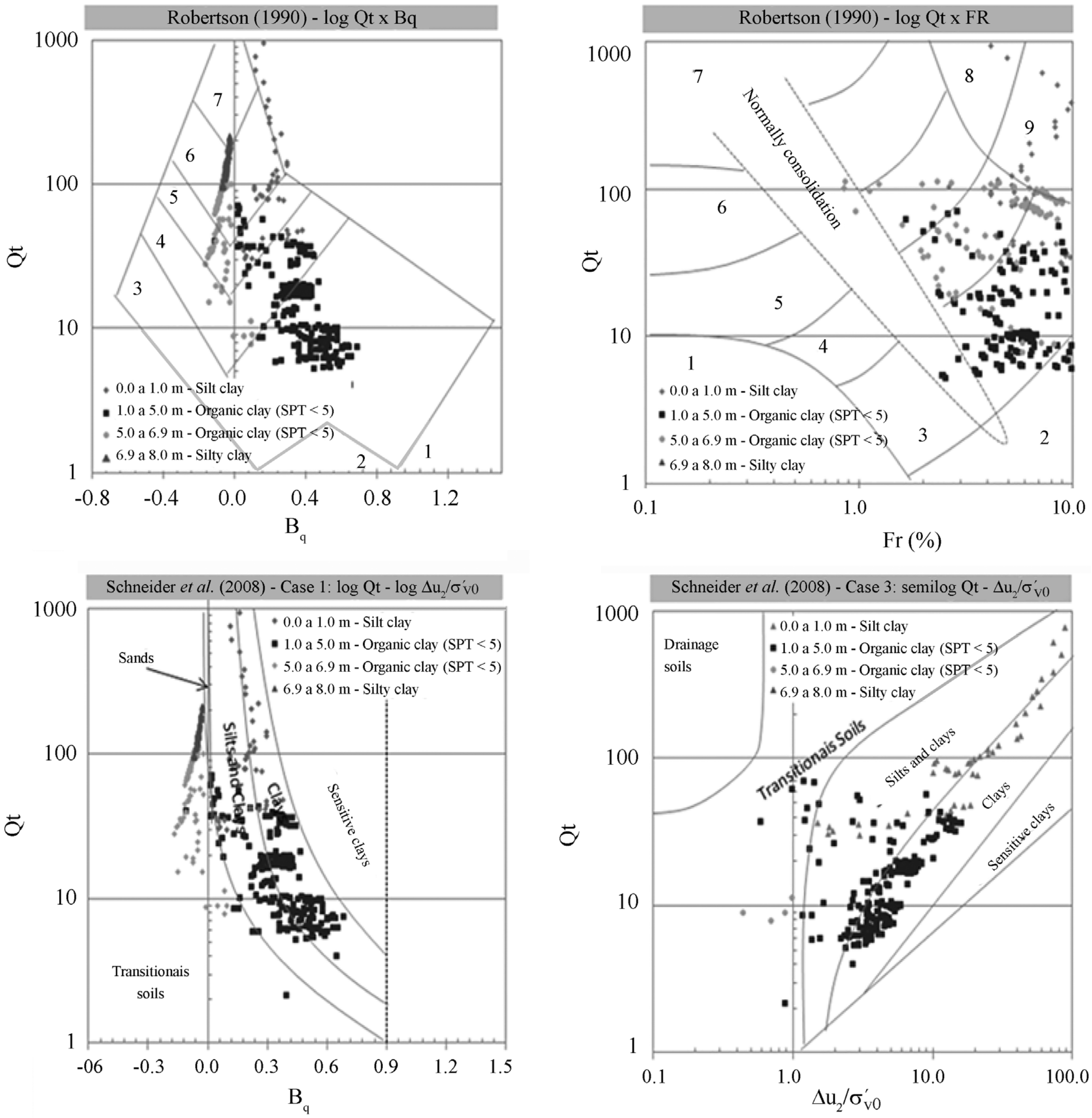

Figure 8 - Comparison between soil classification from grain-size, and piezocone tests - E121 (SUB-AREA C) (Bello, 2011; Bello & Coutinho, 2012).

4. Compressibility Parameters

Laboratory incremental oedometer tests were performed on soil specimens with a diameter of 87 mm and height of 20 mm, using Bishop apparatus, with double drainage. Loads were doubled for each stage, beginning at 5-10 kPa until 640-1280 kPa and then decreased to 10 kPa. Each stage usually took 24 h.

Typical curves of void ratio *vs.* effective stress obtained from oedometer tests are shown in Fig. 9 for the two research sites. It can be seen that the "virgin" portion is not linear. This is consistent with findings in many other investigations (Coutinho, 1976; Coutinho & Lacerda, 1987; Mesri & Choi, 1985). In this study, the virgin portion curve was simplified by two linear parts to obtain the compression index C_c (C_{c1} and C_{c2}).

The quality of samples was evaluated using the proposal presented in Coutinho (2007), which represents the Brazilian experiment, based on the proposal of Lunne *et al.* (1997). This criterion uses the ratio $\Delta e/e_0$ corresponding to the initial effective vertical stress (σ'_{vo}), and can be described as: OCR = 1-2.5; $\Delta e/e_0 < 0.05$; - Very Good to Excellent; $\Delta e/e_0 = 0.05\text{-}0.08$ - Good to Fair; $\Delta e/e_0 = 0.08\text{-}0.14$ - Poor; and $\Delta e/e_0 > 0.14$ - Very Poor. Some samples in this study showed results with considerable disturbance. In the study, these curves e ($\in_v$) *vs.* log p or the compressibility parameters were corrected to obtain results equivalent to

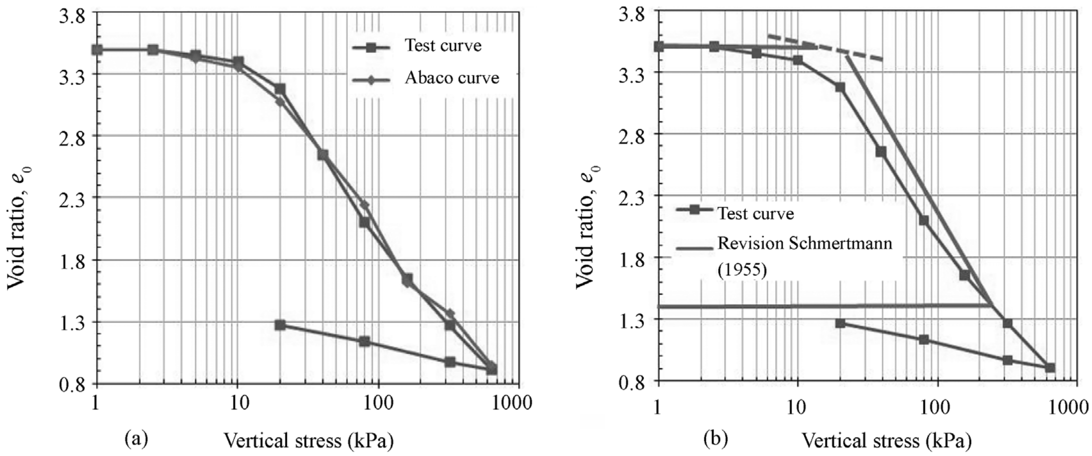

Figure 9 - Experimental curve and curve drawn by the proposed corrections on a good-quality sample E109: (a) proposal by Oliveira (2002); (b) proposal by Schmertmann (1955) (Bello, 2011).

samples of very good to excellent quality. Methodology proposed by Oliveira (2002), Schmertmann (1955), Coutinho (2007) and Futai (2010) was used and are briefly presented in Coutinho & Bello (2012a). In this paper, the results are in general those effectively corrected or initially of very good quality.

Figures 2 and 3 show results of the overconsolidation ratio (OCR = $\sigma'_{vm}/\sigma'_{vo}$) and the compressibility parameters: compression index C_c (first part) and swell index C_s for two sites studied. It can be observed that the deposits have a higher void ratio and very high compressibility.

Statistical correlations (C_c *vs.* e_o and C_c *vs.* w (%)) for Suape soft clays have been developed using all data from the corrected laboratory test database. The results of C_c *vs.* w are shown in Fig. 10). Results of Juturnaíba organic soils (Coutinho, 1986; Coutinho & Lacerda, 1987) are also shown, as are the results from Recife soft clays (Coutinho *et al.*, 1998); Coutinho (2007); and Juturnaiba organic soils (Coutinho, 1986; Coutinho & Lacerda, 1987). The water content w (%), obtained from the SPT testing can be used to have the first estimate of C_c.

The C_c *vs.* w (%) correlations (Figs. 10a and b) are quite similar for the deposit, particularly for clay soils. The Suape clays presenting a smaller inclination: Recife Soft Clay $C_c \cong 0.0126w$ (%) and Suape Soft Clay $C_c = 0.0097w$ (%) $C_c \cong 0.01w$ (%). In general, correlations for clay have higher correlation coefficients (r^2) and lower standard error (lower dispersion) than those for organic soil/peat. Probably for the more difficulty do obtain sample of very good quality.

The organic soft Juturnaíba research site has higher correlation coefficients than Recife and Suape deposits (less dispersion), due to better quality samples. The behavior of these clay deposits under one-dimensional consolidation is strongly affected by sampling disturbance. The general equation between C_c and w (%) for Recife and Suape

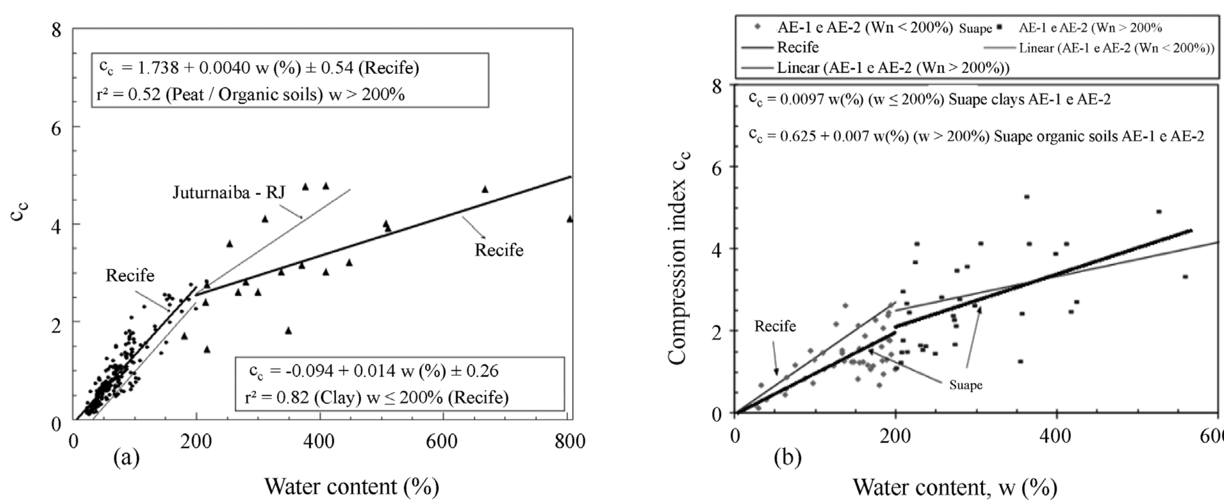

Figure 10 - Statistical correlations for organic soils and soft/medium clays: (a) Recife and Juturnaíba (Coutinho *et al.*, 1998); (b) Suape (Bello, 2011).

clays is very similar to the equation presented by Bowles (1979) for organic silts and clays ($C_c = 0.0115w$), and is also very similar to those presented by Djoenaidi (1985) (see Kulhawy & Mayne, 1990). Almeida *et al.* (2008) plotted C_c *vs.* w values (%) of seven clays from Rio de Janeiro ($C_c = 0.013w$), including Juturnaíba-RJ clays from Coutinho (1986). Koppula (1981) obtained a similar correlation ($C_c = 0.010w$) for the normally densified clays with low sensitivity ($S_t < 1.5$). In general, it has been found that soft clays and soft organic soils $C_c = 0.010$ to $0.015w$ (%) (Coutinho, 2007).

5. Coefficient of Consolidation

The coefficient of consolidation measurement is one of the soil properties major challenges for geotechnical engineering. Parameters for the consolidation rate may be assessed using oedometer (laboratory) and piezocone *in situ* tests by measuring the dissipation or decay of pore pressure through time after penetration ceases (Lunne *et al.*, 1997).

Field stress and pore-pressures around the piezocone can be calculated using the strain path method, according to formulas provided by Baligh & Lavadoux (1986), and Houlsby & Teh (1988).

Baligh & Lavadoux (1986) concluded that dissipation is predominantly in a horizontal direction. The dissipation process can be expressed by a one-dimensional factor of time, as in Eq. 5:

$$T^* = \frac{c_h}{R^2 \sqrt{I}}; \quad c_h = \frac{T^* R^2 \sqrt{I_r}}{t} \tag{5}$$

where R: piezocone radius; T^*: dissipation time; I_r: rigidity index (G/S_u); G: shear modulus.

Houlsby & Teh (1988) presented the following procedure to determine c_h: (a) calculate the difference between pore pressure at the beginning of dissipation, u_i, and the hydrostatic pore pressure, u_o; (b) calculate the percentage of dissipation $u_{50\%} = (u_i - u_o)/2$, and use the experimental curve to determine the actual time taken for 50% of the dissipation to occur, $t_{50\%}$; (c) obtain the T^* value in Table 1, and calculate c_h by using Eq. 5.

Robertson *et al.* (1992) propose a direct estimate of c_h from the t_{50} value using an abacus. This calculation is valid for I_r values varying between 50 and 500, and for cone areas of 10-15 cm^2. Values for c_h obtained from these procedures correspond to soil properties in the preconsolidation band, due to the fact that during penetration, material surrounding the cone undergoes increased levels of deformation, and in this state behaves as soil in recompression (Baligh, 1986; Baligh & Levadoux, 1986). Jamiolkowski *et al.* (1985) proposed estimating c_h in the normal compression band (N.C.) using Eq. 6. The authors presented experimental values for C_s/C_c that varied in the 0.13-0.15 range.

Table 1 - Time factor in function of percentage of pore pressure dissipation (Houlsby & Teh, 1988).

U (%)	Time factor (T^*) in relation to the position of the pore pressure transducer	
	Face of the cone (u_1)	Base of the cone (u_2)
20	0.014	0.038
30	0.032	0.078
40	0.063	0.142
50	0.118	0.245
60	0.226	0.439
70	0.463	0.804
80	1.040	1.600

The coefficient of consolidation in the vertical direction can be estimated using permeability in the horizontal and vertical planes from Eq. 7 (Lunne *et al.*, 1997).

$$c_h(N.C) = \frac{C_s}{C_c} c_h(CPTU) \tag{6}$$

$$c_v(N.C) = \frac{k_v}{h_h} c_h(N.C) \tag{7}$$

where k_h and k_v represent horizontal and vertical permeability, respectively.

In the study area, c_h calculations were carried out according to a formula proposed by Houlsby & Teh (1988). In each CPTU vertical, c_h values were calculated in relation to the depths of the dissipation tests in both study areas, considering $I_r = 50$. Figure 11 shows an example of results of pore pressure of dissipation tests, including the procedure to determine $t_{50\%}$, for the CPTU 120, Sub Area C - AE - 2. Values of c_h were also determined from laboratory trough radial oedometer tests.

Figure 12a shows value variation relating to the depths from the radial oedometer and piezocone tests for the AE-1 study area. In this figure, c_h values are also obtained from piezocone tests in the N.C. band estimated

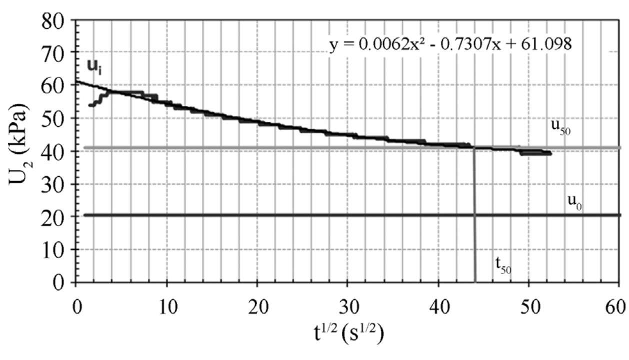

Figure 11 - Results of pore pressure of dissipation tests, including the procedure to determine $t_{50\%}$, for the CPTU 120, Sub Area C - AE - 2.

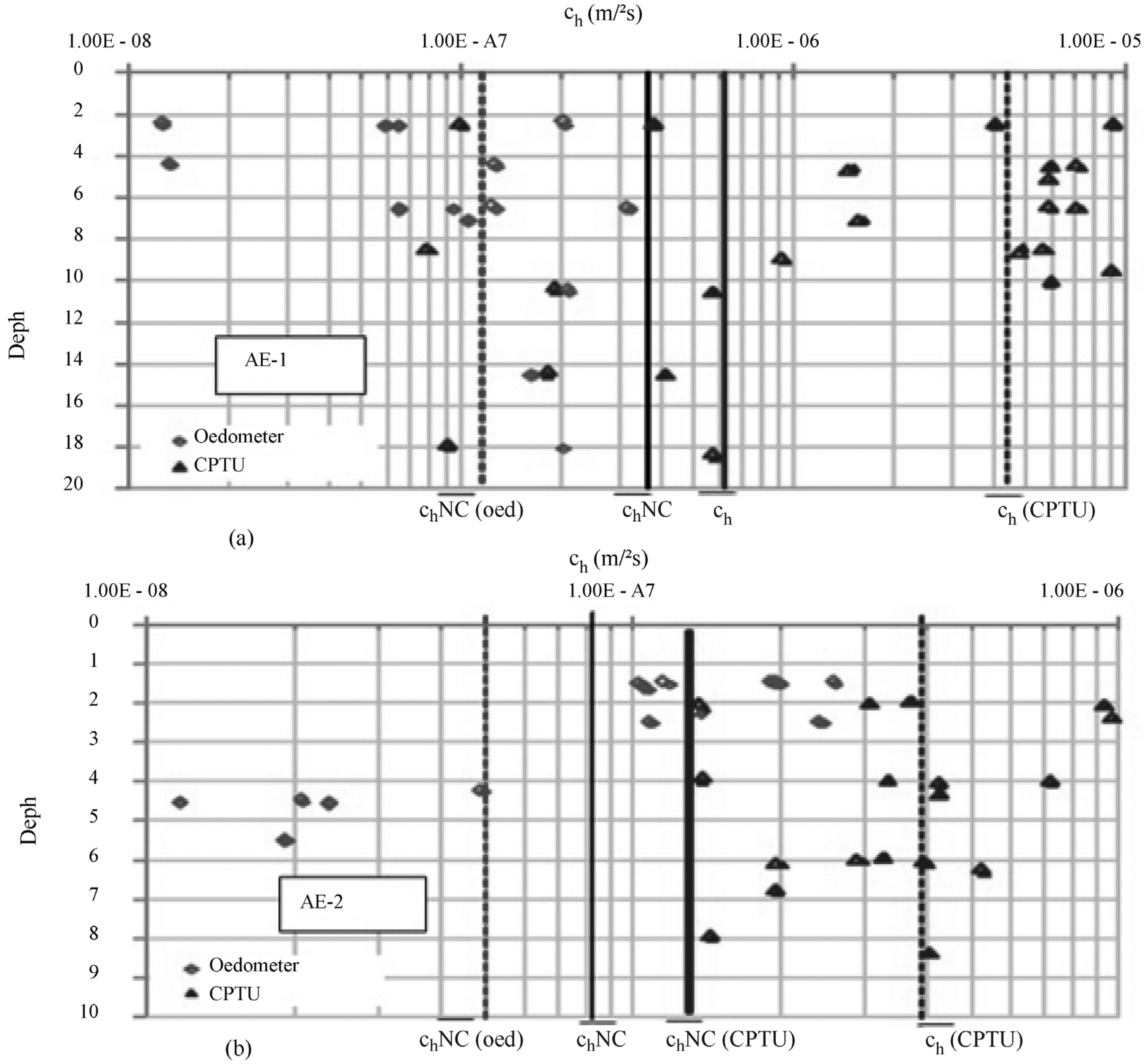

Figure 12 - Coefficient of consolidation values,oedometer and piezocone tests, Suape (Coutinho, 2010; Bello, 2011).

from in the Jamiolkowski *et al.* (1985) proposal. The average c_h value from piezocone tests in the O.C. band was 4.40×10^{-6} m²/s.

In general, the average c_h values varied in the same order of magnitude in both the oedometer (1.15×10^{-7} m²/s) and piezocone tests (6.16×10^{-7} m²/s), considering c_h results in the N.C. band. The overall average c_{hnc} value was 3.65×10^{-7} m²/s.

The variation of c_h values relating to the depths of the oedometer and piezocone tests, for the AE-2 study area is shown in Fig. 12b. The average c_h value from piezocone tests in the O.C. band was 4.03×10^{-7} m²/s. The c_v values obtained in vertical oedometer tests were converted into c_h values according to Eq. 7 ($c_h = 1.5c_v$). The average c_h values varied from 4.94×10^{-8} m²/s in the oedometer tests to 4.03×10^{-7} m²/s in the piezocone tests. The overall average c_h value was 1.34×10^{-7} m²/s. In this study, a wide band of c_h values was measured from oedometer and piezocone tests.

Leroueil & Hight (2003) evaluated the coefficient of consolidation determined by piezocone testing, in addition to other methods (Fig. 13). The *in situ* c_h values within the normal consolidation range are typically 10 times higher than the values deduced from oedometer test results (using the Casagrande method). The *in situ* c_h values in the normal consolidation range are also around two orders of magnitude less than values in the over-consolidated range, deduced from *in situ* observations. The piezocone dissipation tests appear to be somewhere between the field values obtained for the over-consolidated and the normally consolidated ranges (c_v and c_h). This figure also shows the range determined for the laboratory and piezocone c_h values of Suape clays. The ranges is situated in the limits shown by Leroueil & Hight (2003).

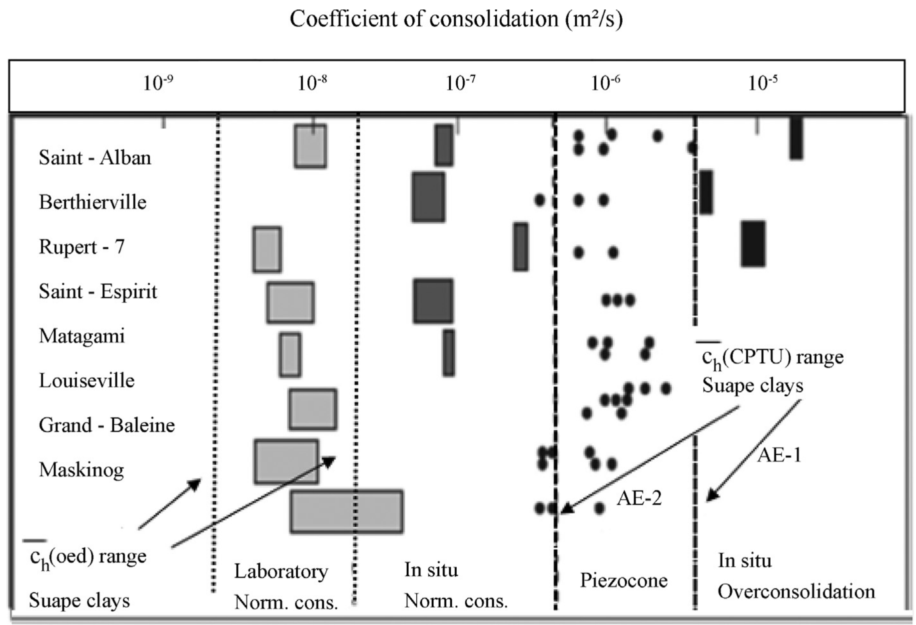

Figure 13 - Coefficients of consolidation (from Leroueil & High, 2003) and Suape clays results.

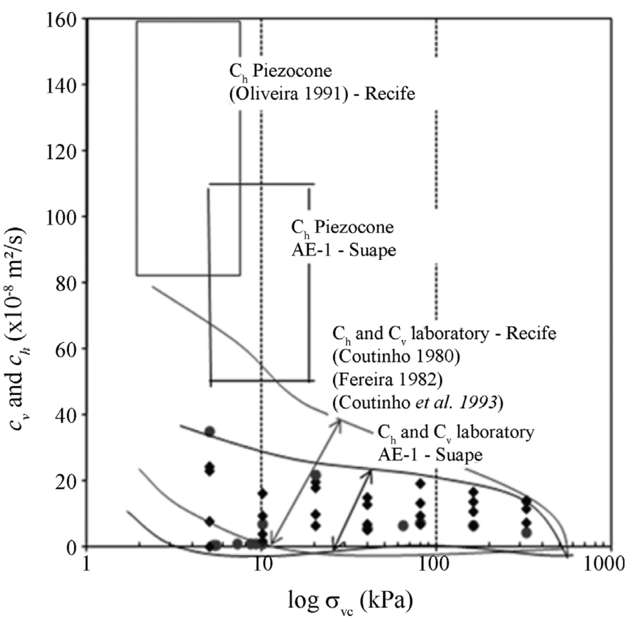

Figure 14 - Values for the c_v, c_h and c_h/c_v relation *vs.* log σ'_{vc} - Recife and Suape (from Coutinho & Bello, 2008).

Figure 14 shows results for c_v and c_h values obtained from oedometer and piezocone tests in the O. C. and N. C. ranges. The c_h (OC range) was much higher (three times as much) in the piezocone test in Recife and Suape clays. Recife soft clays have slightly higher values.

The coefficient of consolidation values obtained from oedometer and piezocone tests are complementary. The oedometer tests are essential for obtaining appropriate compressibility parameters. Results concerning the coefficients of consolidation obtained in the study areas are satisfactory and consistent with results obtained in Brazilian soft soils, and with experience reported in international literature.

6. Undrained and Effective Shear Strength

No single undrained shear strength exists. The *in situ* undrained shear strength depends on the failure mode, soil anisotropy, strain rate and stress history (Lunne *et al.*, 1997).

The triaxial compression, triaxial extension and simple shear laboratory tests with consolidation in the isotropic or anisotropic condition for effective field stress conditions have been used to obtain undrained strength values in geotechnical engineering studies and projects.

Undrained strength can be determined in the field by means of vane and piezocone tests. In order to use in a project, the strength obtained in a vane test must be corrected by Bjerrum's correction factor (1973). In the piezocone test, empirical correlations appropriate for the area under study based on field and laboratory tests should be used.

In the field vane test, undrained strength (S_u) can be determined from maximum torque obtained with the vane rotation (Eq. 8).

$$S_u = \frac{0.86 T_{max}}{\pi D^3} \quad (8)$$

where: T_{max} is the maximum torque measured during the test; D is the vane diameter.

To estimate the value of S_u through the piezocone test, three cone factors are normally used: N_{kt}, N_{ke} and $N_{\Delta u}$, load capacity, effective tip resistance and pore pressure, respectively (Lunne *et al.*, 1997). Undrained shear strength is then defined by Eq. 9. The q_t, q_e and Δu values are determined from the piezocone tests results. The N_{kt}, N_{ke} and $N_{\Delta u}$, factors are based on theoretical work or, more often, on empirical experimental correlations using laboratory or *in situ* tests (Lune *et al.*, 1997).

$$S_u = \frac{q_t - \sigma_{v_0}}{N_{kt}} = \frac{q_t - u_2}{N_{ke}} = \frac{u_2 - u_0}{N_{\Delta u}} \qquad (9)$$

where q_t is cone resistance corrected for pore pressure effects; q_e is the effective cone resistance; Δu is excess pore pressure; σ_{vo} is total vertical pressure.

6.1. Laboratory - Triaxial UU-C_2

The undrained strength profiles obtained in laboratory triaxial UU-C tests for the studied verticals in SUB-AREAS A and C are presented in Figs. 15 and 16. The mean values of S_u obtained in the triaxial tests in SUB-AREA A were 10.8 ± 5.4 kPa for the first 2.0 m of depth, followed by around 7.4 ± 5.0 kPa to 7.0 m in depth. In SUB-AREA C the mean S_u values were 7.8 ± 0.6 kPa throughout the profile. Some of the results obtained in the triaxial UU tests may be influenced by the disturbance of the sample (see Coutinho & Bellom, 2012a), so it is important to compare the results of the triaxial with field vane tests.

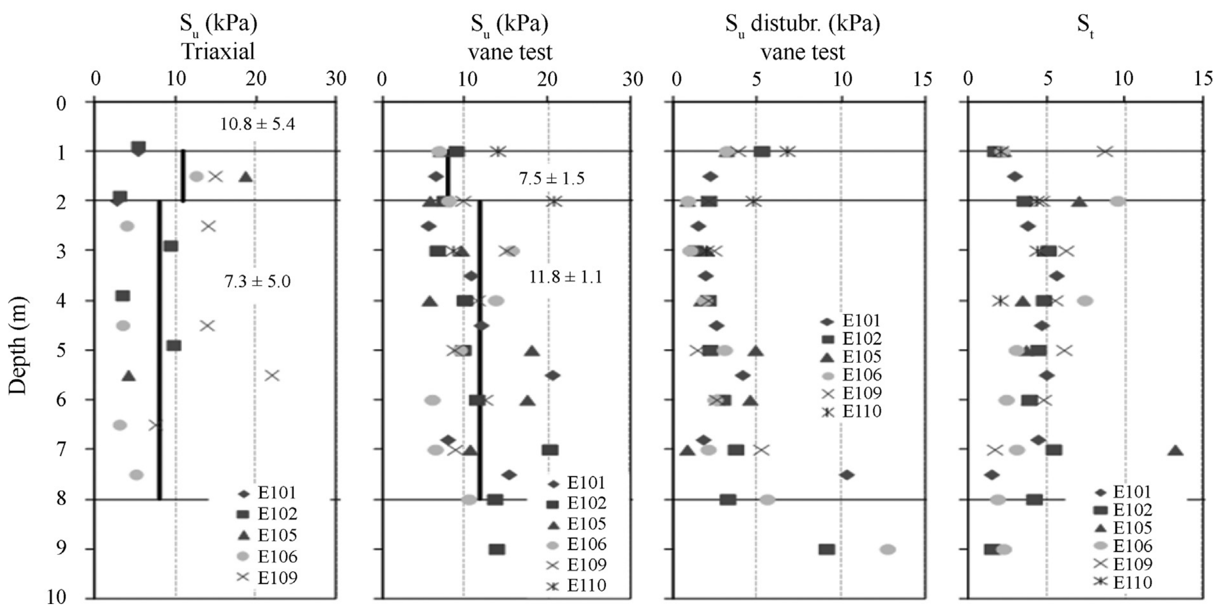

Figure 15 - Results of triaxial and field vane test - SUB-AREA A, study area AE-2 - Suape (Coutinho & Bello, 2012b).

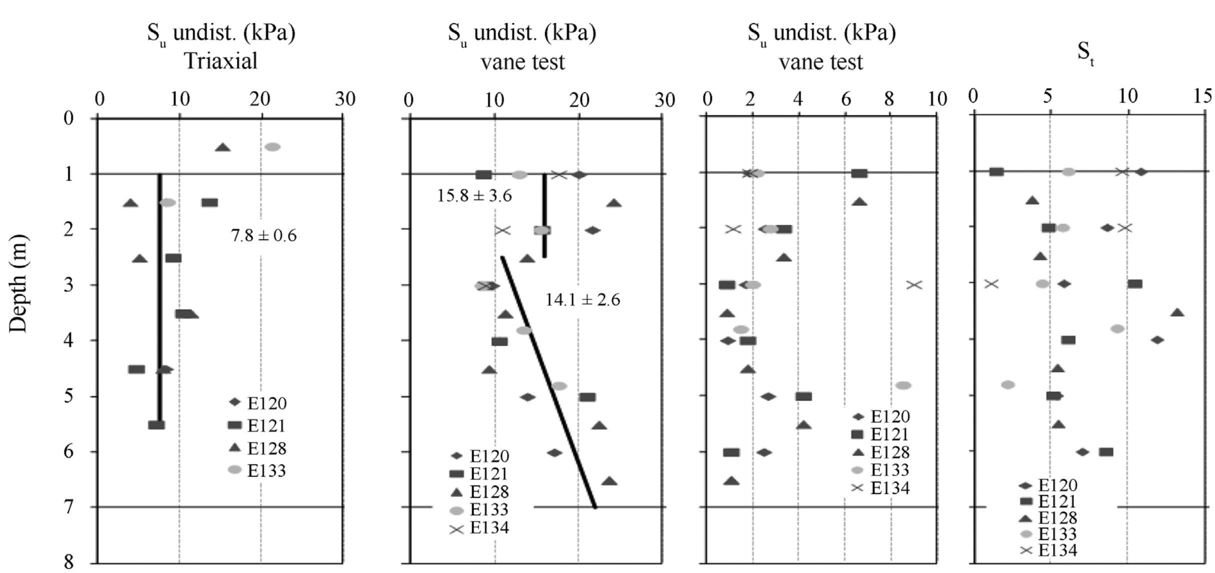

Figure 16 - Results of triaxial and field vane test - SUB-AREA C, study area AE-2 - Suape (Coutinho & Bello, 2012b).

6.2. Vane tests

The undrained strength profiles obtained in the field vane tests for the studied verticals are presented in Figs. 15 and 16. The S_{uvane} results in the verticals of the SUB-AREA A showed a similar trend in behavior, with a mean S_{uvane} value of 7.5 ± 1.5 kPa to a depth of 2.0 m, and with mean values 11.8 ± 1.1 kPa at a depth of 7.0 m. The E110 vertical presented a high S_{uvane} value at a depth of 4.0 m, possibly due to the presence of roots in the soil. Sensitivity had mean values of around 5. The S_u results determined in SUB-AREA C presented mean S_u values of 15.8 ± 3.6 kPa up to 2.5 m in depth, starting from this point, the S_{uvane} values increase linearly reaching 21.0 kPa at 7.0 m. In general the S_t presented mean values in the 5-10 range.

The mean S_u values obtained from the field vane test were generally greater than the S_u laboratory values. These results are similar to those obtained in Recife soft clays (Coutinho, 2007), but in the Suape study the laboratory results are more influenced by the sample quality.

The values of the ratio S_{uvane}/σ'_{vo} *vs.* PI for soils in the areas AE-1 and AE-2 (SUB-AREAS A and C) are presented in Fig. 17. The area AE-1 was divided in two stretches of mangrove deposits.

The two deposits of AE-2 (SUB-AREAS A and C) revealed layers with a similar value range as S_{uvane}/σ'_{vo}, situated above the curve proposed by Bjerrum (1973) for young clays and around the curve of old clays. The range of the mean S_{uvane}/σ'_{vo} values found in the AE-2 study area was 0.45-0.68, much greater than the Recife values (Coutinho *et al.*, 2000). The PI values obtained in the area under study were also much greater than the PI values obtained in Recife.

The mangrove 1 deposit (AE-1) presented values of S_{uvane}/σ'_{vo} situated above the curve proposed by Bjerrum (1973) for young clays, while the mangrove 2 deposit (AE-1) had values of S_{uvane}/σ'_{vo} slightly below the curve for young clays.

Figure 18 shows the ratio S_{uvane}/σ'_{vm} *vs.* PI proposed by Mesri (1975), Coutinho *et al.* (2000) modified from Skempton (1957), Larsson (1980) and Mayne & Mitchell (1988), together with the mean values of various Brazilian clays, including Recife and Suape AE-2 (SUB-AREAS A and C). For Recife and Suape clays, the points fall between the Larsson (1980) and Mesri (1975) correlations, forming upper and lower limits, respectively. The proposal from Coutinho *et al.* (2000) represents satisfactorily clays from Recife, Juturnaíba-RJ, Sarapuí, RJ and for Suape, PE including organic clay from Recife-PE. The σ'_{vm} value of the poor quality samples was corrected (see Coutinho & Bello, 2012b; Bello, 2011).

In order to draw up embankment projects it is necessary to use a correction factor according to Bjerrum's proposal (1973). Considering that the plasticity index results in Suape clays were generally high (values up to 150%), the correction factor soils have a value of about 0.6.

6.3. Piezocone tests

To estimate S_u values using the piezocone test, three experimental parameters were adopted, N_{ku}, N_{ke} and $N_{\Delta u}$. The value of the experimental parameters was determined by the $S_{u\ values}$ from field vane tests.

Figure 19 shows the N_{kt} variation of SUB-AREAS A and C. In general, it is observed that N_{kt} varied between 6 and 14 in SUB-AREA A, with a mean value of 10. In SUB-AREA C, N_{kt} varied between 5 and 16, with a mean value of 9. These results show that the two sub-areas have similar N_{kt} variation ranges with a mean value between 9 and 10. Figure 20 presents the mean value of N_{kt} (12 ±1.0) obtained from S_{uvane} for the Recife research sites. From these results, S_u for Recife soft clay can be estimated with reasonable confidence for practical purposes (Coutinho *et al.*,

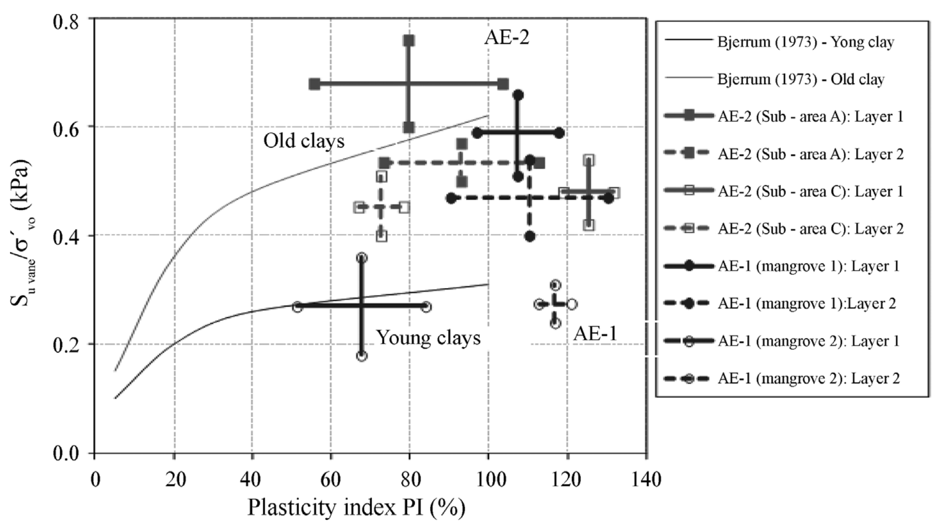

Figure 17 - Resistance ratio-Suape, study areas AE-1 and AE-2 - S_{uvaned}/σ'_{vo} and PI (Bello, 2011).

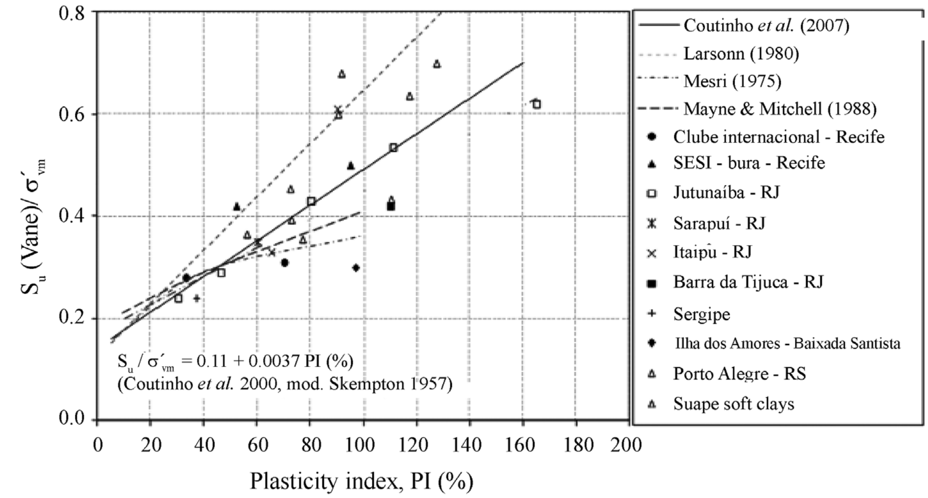

Figure 18 - Resistance ratio-Suape, study area AE-2 - (b) S_{uvane}/σ'_{vm} and IP (Bello, 2011).

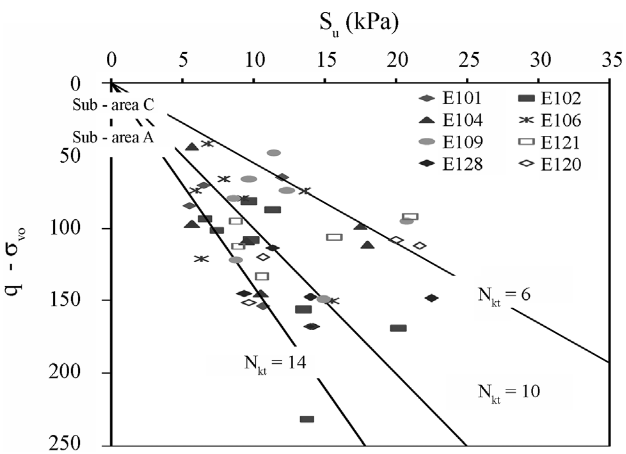

Figure 19 - *Nkt* values obtained from field vane test: Suape clays study area AE-2 (SUB-AREA A and C).

2000). These mean values are about 20-25% greater than the N_{kt} results obtained in Suape.

Almeida *et al.* (2010) found a wide range of N_{kt} mean values (3-20) for deposits of very soft soils in Rio de Janeiro. Schnaid (2009) found N_{kt} values representative of soft clay deposits in Porto Alegre varying between 8 and 16, with a mean value of 11. In general, it can be observed that mean values of Brazilian clays vary around 9 to 12 (Coutinho & Schnaid 2010).

According to Lunne *et al.* (1997) N_{kt} values tend to increase with an increase in plasticity, decrease with an increase in sensitivity and decrease as B_q increases. Brazilian clay results confirm that it is recommended to evaluate in each deposit or at least local experience to obtain representative N_{kt} values.

The variation range of $N_{\Delta u}$ values obtained in the Suape studies areas was between 6.5 and 10.0, with mean

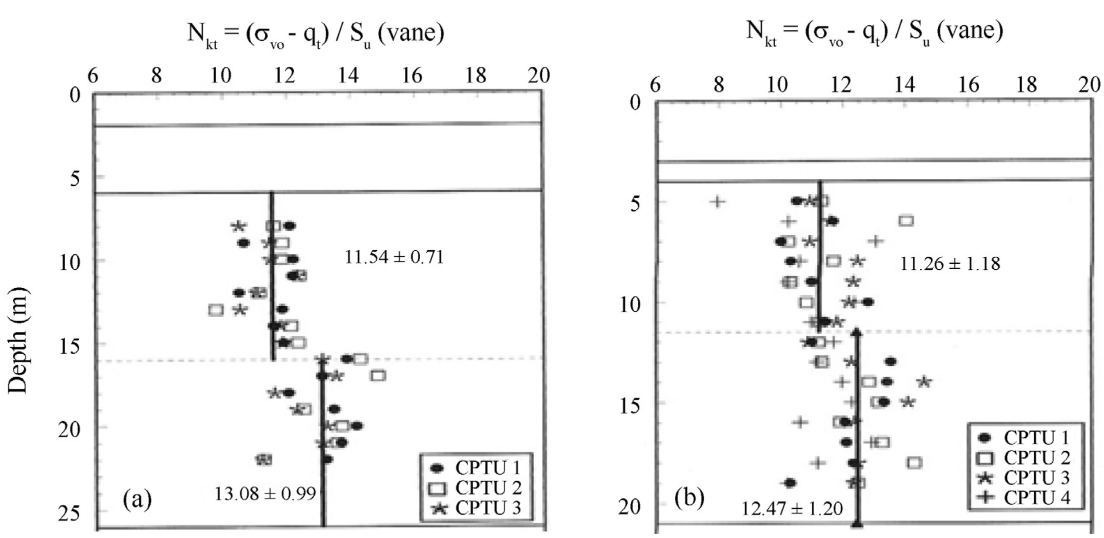

Figure 20 - N_{kt} values - field vane test (a) International Club; (b) SESI-Ibura (Oliveira, 2000; Coutinho, *et al.*, 2000).

values around 8.0. In general, $N_{\Delta u}$ increases linearly with depth (Bello, 2011; Bello & Coutinho, 2012). In Recife and Suape clays, $N_{\Delta u}$ values varied between 7.5 and 11.0 with mean values around 9.5 (Coutinho, 2007, 2008; Coutinho & Schnaid, 2010). La Rochelle *et al.* (1988) obtained for three Canadian clays $N_{\Delta u}$ values between 7 and 9, using as reference S_u values from field vane tests, where the overconsolidation ratio values varied between 1.2 and 50. The variation range of the N_{ke} factor values obtained in the Suape study areas was between 4.0 and 9.0 with mean values around 5.0. In general, N_{ke} increases linearly with depth (Bello, 2011; Bello & Coutinho, 2012).

Figures 21a and b show the undrained strength profiles of the verticals E102 (SUB-AREA A) and E128 (SUB-AREA C), obtained through the piezocone using mean valves of the experimental parameters and field vane tests. The S_u values derived from N_{kt} showed agreements with S_u values obtained from the vane tests. The S_u values derived from $N_{\Delta u}$ showed a greater difference in relation to S_u vane values, because of the difficulty of an accurate Δu measurement, including pore pressure negative values. The S_u values deriving from N_{ke}, showed the highest degree of dispersion, which can be explained by the small effective tip resistance value, q_e, that was the basis for calculating N_{ke}.

6.4. Effective shear strength

The effective shear strength envelope is usually determined by laboratory testing, such as, for example, the triaxial drained compression or excursion test (or undrained with pore pressure measurements). The effective friction angle (ϕ') can be estimated by *in situ* testing, such as the piezocone, or by statistical correlation with plasticity index (PI) proposed by Bjerrum & Simons (1960). Figure 22a shows this statistical correlation with results from five Brazilian clays, including Recife soft clays. Figure 22b gives the results of ϕ' from Suape clays (AE-1 and AE-2) obtained by triaxial CIU-C test. There is dispersion in the results but it is possible to see that the Bjerrum & Simons (1960) proposal is also satisfactory for a preliminary estimation of ϕ' for Suape soft clays. A specific Suape clay statistical correlation is also shown in Fig. 22b.

7. Overconsolidation Ratio

The stress history of the soil can be indicated for the profiles of effective field stress (σ'_{vo}), preconsolidation stress (σ'_{vm}) and the overconsolidation ratio (OCR). It constitutes an indispensable factor for the analysis of behavior of clay deposits. Traditionally obtained in oedometer tests, OCR can be estimated from field vane (Chandler, 1988) and piezocone tests (Lunne *et al.*, 1997).

Critical-state soil mechanics, as well as the SHANSEP method showed that normalized undrained strength (S_u/σ'_{vo}) increases with an increase in OCR (Eq. 10).

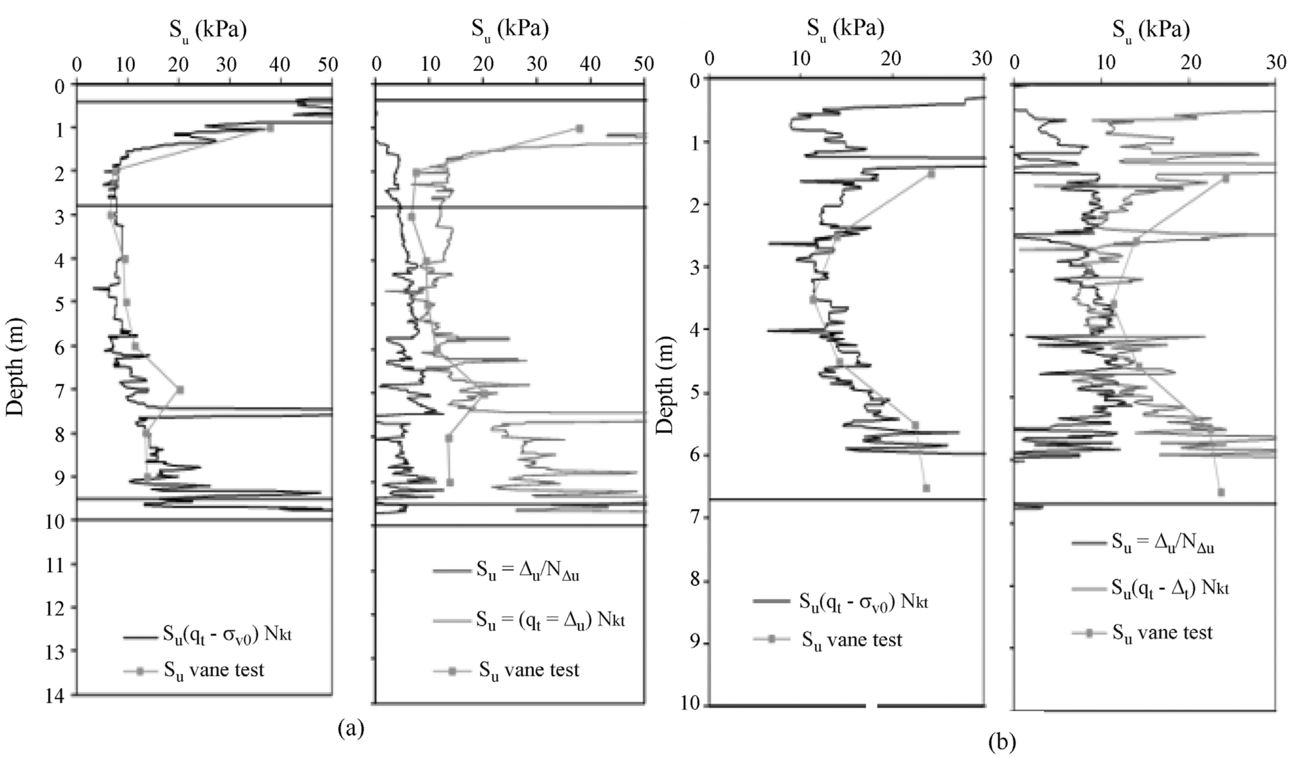

Figure 21 - Suape clays: S_u profile - piezocone and field vane tests. (a) E102 (SUB-AREA A); (b) E128 (SUB-AREA C).

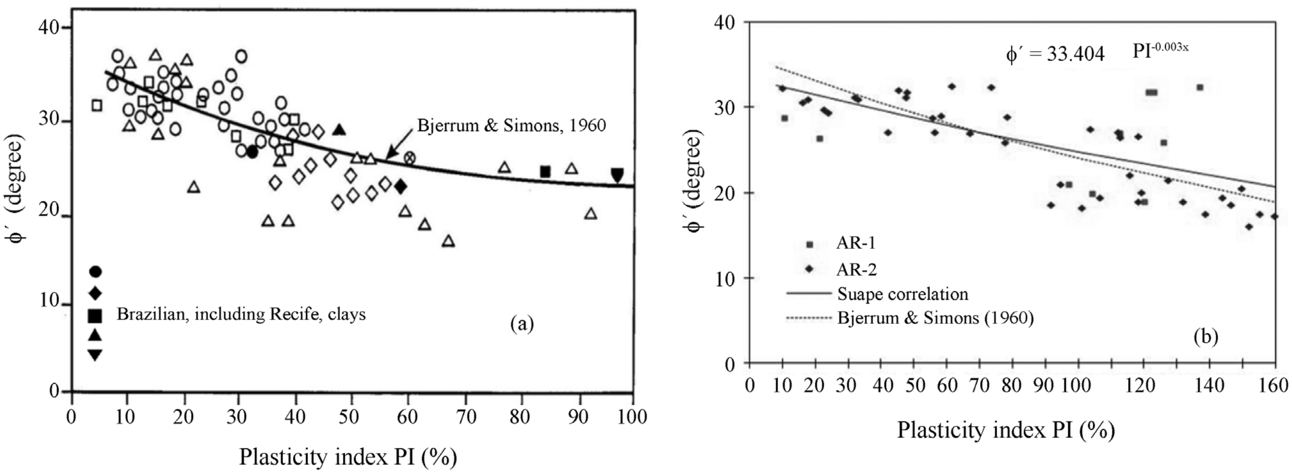

Figure 22 - Relation ϕ’ *vs.* PI: (a) Brazilian Clays; (b) Area AE-1 (Bello, 2011).

$$\left(\frac{S_u}{\sigma'_{v0}}\right)_{\text{O.C.}} = \left(\frac{S_u}{\sigma'_{v0}}\right)_{\text{N.C.}} (\text{OCR})^m \tag{10}$$

where N.C. and O.C. is the normally consolidated and overconsolidated range, respectively.

Chandler (1988) collected data from vane tests of 19 clay deposits, enclosed normally consolidated and overconsolidated clays with OCR up to 7.5, obtaining m value equal to 0.95 (Eq. 11).

$$\text{OCR} = \left[\frac{\left(\dfrac{S_u}{\sigma'_{v0}}\right)_{\text{O.C.}}}{\left(\dfrac{S_u}{\sigma'_{v0}}\right)_{\text{N.C.}}}\right]^{\frac{1}{0.95}} \tag{11}$$

Tavenas & Leroueil (1987) gathered the data used for AAS *et al.* (1986) and Chandler (1988) and plotted them using Bjerrum’s curve (1973) as reference. The authors found the m value equal to 1 (with small dispersions) (Eq. 12).

$$\text{OCR} = \frac{\left(\dfrac{S_{uvane}}{\sigma'_{v0}}\right)_{\text{O.C.}}}{\left(\dfrac{S_u}{\sigma'_{v0}}\right)_{\text{O.C.}}} \tag{12}$$

Mayne & Mitchell (1988) developed a database with results of field vane and oedometer tests including index properties of 96 different clays, in order to define a general correlation that could be used to estimate OCR values from field vane tests (Eq. 13). The deposits showed: 1 < OCR < 40; 3% < PI < 300%; 1.6 kPa < Suvane < 380 kPa and sensitivity varying from 2 up to high values.

$$\text{OCR} = 22(IP)^{-0.48}\left(\frac{S_{uvane}}{\sigma'_{v0}}\right) \tag{13}$$

Lunne *et al.* (1997) stated that methods to derive OCR from piezocone tests data fall into three main categories: (a) methods based on undrained shear strength; (b) methods based on the shape of the CPTU profile; and (c) methods based directly on piezocone tests data.

OCR values can be obtained from CPTU results through correlations in functions of Q_t, where $Q_t = (q_T - \sigma_{vo})/\sigma'_{vo}$ and $\Delta u/\sigma'_{vo}$ (Eqs. 14 to 17).

$$\text{OCR} = f(Q_t) \text{ (Lunne } et\ al.\text{, 1989)} \tag{14}$$

$$\text{OCR} = 0.32(Q_t) \text{ (Kulhawy \& Mayneunne, 1990)} \tag{15}$$

$$\text{OCR} = 0.49 + 1.5\frac{u_1 - u_2}{u_0} \text{ (Sully } et\ al.\text{, 1988)} \tag{16}$$

$$\text{OCR} = f\left(\frac{\Delta u_1}{\sigma'_{v0}}\right) \text{ (Lunne } et\ al.\text{, 1989)} \tag{17}$$

7.1. Oedometer tests

Figure 23 shows the OCR profiles of SUB-AREAS A and C obtained from conventional oedometer tests. In general, $\text{OCR}_{\text{oed.}}$ values were greater than 1.0 up to 2.0 m in depth and a tendency towards the unit value with depth is observed. Poor quality samples had their OCR_{oed} values corrected (see Coutinho & Bello, 2012b; Bello, 2011).

7.2. Vane tests

To estimate the OCR value using the field vane tests performed in the two study areas (AE-1 and AE-2), Chandler (1988), Tavenas & Leroueil (1987) and Mayne & Mitchell (1988) proposals were used. Figure 23a presents the results obtained for the OCR profile of SUB-AREA A, including oedometer tests. The OCR results well differenti-

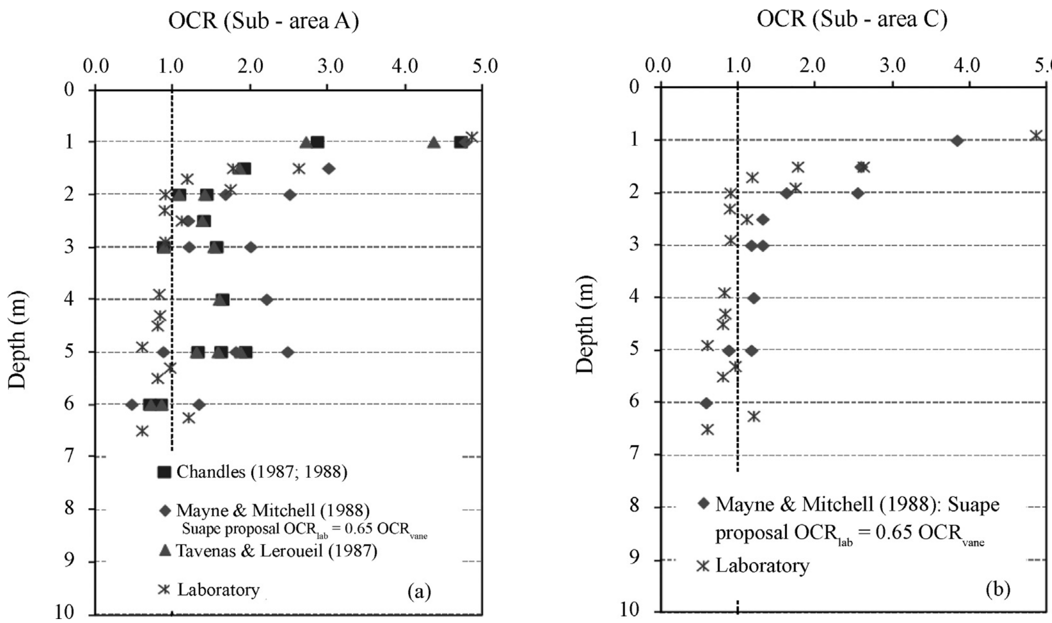

Figure 23 - (a) OCR_{oed}. *vs.* OCR_{vane}; (b) $OCR_{oed.}$ *vs.* OCR from Mayne and Mitchell proposal (1988) for Suape.

ated along the depths but with similar trends in behavior are observed.

Figure 24 shows OCR results determined through the three proposals compared to OCR results obtained in conventional oedometer tests. Mayne & Mitchell (1988) proposal is the one that comes closest to the laboratory OCR values for the Suape study areas, always presenting greater values, as was the case with Recife clays (Coutinho *et al.*, 2000; Coutinho, 2008). Mayne & Mitchell (1988) proposal is being adapted for Suape clays (Eq. 11), considering both Sub-Areas A and C.

$$OCR_{lab} = 0.65\,OCR_{vane} \tag{18}$$

Figure 24b shows the OCR profile obtained in a laboratory and OCR estimated by the Mayne & Mitchell (1988) proposal adapted for Suape clays (Eq. 11). A good correlation can be seen between OCR_{vane} and OCR_{lab} values in good quality samples. These correlations can be useful when no good quality samples are available and to provide complementary results in an investigation.

7.3. Piezocone tests

The OCR values were estimated through the CPTU test using proposals from: Lunne *et al.* (1989) and Kulhawy & Mayne (1990). Results of Recife soft clays are also presented (Coutinho, 2007). Figure 25a shows OCR profiles obtained by the three proposals, together with the OCR results obtained through the oedometer test for SUB-AREAS A and C. It can be seen that the correlations of Lunne *et al.* (1989) and Kulhawy & Mayne (1990) show higher OCR_{CPTU} values than the OCR_{lab} but with similar behavior trends.

Coutinho (2007, 2008) showed OCR profile results from Recife soft clays obtained using oedometer tests and

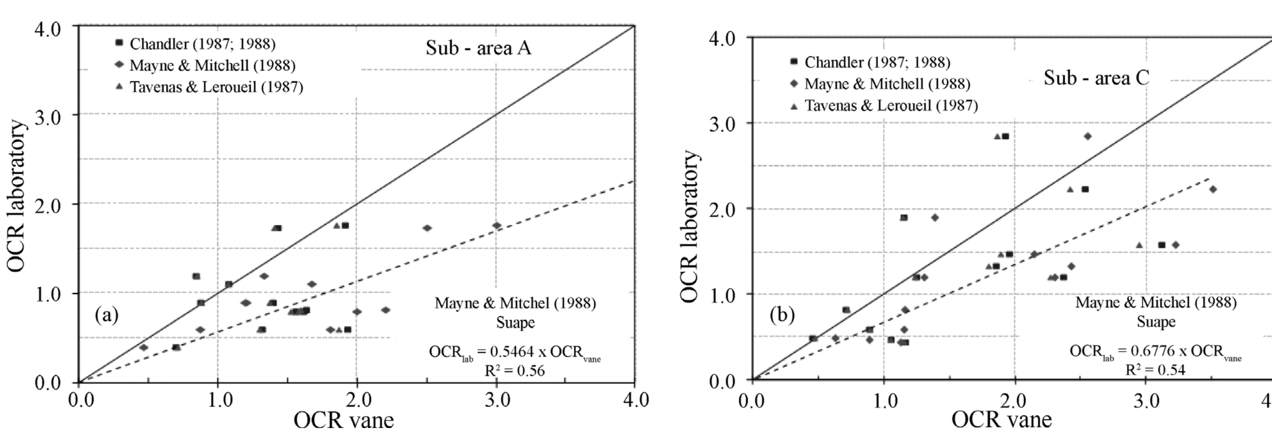

Figure 24 - Comparison between OCR_{lab} *vs.* OCR_{vane}, AE-2: (a) SUB-AREA A; (b) SUB-AREA C.

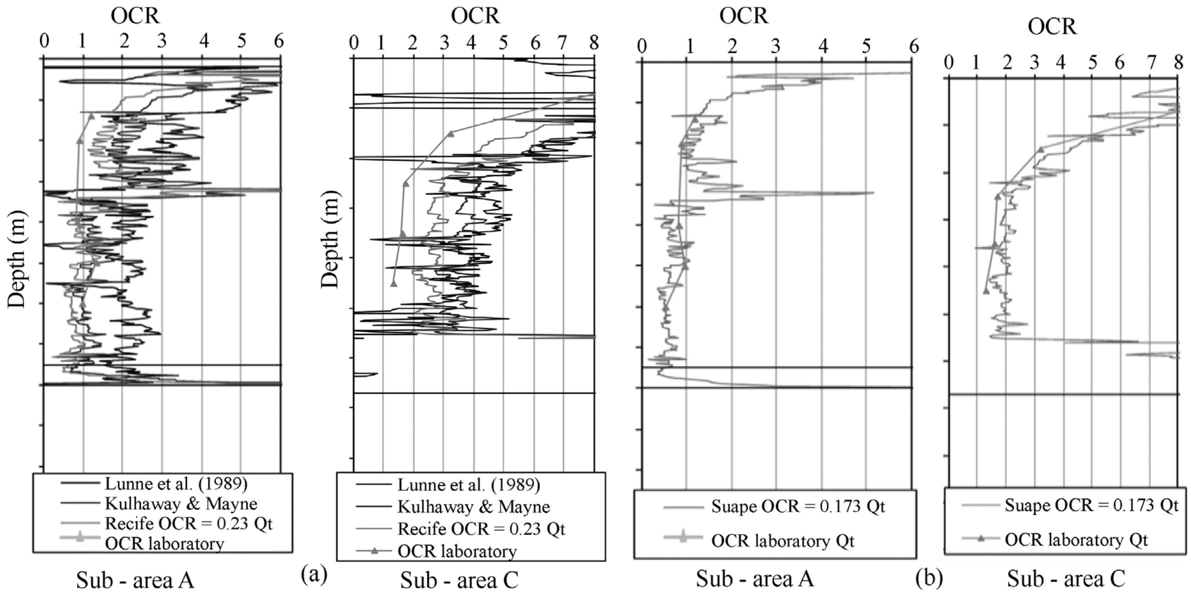

Figure 25 - OCR profile - CPTU and oedometer: E109 (SUB-AREA A) and E128 (SUB-AREA C).

correlations from piezocone (mean values). The Lunne *et al.* (1989) and Kulhawy & Mayne (1990) correlations presented OCR_{lab} values higher than values, particularly if considering OCR from d_{24h}. The exception is the Lunne *et al.* (1989) correlation using $\Delta u/\sigma'_{vo}$ that showed very good results. The values obtained by the Sully *et al.* (1988) correlation were slightly higher than those deduced from laboratory tests. Table 2 shows the summary of results of the comparative study and recommended correlations.

Figure 26 shows the study for obtaining the coefficient of the Kulhawy & Mayne (1990) proposal that is suitable for use in Suape clays. The coefficient obtained was equal to 0.173, almost half the original coefficient (0.32), and smaller than the value of 0.23 found for Recife clays by Coutinho (2007, 2008). Jannuzi (2009) and Baroni (2010) obtained the coefficient of 0.153 for Sarapuí- RJ soft clay and Barra da Tijuca deposits, respectively.

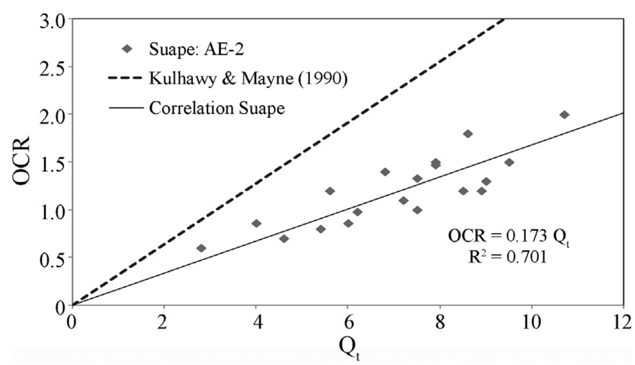

Figure 26 - OCR *vs.* Q_t parameters - Suape clays AE-2.

Table 2 - OCR Comparative Study - CPTU Correlation - Recife Soft Clays - (Coutinho, 2007, 2008).

In situ correlations	Equations	Reference t test	Experiment (Recife)	Recommended correlation
Lunne *et al.* (1989)	$OCR = f\left(\frac{\Delta u_1}{\sigma'_{v0}}\right)$		1.00 ± 0.24	Lunne *et al.* (1989)
Lunne *et al.* (1989)	$OCR = f\left(\frac{q_t - \sigma_{v0}}{\sigma'_{v0}}\right)$	Oedometer (σ'_p for d_{24h})	1.5 ± 0.23	$OCR = \frac{\Delta u_1}{\sigma'_{v0}}$
Kulhawy & Mayne (1990)	$OCR = 0.32x\left(\frac{q_t - \sigma_{v0}}{\sigma'_{v0}}\right)$		1.45 ± 0.18	$OCR = 0.23\left(\frac{q_t - \sigma_{v0}}{\sigma'_{v0}}\right)$
Sully *et al.* (1988)	$OCR = 0.49 + 1.5\left(\frac{u_1 - u_2}{u_0}\right)$		1.30 ± 0.22	

Figure 25b shows the OCR profile obtained in the laboratory and OCR estimated from the Kulhawy & Mayne (1990) proposal adapted for Suape clays (OCR = 0.173Q_t). A good correlation between OCR_{CPTU} values and OCR_{lab} values in good quality samples is observed for Suape Clays. This correlation can be useful when there are no good quality samples available, and for further research.

8. Conclusions

This paper has provided results of a geotechnical site characterization from laboratory and *in situ* tests performed in an important investigation of soft clays in two areas within the Suape Port and Industrial Complex, Brazil.

Soil classification results from the Robertson (1990) and Schneider *et al.* (2008) charts generally agreed with the grain-size distribution and N_{SPT} values. Considering the Brazilian experiment and results obtained from the study areas, the Robertson (1990) proposal confirmed its efficiency for soil classification from piezocone tests. The Schneider *et al.* (2008) proposal was adequate for use in Suape soils; however, it would seem appropriate to carry out further studies elsewhere in Brazil.

Compressibility parameters are discussed, including the development of a statistical correlation C_c = 0.0097 *vs.* w (%) - approximately $C_c \cong 0.01$ w (%). It is also very important to determine the water content in each SPT test.

The horizontal coefficient of consolidation values with depths from the oedometer and piezocone tests for the study areas revealed a wide range of variations considering the O.C. and N.C. ranges. The c_h values in the N.C. range obtained from piezocone tests were higher (around 10 times more) than the c_h values obtained from oedometer tests. These results are in agreement with results from Recife soft clays, along with other soils reported in the literature.

This study confirmed the potential of piezocone tests for use in obtaining adequate predictions for geotechnical classification/consolidation parameters in soft soil deposits.

The values of the ratio S_{uvane}/σ'_{vo} *vs.* PI for Suape clays in general fell between the curves for young and old clays proposed by Bjerrum (1973). For Recife and Suape clays, and other Brazilians clays, the points of the ratio S_{uvane}/σ'_{vm} *vs.* PI fall between the correlations of Larsson (1980) and Mesri (1975), with satisfactory prediction by Coutinho (2007) proposal $S_u/\sigma'_{vm} = 0.11 + 0.0037$ PI (modified from Skempton, 1957). It is possible to make a satisfactory prediction of S_u from CPTU using proposals in the literature (N_{kt}, $N_{\Delta u}$ and N_{ke}). In Suape, satisfactory S_u results were obtained considering N_{kt} of 9-10, in general, with Brazilian clays in the range (9-12), including Recife.

The Mayne & Mitchell (1988) proposal for obtain OCR_{vane} adapted for Suape clays ($OCR_{lab} = 0.65.OCR_{vane}$) presented values with a good correlation with the OCR_{lab} values in good quality samples. Kulhawy & Mayne's (1990) proposal to obtain OCR from CPTU adapted to Suape clays (OCR= 0.173Q_t) provided OCR_{CPTU} values with a good correlation with OCR_{lab} values. The corrected coefficient (0.173) was almost half the original coefficient (0.32), and it was smaller than the value found for Recife clays (0.23) and similar for Rio de Janeiro clay (0.153).

This study confirms that parameters can be obtained through *in situ* tests with correlations suited to local/regional experiment; and it is also important to have a joint laboratory and *in situ* test program. This prediction is fundamental for a proper geotechnical site characterization in research and engineering projects.

Acknowledgments

The authors acknowledge support from specific research projects PRONEX (CNPq/FACEPE); and INCT-REAGEO (CNPq); CNPq for the financial support (fellowship) in research involving the authors; and Gusmão Engineers Associated for the partnership.

References

Aas, G.; Lacasse, S.; Lunne T. & Hoeg, K. (1986) Use of *in situ* tests for foundation design on clay. 6th Conf. on Use of *In Situ* Tests in Geotechnical Engineering, ASCE Special Publication, p. 1-30.

Almeida. M.S.S., M.E.S. Marques. & M. Baroni (2010) Geotechnical parameters of very soft clays obtained with CPTU compared with other site investigation tools. CPT'10 Conference Proceedings, California, USA.

Almeida, M.S.S., Marques, M.E.S. & Miranda, T.C., Nascimento, C.M.C. (2008) Lowland reclamation in urban areas, Proc. TC 41 International Workshop on Urban Infrastructure, Búzios, Brazil.

Baligh, M.M. (1986) Undrained deep penetration II: Pore pressure. Geotechnique, v. 36:4, p. 486-501.

Baligh, M.M. & Lavadoux, J.N. (1986) Consolidation after undrained piezocone penetration II: Interpretation. Journal of Geotechnical Engineering, ASCE, v. 112:7, p. 727-45.

Baroni, M. (2010) Investigação Geotécnica em Argilas Orgânicas Muito Compressíveis em Depósitos da Barra da Tijuca. Master's Dissertation, COPPE, Federal University of Rio de Janeiro, 270 p.

Begemann, H.K.S. (1965) The friction jacket cone as an aid in determining the soil profile. Proc.6th International Conference on Soil Mechanics and Foundation Engineering, ICSMFE, Montreal, v. 2, p. 17-20.

Bello, M.I.M.C.V. & Coutinho, R.Q. (2012) Piezocone testing for use in the classification of soil behavior and flow characteristics: An experiment carried out in Suape, Pernambuco. Coutinho & Mayne (eds) The 4th International Conference on Site Characterization ISC'4, ISSMGE, Recife. Brazil, v. 1. p. 405-413.

Bello, M.I.M.C.V. (2011) Parâmetros Geotécnicos e Banco de Dados de Argilas Moles: o Caso de Suape. D.Sc. Thesis. Federal University of Pernambuco, 320 p.

Bjerrum, L. (1973) Problems of soil mechanics and construction of soft clays and structurally unstable soils. Proceedings of the 8th International Conference on Soil Mechanics and Foundation Engineering, Moscow, v. 2, p. 111-159.

Bjerrum, L. & Simons, N.E. (1960) Comparison of shear strength characteristics of normally consolidated clays. ASCE, Conference on Shear Strength of Cohesive Soils, Boulder, Colorado, p. 711-726.

Chandler R.J. (1988) The *In Situ* Measurements of the Undrained Shear Strength of Clays Using the Field Vane. ASTM, STP, Nº 1014, p. 13-44.

Coutinho, R.Q. (2010) Investigação Geotécnica área Refinaria Petrobrás - Suape-PE. Technical Report, GEGEP/UFPE Agreement, Petrobras Refinery Consortium, Pernambuco.

Coutinho, R.Q. (2008) Investigação Geotécnica de Campo e Avanços para a Prática. Proc. XIV Congresso Brasileiro de Mecânica de Solos e Engenharia Geotécnica, COBRAMSEG'2008, Búzios., v. 1. p. 201-230.

Coutinho, R.Q. (2007) Characterization and Engineering Properties of Recife Soft Clays - Brazil. Tan, Phoon, Hight and Leroueil (eds) The Second International Workshop on Characterization e Engineering Properties of Natural Soils, Singapore, p. 2049-2100.

Coutinho, R.Q. (1980) Estudo de Características Geotécnicas das Argilas Moles do Recife. Relatório Técnico Projeto Pesquisador CNPq - DECivil/UFPE, período 1978-1980.

Coutinho, R.Q. (1976) Características de Adensamento com Drenagem Vertical e Radial em Argila Mole na Baixada Fluminense, M.Sc. dissertation, COPPE/UFRJ, 206 p.

Coutinho, R.Q. & Bello, M.I.M.C.V. (2012a) Evaluation of Sample Quality and Correction of Compressibility Parameters Results to account for the Effects of Sample Disturbance - Experiment at Suape in Pernambuco. Coutinho & Mayne (eds) The 4º International Conf. on Site Characterization, ISC'4, ISSMGE, Recife, Brazil, v. 2, p. 1621-1629.

Coutinho, R.Q. & Bello, M.I.M.C.V. (2012b) Undrained strength and overconsolidation ratio parameters of suape soft clays, Pernambuco. Coutinho & Mayne (eds) The 4th International Conference on Site Characterization, ISC'4, ISSMGE, Recife, Brazil, v. 2. p. 1631-1639.

Coutinho, R.Q. & Schnaid, F. (2010) CPT - Regional Report for South America. CPT10 Conf. Proc., California, USA. v. 1, p. 313-333.

Coutinho, R.Q.; Bello, M.I.M.C.V. & Soares, F.L. (2008) Geotechnical investigation of the Recife soft clays by piezocone test. Proc. ISC'3, Taipei, v. 1.p. 311-319.

Coutinho, R.Q. & Bello, M.I.M.C.V. (2008) Caracterização geotécnica do solo mole do acesso à Ilha de Tatuoca - Porto de Suape/PE. Proc. XIV COBRAMSEG'2008, ABMS, Búzios, Brazil, v. 2, p. 265-269.

Coutinho, R.Q., Oliveira, A.T.J. & Oliveira, J.T.R. (2000) Conferência Palheta: Experiência, Tradição e Inovação. Seminar on Special Foundation Engineering and Geotechnics. SEFE IV, São Paulo, Brazil, v. 3, p. 53-79.

Coutinho. R.Q.; Oliveira, J.T.R. & Oliveira, A.T.J. (1998) Estudo quantitativo da qualidade de amostras de argilas moles brasileiras - Recife e Rio de Janeiro. Proc. XI Brazilian Congresso on Soil Mechanics and Geotechnical Engineering, COBRAMSEG, ABMS, Brasília, v. 2. p. 927-936.

Coutinho, R.Q., Oliveira, J.T.R & Danziger, F.A.B. (1993) Geotechnical characterization of a Recife soft clay. Soils and Rocks, v. 16:4, p. 255-266.

Coutinho, R.Q. & Lacerda, W.A. (1987) Characterization - consolidation of Juturnaíba organic clays. Proc. International Symposium on Geotechnical Engineering of Soft Soils, v. 1, p. 17-24, Mexico. Published also in Soils and Rocks, v. 17:2, p. 145-154 (1994).

Djoenaidi, W.J. (1985) A Compendium of Soils Properties and Correlations. Master's Thesis, University of Sydney, Australia.

Fellenius, B.H. & Eslami, A. (2000) Soil Profile Interpreted from CPTu Data. Year 2000 Geotechnics. Geotechnical Engineering Conference, Asian Institute of Technology, Bangkok, Thailand, 18 p.

Ferreira, S.R.M. (1982) Compressibilidade de uma Argila Orgânica Mole do Recife. Dissertação de M.Sc., Engenharia Civil, COPPE/UFRJ, Rio de Janeiro.

Futai, M.M (2010) Theoretical and Practical Concepts on Behavior Analysis of some Rio de Janeiro Clays. D.Sc. Seminar, COPPE/UFRJ, Rio de Janeiro, 133 p.

Houlsby, G.T. & Teh, C.I. (1988) Analysis of the piezocone in clay. Proc. International Symposium on Penetration Testing, ISOPT-1, Orlando, USA, p. 777-783.

Jannuzi, G.M.F. (2009) Characterization of the Sarapuí II Soft Soil Deposit Through Field Tests. Master's Dissertation, COPPE/UFPE, Rio de Janeiro, Brazil.

Jamiolkowski M., Ladd, C., Germaine & J. T., Lancellota, R. (1985) New developments in field and laboratory testing of soils. Proc. 11th ICSMFE, San Francisco, USA, v. 1, p. 57-153.

Jefferies, M.G. & Davies, M.P. (1993) Use of CPTu to estimate equivalent SPT N60. American Society for Testing and Materials, ASTM, Geotechnical Testing Journal, v. 16:4, p. 458-468.

Koppula, S.D. (1981) Statistical estimation of compression index. Geotechnical Testing Journal, v. 4:2, p. 68-73.

Kulhawy, F.H., Mayne & P.W. (1990) Manual on estimating soil properties for foundation design. Electric Power Research Institute, EPRI, August, 1990.

La Rochelle, P.; Tavena, F. & Leroueil, S. (1988) Clays of Eastern Canada and their contribution to understanding clay behaviour. Canadian Geotechnical Journal, v. 25:3, p. 413-427.

Larsson R. (1980) Undrained shear strength in stability calculation of embankments and foundations on soft clays. Canadian Geotechnical Journal, v. 17:4, p. 591-602.

Leroueil, S. & Hight, D.W. (2003) Characterization of soils for engineering. Characterization and engineering properties of natural soils. Tan, T.S.; Phon, K.K.; Hight, D.W. & Leroueil, S. (eds) Singapore, v. 1, p. 255-236.

Long, M. (2008) Design parameters from *in situ* tests in soft ground - recent developments. Proc. 3rd International Conference on Geotechnical and Geophysical Site Characterization, ISC'3, Taipei, v.1, p. 89-116.

Lunne, T., Robertson, P.K. & Powell, J.J.M. (1997) Cone Penetration Testing in Geotechnical Practice. Blackie Academic & Professional, 312 p.

Lunne, T., Lacasse, S & Rad, N.S. (1989) Pressuremeter testing and recent developments - Part I: All tests except SPT. General Report, 12 ICSMGE, v. 4, p. 2339-2403.

Mayne, P.W. (2007) Synthesis 368 on Cone Penetration Testing: State-of-Practice, NCHRP Project 20-05; Task 37-14, Transportation Research Board, National Academies Press, Washington, D.C., 118 p.

Mayne, P.W. & Mitchell, J.K (1988) Profiling of overconsolidation ratio in clays by field vane. Canadian Geotechnical Journal, v. 25, p. 150-157.

Mesri G. (1975) New design procedure for stability of soft clays. Discussion. Journal of Geotechnical Engineering Division, ASCE, v. 101:GT4, p. 409-412.

Mesri, G. & Choi, Y.K. (1985) Settlement analysis of embankment on soft clays. Journal of Geotechnical Engineering Division, ASCE, JUDGE, v. 111:4, p. 441-464.

Mollé, J. (2005) The accuracy of the interpretation of CPT-based soil classification methods for soft soils. MSc Thesis. Section for Engineering Geology, Department of Applied Earth Sciences, Delft University of Technology. Memoirs of the Centre of Engineering Geology in the Netherlands, No. 242. Report AES/IG/05-25.

Oliveira J.T.R. (2002) Influência da Qualidade da Amostragem no Comportamento Tensão-Deformação-Tempo das Argilas Moles. Doctorate Thesis, COPPE/UFRJ - DEC-UFPE .

Ramsey, N. (2002) A calibrated model for the interpretation of cone penetration tests (CPTs) in North Sea Quaternary Soils. Offshore Site Investigation and Geotechnics - Diversity and Sustainability, Society for Underwater Technology, London, p. 341-356.

Robertson, P.K. (2010) Evaluation of flow liquefaction and liquefied strength using the Cone Penetration Test. American Society of Civil Engineers, ASCE, Journal of Geotechnical & Geoenvironmental Engineering, v. 136:6, p. 842-853.

Robertson, P.K. (1990) Soil Classification by the cone penetration test: Replay. Canadian Geotechnical Journal, v. 27:1, p. 151-158.

Robertson, P.K., Campanella, R.G., Gillespie, D. & Grieg, J. (1986) Use of piezometer cone data. Proc. American Society of Civil Engineers, ASCE, In-Situ 86 Specialty Conference. Geotechnical Special Publication GSP No. 6, p. 1263-1280.

Robertson, P.K. & Campanella, R.G. (1983) Interpretation of cone penetrometer tests, Part I sand. Canadian Geotechnical Journal, v. 20:4, p. 718-733.

Robertson, P.K., Sully, J.P., Woelle, D.J., Lunne, T., Powell, J.J.M. & Gillespie, D.G. (1992) Estimating coefficient on consolidation from piezocone tests. Canadian Geotechnical Journal, v. 29, p. 539-550.

Schmertmann, J.H. (1955) The undisturbed consolidation behavior of clay. Transactions, ASCE, v. 120, p. 1201-1233.

Schmertmann, J.H., Hartmann, J.P. & Brown, P.R. (1978) Improved strain influence factor diagrams. ASCE Journal of the Geotechnical Engineering Division, v. 104:GT8, p. 1131-1135.

Schnaid, F. (2009) *In situ* Testing in Geomechanics. Taylor and Francis, Oxon.

Schnaid, F. (2000) Ensaios de Campo e suas Aplicações à Engenharia de Fundações. 1st ed. Oficina de Textos, São Paulo, 189 p.

Schneider, J.A., Randolph, M.F., Mayne, P.W. & Ramsey, N.R (2008) Analysis of factors influencing soil classification using normalized piezocone tip resistance and pore pressure parameters. Journal of Geotechnical and Geoenvironmental Engineering, ASCE, v.134:11, p. 1569-1586.

Skempton, A.W. (1957) Discussion: The Planning and Design of the New Hong Kong Airport, by K. Grace and J.K.M. Henry. Institution of Civil Engineers, v. 7, p. 305-307.

Sully, J.P.; Campanella, R.G. & Robertson, P.K. (1988) Interpretation of penetration pore pressure to evaluate stress history in clays. Proc. ISOPOT-1, Florida, v. 2, p. 993-999.

Tavenas, F. & Leroueil, S. (1987) State-of-the-Art report: Laboratory and *in situ* stress strain-time behaviour of soft clays. International Symposium on Geotechnical Engineering of Soft Soils, Mexico City, v. 2, p. 3-48.

On the Characterization and Classification of Bauxite Tailings

F. Schnaid, H.P. Nierwinski, J. Bedin, E. Odebrecht

Abstract. Large-scale mining operations generate vast quantities of tailings that are deposited in hydraulic-fill tailing dams in the form of slurries. Stability of these impoundments require investigation of water table configuration, aquifer boundaries, site characterization and determination of short and long term properties of tailings. These aspects are evaluated in this paper from a comprehensive site investigation that comprises both laboratory and field tests from a bauxite tailing deposit in northern Brazil. The purpose is to enhance the understanding on the mechanical properties of bauxite tailings in order to select or develop appropriate constitutive models for predicting the behavior of tailings impoundments. Attention is given to the characterization and classification of silt tailings from the combination of measurements from independent tests expressed on the basis of the ratio of the elastic stiffness to penetration tip resistance.

Keywords: bauxite tailings, critical state, piezocone, liquefaction.

1. Introduction

Many countries with large mining industry operations are active in implementing effective environmental legislation to ensure sustainable development with minimum ecosystem degradation. Tailing storage facilities is one subject of major concern, given the potential environmental impact in discharge areas. The most popular type of embankment for tailings dams is the upstream construction where new parts of the embankment are built on top of the slurries impounded during the previous stage (i.e. the dam crest moves "upstream" during construction). Although this is a low cost process, the upstream embankment type is a high risk operation, particularly because (a) upstream dams are particularly susceptible to liquefaction under seismic ground motion and (b) dam stability is endangered if the raising rate of the dam is high due to excess pore pressure built within the deposit during construction. Since tailings have different properties compared to natural materials and the way of testing tailings material need to be calibrated for these differences, there is a need for field and laboratory studies of physico-mechanical characteristics of tailing dam deposits.

Recent research projects in Brazil comprise comprehensive *in situ* (CPTU, DMT, Vane) and laboratory characterization (triaxial and oedometer) in active iron ore, gold, bauxite and zinc residue storages. This includes a decade of consecutive site investigation research all over Brazil, providing an opportunity to examine the state of tailings from the beginning of operations to closure (*e.g.* Schnaid, 2005; Bedin *et al.*, 2008; 2012; Schnaid *et al.*, 2013). This paper explores some features of this study with focus on fundamental aspects of behavior, as well as the characterization and classification of bauxite tailings in storage facilities.

2. Laboratory Testing Program

An extensive laboratory testing program has been carried out to study the geotechnical properties and behavior of gold, bauxite and zinc (*e.g.* Bedin *et al.*, 2012; Schnaid *et al.*, 2013). Some characteristic features are common to all silty tailings and are highlighted here from tests carried out on bauxite. Characterization comprises identification of minerals, grain size distribution and microscopy (Table 1). The material disposed in ponds is predominantly low to non-plastic, silty clay (typically 80% silt, 15% clay and 5% sand) with an average unit weight of 16 kN/m^3 and high specific gravity ($2.70 < G < 3.00$) reflecting the high iron content of the tailings. Microscopy reveals well-rounded as well as angular grains, forming loosely arranged structure that due to angularity may result in relatively high drained shear strength.

Undisturbed samples in silts are typically too difficult or costly to obtain and, for this reason, reconstituted samples need to be prepared for laboratory testing. Disturbed samples were retrieved using a bucket type of sampler which allows samples to be extracted without losing water. The moist tamping method has been used to reconstitute specimens at their average in situ density. Samples were prepared by mixing the soil with small amount of water and compacting the mixture in a mold, in layers prepared of equal volume lifts to produce homogeneous mixtures (*e.g.* Lade, 1978). The mixture is partially saturated when placed and the inter-particle suction is utilized to allow high voids ratio to be achieved.

F. Schnaid, Ph.D., Full Professor, Departamento de Engenharia Civil, Universidade Federal do Rio Grande do Sul, Porto Alegre, RS, Brazil. e-mail: fernando@ufrgs.br.
H.P. Nierwinski, MSc. Student, Programa de Pós Graduação em Engenharia Civil, Universidade Federal do Rio Grande do Sul, Porto Alegre, RS, Brazil. e-mail: helnier@gmail.com.
J. Bedin, D.Sc. Student, Programa de Pós Graduação em Engenharia Civil, Universidade Federal do Rio Grande do Sul, Porto Alegre, RS, Brazil. e-mail: juceliabedin@gmail.com.
E. Odebrecht, D.Sc., Associate Professor, Departamento de Engenharia Civil, Universidade do Estado de Santa Catarina, Joinville, SC, Brazil. e-mail: edgar@geoforma.com.br.
Submitted on June 19, 2014; Final Acceptance on December 15, 2014; Discussion open until April 30, 2015.

Table 1 - Bauxite tailings composition.

Element	% by weight
Na	14.33
Al	16.85
Si	12.58
Ca	2.86
Ti	6.70
Fe	46.65
Total	99.96

One dimensional compression and hydraulic conductivity tests have been carried out in specimens reconstituted at different void ratios, ranging from 2.6 to 1.4, which covers the maximum and minimum determined *in situ* values. The vertical effective stress-void ratio relationship presented in Fig. 1 gives a description of the soil compressibility. The vertical stresses were not sufficiently high to identify the normal compression line (NCL), and an attempt to fit a straight line to points measured at high stresses give a slope λ equal to 0.093 to an initial void ratio of 1.7. The hydraulic conductivity has been determined by constant head tests carried out in the oedometer cells at different vertical stresses. An average value of 2 x 10^{-8} m/s was taken as representative.

Undrained triaxial tests were performed to evaluate the stress-strain-pore pressure response of bauxite tailings. Saturation of soil specimens was accomplished by application of a back pressure of around 500 kPa to produce *B* values higher than 95%. All reported test specimens were isotropically consolidated from a single initial void ratio to their desired consolidation pressure before shearing at 0.1 mm/min under undrained conditions. Results on saturated samples are presented in Fig. 2, in which deviatoric stress (σ1 - σ3) and pore pressures are plotted against axial strains. Tests generate considerable excess pore pressure and gentle strain softening. Fifteen percent maximum axial strain was sufficient to establish critical state conditions in these undrained tests, as shown in Fig. 2 using the Cambridge (p‘ - q) and (e - ln p‘) planes. The isotropic and oedometric compression lines are presented in the same diagram for reference. Results show the idealized behavior of a unique critical state line (CSL) described by parallel ICL and CSL (despite the fact that NCL and ICL do not produce a match) The shear strength properties were zero cohesion and effective angle of internal friction angle typically of 36°, and the state parameter of the order of 0.08.

3. Field characterization

Field tests are the preferable alternative to assess tailing properties and hydrogeologic conditions within the impoundment. *In situ* water content, unit weight and specific gravity in this bauxite tailings are shown in Fig. 3. Typical profiles from a series of SCPTU are shown in Fig. 4. Measured cone resistance q_t, sleeve friction f_s and pore pressure u_2 are plotted against depth revealing a relatively homogeneous profile down to about 16 m. Although the piezocone tests were conducted about 10 m away from each other, two profiles revealed lenses of granular materials that are not taken into consideration in the forgoing analysis. Shear

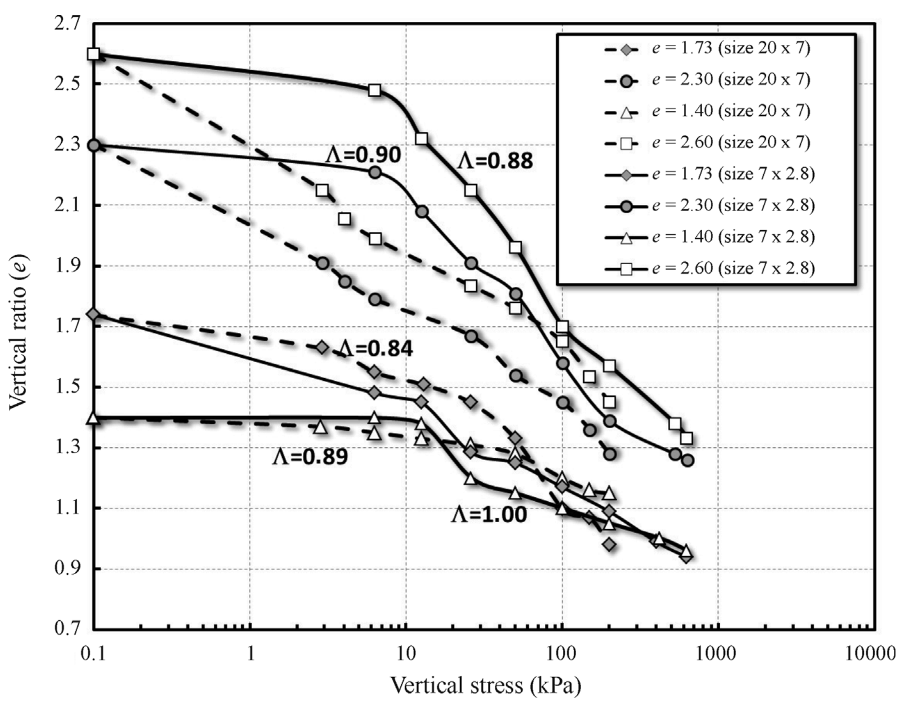

Figure 1 - Results from oedometer tests.

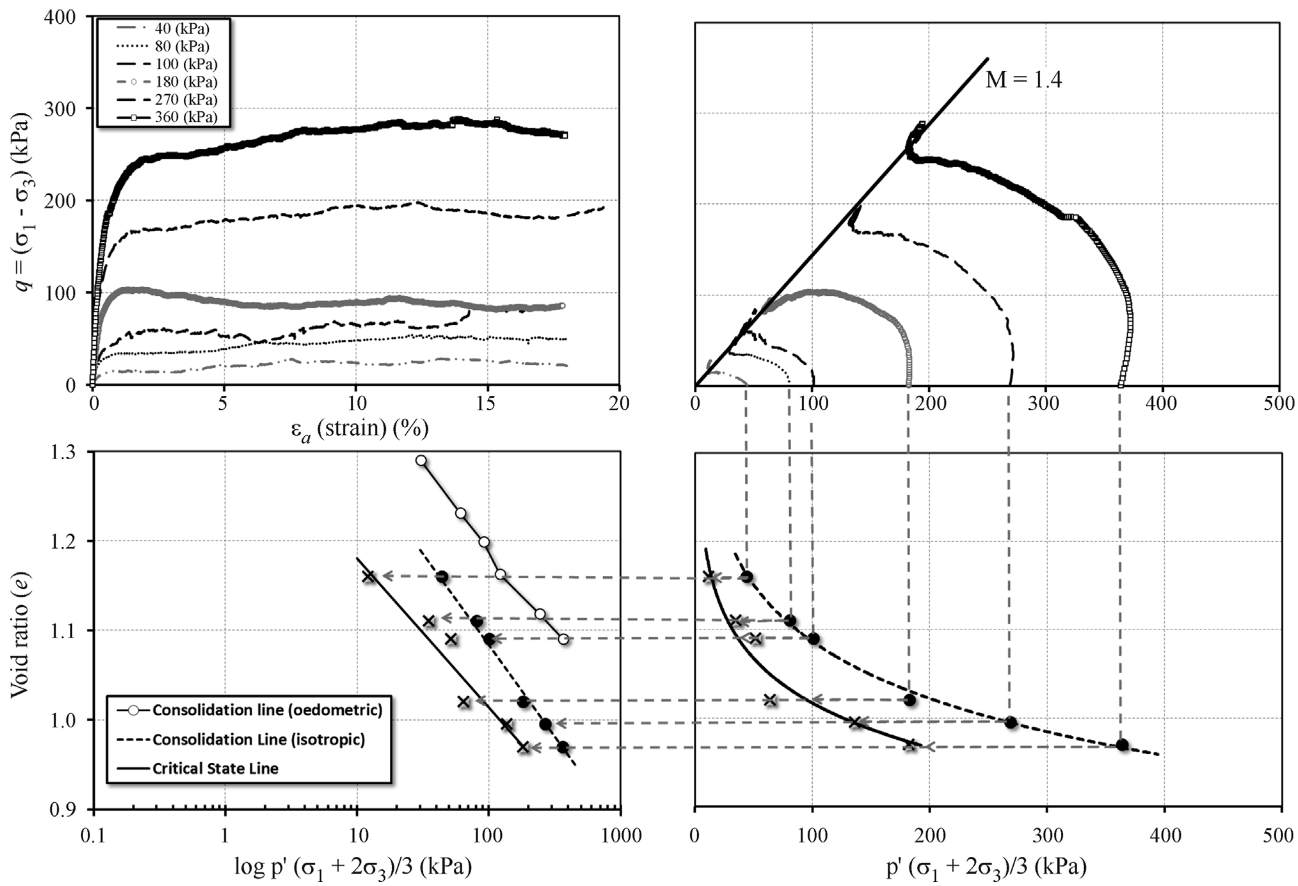

Figure 2 - Bauxite critical state conditions.

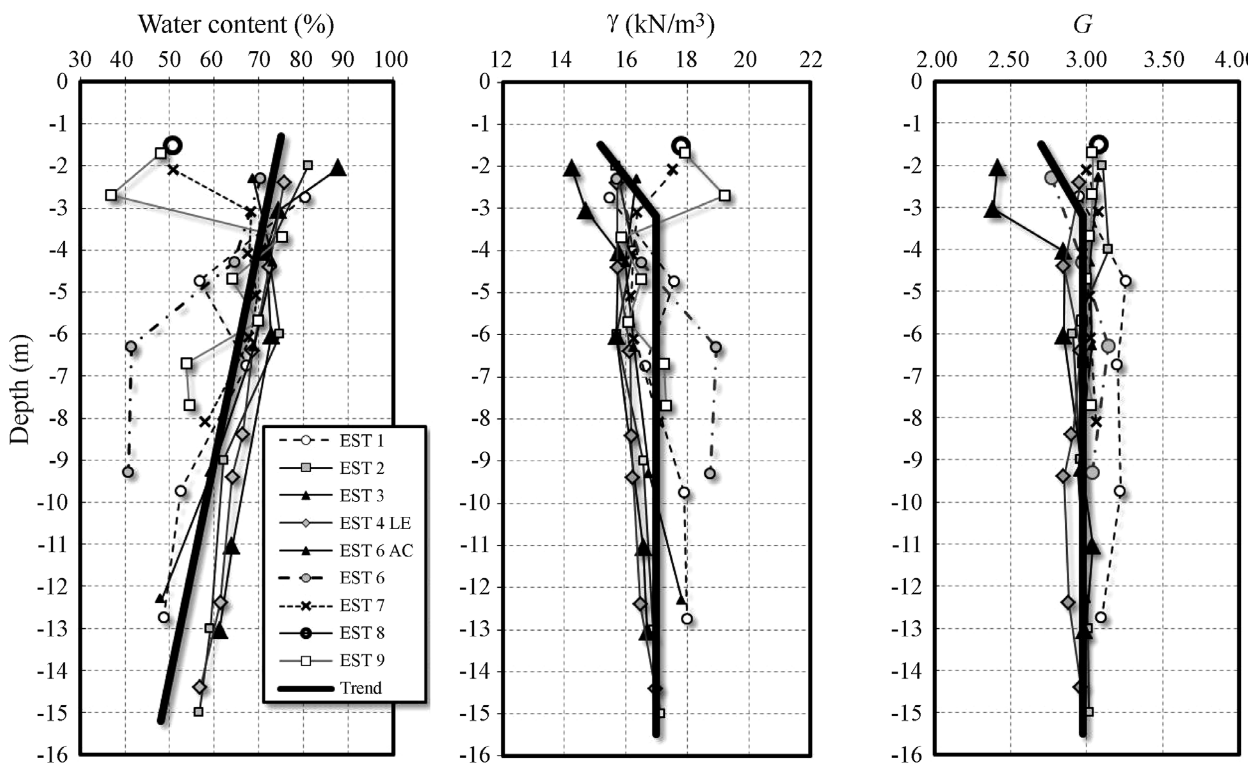

Figure 3 - *In situ* water content, unit weight and specific gravity in the bauxite tailing dam.

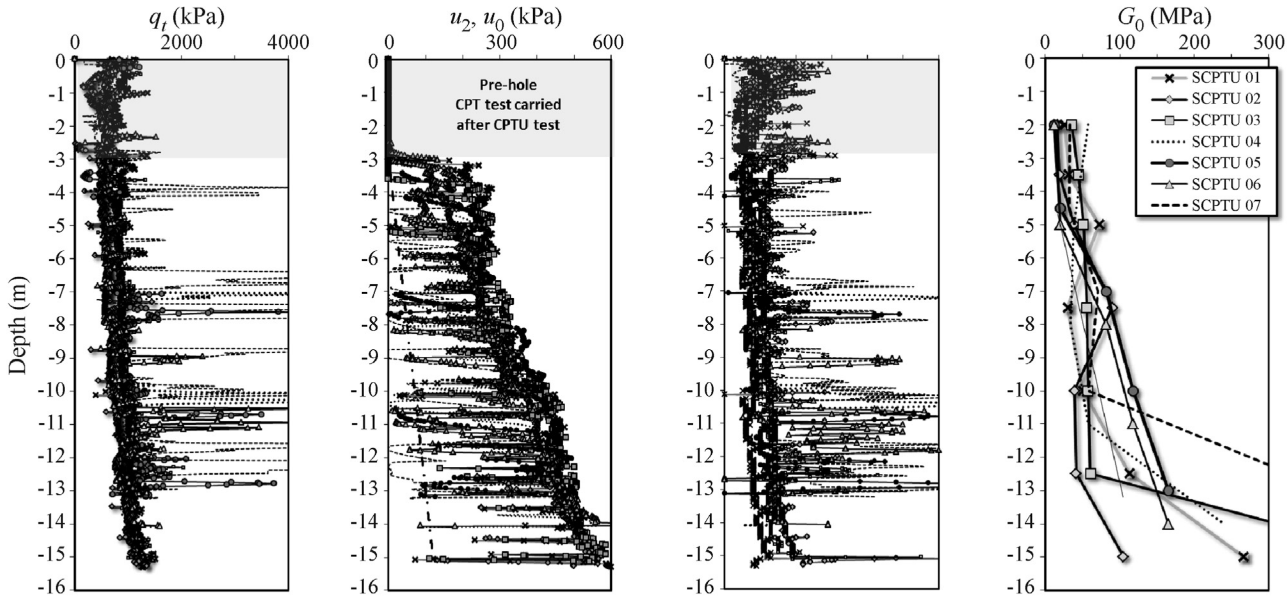

Figure 4 - Typical CPTU profiles.

wave velocity measurements show monotonic increase with depth and yield shear modulus in the range of 20 to 50 MPa.

Values of the pore pressure parameter B_q range from 0.5 to 0.8 indicating undrained paths during cone penetration. High B_q is consistent with the measured hydraulic conductivity values and the contractive response in shear.

In these site investigations, close attention has been given to a precise determination of the position of the water table at the time of the investigation programme, which changes with time in these recently deposited, under consolidation slurries placed over a pervious free drained deposit foundation. This is achieved by a close inspection of a series of dissipation tests obtained by recording the values of the pore water pressure with time during a pause in pushing and whilst the cone penetrometer is held stationary. Although dissipation tests are often held for the time that takes for 50% consolidation, t_{50}, in tailings a special recommendation is made to held the penetrometer stationary for longer periods corresponding to a time interval between t_{90} to t_{100}.

Values of c_h and c_v can be also estimated from these dissipation tests following the analysis proposed by Houlsby & Teh (1988). A summary of values obtained in the alumina STF is summarized in Fig. 5. Although values of c_h range between 2 x 10^{-6} and 8 x 10^{-5} cm^2/s, there is no distinct variation trend with depth. An average c_h value of about 8 x 10^{-6} is representative of this alumina tailing deposit.

4. Classification

Several attempts have been made to combine the piezocone measurements in order to produce classification charts designed to describe soil type for engineering applications (Douglas & Olsen, 1981; Senneset & Janbu, 1985; Robertson *et al.*, 1986; Robertson, 1990; Jefferies & Davies, 1991). Published CPTU soil classification charts are typically constructed from dimensionless ratios such as Q_t (=(q_t - σ_{vo})/σ'_{vo}), B_q (=(u - u_o)/(q_t - σ_{vo})) and F_r (=(f_s/q_t - σ_{vo})x 100%). The original chart by Robertson (1990) produces very scattered data with soil ranging from sandy-silt to clay (Fig. 6).

The normalized soil behavior index I_c proposed by Robertson (1990) is shown in the Fig. 7 and indicates/characterizes silty-sand and sandy-silt soils (1.90 < I_c < 2.82).

An alternative relationship uses the ratio of the elastic stiffness to penetration tip resistance (G_o/q_c), following the concept that a material that is stiffer in deformation may be stronger in strength. An approach developed by Robertson (2010) correlating G_o/q_c and Q_t is shown in Fig. 8. In addition CPT data can be expressed in the unified plot proposed by Shuttle & Cunning (2007) using the $Q(1 - Bq)+1$ *vs.* F space (Fig. 9), where strain softening is a predominantly response.

A similar plot has been suggested by Schnaid *et al.* (2004) and Schnaid (2005) in which the the G_o/q_c ratio is related to the normalized dimensionless parameter q_{c1}, defined as:

$$q_{c1} = \left(\frac{q_c}{p_a}\right)\sqrt{\frac{p_a}{\sigma'_v}} \tag{1}$$

where p_a is the atmospheric pressure. Results shown in Fig. 10 define a specific region in the G_o/q_c *vs.* q_{c1} space that falls outside, above and to the left of the region established for sand. Independent sets of data from gold and zinc high

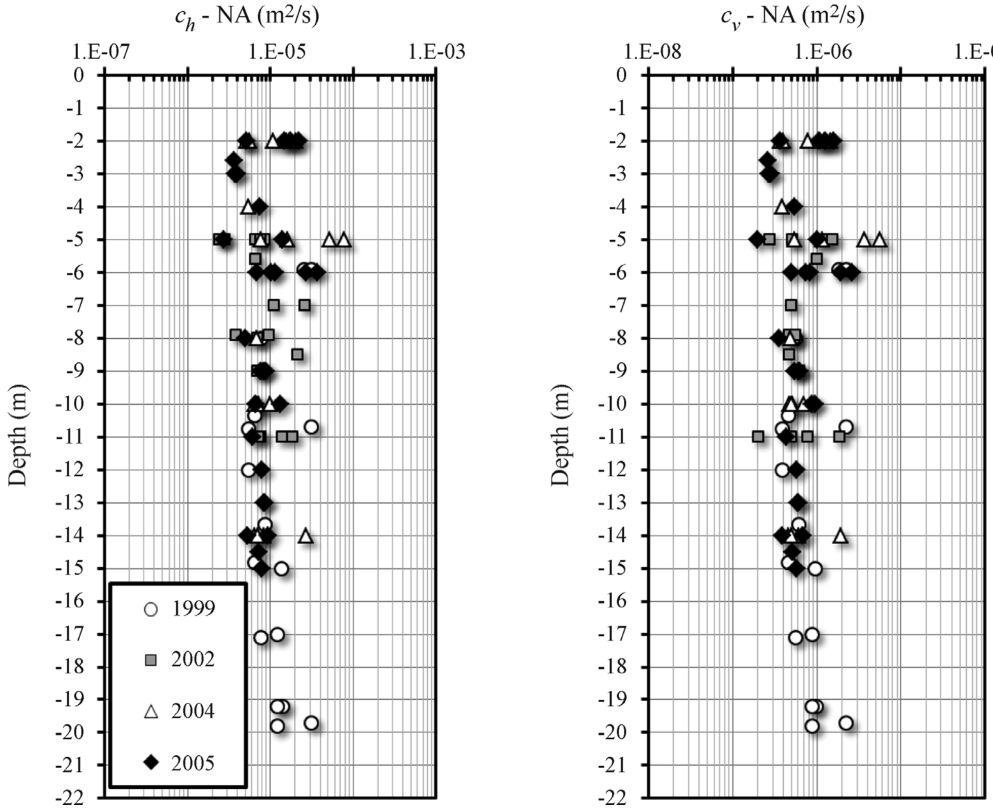

Figure 5 - Values of coefficient of consolidation.

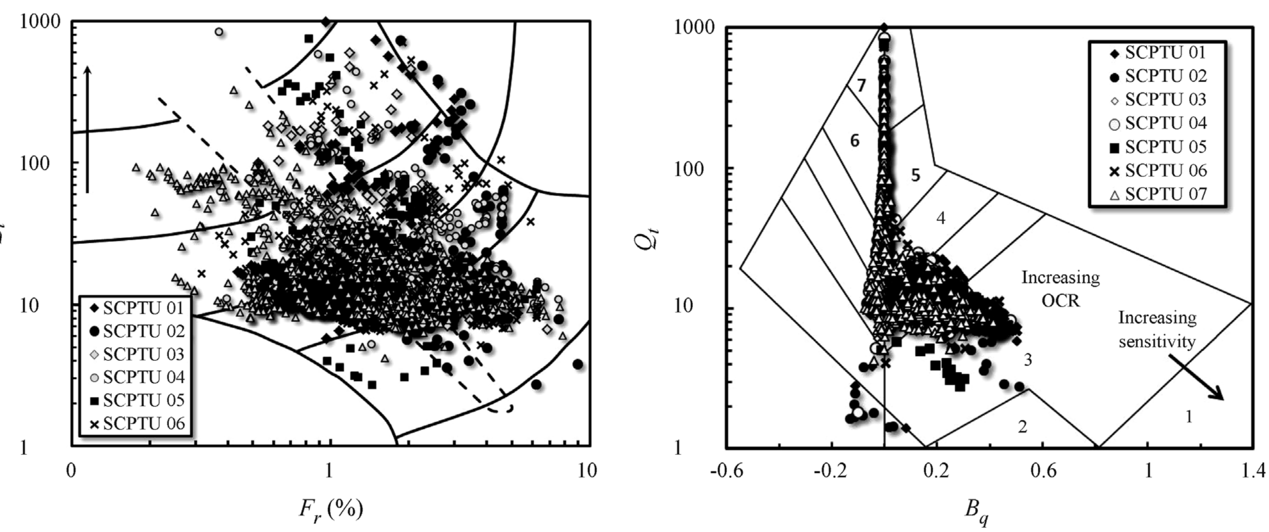

Zone	Soil behaviour type	Zone	Soil behaviour type
1	Sensitive fine grained	7	Silty sand to sandy silt
2	Organic material	8	Sand to silty sand
3	Clay	9	Sand
4	Silty clay to clay	10	Gravelly sand to sand
5	Clayey silt to silty clay	11	Very stiff fine grained*
6	Sandy silt to clayey silt	12	Sand to clayey sand*

* Overconsolidated or cemented

Figure 6 - Classification of bauxite tailings on the chart proposed by Robertson (1990).

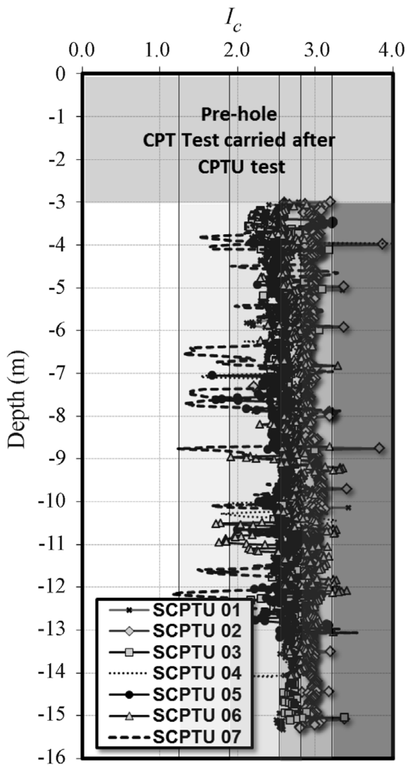

Figure 7 - Normalized soil behavior index I_c of bauxite tailings proposed by Robertson (1990).

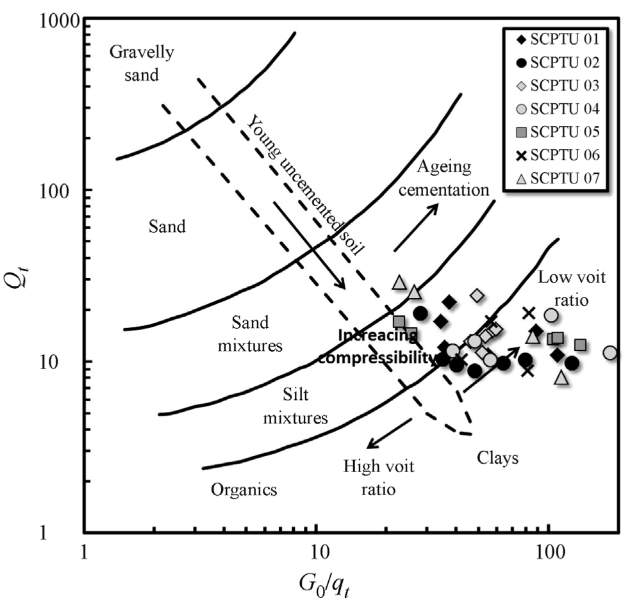

Figure 8 - Classification of bauxite tailings on the chart proposed by Robertson and Fear (1995).

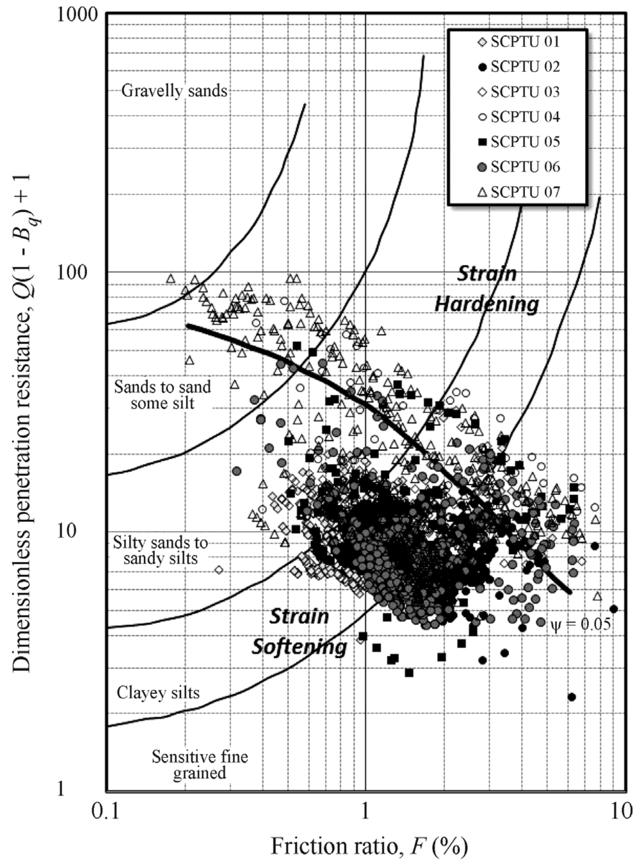

Figure 9 - Unified classification chart (Shuttle & Cunning (2007 & 2008)).

plasticity slurries have been added to the same plot, falling on the very same region established for bauxite tailings. The classification method was then considered to provide an adequate representation of the fines influence by grouping all materials in a single area that appears to be representative of compressible materials that may exhibit strong strain softening (*e.g.* Schnaid *et al.*, 2013). This evidence is in accordance to laboratory observations.

5. Conclusion

The purpose of this paper is to study the mechanical properties of bauxite tailings and to evaluate how the current site investigation practice is able to identify factors related to tailing response and to stability problems of impoundments. The hydraulic conductivity of tailings varies from point to point in a deposit and, for the present study, a location representative of fine, non-plastic, silt tailings has been selected. Laboratory tests were carried out on reconstituted samples leading to measured coefficient of hydraulic conductivity of the order of 2×10^{-8} m/s, zero cohesion, friction angle of 36° and state parameter of 0.08. Drained shear strength is often higher than that for similar natural soils due to high particle angularity.

The piezocone test is the most popular technique used to characterize tailing impoundments and it successfully delineated the stratigraphy of bauxite. Predominantly undrained penetration enabled strength and stiffness to be assessed with reasonable accuracy. The coefficient of consolidation of bauxite slurries is in the range shown by

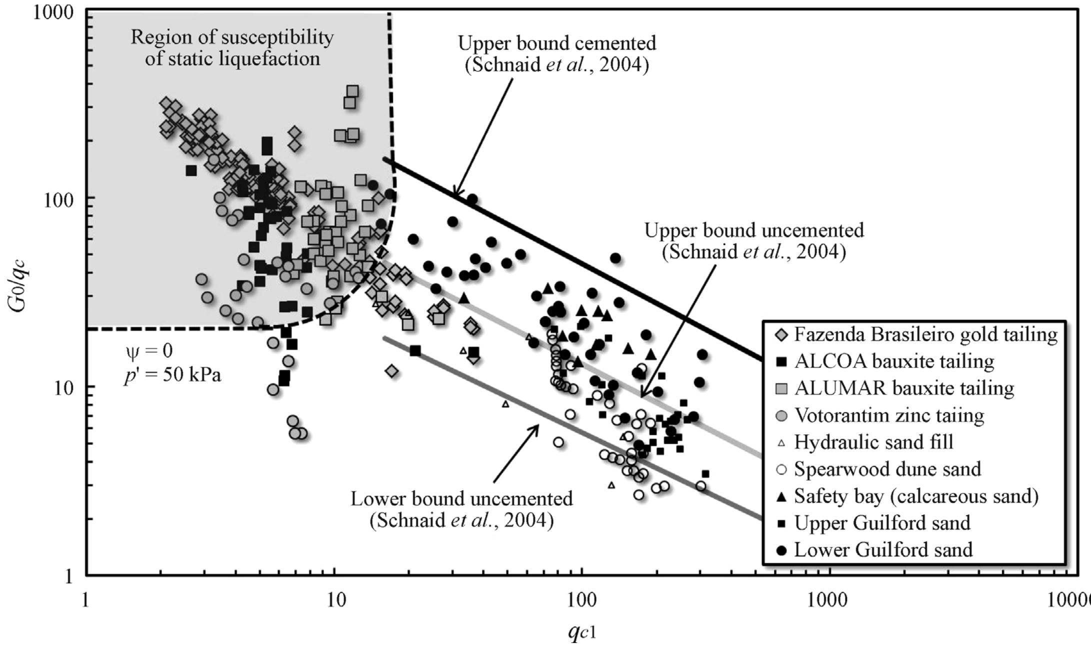

Figure 10 - Classification of bauxite tailings represented in the G_o/q_c *vs.* q_{c1} space.

natural clays. Undrained strength of these slurries is important in evaluation of liquefaction behaviour.

Finally the usefulness of the G_o/q_c ratio in tailings classification is highlighted, because combination of elastic stiffness to ultimate strength provides direct means to identify deposits that are highly compressible and may be susceptible to liquefaction.

Acknowledgments

The work described in this paper was carried out with the support from ALUMAR. The authors are particular grateful to the engineers Leandro Moura Costa Filho for his fruitful contribution and collaboration.

References

Bedin, J.; Schnaid, F. & Costa Filho, L.M. (2008) Study of geotechnical properties of gold tailing mining. Proc. IV Luso Brazilian Congress of Geotechnics, IV GEO 2008, Coimbra, Portugal, v. 1, p. 25-32.

Bedin, J.; Schnaid, F.; Fonseca, A.J.P.V. & Costa Filho, L.M. (2012) Gold tailings liquefaction under critical state soil mechanics. Geotechnique, v. 62, p. 263-267.

Douglas, B.J. & Olsen, R.S. (1981) Soil classification using electric cone penetrometer. Proc. ASCE National Convention, St. Louis, p. 209-227.

Houlsby, G.T. & Teh, C.I. (1988) Analysis of the piezocone in clay. Proc. International Symposium on Penetration Test, Rotterdam, Netherlands, v. 1, p. 777-783.

Jefferies, M.G. & Davies, M.O. (1991) Soil classification by the cone penetration test: Discussion. Canadian Geotechnical Journal, v. 281, p. 177-176.

Lade, R.S. (1978) Preparing test specimens using undercompaction. Geotechnical Testing Journal, Philadelphia, v. 1:1, p. 16-23.

Robertson. P.K., Campanella, R.G., Gillespie, D. & Greig, J. (1986) Use of piezometer cone data. Proc. ASCE Specialty Conference, In-Situ'86: Use of In-situ testing in Geotechnical Engineering, Blacksburg, p. 1263-1280.

Robertson, P.K. (1990) Soil classification using the cone penetration test. Canadian Geotechnical Journal, v. 27:1, p. 151-158.

Robertson, P.K. & Fear, C.E. (1995) Liquefaction of sands and its evaluation. Proc. First International Conference on Earthquake Geotechnical Engineering, keynote lecture, Tokyo, Japan.

Robertson, P.K. (2010) Evaluation of flow liquefaction and liquefied strength using the cone penetration test. Journal of Geotechnical Geoenvironmental Engineering, ASCE, v. 136:6, p. 842:853.

Schnaid, F. (2005) Geo-characterization and properties of natural soils by *in situ* tests. Proc. 16th ICSMGE, Osaka, Millpress, Rotterdam, v. 1, p. 3-45.

Schnaid, F.; Lehane, B.M. & Fahey. M. (2004) In situ test characterization of unusual geomateriais. Proc. 2nd ISC, keynote lecture, Porto, Millpress, Rotterdam, v. 1, p. 49-74.

Schnaid, F.; Bedin, J.; Viana da Fonseca, A.J.P. & Costa Filho, L.M. (2013) Stiffness and strenght governing the static liquefaction of tailings. Journal Geotechnical Geoenvironmental Engineerimg, v. 139:12, p. 2136-2144.

Senneset, K. & Janbu, N. (1985) Shear strength parameters obtained from static cone penetration tests. Proc. Symp. Shear Strength of Marine Sediments, ASTM Special Technical Publication, STP. 883, p. 41-54.

Shuttle, D.A. & Cunning, J. (2007) Liquefaction potential of silts from CPTU. Canadian Geotechnical Journal, v. 44:1, p. 1-19.

Shuttle, D.A. & Cunning, J. (2008) Discussion: Liquefaction Potential of Silts from CPTu. Canadian Geotechnical Journal, v. 45, p. 142-145.

SOILS and ROCKS
An International Journal of Geotechnical and Geoenvironmental Engineering

Publication of
ABMS - Brazilian Association for Soil Mechanics and Geotechnical Engineering
SPG - Portuguese Geotechnical Society
Volume 37, N. 3, September-December 2014

Author index

Instructions for Submission of Manuscripts

Category of the Papers

Soils and Rocks is the international scientific journal edited by the Brazilian Association for Soil Mechanics and Geotechnical Engineering (ABMS) and the Portuguese Geotechnical Society (SPG). The aim of the journal is to publish (in English) original research and technical works on all geotechnical branches.

According to its content the accepted paper is classified in one of the following categories: Article paper, Technical Note, Case Study or Discussion. An article paper is an extensive and conclusive dissertation about a geotechnical topic. A paper is considered as a technical note if it gives a short description of ongoing studies, comprising partial results and/or particular aspects of the investigation. A case study is a report of unusual problems found during the design, construction or the performance of geotechnical projects. A case study is also considered as the report of an unusual solution given to an ordinary problem. The discussions about published papers, case studies and technical notes are made in the Discussions Section.

When submitting a manuscript for review, the authors should indicate the category of the manuscript, and is also understood that they:

a) assume full responsibility for the contents and accuracy of the information in the paper;

b) assure that the paper has not been previously published, and is not being submitted to any other periodical for publication.

Manuscript Instructions

Manuscripts must be written in English. The text is to be typed in a word processor (preferably MS Word), **single column**, using ISO A4 page size, left, right, top, and bottom margins of 25 mm, Times New Roman 12 font, and line spacing of 1.5. All lines and pages should be numbered. The text should be written in the third person.

The first page of the manuscript must include the title of the paper followed by the names of the authors with the abbreviation of the most relevant academic title. The affiliation, address and e-mail must appear below each author´s name. An abstract of 200 words follows after the author´s names. A list with up to six keywords at the end of the abstract is required.

Although variations on the sequence and title of each section are possible, it is suggested that the text contains the following sections: Introduction, Material and Methods, Results, Discussions, Conclusions, Acknowledgements, References and List of Symbols. A brief description of each section is given next.

Introduction: This section should indicate the state of the art of the problem under evaluation, a description of the problem and the methods undertaken. The objective of the work should be clearly presented at the end of the section.

Materials and Methods: This section should include all information needed to the reproduction of the presented work by other researchers.

Results: In this section the data of the investigation should be presented in a clear and concise way. Figures and tables should not repeat the same information.

Discussion: The analyses of the results should be described in this section.

Conclusions: The content of this section should be based on the data and on the discussions presented.

Acknowledgements: If necessary, concise acknowledgements should be presented in this section.

References: References to other published sources must be made in the text by the last name(s) of the author(s), followed by the year of publication, similarly to one of the two possibilities below:

…while Silva and Pereira (1987) observed that resistance depended on soil density… or *It was observed that resistance depended on soil density (Silva and Pereira, 1987).*

In the case of three or more authors, the reduced format must be used, *e.g.*: Silva *et al.* (1982) or (Silva *et al.*, 1982). Two or more citations belonging to the same author(s) and published in the same year are to be distinguished with small letters, *e.g.*: (Silva, 1975a, b, c.). Standards must be cited in the text by the initials of the entity and the year of publication, *e.g.*: ABNT (1996), ASTM (2003).

Full references shall be listed alphabetically at the end of the text by the first author´s last name. Several references belonging to the same author shall be cited chronologically. Some examples are listed next:

Papers: Bishop, A.W. & Blight, G.E. (1963). Some aspects of effective stress in saturated and unsaturated soils. Geotechnique, 13(2): 177-197.

Books: Lambe, T.W & Whitman, R.V. (1979). Soil Mechanics, SI Version. John Wiley & Sons, New York, 553 p.

Book with editors: Sharma, H.D.; Dukes, M.T. & Olsen, D.M. (1990). Field measurements of dynamic moduli and Poisson's ratios of refuse and underlying soils at a landfill site. Landva, A. & Knowles, G.D. (eds), Geotechnics of Waste Fills - Theory and Practice, American Society for Testing and Materials - STP 1070, Philadelphia, pp. 57-70.

Proceedings (printed matter or CD-ROM): Jamiolkowski, M.; Ladd, C.C.; Germaine, J.T & Lancellotta, R. (1985). New developments in field and laboratory testing of soils. Proc. 11th Int. Conf. on Soil Mech. and Found. Engn., ISSMFE, San Francisco, v. 1, pp. 57-153.(specify if CD ROM).

Thesis and dissertations: Lee, K.L. (1965). Triaxial Compressive Strength of Saturated Sands Under Seismic Loading Conditions. PhD Dissertation, Department of Civil Engineering, University of California, Berkeley, 521 p.

Standards: ASTM (2003). Standard Test Method for Particle Size Analysis of Soils - D 422-63. ASTM International, West Conshohocken, Pennsylvania, USA, 8 p.

Internet references: Soils and Rocks available at http://www.abms.com.br and downloaded on August 6th 2003.

On line first publications must also bring the digital object identifier (DOI) at the end.

Figures shall be either computer generated or drawn with India ink on tracing paper. Computer generated figures must be accompanied by the corresponding digital file (.tif, .jpg, .pcx, etc.). All figures (graphs, line drawings, photographs, etc.) shall be numbered consecutively and have a caption consisting of the figure number and a brief title or description of the figure. This number should be used when referring to the figure in text. Photographs should be black and white, sharp, high contrasted and printed on glossy paper.

Tables shall be numbered consecutively in Arabic and have a caption consisting of the table number and a brief title. This number should be used when referring to the table in the text. Units should be indicated in the first line of the table, below the title of each column. Acronyms should be avoided. When applicable, the units should come right below the corresponding column heading. Additional comments can be placed as footnotes.

Equations shall appear isolated in a single line of the text. Numbers identifying equations must be flushed with the right margin. International System (SI) units must be used. The definitions of the symbols used in the equations must appear in the List of Symbols. It is recommended that the symbols used are in accordance with Lexicon in 8 Languages, ISSMFE (1981) and the ISRM List of Symbols.

The text of the submitted manuscript (including figures, tables and references) intended to be published as an article paper or a case history should not contain more than 30 pages, formatted according to the instructions mentioned above. Technical notes and discussions should have no more than 15 and 8 pages, respectively. Longer manuscripts may be exceptionally accepted if the authors provide proper explanation for the need of the required extra space in a cover letter.

Discussion

Discussions must be written in English. The first page of a discussion should contain:

The title of the paper under discussion;

Name of the author(s) of the discussion, followed by their position, affiliation, address and e-mail. The author(s) of the discussion should refer to himself (herself/themselves) as the reader(s) and to the author(s) of the paper as the author(s).

Figures, tables and equations should be numbered following the same sequence of the original paper. All instructions previously mentioned for the preparation of article papers, case studies and technical notes also apply to the preparation of discussions.

Editorial Review

Each paper will be evaluated by reviewers selected by the editors according to the subject of the paper. The authors will be informed about the results of the review process. If the paper is accepted, the authors will be required to submit a version of the revised manuscript with the suggested modifications. If the manuscript is rejected for publication, the authors will be informed about the reasons for rejection. In any situation comprising modification of the original text, classification of the manuscript in a category different from that proposed by the authors, or rejection, the authors can reply presenting their reasons for disagreeing with the reviewer comments.

Submission

The author(s) must upload a digital file of the manuscript to the Soils and Rocks website.

Follow Up

The online management system will provide a password to the corresponding author, which will enable him/her to follow the reviewing process of the submitted manuscript at the Soils and Rocks website.